First Principles Based Modeling of Pyrolysis of Cycloalkanes

Muralikrishna Khandavilli

UNIVERSITEIT
GENT

EXAMINATION BOARD

Faculty reading committee

Hans-Heinrich Carstensen,
Researcher, Fundación Agencia Aragonesa para la Investigación y Desarrollo (ARAID),
University of Zaragoza, Spain

Prof. dr. ir. Maarten Sabbe
Laboratory for Chemical Technology
Vakgroep Chemische Proceskunde en Technische Chemie
Faculteit Ingenieurswetenschappen en Architectuur
Universiteit Gent

Prof. ir. Marie-Francoise Reyniers
Laboratory for Chemical Technology
Vakgroep Chemische Proceskunde en Technische Chemie
Faculteit Ingenieurswetenschappen en Architectuur
Universiteit Gent

Prof. dr. Olivier Herbinet
Laboratoire Réactions et Génie des Procédés
Université de Lorraine, Nancy

Dr. Luc-Sy TRAN
CNRS Research Scientist
PC2A-CNRS-University of Lille,
France

Other members

Prof. dr. ir. Guy B. Marin [promotor]
Laboratory for Chemical Technology
Vakgroep Materialen, Textiel en Chemische Proceskunde
Faculteit Ingenieurswetenschappen en Architectuur
Universiteit Gent

Prof. dr. ir. Kevin Van Geem [promotor]
Laboratory for Chemical Technology
Vakgroep Chemische Proceskunde en Technische Chemie
Faculteit Ingenieurswetenschappen en Architectuur
Universiteit Gent

Prof. dr. ir. Filip De Turck [voorzitter]
Internet Technology and Data Science Lab
Vakgroep Informatietechnologie
Faculteit Ingenieurswetenschappen en Architectuur
Universiteit Gent

Acknowledgement

Wiele, who I found to be very smart. I also interacted with Maarten Sabbe, Carl Schietekat, Ruben de Bruycker and Alexander Vervust who added to my knowledge in a field which was very new to me at the beginning of my PhD. If I know something about this field now, a lot of credit goes to the above persons, and many more in the LCT group. After my PhD, I would like to pursue research in a similar field, possibly expand to quantum chemical calculations or to combustion/ oxidation related topics. Hence, it is possible that our paths would cross. I would like to keep in touch with the above persons in future. Not lastly, but firstly, my family is my backbone, and I could not have done it without the support and encouragement of my father Venkatacharyulu (aged 74 years), mother Nagamani (aged 65 years) and my son Aryan (aged 11 years). I would like to acknowledge Prof K. P. Madhavan from IIT Bombay for always having encouraged me. The innovative thinking that he encouraged during my dual degree project at IIT Bombay Chemical Engineering Department has always been helpful in my life. Prof U. V. Shenoy of IIT Bombay with whom I published my first paper while in the 3rd year of my B.Tech always told me that I belong to the research field. I would like to thank Dr. Chittoor Lakshmanan and Dr. Shekhar Krishnan of GE for having assigned me research based projects, based on my temperament. Yatin Tayalia of GE also inspired me to think deep and innovate. The discussions with Walter Postula, Jan Dierickx, Laxmi Narasimhan and Anand Sundarrajan while at Shell gave me insights into the pyrolysis process in general and further influenced my decision to do something worthwhile in the field of mechanistic modeling of pyrolysis process. Phani Kumar Docca has always been a friend through my ups and downs and I am glad to have his encouragement. And here I am now, submitting my PhD thesis, along with 2 published journal articles and 3 conference articles and a mechanistic model that can predict pyrolysis of light alkanes and some cycloalkanes. A final thanks to all who influenced me and helped me achieve my PhD.

<div align="right">Muralikrishna V. Khandavilli</div>

Table of Content

(#) Khandavilli, M. V.; Vermeire, F. H.; Van de Vijver, R.; Djokic, M.; Carstensen, H. H.; Van Geem, K. M.; Marin, G. B., Group additive modeling of cyclopentane pyrolysis, Journal of Analytical and Applied Pyrolysis 2017, 128, 437-450.

(##) Khandavilli, M. V.; Djokic, M.; Vermeire, F. H.; Carstensen, H. H.; Van Geem, K. M.; Marin, G. B., Experimental and kinetic modeling study of cyclohexane pyrolysis, Energy & Fuels 2018, 32, 7153-7168.

Glossary

Ab initio
Calculations based on first principles for the determination of molecular properties using quantum chemical calculations.

Base mechanism
A kinetic model that has thermodynamic properties for the smallest species and reactions that occur between the smallest species. Often used to complement a kinetic model that is generated automatically.

Group additivity method
A method that allows to calculate properties of molecules or reaction by summing contributions for each group the molecule or reaction exists of. A group is a submolecular pattern existing of a small number of atoms.

Internal standard
A known concentration of a substance that is added to the analyzed sample to allow quantification.

Continuous Flow reactor
A reactor (that can be modeled as an ideal plug flow reactor) typically used for pyrolysis studies.

Level of theory
Property of quantum chemical calculations that describes the treatment of the electron correlations and defines the basis set

Microkinetic model
A kinetic model with a set of elementary reactions that are thought to be relevant for the overall chemical transformation.

Photoionization
The physical process in which an ion is formed from the interaction of a photon and an atom or molecule.

Photoionization cross-section
A quantity for the probability that an electron is emitted from its electronic state.

Single events
A factor introduced in the rate coefficient to account for equivalent ways for the reaction to occur. Also referred to as reaction path degeneracy.

Steam cracking
A petrochemical process in which saturated hydrocarbons are broken down into smaller unsaturated hydrocarbons.

Thermodynamic consistency
A reaction is thermodynamic consistent if the ratio of the forward and reverse rate coefficients equals the equilibrium coefficient of the reaction.

List of symbols and Acronyms

$k_{TST}(T)$ rate coefficient at temperature T, $m^3.mol^{-1}.s^{-1}$ for bimolecular, s^{-1} for unimolecular

$\chi(T)$ quantum mechanical tunneling correction factor

k_B Boltzmann constant, $m^2.kg.s^{-2}.K^{-1}$

h Planck constant, $m^2.kg.s^{-1}$

$\dfrac{RT}{p}$ Molar volume at 1 atm, m^3

Δn Molecularity of the reaction (2 for bimolecular, 1 for unimolecular reactions)

$\Delta G^{\ddagger}$ Gibbs free energy difference between transition state and reactant(s) without the transitional mode, kJ

A Pre-exponential factor $m^3.mol^{-1}.s^{-1}$ for bimolecular, s^{-1} for unimolecular

$\tilde{A}$ Single-event pre-exponential factor $m^3.mol^{-1}.s^{-1}$ for bimolecular, s^{-1} for unimolecular

E_a Activation energy of a reaction, kJ/mol

$\Delta GAV^{\circ}(\log \tilde{A})$ Standard Δ group additive value for single-event pre-exponential factor

$\Delta GAV^{\circ}(E_a)$ Standard Δ group additive value for activation energy, kJ/mol

n_e Number of single events

NNI   Non-nearest neighbor Interaction (for $\log\tilde{A}$ and E_a)

exo   Exocyclic ring intra-molecular carbon centered radical addition

endo   Endocyclic ring intra-molecular carbon centered radical addition

Summary

The big picture

The work presented in this PhD thesis is relevant for the production of renewable chemicals. Renewable chemicals are those derived from renewable sources (biomass sources) such as wood, biogas, etc. Chemicals such as ethylene may be produced from these bio-derived feeds. More specifically, this work focuses on understanding the pyrolysis of cycloalkanes (naphthenes). The cycloalkanes form a significant fraction of bio-derived feeds from which important olefins such as ethylene, propylene, butadiene, etc. are produced via well-established industrial processes such as steam cracking. Olefins like ethylene, propylene, butenes and butadiene are highly reactive and hence major building blocks for polymers, chemical intermediates and synthetic rubber. There has been a tremendous growth in the demand for olefins in the recent years due to the increasing human population and its basic needs. Industrial steam cracking or thermal pyrolysis is the most important process for the production of olefins. The choice of the feedstock for the same depends on availability and cost of raw materials. Conventional and preferred feedstocks include fossil-based fuels: ethane, liquefied petroleum gas and naphtha containing predominantly paraffinic molecules. Most of the unconventional feedstocks also happen to be advantaged, meaning they are available at a premium compared to conventional ones. Examples of unconventional fossil-based feedstocks are: shale oil, raw crude oil and vacuum gas oil. These unconventional inexpensive feedstocks contain mainly naphthenic and aromatic molecules. Recently, there has been a trend in the petrochemical industry to invest in direct cracking of full-range crude oil instead of the conventional distillate cracking. This process is expected to render a few process steps redundant in the refinery and petrochemical complexes, thus bringing down the investment cost of a grass-roots plant. However, crude oils can have a naphthenic content as high as 40%, hence understanding the pyrolysis behavior of naphthenes is important.

Bio-fuels are derived from biomass such as wood (lignin, cellulose, hemi-cellulose), municipal waste, manure, biogas, etc. Modern society faces a number of challenges related to the anticipated scarcity of geologically derived fuel and chemical sources in the next few decades. Lignocellulosic biomass offers a promising alternative to petroleum oil as a feedstock for the production of chemicals, materials and energy. Considering that it is composed of cellulose (a semi-crystalline polysaccharide), hemicellulose (a multicomponent polysaccharide) and lignin (an amorphous phenylpropanoid polymer), its conversion has the potential to provide furan-derived compounds, carbohydrates, aromatics, and many other platform chemicals. Lignin represents the most abundant reservoir of renewable carbon. Its valorisation is a key step for profitable and sustainable bio-refinery operations. So far, lignin has been mostly used as a low-grade fuel in pulp and paper industries. Such low-value applications are often insufficient for bio-based industries to be profitable. Therefore, production of value-added compounds derived from olefins is important, justifying the need

to understand the pyrolysis behavior of naphthenes which form a major fraction of bio-derived fuels.

The small picture

The pyrolysis characteristics of naphthenes are not as well established as linear and branched paraffins. The present thesis aims to study the pyrolysis of naphthenic molecules from first principles. Detailed fundamental kinetic modeling has been done for pyrolysis of cycloalkanes – cyclopentane, cyclohexane, methyl-cyclohexane and ethyl-cyclohexane, in addition to light alkanes – propane, n-butane, iso-butane. The mechanism has been generated automatically using the automatic mechanism generation tool, 'Genesys'. Genesys is an in-house developed automatic kinetic model generation tool, in which the size of the kinetic model is controlled by a rule-based termination criterion. In Genesys, starting from the user-defined reaction families and the initial feed molecules, an exhaustive mechanism is generated which is terminated by the user-defined constraints on product species, e.g. constraints on the maximum carbon number allowed, and constraints on the reaction families, e.g. limiting the size of the abstracting and adding species. The reaction families are defined by the user in Genesys by supplying a reaction recipe, the possible reactive center by the user-friendly SMARTS language and constraints on the appearance of the reaction family or the products formed by this reaction family. Owing to the ever increasing power of computers and speed of ab-initio calculations, new types of elementary reactions are being discovered and will be discovered in future. However, for the choice of elementary reaction families in Genesys, current knowledge and experience is applied. The completeness of the mechanism generated by Genesys depends on the selected reaction families. The reaction families list applied in Genesys is a subjective choice of the user based on prior experience. Genesys can now also be used using on the fly calculations. The kinetics of the elementary reaction model have been derived ab-initio or from an ab-initio based group additive methodology. The model has been validated using in-house experimental data from a continuous flow tubular reactor with GC×GC analysis. The operating conditions typically were 1.7 bara, 0.5 second residence time, temperature 900-1100K. The analysis section enabled on-line identification and quantification of the entire product stream. Two different gas chromatographs were used for a detailed analysis of the reactor effluent: a refinery gas analyzer (RGA) and a GC×GC-FID/TOF-MS setup. The model has also been validated by experimental data from a different laboratory using a continuous flow reactor and a SVUV-PIMS analysis section. The corresponding operating conditions of 0.8 mbara, 50 micro-s residence time, temperature 1100-1400K, were very different from the in-house experiment, so these two data sets provide a wide range of operating conditions for model validation. Some feeds like cyclohexane, n-butane and iso-butane have been experimentally studied in both of the setups, and the model is able to capture both of the data sets. For each feed molecule, reaction path analysis has been done to investigate the dominant reactions toward major products. An example product spectrum of cyclopentane includes: hydrogen, methane, ethylene, propylene, 1,3-butadiene, cyclopentene, 1,3-cyclopentadiene, ethane, propane, benzene, indene and naphthalene. A comparison is made of the in-house model result with that of popular optimized models from literature for

all the experimental data considered. Based on this, the Genesys model has been shown to perform as good or better than the other optimized models from the literature . The feeds tested in the in-house experimental setup were: propane, n-butane, iso-butane, cyclopentane and cyclohexane. The feeds tested in SVUV-PIMS were n-butane, iso-butane, cyclohexane, methyl-cyclohexane and ethyl-cyclohexane Overall, the present thesis aims to further the understanding of cycloalkane pyrolysis chemistry and shows that an elementary reaction mechanism of high pressure limit reactions, generated automatically, having ab-initio i.e. unaltered kinetics can compete with popular global lumped adjusted literature models. The model is validated by experimental data from different laboratory sources spanning a wide range of operating conditions. The research on cycloalkane pyrolysis finally helps understanding the pyrolysis of biomass-derived fuels, unconventional fossil fuels, full range crude oils, for all of which cycloalkanes form a significant fraction.

Samenvatting

Het groter geheel

Het werk uit dit doctoraatsthesis is relevant voor de productie van hernieuwbare chemicaliën. Deze laatsten worden afgeleid van hernieuwbare grondstoffen (uit biomassa) zoals hout, biogas, enz. Chemicaliën zoals ethyleen kunnen geproduceerd worden uit deze van biomassa afgeleide voedingen. Meer specifiek focust dit werk zich op begrijpen van de pyrolyse van cycloalkanen (naphtenen). Cycloalkanen vormen een significante fractie van uit biomassa afgeleide voedingen waaruit belangrijke olefinen zoals ethyleen, propyleen, butadieen, enz. worden geproduceerd via erkende industriële processen zoals stoomkraken. Olefinen zoals ethyleen, propyleen, butenen en butadieen zijn uiterst reactief en zijn daarom belangrijke bouwstenen voor polymeren, chemische intermediairen en synthetisch rubber. In de laatste jaren is er een enorme groei in de vraag naar olefinen door de stijgende menselijke populatie en diens levensbehoeften. Industrieel stoomkraken of thermische pyrolyse is het belangrijkst proces voor de productie van olefinen. De keuze van de voeding voor dit proces hangt af van de beschikbaarheid en kost van grondstoffen. Conventionele en voorkeursvoedingen zijn gebaseerd op fossiele grondstoffen: ethaan, LPG en nafta bestaande uit vooral parafine moleculen. De meeste onconventionele grondstoffen zijn beschikbaar aan goedkopere prijzen vergeleken met conventionele grondstoffen. Voorbeelden van onconventionele fossiele grondstoffen zijn schalie olie, ruwe aardolie en vacuümgasolie. Deze onconventionele en goedkope grondstoffen bevatten voornamelijk naftenen en aromatische componenten. Er is de laatste jaren een trend in de petrochemische industrie om te investeren in het onmiddellijk kraken van ruwe aardolie in de plaats van conventionele gedestilleerde fracties. Dit maakt een aantal processen overbodig in raffinaderijen en petrochemische bedrijven, en zorgt voor een daling van de investeringskost van de fundamentele fabrieken. Echter, ruwe aardolie bevat tot 40% naftenen, en een inzicht in het pyrolysegedrag van naftenen is dus belangrijk.

Biobrandstoffen zijn afgeleid uit biomassa zoals hout (lignine, cellulose, hemicellulose), gemeentelijk afval, mest, biogas, enz. De moderne maatschappij staat voor een aantal uitdagingen gerelateerd aan de verwachte schaarste aan geologisch afgeleide brandstoffen en chemische grondstoffen in de komende decennia. Lignocellulose biedt een veelbelovend alternatief voor aardolie als grondstof voor de productie van chemicaliën, materialen en energie. Omdat lignocellulose bestaat uit cellulose (een semi-kristallijn polysacharide), hemicellulose (een polysacharide bestaande uit verschillende componenten) en lignine (een amorfe fenylpropanoïde polymeer), heeft diens conversie het potentieel om furanen, koolhydraten, aromaten en andere platformchemicaliën te vormen. Lignine vormt het grootste aandeel aan hernieuwbaar koolstof. De valorisatie van lignine is onontbeerlijk voor een winstgevende en duurzame bioraffinaderij. Tot op heden is lignine vooral gebruikt als lage-kwaliteitsbrandstof in de pulp- en papierindustrie. Dergelijke toepassingen met beperkte waarde zijn onvoldoende voor een rendabele bio-gebaseerde industrie. Daarom is de

productie van componenten met toegevoegde waarde gevormd uit olefinen belangrijk, wat de nood aan het volledig begrijpen van de pyrolyse van naftenen verantwoord. De laatsten vormen een grote fractie in bio-gebaseerde brandstoffen.

Het kleiner geheel

De pyrolyseeigenschappen van naftenen is tot op heden niet goed gekend vergeleken met lineaire en vertakte paraffines. Deze thesis heeft als doel de pyrolyse van naftenen vanuit de grondbeginselen te bestuderen. Gedetailleerd fundamenteel kinetisch modelleren werd gedaan voor de pyrolyse van cycloalkanen – cyclopentaan, cyclohexaan, methylcyclohexaan en ethylcyclohexaan, bovenop lichte alkanen – propaan, n-butaan en iso-butaan. Het mechanisme is automatisch gegenereerd gebruik makende van het automatische mechanisme genereringsprogramma 'Genesys'. Genesys is een programma voor automatische kinetisch modelgenerering ontwikkeld aan de Universiteit Gent, waarin de grootte van het kinetisch model wordt gecontroleerd door het regel-gebaseerd terminatiecriterium. In Genesys, startende van reactiefamilies en initiële voedingsmoleculen gedefinieerd door de gebruiker, wordt er nauwgezet een mechanisme gegenereerd, en wordt de generering stopgezet door voorwaarden – tevens gedefinieerd door de gebruiker – op te leggen op product species, b.v. voorwaarden op het maximum aantal koolstofatomen, en op de reactiefamilies, b.v. door de grootte van abstraherende en adderende species te limiteren. The reactiefamilies zijn gedefinieerd door de gebruiker in Genesys door het opstellen van een reactierecept, de mogelijke reactiecentra via de gebruiksvriendelijke SMARTS notatie en voorwaarden op de toepasbaarheid van de reactiefamilie op de product species gevormd door deze familie. Dankzij de steeds toenemende kracht van computers en de snelheid van kwantumchemische berekeningen, worden nieuwe types aan elementaire reacties ontdekt, en zullen er meer worden ontdekt in de toekomst. Desalniettemin is de huidige kennis en ervaring toegepast voor de keuze van de elementaire reactiefamilies in Genesys. The volledigheid van het mechanisme gegenereerd door Genesys hangt af van de geselecteerde reactiefamilies. De lijst aan reactiefamilies toegepast in Genesys is een subjectieve keuze van de gebruiker en is gebaseerd op voorkennis en ervaring. Genesys kan ook worden gebruikt voor rechtstreekse kwantumchemische berekeningen. De kinetiek van de elementaire reacties in het model werden afgeleid van kwantumchemische berekeningen of van een groepadditiveitsmethode gebaseerd op kwantumchemische berekeningen. Het model is gevalideerd gebruik makende van experimentele data van een continue buisreactor met GC×GC analyse. De reactorcondities zijn een druk van 1.7 bara, een verblijftijd van 0.5 seconden en een temperatuur tussen 900 en 1100K. The analysesectie laat online identificatie en kwantificatie van de volledige productstroom toe. Twee verschillende gaschromatografen werden gebruikt voor een gedetailleerde analyse van de effluent van de reactor: een *refinery gas analyzer (RGA)* en een GC×GC-FID/TOF-MS opstelling. Het model werd ook gevalideerd gebruik makende van experimentele data uit een ander laboratorium opgemeten met een continue buisreactor en een SVUV-PIMS analysesectie. De overeenkomstige experimentele condities van een druk van 0.8 mbara, een verblijftijd van 50 micro-s en een temperatuur van 1100-1400K, waren verschillend van de eigen experimenten. Deze twee datasets laten toe het model

te valideren bij uiteenlopende condities. Bepaalde voedingen zoals cyclohexaan, n-butaan en iso-butaan werden experimenteel onderzocht op beide opstellingen, en het model is in staat om beide datasets te reproduceren. For elke voedingsmolecule werd een reactiepadanlyze uitgevoerd om de dominante reactie naar de voornaamste producten te onderzoeken. Een voorbeeld van het product spectrum van cyclopentaan is: waterstof, methaan, ethyleen, propyleen, 1,3-butadieen, cyclopenteen, 1,3-cyclopentadieen, ethaan, propaan, benzeen, indeen en naftaleen. Een vergelijking is gemaakt tussen de eigen modelresultaten met modelresultaten van populaire geoptimaliseerde modellen uit de literatuur voor alle beschouwde experimentele data. Hieruit bleek dat het model van Genesys even goed of beter presteert vergeleken met de literatuurmodellen. De voedingen onderzocht in SVUV-PIMS waren n-butaan, iso-butaan, cyclohexaan, methyl-cyclohexaan en ethyl-cyclohexaan. In het algemeen verbreed deze thesis het inzicht in de pyrolyse van cycloalkanen en toont het aan dat een automatisch gegenereerd model bestaande uit elementaire reacties met hogedruklimiet snelheidscoëfficiënten, bepaald uit kwantumchemische berekeningen en zonder die aan te passen aan experimentele data, kan concurreren met populaire globale gelumpte en aangepaste literatuurmodellen. Het model is gevalideerd voor experimentele data van verschillende laboratoriumbronnen met een breed bereik aan reactorcondities. Het onderzoek van de pyrolyse van cycloalkanen helpt ten slotte het inzicht van de pyrolyse van uit biomassa afgeleide brandstoffen, onconventionele fossiele brandstoffen en aardolie, die elk een hoge fractie aan cycloalkanen bevatten, te vergroten.

1

Introduction

Olefins like ethylene, propylene, butenes and butadiene are highly reactive and hence major building blocks for polymers, chemical intermediates and synthetic rubber. There has been a tremendous growth in the demand for olefins in the recent years due to the increasing human population and its basic needs. Industrial steam cracking or thermal pyrolysis is the most important process for the production of olefins. The choice of the feedstock for the same depends on availability and cost of raw materials. Conventional and preferred feedstocks include ethane, liquefied petroleum gas and naphtha having predominantly paraffinic molecules. Most of the unconventional undesirable feedstocks also happen to be advantaged, meaning they are available at a premium compared to conventional ones. Examples of unconventional feedstocks are shale oil, raw crude oil, vacuum gas oil, etc. These unconventional inexpensive feedstocks contain mainly naphthenic and aromatic molecules. The pyrolysis characteristics of such molecules are not as well established as linear and branched paraffins. The present thesis aims to study the pyrolysis of naphthenic molecules from fundamental principles. Detailed fundamental kinetic modeling has been done for pyrolysis of cycloalkanes – cyclopentane, cyclohexane, methyl-cyclohexane and ethyl-cyclohexane. The kinetics of the elementary reaction model has been derived ab-initio or from an ab-initio based group additive methodology. The mechanism has been generated automatically using the automatic mechanism generation tool, 'Genesys'. The model has been validated using in-house experimental data as well as that from a different laboratory. Effect of feed impurities on model trends have been shown. Overall, the present thesis aims to further the understanding of cycloalkane pyrolysis chemistry and shows that an elementary reaction mechanism generated automatically with ab-initio unaltered kinetics can compete with popular global lumped adjusted literature models.

1.1. Bird's eye-view of the thesis

This thesis studies the pyrolysis of seven molecules – propane, n-butane, iso-butane, cyclopentane, cyclohexane, methyl-cyclohexane and ethyl-cyclohexane. A snapshot of what has been accomplished in the thesis is shown in Figure 1.
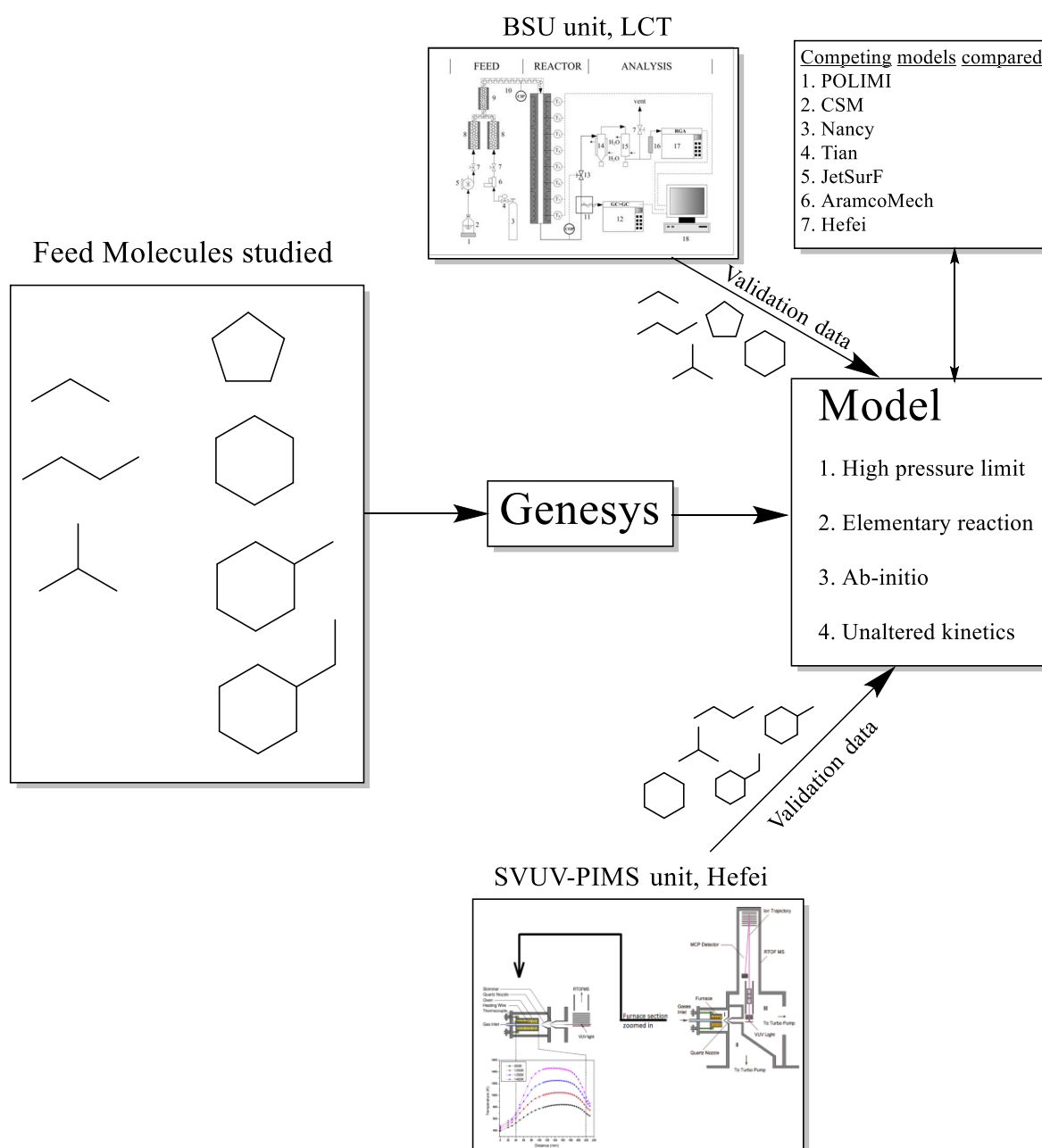
Figure 1.1: A snapshot of the contents of the thesis

An automatic mechanism generation tool "Genesys"[1, 2] has been used to generate a high pressure limit, elementary reaction, ab-initio/ group additive, unaltered model. The sub-mechanism that represents the pyrolysis of propane, n-butane and iso-butane forms the core of the model and the reactions for these small molecules are relevant also for the pyrolysis of the larger cyclic molecules – cyclopentane, cyclohexane, methyl-cyclohexane and ethyl-cyclohexane. The model has been validated by experimental data from two different laboratories – (1) In-house experiments on bench scale unit (BSU) at LCT and (2) Synchrotron Vacuum Ultra-Violet Photo Ionization Mass Spectrometer (SVUV-PIMS) unit at Hefei, China. The BSU generated pyrolysis data for the feeds propane, n-butane, iso-butane, cyclopentane and cyclohexane have been obtained at 0.17 MPa, 700-950ºC, around 0.4 s residence time. The SVUV-PIMS unit generated pyrolysis data for n-butane, iso-butane, cyclohexane, methyl-cyclohexane and ethyl-cyclohexane at different pressures ranging from 0.004 MPa to 0.1 MPa, 900-1300ºC, 50 micro.s residence time. Hence, we have experimental data sourced from different laboratories at broad ranges of pressures, temperatures and residence times. Also, there is an overlap of feed molecules tested between the two laboratories – n-butane, iso-butane and cyclohexane. Hence, these experimental data of overlapping feed molecules between the two data sets provide a good opportunity to check if the Genesys model can predict a product spectrum at different operating conditions (including at low pressures and high temperatures) across different laboratories. Another aspect covered in the thesis is – comparison to existing popular literature models – POLIMI[3], CSM[4], Nancy[5], Tian[6], JetSurF[7], AramcoMech[8] and Hefei[9-11]. These models have different underlying philosophies, and have lumping present to various extents. Some have adjusted parameters, while some have pressure dependence built in them. So, their comparison with the high pressure limit, elementary, ab-initio, unaltered Genesys model would be interesting. These aspects have been covered in this thesis. Even though pyrolysis of seven molecules have been studied, the most interesting are four of them – the cycloalkanes – cyclopentane, cyclohexane, methyl-cyclohexane and ethyl-cyclohexane.

1.2. Why study cycloalkane pyrolysis?

Let us start this section with a latest news item[12]. In April 2019, it was reported that *"Aramco and SABIC have already announced a joint crude-oil-to-chemicals project of*

400,000 barrels per day capacity, which is expected to become operational in the mid-2020s. A flagship technology initiative-crude oil to chemicals (C2C) programme, developed by Aramco is expected to play a crucial role in future production and maximise the profit. This technology, according to Aramco researchers, will remove or streamline several conventional industrial processes, resulting in chemicals that are less expensive to produce while at the same time reducing the carbon footprint associated with the use of oil."

The above news clipping means that ethylene and other chemicals will henceforth be produced not just by naphtha or conventional fuel cracking, but also directly by crude oil cracking. This process is expected to render a few process steps redundant in the refinery and petrochemical complexes, thus bringing down the investment cost of a grassroots plant. What does the crude oil consist of? Table 1.1 shows the composition - PNA (Paraffins, Naphthenes, Aromatics) of a few sample crude oils compiled from the crude assays given on the website of ExxonMobil[13].

Table 1.1: Crude oil PNA composition of some sample crudes[13]

Crude	Azeri light	Alaska North slope	Balder blend	Basrah	Basrah heavy	Brent blend	Marib light	Ormen Lange	Yoho
Paraffins vol%	35	30	21	38	33	39	47	59	38
Naphthenes vol%	40	31	40	20	17	33	30	34	39
Aromatics vol%	25	39	39	41	50	28	23	7	23

Table 1.1 shows that crude oil can have a very high content of naphthenes (cycloalkanes). Azeri light, Balder Blend and Yoho crudes have close to 40 vol% naphthenes. Almost all the crudes in the above example have a naphthenic content of 30% or more. Generally crude oils originating from mid-continent United States have very high naphthenic (cycloalkane) content. Typically this cut consists of substituted and unsubstituted cyclopentane and cyclohexane. The new C2C technology will benefit greatly if the pyrolysis characteristics of cyclopentane and cyclohexane are well understood. Among cycloalkanes, this thesis studies pyrolysis of cyclopentane, cyclohexane, methyl-cyclohexane and ethyl-cyclohexane.

Pyrolysis study of cycloalkanes would also be relevant to the pyrolysis and combustion of bio-fuels, which are fuels derived from biomass such as wood (lignin, cellulose, hemi-cellulose), municipal waste, manure, biogas, etc. Modern society faces a number of challenges related to the anticipated scarcity of geologically derived fuel and chemical

sources. Lignocellulosic biomass offers a promising alternative to petroleum oil as a feedstock for the production of chemicals, materials and energy. Considering that it is composed of cellulose (a semi-crystalline polysaccharide), hemicellulose (a multicomponent polysaccharide) and lignin (an amorphous phenylpropanoid polymer), its conversion has the potential to provide furan-derived compounds, carbohydrates, aromatics, and many other platform chemicals. Lignin represents the most abundant reservoir of renewable carbon. Its valorisation is a key step for profitable and sustainable bio-refinery operations. So far, lignin has been mostly used as a low-grade fuel in pulp and paper industries. Such low-value applications are often insufficient for bio-based industries to be profitable. Therefore, production of value-added compounds is crucial. However, the cost of purification of platform molecules often significantly impacts the overall process economy. Improvements in the bio-refining processes are needed in order to competitively produce high-value products such as polymer additives, bitumen, carbon fibers, phenolic resins and adhesives.

Catalytic hydrodeoxygenation (HDO) is an effective route for lignin valorisation; by using hydrogen at elevated pressure (2–30MPa) and relatively moderate temperatures (200–450°C), chemically bonded oxygen can be removed. It can occur via two pathways: either with ring hydrogenation followed by subsequent deoxygenation or with direct deoxygenation. After hydrodeoxygenation, we are left with a predominantly cycloalkane bio-fuel, which can be used in various areas such as jet fuel. Figure 1.2 shows the HDO process for lignin model compound eugenol[14]. The circled products represent cyclopentane and cyclohexane moieties which are blended with jet fuel or directly used as bio-jet fuel, among other applications.
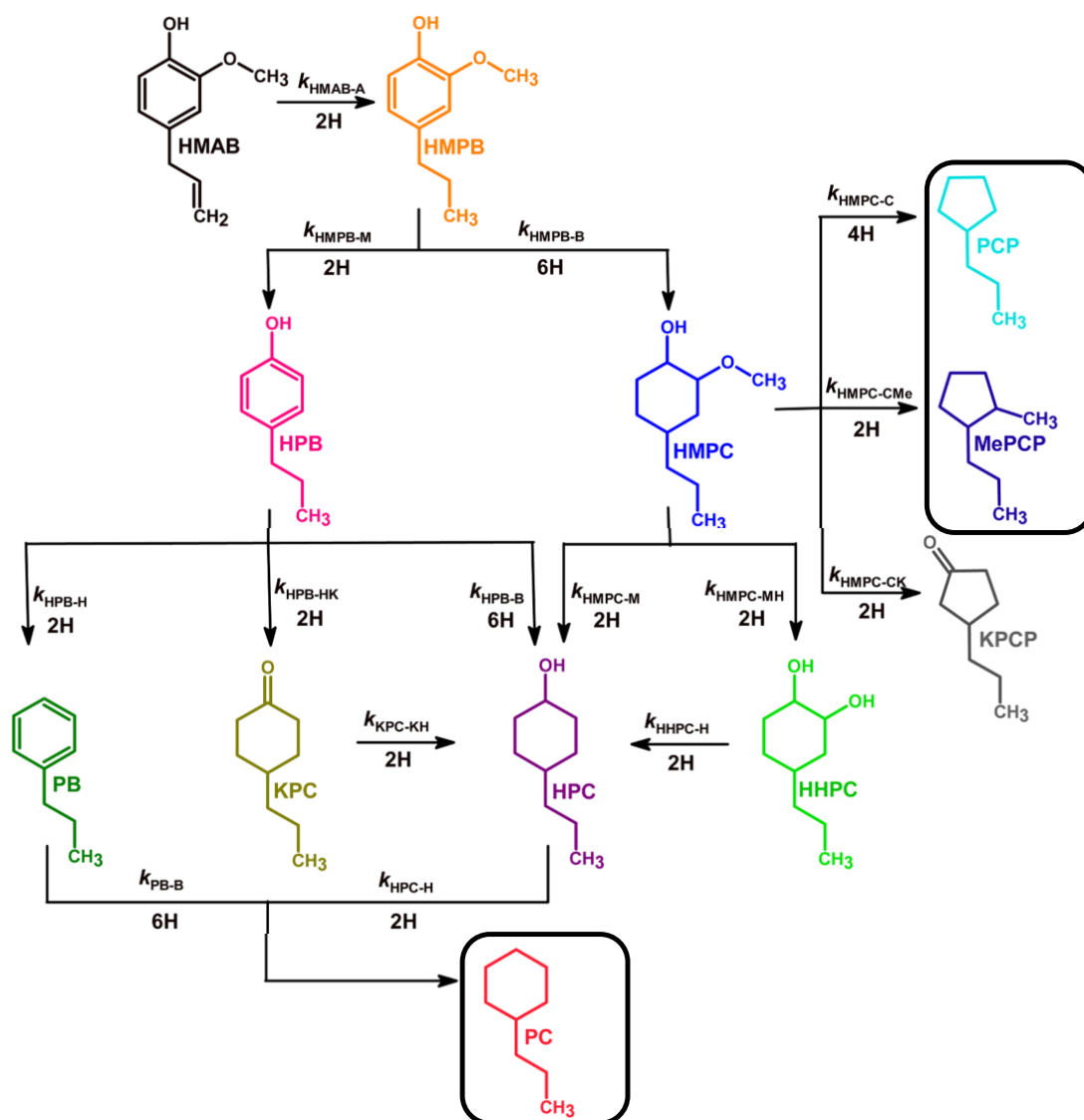
Figure 1.2: Hydrodeoxygenation of lignin model compound eugenol[14] to produce cycloalkane rich product (circled)

Other workers[15] have also done research on this topic and found the treated lignin effluent to contain naphthene-rich liquid. Figure 1.3 shows the GC-MS spectrum of the effluent of lignin treatment by HDO. It can be seen that the presence of cycloalkane moiety is very dominant, justifying our interest in studying the pyrolysis behavior of this class of molecules.
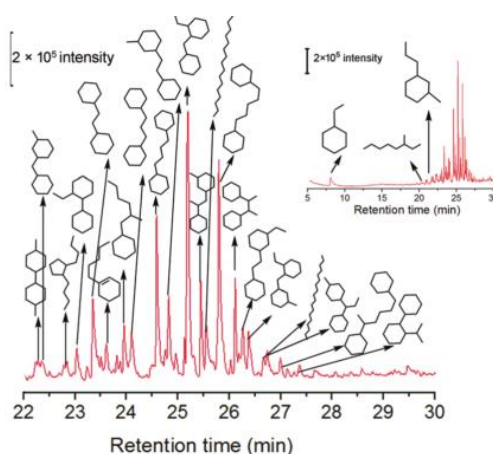
Figure 1.3: GC-MS of effluent of lignin conversion to biofuels via hydrodeoxygenation[15]

This section shows the relevance of studying cycloalkane pyrolysis chemistry, specifically for cyclopentane and cyclohexane. Once the bio-fuel is generated from biomass, typically, we may use it directly as jet fuel in jet engines or use it as a substitute for petrochemical feedstocks to produce olefins. A typical steam cracker produces important olefins from hydrocarbon feedstocks. The details of this well-established industrial process are briefly touched upon below.

1.3. Industrial pyrolysis

Petrochemical feedstocks and biomass derived liquid fuels are complex mixtures composed of various molecule classes such as paraffins, isoparaffins, olefins, naphthenes and aromatics. They are used for pyrolytic or combustion applications. Among pyrolysis modeling, the thermal decomposition chemistry plays a central role in the prediction of product yields from industrial steam cracking[16, 17], biomass fast pyrolysis[18], waste fractions[19], scram jet modelling[20-23], naphtha steam cracking[24] and undesired auto ignition of gasoline[5, 25, 26]. Therefore the pyrolysis chemistry of hydrocarbons has been the subject of research for many years. While the gas-phase chemistry of open-chain hydrocarbons is well understood, the knowledge of the pyrolysis chemistry of cyclic hydrocarbons is less understood[5, 27]. This is even true for the simplest cycloalkanes, such as cyclopentane and cyclohexane which can make up a significant part of steam cracking feedstocks like naphtha. Steam cracking is the most important route for production of olefins. Olefins like ethylene, propylene, butenes and butadiene are highly reactive and hence major building

blocks for polymers, chemical intermediates and synthetic rubber. There has been a tremendous growth in the demand for olefins in the recent years due to the increasing human population and its basic needs. The choice of the feedstock for industrial steam cracking depends on availability and cost of raw materials. Conventional and preferred feedstocks include ethane, liquefied petroleum gas, naphtha having predominantly paraffinic molecules. Most of the unconventional undesirable feedstocks are also advantaged, meaning they are available at a premium compared to conventional ones. Examples of unconventional feedstocks are shale oil, raw crude oil, vacuum gas oil, etc. These unconventional cheap feedstocks contain mainly naphthenic and aromatic molecules. The pyrolysis characteristics of such molecules are not as well established as linear and branched paraffins. The study of cycloalkane pyrolysis is the main subject of this thesis. However, in this section, the process steps of industrial steam cracking will be elaborated upon. Figure 1.4 shows the schematic diagram of industrial steam cracking. It consists of 3 parts – Hot section, quench section and cold section. The hot section consists of convection and radiation zone. In the convection zone, hydrocarbon feedstock is preheated and mixed with steam and heated to high temperature. In the radiation zone, the actual pyrolysis (cracking) reaction takes place where thermal degradation of feedstock takes place. In the radiation section, feedstock that is vaporized in convection section passes through metal coils stationed in a direct fired furnace that can have floor burners or wall burners or both. Pyrolysis is an endothermic reaction. The furnace temperatures can reach up to 2000K. At these temperatures, the heat transfer to the process gas happens mainly by radiation and not by convection mode. Hence, this section is called the radiation section.
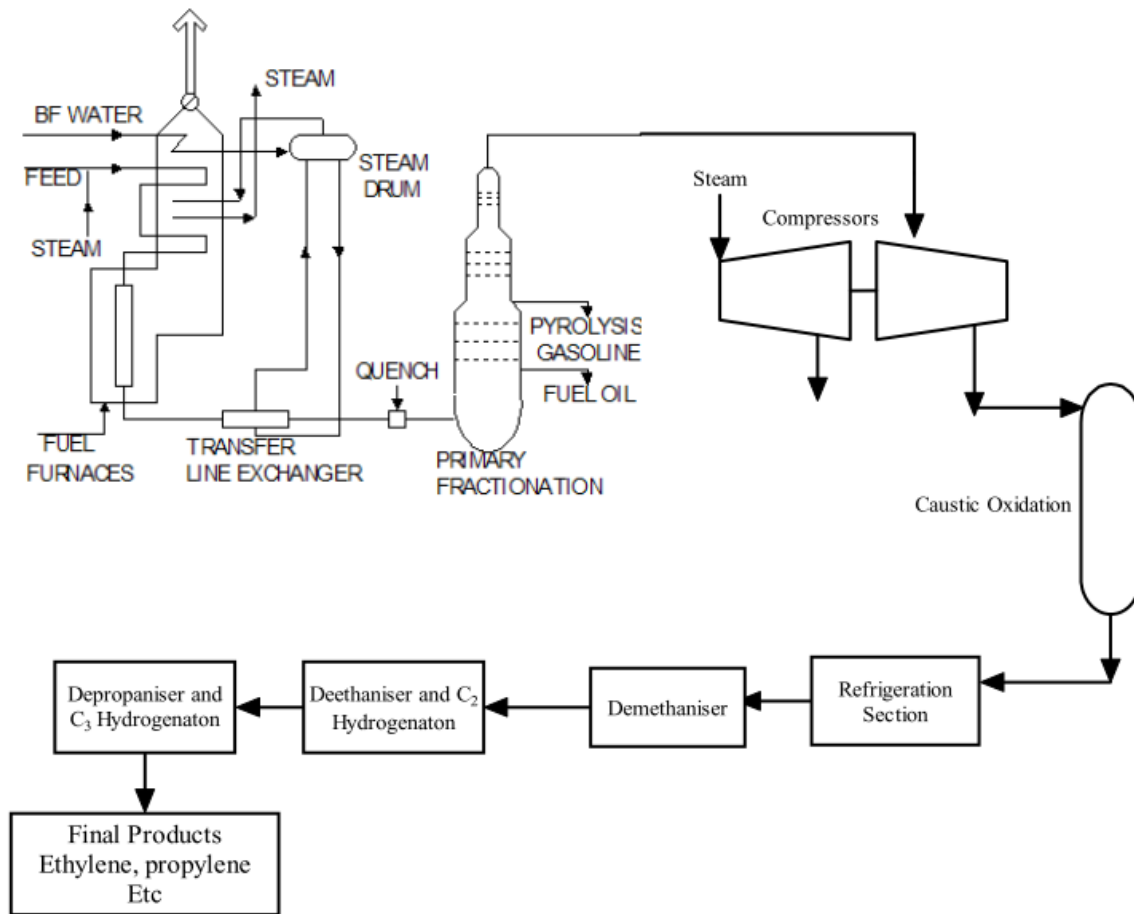
Figure 1.4: Schematic diagram of a typical industrial steam cracker

Steam is added as a diluent to decrease the partial pressure of the hydrocarbon feedstock. This is done so as to ease its evaporation and drive the pyrolysis reaction toward increasing number of moles in product, which is typical of pyrolysis. Another reason why steam is added is to decrease coke deposition on the inner metal skin of the radiant coils. The steam dilution employed for ethane cracking is usually 0.2-0.4 kg steam/kg ethane. For propane cracking, it is 0.3-0.5 kg/kg. For naphtha cracking, it is 0.4-0.8 kg/kg. For gas oil, it is 0.8-1.0 kg steam/kg gasoil. This shows that with increasing feed molecular weight, more steam is needed for the same weight of feed. This is because heavier feeds have more coking tendency owing to the presence of cyclic compounds, so it is more important to decrease the partial pressure of heavy feeds in the radiant section. The residence time of the feed in the radiant section is around 0.4 second. Recent technological advances have tended toward decreasing residence time while increasing the temperature in the furnace. This also encouraged research on radiant coil alloy material which could allow a high enough tube

skin temperature. The overall pressure in the radiant coil is about 2-4 atm. After a few days run in an actual plant, enough coke accumulates on the inner skin of the radiant coil and the transfer line exchanger (discussed later), indicated by pressure drop across the tubes and the furnace is shut down for decoking. The "at-a-stretch" operational run length for gas based furnaces are usually 20-60 days, while for liquid based furnaces are 20-40 days.

Quench section has the transfer line exchanger. After the feed exits the radiant coil, in order to avoid subsequent reaction in the effluent, it is quenched first by indirect quench in a heat exchanger by water, to 400-450ºC in a transfer line exchanger, also called quench boiler. The hot water from this section is used for steam production in the plant. Next, heavy product from the pyrolysis directly quenches the transfer line effluent. After compression, caustic scrubbing and drying, the light effluents enter the cold section of the unit, which performs the separation of hydrogen, ethylene, propylene, C_4 cut and pyrolysis gasoline rich in aromatics. In the de-methanizer, methane is condensed at the top at around -100ºC. De-ethanizer separates ethane from ethylene, and unreacted ethane is recycled back to the cracker. Sometimes, acetylene is selectively hydrogenated using Palladium or Nickel catalyst at 40-80ºC. The focus of this thesis is to investigate what reactions happen in the radiant coil, more specifically, what happens to the cycloalkane cut of the feed. In order to investigate this, a 2-pronged approach is needed (1) Laboratory experiments with pure cycloalkane feeds and (2) Pyrolysis modeling. There have been numerous attempts at both over the past century to do this, which is discussed in section 1.4.

1.4. A century of cycloalkane pyrolysis study

The simplest and the most occurring cycloalkane compound in feeds like naphtha is cyclohexane. Though literature on pyrolysis of cycloalkanes is relatively scarce, among them cyclohexane has been more studied experimentally and mechanism-wise over the past 100 years, when there were no advanced techniques like the gas chromatography. The first worker to ever pyrolyze cyclohexane non-catalytically in a laboratory was Jones in the year 1915[28]. It was a case of heating the cyclohexane liquid in a porcelain enclosure at 773K and analyzing the gas evolved using titration methods known at that time. He compared the results with those of methyl cyclohexane pyrolysis. The major products formed were hydrogen, methane, ethane, ethylene, acetylene, benzene and higher olefins. The first

known continuous flow tubular reactor experimental pyrolysis of cyclohexane was done by Frolich, Simard and White[29] in the year 1930, at 927 K, however they focused on the detection of butadiene, benzene, naphthalene and tar, and did not report the formation of lighter products. The review article by Egloff et al[30] describes these 2 experiments and those on other cycloparaffins and cyclo-olefins with and without catalyst. One of the earliest detailed studies on cyclohexane pyrolysis was done in 1933 by Pease and Morton[31]. In this, pyrolysis was conducted in a batch as well as a pyrex continuous flow tubular reactor at 1 atmosphere and 873-973K with 4 categories of feeds – open chain alkane, olefin, cycloalkane (included cyclohexane) and aromatics and product yields were compared. A limited set of products was analyzed, and it was done by laboratory titration methods. Light olefins yield was measured by dissolving product gas emanating from the cold trap into concentrated sulphuric acid and bromine water. Hydrogen, methane and ethane yields were measured by passing the uncondensed product over heated copper oxide. Butadiene content was measured by brominating the product and forming butadiene tetrabromide and weighing the same. The rate of decomposition of cyclohexane was measured by recording the pressure increase over time in the batch reactor. Based on this, for the first time, an induction period especially for cyclohexane was discovered during which initial period, the pressure is stable. The presence of this induction period was to be confirmed by other workers many decades later. This work, though very old and limited in terms of analytical technique, was one of the first detailed studies where comparison of different classes of feeds was made. The main conclusions were that cyclohexane decomposition is typical first order, and that it is less stable than aromatic feeds when rates of conversions are compared. It also opined that cyclohexane decomposition mechanism can be compared to that of a C6-olefin, the earliest study to predict that. Also, global rate parameters were reported.

The next major study on cyclohexane pyrolysis was reported a few decades later, by Levush[32] in 1969. The experiment was done in a porcelain tubular flow reactor at atmospheric pressure for reactor temperatures between 1173-1373K, which is higher compared to steam cracking conditions, but relevant for combustion conditions. Analysis of major products ethylene, propylene, butadiene and acetylene was done by chromatographic columns filled with different types of packings. Cyclohexane conversion was determined by first order decay and a short global mechanism was proposed without the usage of

radicals to explain the formation of major products. In 1978, Tsang[33, 34] measured the initial decomposition kinetics of cyclopentane, cyclohexane and 1-hexene in a single pulse shock tube reactor at 1000K to 1200K using the decyclization process of cyclohexene for rate comparison. Tsang concluded that 1-hexene is the initial decomposition product of cyclohexane and global rate coefficients were derived based on experimental data. The next major stride in the understanding of cyclohexane pyrolysis was taken by Aribike, Susu and Ogunye[35-37] in their papers of 1979, 1981 and 1988. In these, a SS304 tubular reactor and annular reactor each was operated in a continuous flow mode. At temperatures of 1003K to 1133K and residence times in the range of 0.16 to 0.48 s at atmospheric pressure with nitrogen dilution, the conditions were so far the closest to those of industrial steam cracking. Also, for the first time, analysis of products were done using gas chromatography. There were however a few points lacking from the perspective of a complete understanding of the mechanism. The reactor material of SS304 acted as an active catalyst site, as the workers noticed considerable difference between the product yield results from an annular reactor and the tubular reactor owing to different surface area to volume ratios of the two reactors. Also, the entire temperature profile was not reported and the calculation of residence time was based on assumptions of temperature profile. Though the GC results yielded the numbers for hydrogen, methane, ethane, ethylene, propylene, propane, acetylene, butadiene and butenes, higher molecular weight compounds like cyclopentadiene, benzene and polyyclic aromatic hydrocarbons were not reported either because they were not observed or because of the lack of GC technique. It is to be noted that benzene and naphthalene had been observed in cyclohexane pyrolysis 50 years earlier, in 1930 at much milder conditions[29], so that detail was missing here. Moreover, the conversions achieved were in the range of 23% to 70%. Based on the experimental data, a non-elementary molecular mechanism was put together and rate parameters were estimated. In the 1988 study[35], the same workers injected a liquid pulse of cyclohexane into the nitrogen stream entering the pyrolysis reactor and measured effluent composition. This is also something like a pulse injection into a pyrolysis GC that Zamostny did in 2010[38] where he evaluated the relative pyrolytic behavior of various families of chemicals including cycloalkanes. However, the challenge with such experiments is that the reactor model itself is not simple and a lot of assumptions go into how the pulse vaporizes and achieves the tube temperature and if the pulse length is uniform, etc. Under such clouded conditions, it is

difficult to correlate product composition to a set of input conditions like temperature profile, flow rates, residence time and pressure, as it is strictly not a continuous flow reactor like in the studies of 1930, 1969 and 1981.

Lai and Song[39] in 1996 did the pyrolysis experiment on cyclohexane at super-critical conditions. The temperature was low, at 723K, and the batch reactor temperature was maintained for a period of 480 minutes during which time the pressure was continuously increasing and reached 2 MPa. Comprehensive product analyses were done, including aromatics, but this experiment catered to very different conditions than what we are interested in. One strong conclusion from their study was that when there is a long chain substituent on a cycloalkane, the immediate pyrolytic step would be to break the chain rather than open the core ring. Many substituted cyclohexanes were tested in this study. In 2009, Kiefer[40] et al pyrolyzed diluted cyclohexane gas mixtures in a shock tube and using laser-schlieren technique, derived the rate coefficient of cyclohexane isomerization to 1-hexene and 1-hexene homolytic scission to allyl and propyl radicals at 1300K to 2000K. The pressures employed were 25-200 Torr and cyclohexane content was 2-20% in Krypton gas. RRKM extrapolation using the Gorin model was used to estimate the high pressure limit rate coefficients of these 2 reactions and they matched those of Tsang's findings[34] of 1978, and also those of Sirjean's ab-initio derived rate coefficients in year 2006[41]. Peukert[42, 43] in the years 2011 and 2012 studied the cyclohexane pyrolysis in shock tubes. However, the focus of the study was on hydrogen atom generation and hydrogen atom reaction with cyclohexane. Hence, it was not a complete pyrolysis experiment.

In 2012, Wang[9] et al reported a very low pressure pyrolysis study of cyclohexane. The experiment was done at less than 1 mbar cyclohexane and temperatures were more in the range of combustion rather than steam cracking. Extensive product spectrum was analyzed by SVUV-PIMS equipment in Hefei. The kinetic model proposed by them had adjustments made to suit the experimental data. Their model was a mixture of ab-initio data, estimates and altered parameters and some global reactions too. There are other references in literature which deal with the subject of cyclohexane pyrolysis, but none of them report detailed experimental data nor a purely elementary reaction high pressure limit kinetic model. Same is the case with cyclopentane pyrolysis. There are however popular models in literature which have cyclohexane decomposition as one of their sub-mechanisms, which can be tested against any new experimental data. These are JetSurF[7]

and POLIMI[3]. In 2015, Wang[4] proposed a comprehensive ab-initio based kinetic model for propylene pyrolysis with extensive potential energy surface scans of species including cyclohexane. Though originally intended for predicting propylene pyrolysis, it has the capability to attempt prediction of cyclopentane and cyclohexane pyrolysis too. However, the Wang model uses single-step lumped reactions to form aromatics like benzene, toluene, styrene, indene and naphthalene from 1,3-cyclopentadiene, so it is not a completely elementary reaction model. It has a mixture of pressure dependent kinetics, high pressure limit rate coefficients, for some reactions altered kinetic parameters and global lumped kinetics for aromatics formation. It is also a fitted model for the most important reaction of cyclohexane pyrolysis: isomerization to 1-hexene where there is a factor of 33 difference compared to the ab-initio value reported by Sirjean[41]. This model can also be used for comparison with experimental data. Hence so far, there has been no experiment with pure cyclohexane feed or pure cyclopentane feed without dilution in a flow reactor leading to a full range of conversions at conditions close to atmospheric pressure and temperature range 900 to 1100K, and a residence time of around 0.5s with a detailed analysis of the product spectrum right from hydrogen to polycyclic aromatic hydrocarbons. Nor was a corresponding elementary, ab-initio, high pressure limit, unaltered model built. Hence, an experiment was done in the bench scale unit at LCT, UGent to get the first experimental data on these lines. The apparatus is discussed next, the model is discussed later.

1.5. Bench scale pyrolysis unit at LCT, UGent

The experimental pyrolysis apparatus at LCT, UGent is a continuous flow bench scale unit with a tubular reactor with GC×GC analysis section. It is described in detail here. The length of the tubular reactor is 1.47m with 6mm internal diameter, made of Incoloy 800HT (Ni, 30-35; Cr, 19-23; and Fe, >39.5 wt %). The reactor is placed vertically in a rectangular furnace and heated. In all experiments, the reactor is operated nearly isothermally, i.e. with a steep temperature increase at the reactor inlet and a steep temperature drop at the outlet of the reactor. The isothermal region is from around 20 cm to 120 cm axial distance from the inlet. Thermocouples monitor the process gas temperature at eight axial positions (Figure 1.5). In the setup, Type K thermocouples are used for which the manufacturer calibrated accuracy is ±2.2°C for temperature range 0-1250°C or 0.75% of reading in °C whichever is

greater. The pressure in the reactor is controlled by an outlet pressure restriction valve. Two manometers, situated at the inlet and outlet of the reactor, allow measuring the coil inlet pressure (CIP) and the coil outlet pressure (COP), respectively. The pressure drop over the reactor was found to be negligible, with the pressure remaining constant in the reactor at 1.7 bara. The typical reactor pressure drop is <0.01 bar (0.5% of inlet pressure of 1.7bara). This pressure change has a negligible effect on simulation results. The process gas temperature profile is not perfectly isothermal, but close. This is due to the changes in heat flux over the length of the reactor, the endothermic character of the pyrolysis reactions and the number of heating zones that are used (in this case 8). In simulating the experiment, real temperature profiles are used as input to the plug flow reactor model in the CHEMKIN[49] simulations because the process gas temperatures are measured and not the wall temperatures. The uncertainty of temperature measurement leads to less than 5% relative error on product yields for all temperatures based on CHEMKIN simulations with a varying temperature profile. The properties and dimensions of the reactor are given in Table 1.2.

The analysis section of the pyrolysis set-up has been described in detail previously [44-46]. The analysis section enables on-line identification and quantification of the entire product stream. Two different gas chromatographs were used for a detailed analysis of the reactor effluent: a refinery gas analyzer (RGA) and a GC×GC-FID/TOF-MS setup (Thermo Scientific, Interscience Belgium), as can be seen in Figure 1.5. An overview of the GC×GC-FID/TOF-MS settings used in this work can be found in Table 1.3.

The reactor effluent enters a heated sampling system that consists of two high temperature 6-port 2-way valves and that is kept at 575K to prevent condensation of high molecular weight components. As shown by Van Geem et al. [47], the temperature at which sampling occurs is well above the dew point of the effluent sample. Using this valve-based sampling manifold and uniformly heated transfer lines a gaseous sample of the reactor effluent is injected onto the GC×GC. The former is equipped with both an FID and a TEMPUS TOF-MS (Thermo Scientific, Interscience Belgium), enabling both qualitative and quantitative on-line analyses of the entire product stream, from permanent gases to PAHs [44, 46].

Further downstream the reactor effluent is cooled to approximately 323 K using a water-cooled heat exchanger. Condensed products are collected in a liquid separator, while the remainder of the effluent stream is sent directly to the vent. Before reaching the vent, a

fraction of the effluent is withdrawn and automatically injected onto the RGA using built-in gas sampling valves (353 K). This chromatograph is equipped with one FID and two TCD detectors. This analysis allows separation and detection of all permanent gases that are present in the effluent, as well as an additional analysis of the lighter hydrocarbons, i.e. C_1 – C_4 hydrocarbons.

Before analysis, an internal standard N_2 is mixed with the reactor effluent. With this internal standard, the flow rates of the compounds in the reactor effluent can be quantified. The flow rates of hydrogen, methane, and hydrocarbons up to C_2 are calculated using the peak surface areas obtained from the thermal conductivity detector (TCD) channels of the RGA. Quantification of the peaks of the hydrocarbons with higher molecular masses on the flame ionization channel of the RGA and GC×GC-FID is accomplished by considering methane as a secondary internal standard for these detectors. Peak integration of the chromatograms obtained from GC×GC is performed by a commercial integration package, GC-Image (Zoex Corp.). The identification of compounds is accomplished using two independent orthogonal parameters, Kovats retention indices and the associated mass spectra obtained from GC×GC-TOF-MS analyses. Response factors of all permanent gasses (H_2, CH_4) and light hydrocarbons (C_1-C_4) were determined by means of a gaseous calibration mixture (Air Liquide, Belgium). The response factors of all C_{5+} hydrocarbons were determined using the effective carbon number method, relative to methane [48]. For each studied temperature, at least 3 repeat analyses were performed on RGA chromatograph. Deviations in the obtained results are attributed to uncertainties on the mass flow rates of both feed and the internal standard (N_2) and on uncertainties on the measured temperature profile. This yields, based on experience, a relative error of less than 10% on the mass fractions of products. The carbon balance is closed within 1% for all reported experimental conditions.

Table 1.2: Properties and dimensions of the reactor

Reactor material	Incoloy 800HT
Reactor diameter (ID), mm	6
Reactor length, m	1.47

Surface-to-volume ratio, mm^{-1}	0.66
HC mass flow rate, (g.h^{-1})	240
N_2 dilution mass flow rate, (g.h^{-1})	0
N_2 internal standard mass flow rate, , (g.h^{-1})	20 to 70

Table 1.3: GC × GC settings for on-line effluent analysis

Detector	FID, 300°C	TOF-MS, 25-350 amu
Injections (SSL)	Gas injection, split flow 50 ml/min, 280°C	
First column	RTX-1 PONA 60 m L × 0.25 mm I.D. × 0.25 μm df	
Second column	BPX-50^b 2 m L × 0.15 mm I.D. × 0.15 μm df	
Oven temperature	**-40**°C (4 min hold) → 40°C at 5°C/min → 300°C for RTX-1) at 4°C/min	
Modulation Period	5 s (cryogenic CO_2)	
Carrier gas	He, constant flow 2.1 ml/min	He, constant flow 3.5 ml/min

[a] dimethyl polysiloxane (Restek); [b] 50% phenyl polysilphenylene-siloxane (SGE)
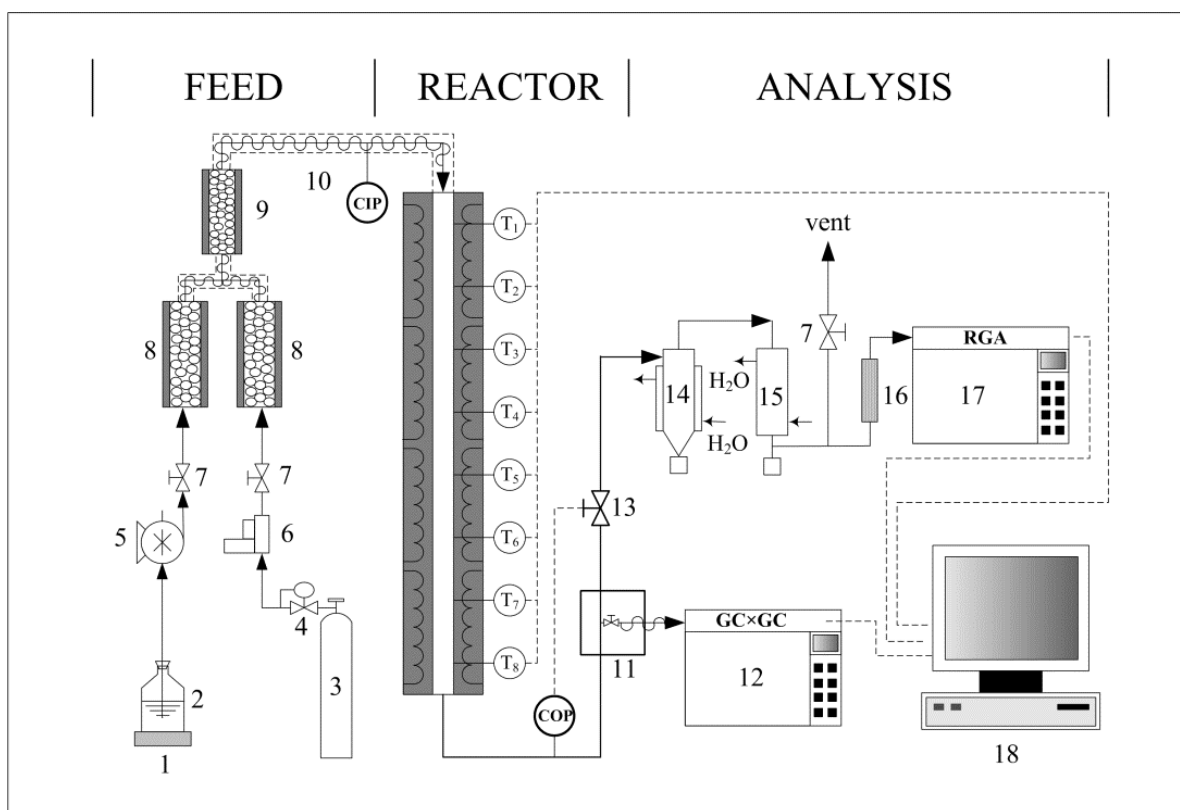
Figure 1.5: Schematic diagram of the experimental setup for cyclopentane pyrolysis indicating process gas temperatures (Ti) and pressure measurements (CIP & COP) (1-electronic balance; 2-liquid feed reservoir; 3-dilution (not added); 4-pressure reducing valve; 5-coriolis flow meter controlled pump; 6-coriolis mass flow controller; 7-valve; 8-evaporator/heater; 9-mixer; 10-heater; 11-heated sampling oven; 12-GC×GC-FID/TOF-MS for C5+; 13-outlet pressure restriction valve; 14-cyclone separator; 15-condenser; 16-dehydrator; 17-Refinery Gas Analyzer (RGA) for C4⁻; 18-data acquisition system)

GC×GC is an arrangement of 2 columns in series with a modulator in between them, all situated in a single oven with programmable temperature. The first column typically separates compounds based on volatility and the second column does so based on polarity. If there were only the conventional 1st dimension GC, then all close boiling pyrolysis products would elute out at the same time. In that case, the peak identification and separation would be difficult. An example would be the isomers cyclopentene and 1,3-pentadiene. Both have a boiling point of 44°C, and have the same molecular mass. Hence, they are expected to elute together in a conventional 1-D GC. Separating the 2 peaks would be a challenge and accurate product quantification cannot be obtained. Connecting a mass spectrometer to the GC is one possible option of resolving such isomers. However, as the

carbon number increases, there may be more such isomers with unknown fragmentation patterns making it difficult to separately identify each isomer. Hence, GC×GC provides a practical solution in the form of the 2nd dimension GC column which quickly separates a sample based on polarity, or in our case: paraffins, isoparaffins, olefins, naphthenes and aromatics. In the example discussed, cyclopentene is a cyclic olefin and 1,3-pentadiene is an open chain di-olefin. The electron charge delocalization is different between the 2 molecules, leading to different polarities. Hence, the 2nd dimension column is expected to separate these 2 peaks, thereby giving a good qualitative separation. Also, since the eluent from the 2nd dimension column is sent to a flame ionization detector which has measurement capability down to ppb levels, the quantitative accuracy is unsurpassed. In the LCT setup, GC×GC setup is already established and validated for analyses of typical pyrolysis products. An important drive that propelled us to design and build the GC×GC setup in the first place was the increased signal to noise ratio. GC×GC is the best technique for analysis of hydrocarbon sample with a wide boiling range compared with traditional GC-MS techniques. In our case, we intend to quantify hydrocarbons from methane till naphthalene. Separation and analysis using comprehensive two-dimensional gas chromatography (GC×GC) is much more powerful than using one-dimensional gas chromatography (1D-GC). The 2nd GC has much higher elution speed than the 1st GC. Qualitative analysis is more reliable because each eluent has two identifiers (retention times) rather than one. If proper orthogonal conditions are selected separations are likely to be more structured in the GC×GC leading to recognizable patterns. This enables a fast group-type analysis and provisional classifications of unknowns. In short, quantification in GC×GC has several potential advantages over 1D-GC such as:

    a. Ordering which makes interference due to peak overlap less likely.

    b. Greater sensitivity or detectability due to the high speed of the second column. The resulting peaks are sharper and, therefore, exhibit a higher signal response.

    c. Reliable presence of a true baseline for peak integration

The residence time of the hydrocarbon feed in the reactor is calculated to be around 0.5 s, as is typical of an industrial steam cracker. The experimental data are used as a validation basis for an automatically generated mechanism, which is an elementary reaction network

with kinetics based on group additive methodology. In the next section, group additive methodology is discussed.

1.6. Group additive methodology

Group additive methodology has been extensively discussed in literature[16, 50-55]. However, here it is illustrated with an example how the kinetic parameters of a H-shift reaction are calculated starting from the standard group additive values listed and the kinetic parameters for the reference reaction of that family. In an intra-cyclopentadiene (intra-CPD) H-shift, a hydrogen atom from the single bonded carbon of the 1,3-cyclopentadiene moiety shifts and bonds to the neighboring carbon atom, thereby causing a re-arrangement of the double bonds. The simplest reaction for this family is in general the reference reaction for that family. In this case, this is the identical intra-molecular hydrogen shift reaction in cyclopentadiene, (Ref) as given in Figure 1.6.
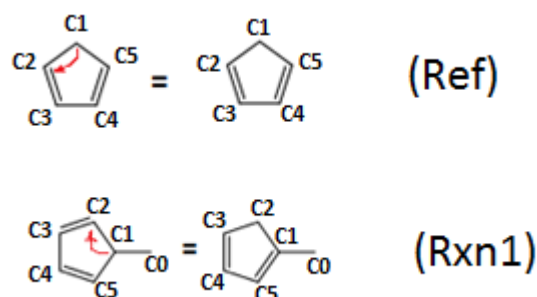
Figure 1.6: Illustration of How Arrhenius parameters are calculated for an example reaction (Rxn1) starting from group additive values and Arrhenius parameters for the reference reaction of the reaction family (Ref).

For this reaction, the Arrhenius parameters (A_{ref}, $E_{a,ref}$) calculated at the CBS-QB3 level of theory are: 4.8 10^{13} s^{-1}, and 107.8 kJ mol^{-1} respectively. The number of single events n_e for this reaction equals 4. Hence, the single event pre-exponential factor is $\tilde{A}_{ref}$ = 4.8 10^{13}/4 s^{-1} = 1.2 10^{13} s^{-1}, i.e. log($\tilde{A}_{ref}$) = 13.079. The Arrhenius parameters for the reference reaction are further used for the calculation of the Arrhenius parameters for other reactions in this family. The intra-molecular hydrogen shift reaction in methyl cyclopentadiene is used as an example reaction (Rxn1 in Figure 1.6). With the use of the Arrhenius parameters for the reference reaction and the ΔGAV^o values from the group additive database, new Arrhenius parameters can be estimated for this reaction.

In Rxn 1, there is only one hydrogen atom bonded to C1, and it shifts to the neighboring carbon causing the re-arrangement of double bonds, as shown in figure 1.6. C1 of the cyclopentadiene moiety is bonded to a hydrogen and a branch - carbon indicated as C0. So, the relevant group is C1-C, which means a single bonded carbon attached to C1. The number of single events n_e for this reaction is 2. Hence, the single event Arrhenius pre-exponential factor for Rxn1 is calculated by:

$$\log(\tilde{A}_{Rxn1}) = \log(\tilde{A}_{ref}) + \Delta GAV^{\circ}(\tilde{A}_{C1C}) \tag{1.1}$$

Hence,

$$\log(\tilde{A}_{Rxn1}) = 13.079 + 0.317 = 13.396 \tag{1.2}$$

Note that the group additive value $\Delta GAV^{\circ}(\tilde{A}_{C1-C}) = 0.317$ is the group additive value from databases[56].

This gives a single event pre-exponential factor equal to:

$$\tilde{A}_{Rxn1} = 2.59 \; 10^{13} \; s^{-1}. \tag{1.3}$$

If the number of single events for Rxn1 are accounted for, the pre-exponential factor and the activation energy for the reaction become:

$$A_{Rxn1} = n_{e,Rxn1} \times 2.59 \; 10^{13} = 2 \times 2.59 \; 10^{13} = 4.98 \; 10^{13} \; s^{-1} \tag{1.4}$$

$$E_{a,Rxn1} = E_{a,ref} + \Delta GAV^{\circ}(E_{a,C1-C}) = 107.8 + 0.92 = 108.72 \; kJ \; mol^{-1} \tag{1.5}$$
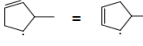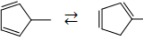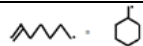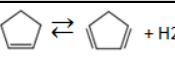
Note that also the group additive value $\Delta GAV^{\circ}(E_{a,C1-C}) = 0.92$ is obtained from databases[56]. This is the methodology for calculating the kinetics of the elementary reactions. The group additive values are derived ab-initio from CBS-QB3 based kinetics and are reliable and proven to work. The mechanism of elementary reactions, however, is generated using an automatic mechanism generation tool, 'Genesys', discussed next.

1.7. Automatic mechanism generation using Genesys

Genesys[1, 2] is an in-house developed automatic kinetic model generation tool, in which the size of the kinetic model is controlled by a rule based termination criterion. In Genesys, starting from the user-defined reaction families and the initial feed molecules, an exhaustive mechanism is generated which is terminated by the user-defined constraints on product species, like constraints on the maximum carbon number allowed, and constraints on the reaction families, like limiting the size of the abstracting and adding species. The reaction families are defined by the user in Genesys by supplying a reaction recipe, the possible

reactive center by the user-friendly SMARTS language and constraints on the appearance of the reaction family or the products formed by this reaction family. Examples of reaction families and constraints are shown in Table 1.4. Owing to the ever increasing power of computers and speed of ab-initio calculations, new types of elementary reactions are being discovered[57] and will be discovered in future. However, for the choice of elementary reaction families in Genesys, current knowledge and experience is applied. Figure 1.7 shows the algorithm in Genesys for the generation of the kinetic model. The completeness of the mechanism generated by Genesys depends on the selected reaction families. The reaction families applied in Genesys is a subjective choice of the user based on prior experience. Genesys can now also be used using on the fly calculations.

Table 1.4: Example of reaction families and constraints – input to Genesys[2]

Reaction family	Description/ Example	Kinetics	Constraint on carbon number
Hydrogen transfer		Reference	Objective – to limit C no. to 10
Inter-molecular H-abstraction	by C• by H•	55	10 for molecule, 4 for C• radical
Intra-molecular H-abstraction (acyclics)	C-(C)$_n$-C• ⇄ •C-(C)$_n$-C	58	10 for C• radical
Intra-molecular H-abstraction (cyclics)		58	10 for cyclic C• radical
Intra-CPD-H-shift		58	7 (includes methyl and ethyl CPD)
Addition			
Inter-molecular C-radical addition	C=C + •C ⇄ •C-C-C	52	6 for molecule, 4 for C• radical
Intra-molecular C-radical addition		58	10 for C• radical (naphthalene routes)
Hydrogen atom addition	•C-C-H ⇄ C=C+ •H	53	10 for C• radical
Recombination			
C-C recombination	•C + •C ⇄ C-C	16	4 for C• radical
C-H recombination	•C + H ⇄ C-H	16	5 for C• radical
H2 elimination			
Direct release of H2 gas		58	Cyclopentene molecule
Diels-Alder			
Molecular mechanism – rearrangement of double bonds		16	Specific to ethylene and BD substrates
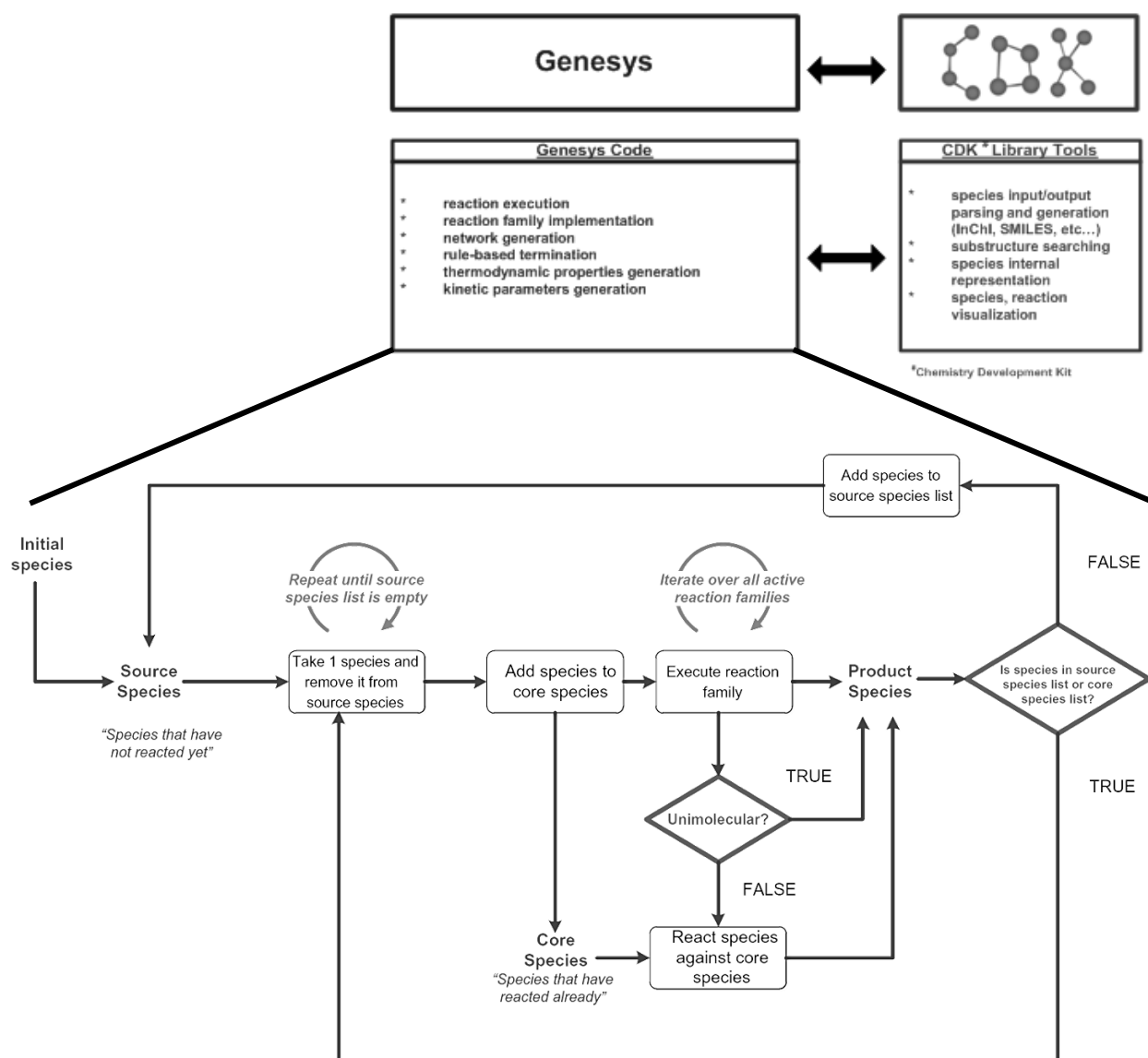
Figure 1.7: Algorithm of the generation of a kinetic model with the use of the rule based termination criterion in Genesys

The model that is generated by Genesys is used in ChemKin simulations for finding the predicted yields.

1.8. Overview of thesis chapters

Genesys was first employed to generate a model for light alkanes – propane, n-butane and iso-butane. This is discussed in chapter 2, and the model was validated with in-house experiments with the 3 feeds, respectively. The operating conditions were similar to those

in the industrial steam cracking, 700-900ºC, ~ 0.5 sec, 1.7 bara pressure, with steam as diluent. Experimental data on n-butane and iso-butane at a much higher temperature and much lower pressure and residence times from a different laboratory was also selected[59] and the Genesys model predictions were compared. This comparison wass all the more interesting because Genesys model is a high pressure limit ab-initio based un-altered elementary reaction model, while the experimental data[59] was at a pressure of 0.004 MPa, 50 micro.sec, 1100-1400K. Reaction path analysis was done to show the dominant routes toward major products. The Genesys model was then extended to predict the pyrolysis of cyclopentane (chapter 3). Cyclopentane is one of the least studied in pyrolysis feeds in literature. Hence, chapter 3 and the related publication[56] was the first to report experimental data of a large spectrum of products from cyclopentane pyrolysis. This was again done at steam cracking relevant conditions. Even though experimental data on cyclopentane pyrolysis in literature is   scarce, there have been articles on ignition studies of cyclopentane[6], and models have been developed with that objective. Genesys model predictions were compared to experimental results and other model predictions too. Reaction path analysis shows the major pathways, and as the basic feed is cyclopentane, one of the reaction families that becomes more relevant than for other feeds is the cyclopentadiene H-shift. . Chapter 4 reports experimental data and model results for cyclohexane pyrolysis. Cyclohexane pyrolysis has been more widely studied as compared to cyclopentane, but there is a gap in literature for a purely elementary reaction high pressure limit model with un-altered ab-initio kinetics. Chapter 4 and the related article[60] addresses this gap in literature. In addition, experimental results have been reported for conditions close to steam cracking. As compared to cyclopentane, there were more literature models for cyclohexane. Their predictions were compared to those of the Genesys model. Experimental data from a different laboratory[61] were also predicted well by the Genesys model. This is interesting because the other data is at very low pressure and high temperature. Reaction path analysis showed the major pathways, and these were in contrast to the lumped schemes of popular literature models, where it is difficult to understand the underlying elementary mechanism. Chapter 5 extended the cycloalkane model to predict methyl-cyclohexane pyrolysis and the model was validated using laboratory data from Hefei[10]. Chapter 6 further extended the model to predict ethyl-cyclohexane pyrolysis, validated using experimental data from Hefei[11]. The Genesys model for methyl- and ethyl-

cyclohexane was compared to other literature models and reaction path analyses is presented. In these two chapters, experimental data of different pressures are compared and it is realized that pressure has a limited effect on the major product trends. Conversion and some product where the pressure does play a major role, the high pressure limit Genesys model was able to capture the trends from 0.004 MPa to 0.17 MPa. Chapter 7 discusses the conclusions and way forward. It is to be noted that the experiments in chapters 2, 3, 4 were performed by the collaborators of the author, and these collaborators are co-authors on the papers published based on this thesis.

1.9. References

1.Van de Vijver, R.; Vandewiele, N. M.; Vandeputte, A. G.; Van Geem, K. M.; Reyniers, M. F.; Green, W. H.; Marin, G. B., Rule-based ab initio kinetic model for alkyl sulfide pyrolysis. *Chemical Engineering Journal* **2015,** 278, 385-393.

2.Vandewiele, N. M.; Van Geem, K. M.; Reyniers, M. F.; Marin, G. B., Genesys: Kinetic model construction using chemo-informatics. *Chemical Engineering Journal* **2012,** 207, 526-538.

3.Ranzi, E.; Frassoldati, A.; Grana, R.; Cuoci, A.; Faravelli, T.; Kelley, A. P.; Law, C. K., Hierarchical and comparative kinetic modeling of laminar flame speeds of hydrocarbon and oxygenated fuels. *Progress in Energy and Combustion Science* **2012,** 38, (4), 468-501.

4.Wang, K.; Villano, S. M.; Dean, A. M., Fundamentally-based kinetic model for propene pyrolysis. *Combustion and Flame* **2015,** 162, (12), 4456-4470.

5.Sirjean, B.; Buda, F.; Hakka, H.; Glaude, P. A.; Fournet, R.; Warth, V.; Battin-Leclerc, F.; Ruiz-Lopez, M., The autoignition of cyclopentane and cyclohexane in a shock tube. *Proceedings of the Combustion Institute* **2007,** 31, 277-284.

6.Tian, Z. M.; Tang, C. L.; Zhang, Y. J.; Zhang, J. X.; Huang, Z. H., Shock Tube and Kinetic Modeling Study of Cyclopentane and Methylcyclopentane. *Energy & Fuels* **2015,** 29, (1), 428-441.

7.H. Wang, E. D., B. Sirjean, D. A. Sheen, R. Tango, A. Violi, J. Y. W. Lai, F. N. Egolfopoulos, D. F. Davidson, R. K. Hanson, C. T. Bowman, C. K. Law, W. Tsang, N. P. Cernansky, D. L. Miller, R. P. Lindstedt *JetSurF*, 2.0; http://web.stanford.edu/group/haiwanglab/JetSurF/JetSurF2.0/index.html, 2010.

8.Li, Y.; Zhou, C. W.; Somers, K. P.; Zhang, K. W.; Curran, H. J., The oxidation of 2-butene: A high pressure ignition delay, kinetic modeling study and reactivity comparison with isobutene and 1-butene. *Proceedings of the Combustion Institute* **2017,** 36, (1), 403-411.

9.Wang, Z.; Cheng, Z.; Yuan, W.; Cai, J.; Zhang, L.; Zhang, F.; Qi, F.; Wang, J., An experimental and kinetic modeling study of cyclohexane pyrolysis at low pressure. *Combustion and Flame* **2012,** 159, (7), 2243-2253.

10.Wang, Z. D.; Ye, L. L.; Yuan, W. H.; Zhang, L. D.; Wang, Y. Z.; Cheng, Z. J.; Zhang, F.; Qi, F., Experimental and kinetic modeling study on methylcyclohexane pyrolysis and combustion. *Combustion and Flame* **2014,** 161, (1), 84-100.

11.Wang, Z. D.; Zhao, L.; Wang, Y.; Bian, H. T.; Zhang, L. D.; Zhang, F.; Li, Y. Y.; Sarathy, S. M.; Qi, F., Kinetics of ethylcyclohexane pyrolysis and oxidation: An experimental and detailed kinetic modeling study. *Combustion and Flame* **2015,** 162, (7), 2873-2892.

12.Alaraby, Saudi Aramco shifts to new 'crude to chemical' strategy. *The New Arab:* *https://www.alaraby.co.uk/english/indepth/2019/4/17/saudi-aramco-shifts-to-new-crude-to-chemical-strategy* April 17, 2019, 2019.

13.ExxonMobil, h. c. e. c. e. c.-o. c.-t. a.-a.-f.-d. Crude oil assays. https://corporate.exxonmobil.com/en/crude-oils/crude-trading/assays-available-for-download

14.Bjelic, A.; Grilc, M.; Hus, M.; Likozar, B., Hydrogenation and hydrodeoxygenation of aromatic lignin monomers over Cu/C, Ni/C, Pd/C, Pt/C, Rh/C and Ru/C catalysts: Mechanisms, reaction micro-kinetic modelling and quantitative structure-activity relationships. *Chemical Engineering Journal* **2019,** 359, 305-320.

15.Wang, H. L.; Ruan, H.; Pei, H. S.; Wang, H. M.; Chen, X. W.; Tucker, M. P.; Cort, J. R.; Yang, B., Biomass-derived lignin to jet fuel range hydrocarbons via aqueous phase hydrodeoxygenation. *Green Chemistry* **2015,** 17, (12), 5131-5135.

16.Sabbe, M. K.; Van Geem, K. M.; Reyniers, M. F.; Marin, G. B., First Principle-Based Simulation of Ethane Steam Cracking. *Aiche Journal* **2011,** 57, (2), 482-496.

17.Van Geem, K. M.; Reyniers, M. F.; Marin, G. B.; Song, J.; Green, W. H.; Matheu, D. M., Automatic reaction network generation using RMG for steam cracking of n-hexane. *Aiche Journal* **2006,** 52, (2), 718-730.

18.Djokic, M. R.; Dijkmans, T.; Yildiz, G.; Prins, W.; Van Geem, K. M., Quantitative analysis of crude and stabilized bio-oils by comprehensive two-dimensional gas-chromatography. *Journal of Chromatography A* **2012,** 1257, 131-140.

19.Vargas, D. C.; Alvarez, M. B.; Portilla, A. H.; Van Geem, K. M.; Streitwieser, D. A., Kinetic Study of the Thermal and Catalytic Cracking of Waste Motor Oil to Diesel-like Fuels. *Energy & Fuels* **2016,** 30, (11), 9712-9720.

20.Vandewiele, N. M.; Magoon, G. R.; Van Geem, K. M.; Reyniers, M. F.; Green, W. H.; Marin, G. B., Kinetic Modeling of Jet Propellant-10 Pyrolysis. *Energy & Fuels* **2015,** 29, (1), 413-427.

21.Vandewiele, N. M.; Magoon, G. R.; Van Geem, K. M.; Reyniers, M. F.; Green, W. H.; Marin, G. B., Experimental and Modeling Study on the Thermal Decomposition of Jet Propellant-10. *Energy & Fuels* **2014,** 28, (8), 4976-4985.

22.Gascoin, N.; Abraham, G.; Gillard, P., Synthetic and jet fuels pyrolysis for cooling and combustion applications. *Journal of Analytical and Applied Pyrolysis* **2010,** 89, (2), 294-306.

23.Yang, Q. C.; Chetehouna, K.; Gascoin, N.; Bao, W., Experimental study on combustion modes and thrust performance of a staged-combustor of the scramjet with dual-strut. *Acta Astronautica* **2016,** 122, 28-34.

24.Pyl, S. P.; Schietekat, C. M.; Reyniers, M. F.; Abhari, R.; Marin, G. B.; Van Geem, K. M., Biomass to olefins: Cracking of renewable naphtha. *Chemical Engineering Journal* **2011,** 176, 178-187.

25.Buda, F.; Bounaceur, R.; Warth, V.; Glaude, P.; Fournet, R.; Battin-Leclerc, F., Progress toward a unified detailed kinetic model for the autoignition of alkanes from C-4 to C-10 between 600 and 1200 K. *Combustion and Flame* **2005,** 142, (1-2), 170-186.

26.Buda, F.; Glaude, P. A.; Battin-Leclerc, F.; Porter, R.; Hughes, K. J.; Griffiths, J. F., Use of detailed kinetic mechanisms for the prediction of autoignitions. *Journal of Loss Prevention in the Process Industries* **2006,** 19, (2-3), 227-232.

27.Serinyel, Z.; Herbinet, O.; Frottier, O.; Dirrenberger, P.; Warth, V.; Glaude, P. A.; Battin-Leclerc, F., An experimental and modeling study of the low- and high-temperature oxidation of cyclohexane. *Combustion and Flame* **2013,** 160, (11), 2319-2332.

28.Jones, D. T., CLXXVII. - The thermal decomposition of hydrogenated aromatic hydrocarbons. *Journal of the Chemical Society, Transactions* **1915,** 107, 1582-1588.

29.Frolich, P. K.; Simard, R.; White, A., Formation of Butadiene by Cracking of Hydrocarbons1. *Industrial & Engineering Chemistry* **1930,** 22, (3), 240-241.

30.Egloff, G.; Bollman, H. T.; Levinson, B. L., Thermal reactions of cycloparaffins and cycloölefins. *Journal of Physical Chemistry* **1931,** 35, (12), 3489-3552.

31.Pease, R. N.; Morton, J. M., Kinetics of dissociation of typical hydrocarbon vapors. *Journal of the American Chemical Society* **1933,** 55, (8), 3190-3200.

32.Levush, S. S.; Abadzhev, S. S.; Shevchuk, V. U., Pyrolysis of cyclohexane. *Petroleum Chemistry* **1969,** 9, (3), 185-&.

33.Tsang, W., Thermal decomposition of cyclopentane and related compounds. *International Journal of Chemical Kinetics* **1978,** 10, (6), 599-617.

34.Tsang, W., Thermal stability of cyclohexane and 1-hexene. *International Journal of Chemical Kinetics* **1978,** 10, (11), 1119-1138.

35.Aribike, D. S.; Susu, A. A., Kinetics of the pyrolysis of cyclohexane using the pulse technique. *Industrial & Engineering Chemistry Research* **1988,** 27, (6), 915-920.

36.Aribike, D. S.; Susu, A. A.; Ogunye, A. F., Mechanistic and mathematical modeling of the thermal decomposition of cyclohexane. *Thermochimica Acta* **1981,** 51, (2-3), 113-127.

37.Aribike, D. S.; Susu, A. A.; Ogunye, A. F., Kinetics of the thermal decomposition of cyclohexane. *Thermochimica Acta* **1981,** 47, (1), 1-14.

38.Zamostny, P.; Belohlav, Z.; Starkbaumova, L.; Patera, J., Experimental study of hydrocarbon structure effects on the composition of its pyrolysis products. *Journal of Analytical and Applied Pyrolysis* **2010,** 87, (2), 207-216.

39.Lai, W. C.; Song, C. S., Pyrolysis of alkylcyclohexanes in or near the supercritical phase. Product distribution and reaction pathways. *Fuel Processing Technology* **1996,** 48, (1), 1-27.

40.Kiefer, J. H.; Gupte, K. S.; Harding, L. B.; Klippenstein, S. J., Shock Tube and Theory Investigation of Cyclohexane and 1-Hexene Decomposition. *Journal of Physical Chemistry A* **2009,** 113, (48), 13570-13583.

41.Sirjean, B.; Glaude, P. A.; Ruiz-Lopez, M. F.; Fournet, R., Detailed kinetic study of the ring opening of cycloalkanes by CBS-QB3 calculations. *Journal of Physical Chemistry A* **2006,** 110, (46), 12693-12704.

42.Peukert, S.; Naumann, C.; Braun-Unkhoff, M.; Riedel, U., The reaction of cyclohexane with H-atoms: A shock tube and modeling study. *International Journal of Chemical Kinetics* **2012,** 44, (2), 130-146.

43.Peukert, S.; Naumann, C.; Braun-Unkhoff, M.; Riedel, U., Formation of H-Atoms in the Pyrolysis of Cyclohexane and 1-Hexene: A Shock Tube and Modeling Study. *International Journal of Chemical Kinetics* **2011,** 43, (3), 107-119.

44.Pyl, S. P.; Schietekat, C. M.; Van Geem, K. M.; Reyniers, M.-F.; Vercammen, J.; Beens, J.; Marin, G. B., Rapeseed oil methyl ester pyrolysis: On-line product analysis using comprehensive two-dimensional gas chromatography. *Journal of Chromatography A* **2011,** 1218, (21), 3217-3223.

45.Pyl, S. P.; Van Geem, K. M.; Puimège, P.; Sabbe, M. K.; Reyniers, M.-F.; Marin, G. B., A comprehensive study of methyl decanoate pyrolysis. *Energy* **2012,** 43, (1), 146-160.

46.Djokic, M.; Carstensen, H.-H.; Van Geem, K. M.; Marin, G. B., The thermal decomposition of 2,5-dimethylfuran. *Proceedings of the Combustion Institute* **2013,** 34, (1), 251-258.

47.Geem, K. M. V.; Dhuyvetter, I.; Prokopiev, S.; Reyniers, M.-F. o.; Viennet, D.; Marin, G. B., Coke Formation in the Transfer Line Exchanger during Steam Cracking of Hydrocarbons. *Industrial & Engineering Chemistry Research* **2009,** 48, (23), 10343-10358.

48.Beens, J.; Boelens, H.; Tijssen, R.; Blomberg, J., Quantitative Aspects of Comprehensive Two-Dimensional Gas Chromatography (GC×GC). *Journal of High Resolution Chromatography* **1998,** 21, (1), 47-54.

49.   *CHEMKIN-PRO 15131*, Reaction Design: San Diego, 2013.

50.Paraskevas, P. D.; Sabbe, M. K.; Reyniers, M. F.; Papayannakos, N.; Marin, G. B., Group Additive Values for the Gas-Phase Standard Enthalpy of Formation, Entropy and Heat Capacity of Oxygenates. *Chemistry-a European Journal* **2013,** 19, (48), 16431-16452.

51.Sabbe, M. K.; De Vleeschouwer, F.; Reyniers, M. F.; Waroquier, M.; Marin, G. B., First Principles Based Group Additive Values for the Gas Phase Standard Entropy and Heat Capacity of Hydrocarbons and Hydrocarbon Radicals. *Journal of Physical Chemistry A* **2008,** 112, (47), 12235-12251.

52. Sabbe, M. K.; Reyniers, M. F.; Van Speybroeck, V.; Waroquier, M.; Marin, G. B., Carbon-centered radical addition and beta-scission reactions: Modeling of activation energies and pre-exponential factors. *Chemphyschem* **2008,** 9, (1), 124-140.

53. Sabbe, M. K.; Reyniers, M. F.; Waroquier, M.; Marin, G. B., Hydrogen Radical Additions to Unsaturated Hydrocarbons and the Reverse beta-Scission Reactions: Modeling of Activation Energies and Pre-Exponential Factors. *Chemphyschem* **2010,** 11, (1), 195-210.

54. Sabbe, M. K.; Saeys, M.; Reyniers, M. F.; Marin, G. B.; Van Speybroeck, V.; Waroquier, M., Group additive values for the gas phase standard enthalpy of formation of hydrocarbons and hydrocarbon radicals. *Journal of Physical Chemistry A* **2005,** 109, (33), 7466-7480.

55. Sabbe, M. K.; Vandeputte, A. G.; Reyniers, M. F.; Waroquier, M.; Marin, G. B., Modeling the influence of resonance stabilization on the kinetics of hydrogen abstractions. *Physical Chemistry Chemical Physics* **2010,** 12, (6), 1278-1298.

56. Khandavilli, M. V.; Vermeire, F. H.; Van de Vijver, R.; Djokic, M.; Carstensen, H. H.; Van Geem, K. M.; Marin, G. B., Group additive modeling of cyclopentane pyrolysis. *Journal of Analytical and Applied Pyrolysis* **2017,** 128, 437-450.

57. Green, S., Automated Discovery of Elementary Chemical Reaction Steps Using Freezing String and Berny Optimization Methods. *Journal of Chemical theory and Computation* **2015,** 11, (9), 4248-4259.

58. Merchant, S. Molecules to Engines: Combustion chemistry of Alcohols and their application to advanced engines. MIT, 2015.

59. Li, W.; Wang, G. Q.; Li, Y. Y.; Li, T. Y.; Zhang, Y.; Cao, C. C.; Zou, J. B.; Law, C. K., Experimental and kinetic modeling investigation on pyrolysis and combustion of n-butane and i-butane at various pressures. *Combustion and Flame* **2018,** 191, 126-141.

60. Khandavilli, M. V.; Djokic, M.; Vermeire, F. H.; Carstensen, H. H.; Van Geem, K. M.; Marin, G. B., Experimental and Kinetic Modeling Study of Cyclohexane Pyrolysis. *Energy & Fuels* **2018,** 32, (6), 7153-7168.

61. Zhandong, W. Experimental and Kinetic Modeling Study of Cyclohexane and Its Mono-alkylated Derivatives Combustion. University of Science and Technology of China,Hefei

2

An experimental and kinetic modeling study of pyrolysis of propane, n-butane and iso-butane

Pyrolysis of propane, n-butane and iso-butane was conducted in a bench scale continuous flow unit with steam as diluent. The operating conditions were comparable to industrial steam cracking, at reactor temperatures of 1073 to 1123K, pressure 0.17 MPa, residence times around 0.5 s, with steam dilutions around 30% by mass. Single pass conversions of more than 50% were realized and a range of compounds from hydrogen to toluene were detected and measured in the effluent. A rule-based automatic reaction mechanism generator software tool called Genesys was used to build a high pressure limit mechanism consisting of solely elementary reactions to predict the experimental results. Rate coefficients of the reactions and all thermodynamic parameters were derived either from ab-initio calculations or by using an ab-initio based group additive methodology. No adjustment of the reaction rate coefficients was done to assess the predictive capabilities of Genesys. Aromatics formation mechanism was adopted from two literature sources – for benzene formation starting from vinyl and 1,3-butadiene based on an ethane pyrolysis model, and toluene, indene, naphthalene mechanism from a model for cyclopentadiene-ethylene mixture pyrolysis. A reasonable agreement with experimental data was obtained for the products for our (LCT) experimental data as well as for data generated in Hefei at a different temperature and pressure range (pyrolysis of n-butane and iso-butane at 1100-1400K, 0.004 MPa, 50 μ.s residence time). This chapter demonstrates the effectiveness of an ab-initio based high pressure limit model generated automatically and how its predictions compare well with popular optimized literature models for a wide range of temperature, pressure and residence time conditions, experiments done in-house as well as those obtained from another laboratory.

2.1. Introduction

Steam cracking is the most commercially viable route to form important lower olefins such as ethylene, propylene and butadiene.[1] These lower olefins are in turn raw materials for important polymers and chemicals. Typical feedstocks of steam cracking come from natural gas, crude oil or shale resources. They range from light feeds such as ethane and LPG to heavy feeds such as vacuum gas oils. Typical steam cracking temperatures are in the range of 973 K to 1173 K, pressures vary between 0.2 and 0.4 MPa and residence times of 0.1 to 1 seconds are achieved.[2] Due to the large throughputs employed in the steam cracking industry, any improvement in process conditions or change of feedstock can lead to a significant economic impact. For a knowledge driven improvement hence, a good understanding of the steam cracking process is desirable. This involves the mechanistic understanding of the gas-phase pyrolysis reactions, which are elementary radical reactions[3-6] such as additions, hydrogen abstractions, recombinations and their reverse reactions. Typically the reactive phase consists of hundreds of species involved in thousands of elementary reactions.[7-9] Uncertainty in rate coefficients is a major contributor to the model deviations.[10] Measuring the kinetics of all these reactions is time consuming and costly. Hence, kinetic estimation procedures are usually used for most of the reactions in a model. Understanding the pyrolysis chemistry of light hydrocarbons such as ethane, propane, butanes forms the basis of mechanistic understanding of pyrolysis of any real life feed. This is because ultimately the most important products are generally formed starting from small molecules and radicals, once the large feed molecules crack down to smaller ones[2]. Most of the literature on experimental pyrolysis of propane and butanes is focused on catalytic pyrolysis. However, there are a few articles which discuss non-oxidative gas phase non-catalytic pyrolysis of butanes. In 2013, Zhang et al[30] did continuous flow experiments with n-butane and iso-butane feeds in an electrically heated furnace at reactor temperatures 823-1823 K and very low pressures. The objective was to identify the products using photo-ionization/ mass spectrometry. The focus was mainly on differentiating between the sooting tendency of the 2 feeds. A detailed report of product yields versus operating conditions was not given. Pyun et al.[31] measured the time history of methane and ethylene in n-butane and n-heptane pyrolysis behind reflected shock waves at 1200-1600K, 0.15MPa. This

experiment did not intend to measure the whole product spectrum though. Tang et al.[32] did experiments with n-butane in a coupled system of a flash pyrolysis micro-reactor with threshold photoelectron photo-ion coincidence (TPEPICO) spectroscopy at Hefei synchrotron laboratory to investigate thermal decomposition of n-butane. Primary products in the pyrolysis were determined with TPEPICO time-of-flight mass spectra and mass-selected threshold photoelectron spectra (TPES). The operating conditions were in the range of 1600K and 10 micro.second at 0.001 MPa. These conditions are more in the range of combustion than for steam cracking. Shrestha et al.[33] did a continuous flow pyrolysis experiment using n-butane, ethane and dodecane feeds. The reactor was of quartz and the operating conditions were in the range of 1100K and 0.05 seconds at 1 atm pressure, conditions not being in the steam cracking regime. Li et al from Hefei most recently generated experimental data on n-butane and iso-butane pyrolysis[12] in which the feed hydrocarbon was present at a dilution of 2 mol%. The reactor peak temperature varied from 861 to 1347 K. The feed flow rate was $1.67*10^{-5}$ standard cubic meter per second. The reactor was operated at 3 different pressures – 0.00405 MPa, 0.0203 MPa and 0.1013 MPa at a few micro-seconds residence time. It can be seen from this review that there is a gap in literature with respect to light alkane pyrolysis data at conditions 1073-1173K at close to atmospheric pressures and around 0.5 second residence time, conditions of interest for industrial steam cracking. In 2015, Wang et al[22] did experiments on propylene pyrolysis and developed a comprehensive model which can also be used for modeling of light alkanes pyrolysis.

In this chapter, pyrolysis experiments have been done with propane, n-butane and iso-butane feeds in the temperature range of 973-1173 K, 0.17 MPa, 0.5 s residence time. There is no prior literature at these conditions. A model which is entirely based on first principles containing solely elementary reactions has been generated automatically using an in-house tool called Genesys[11] and validated using the experimental data. Next, the model is also used to predict the experimental data from a different laboratory on n-butane and iso-butane pyrolysis at higher temperature range and low pressures[12]. Also, predictions of popular models in literature – POLIMI (Ranzi)[24], CSM[22], Hefei[12] and Aramco Mechanism[25] models have been compared with those of the new model, so as to check if the new high pressure limit automatic mechanisms can perform well when compared to optimized models from literature, that too at extreme ranges of pressure and temperature.

2.2. Methodology

2.2.1. Experimental setup and procedure

Propane, n-butane and iso-butane pyrolysis experiments were carried out in the Laboratory for Chemical technology at Ghent University on a bench scale unit which consisted of three main sections – feed section, reactor section and product analysis section. The setup has been described in detail elsewhere [13, 14]. Only the specifics related to this work will be given. The light gases were procured from Air Liquide, Belgium in diluted form as gas cylinders. The feed was fed to an electrically heated tubular reactor made of Incoloy 800HT. The length of the reactor is 1.47m with 0.006 m internal diameter. The flow rate was chosen so as to obtain a residence time calculated based on inlet conditions in the order of 0.5 s. The pressure was maintained at 0.17 MPa using an outlet pressure restriction valve situated at the exit of the effluent line. In all the experiments, the reactor was operated nearly isothermally in the temperature range from 1073K to 1173K, i.e. with a steep temperature increase at the reactor inlet and a steep temperature drop at the outlet of the reactor.

The product analysis section consisted of two different gas chromatographs for a detailed analysis of the reactor effluent: a so-called refinery gas analyzer (RGA) and a GC×GC-FID/TOF-MS. The former enabled analysis of permanent gases and light hydrocarbons ($C_1 - C_4$), while the latter analyzed the whole product spectrum. Response factors for the former were determined by calibration with a synthetically created gas mixture (supplied by Air Liquide, Belgium). The response factors of the C_5+ compounds were determined using the effective carbon number method relative to methane. The relative error on the mass fractions of products was less than 3% based on prior experience[13,14]. For each temperature and flow condition, 3 RGA injections were done to make sure the effluent is stable in composition.

Separation and analysis using comprehensive two-dimensional gas chromatography (GC×GC) is much more powerful than using one-dimensional gas chromatography (1D-GC)[15]. Qualitative analysis is more reliable because each eluent has two identifiers (retention times) rather than one. If proper orthogonal conditions are selected separations are likely to be more structured in the GC×GC leading to recognizable patterns [16, 17]. This

enables a fast group-type analysis and provisional classifications of unknowns [18]. Moreover, quantification in GC×GC has several potential advantages over 1D-GC such as:

   a. Ordering which makes interference due to peak overlap less likely [17, 19].

   b. Greater sensitivity or detectability due to the high speed of the second column. The resulting peaks are sharper and, therefore, exhibit a higher signal response [17].
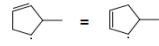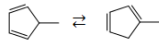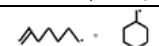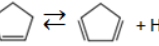
Reliable presence of a true baseline for peak integration [17].

2.2.2. Kinetic model generation

The objective is to create a light gases pyrolysis model consisting of only elementary reversible reactions whose kinetics and thermodynamics are based on ab-initio electronic structure calculations. The first step is to select the relevant reaction families. For ethane cracking [20], Sabbe et al. used the following reaction families: hydrogen abstraction, hydrogen atom addition, carbon radical addition and recombination (and their reverse reaction families). Based on related literature [21-23], the following reaction families and reactions also have been considered: Intra-molecular carbon centered radical addition, Intra-cyclopentadiene hydrogen shift, Intra-molecular hydrogen abstraction, Diels-Alder reaction, H_2 elimination. Table 1 shows the complete list of reaction families considered. In order to limit the mechanism size to a carbon number of 10 (representing naphthalene product), constraints were imposed on the different reaction families. With reference to Table 1 for example, for intermolecular carbon radical based hydrogen abstraction, the attacking carbon based radical was limited to a size of C_4 because usually a bigger radical than this may preferably undergo unimolecular decomposition by β-scission. The substrate molecule was limited to a carbon number of C_{10}. Similarly, for Carbon radical addition family, the attacking radical had a maximum size of C_4 while the substrate had a maximum of C_6 to limit the final radical size to 10. The huge model that is generated (having ~ 20000 reactions) is later on compressed to around 800 dominant reaction-model using principal component analysis, rate of production analysis and reaction path analysis - From the huge mechanism of around 20000 reactions, firstly, reactions involving rare species (bi-radicals, tri-radicals, di-ynes, 1,2,3-tri-enes, duplicates of resonance stabilized species) are eliminated. This reduces the mechanism to around 4000 reactions. Principal Component

Analysis is performed on this reduced mechanism by the procedure of Vajda, Valko and Turanyi[34] to further compress it. It is briefly described – first, all reactions are converted to irreversible form (to account for sensitivity of independent forward and reverse directions of each reaction. Reverse rate coefficient can be found by thermodynamic calculations). Next a sensitivity matrix is generated based on perturbation of rate coefficient one reaction at a time and finding its effect on a set of important products' mole fractions[34]. $S=[\partial \ln(y_i)/\partial \ln(k_j)]_{i,j}$ where 'i' is an important product and 'j' is reaction number. An eigenvector decomposition of $S^T S$ is done using MATLAB commands. From this, we get eigenvalues corresponding to each reaction. The magnitude of eigenvalue is proportional to the importance of that particular reaction for the overall product spectrum of interest. Based on this, the top ~ 1500 important reactions are chosen and the mechanism is recast in reversible form to make it around 800 reversible reactions. Independently, this was also done using ChemKin-PRO where sensitivities are calculated in rate of production analysis. Reaction path analysis shows no loss of information of dominant reactions due to the compression of the model. This was later re-verified by actual simulation of experiments.

Table 1: Reaction families considered in this work

Reaction family	Description/ Example	Kinetics	Constraint on carbon number
Hydrogen transfer		Reference	Objective – to limit C no. to 10
Inter-molecular H-abstraction	by C• by H•	26	10 for molecule, 4 for C• radical
Intra-molecular H-abstraction (acyclics)	C-(C)$_n$-C• ⇌ •C-(C)$_n$-C	20	10 for C• radical
Intra-molecular H-abstraction (cyclics)	=	22, 23	10 for cyclic C• radical
Intra-CPD-H-shift	⇌	23	7 (includes methyl and ethyl CPD)
Addition			
Inter-molecular C-radical addition	C=C + •C ⇌ •C-C-C	27	6 for molecule, 4 for C• radical
Intra-molecular C-radical addition		22, 23	10 for C• radical (naphthalene routes)
Hydrogen atom addition	•C-C-H ⇌ C=C+ •H	28	10 for C• radical
Recombination			
C-C recombination	•C + •C ⇌ C-C	20, 22, 23	4 for C• radical
C-H recombination	•C + H ⇌ C-H	20, 22, 23	5 for C• radical
H2 elimination			
Direct release of H2 gas	⇌ + H2	23, 29	Cyclopentene molecule
Diels-Alder			
Molecular mechanism – rearrangement of double bonds	+ ⇌	23	Specific to ethylene and BD substrates

The in-house automatic mechanism generation tool, "Genesys" [11] was used to generate the mechanism. The C_0-C_4 base chemistry has been completely generated in-house using Genesys. Genesys contains large databases of thermodynamic and kinetic parameters from ab initio sources and uses these as primary source for the assignment of parameters during the kinetic model generation. If no entry is present in these databases for thermodynamic properties or kinetics, these are estimated by group additivity methods. A detailed example of how these group additive methods work is given in Chapter 4. The aromatics chemistry is based on various literature sources. The ethane pyrolysis model of Sabbe et al.[20] contains ab-initio kinetics of elementary reactions leading to benzene formation starting from 1,3-butadiene and vinyl radical. Merchant's model for the pyrolysis of cyclopentadiene-ethene mixture[23] has the kinetics for H-shift reactions, most importantly that concerning the 1,3-cyclopentadiene moiety and many reactions of intra-molecular carbon radical addition from which group additive values were derived and made part of Genesys databases, as discussed in detail in Chapter 4. These groups of reactions play an important role in ring formation and ring expansion, ultimately leading to the formation of aromatics higher than benzene like toluene, styrene, indene and naphthalene. In Genesys, the size of the kinetic model is controlled by a rule based termination criterion. starting from the user-defined reaction families and the initial feed molecules, an exhaustive mechanism is generated which is terminated by the user-defined constraints on product species, e.g. constraints on the maximum carbon number allowed, and constraints on the reaction families, e.g. limiting the size of the abstracting and adding species. The reaction families are defined by the user in Genesys by supplying a reaction recipe, the possible reactive center by the user-friendly SMARTS language and constraints on the appearance of the reaction family or the products formed by this reaction family. The reaction families, and an example of how the iterations take place in Genesys is discussed in Chapter 4. Polycyclic aromatic hydrocarbons were limited up to naphthalene. Algorithmic details about mechanism generation using Genesys, including schematics can be found in [11]. Also, predictions of popular models in literature – POLIMI (Ranzi)[24], CSM[22], Hefei[12] and AramcoMech models have been compared with those of the new model, so as to check if the new high pressure limit automatic mechanism compares well with existing optimized literature models.

2.3. Results and discussion

2.3.1 Experimental data and model trends for propane pyrolysis

Experimental results of the main products of propane pyrolysis and model trends of Genesys, Ranzi[24], CSM[22], Hefei[12] and Aramco[25] models are shown in Figure 2.1. and Figure 2.2. It can be seen that the conversion trends of Genesys and Aramco models are the best for propane pyrolysis. Ranzi overpredicts conversion, while CSM and Hefei underpredict it. Ethylene predictions of CSM, Ranzi and Genesys are good, while Hefei overpredicts it and Aramco underpredicts it. Methane is slightly underpredicted by Genesys and Aramco while the other 3 models are good. Propylene trends is captured well by all models, but CSM and Ranzi show better predictions. Butadiene is best predicted by Genesys and Ranzi, followed by CSM. Hefei and Aramco overpredict it. Genesys is the best model for ethane, acetylene, toluene, benzene and hydrogen. For these products, CSM and Ranzi make reasonable predictions, while Hefei and Aramco mechanisms are not good.
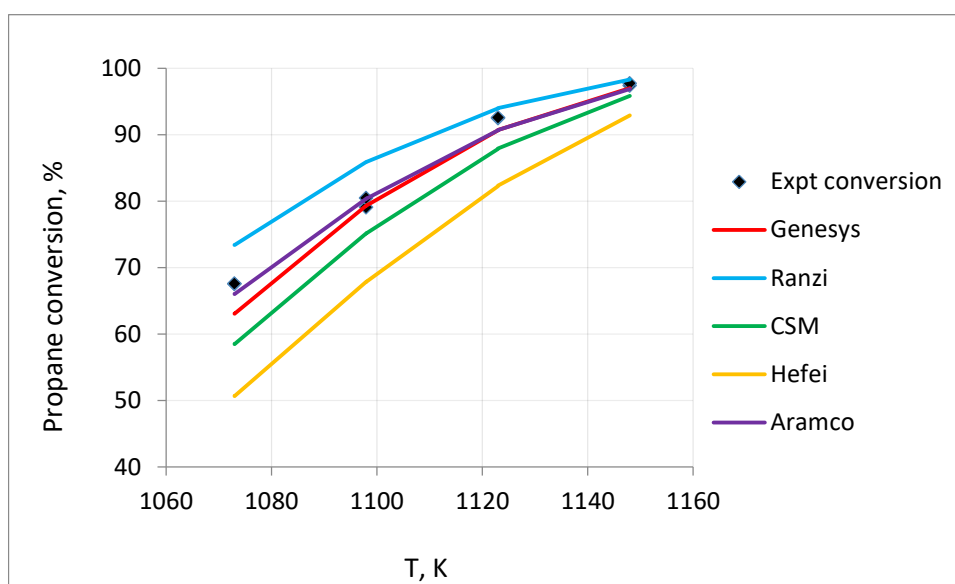
Figure 2.1: Propane conversion % vs. temperature, K: LCT experiment vs. models (temperature is the average of measured temperature in the isothermal region of reactor temperature profile)
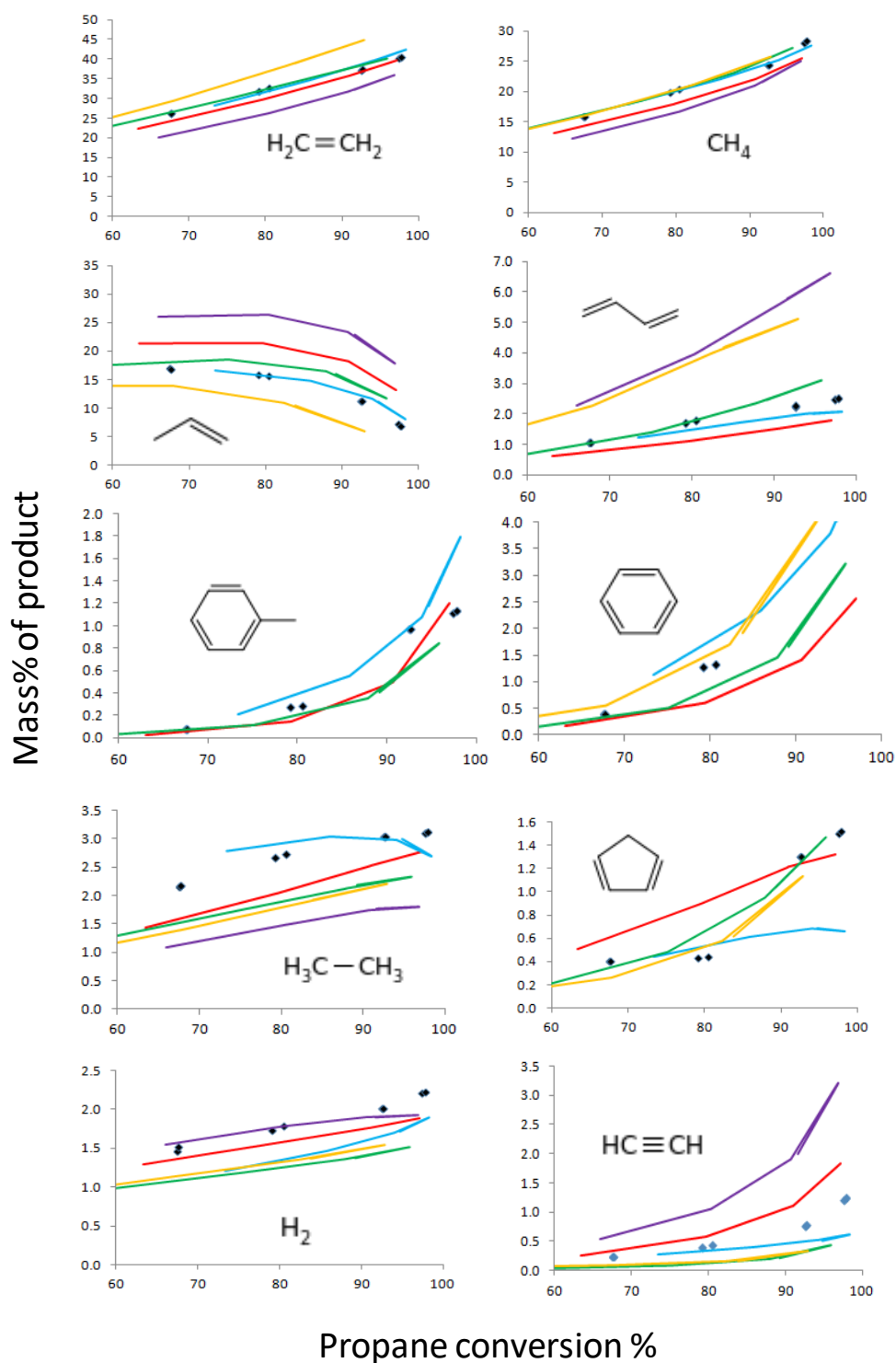
Figure 2.2: LCT experimental trends vs. Model predictions for propane pyrolysis. X-axis=propane conversion %, Y-axis=product mass%. Legends: ◆ **Experiment,** —— **Genesys,** —— **Ranzi,** —— **CSM,** —— **Hefei,** —— **Aramco**

A rate of production analysis was carried out to identify the dominant reaction pathways for the different kinetic models. From this analysis the following conclusions can be drawn:

Propane conversion routes:- Propane is converted primarily by H-assisted abstraction to i-propyl and n-propyl, followed by homolytic scission to methyl and ethyl radicals. The next dominant routes are hydrogen abstractions by methyl, allyl and ethyl. It is to be noted that the hydrogen abstractions take place to preferably form iso-propyl instead of n-propyl.

Propylene formation:- The iso-propyl radical formed at the initiation step loses a hydrogen atom via C-H β-scission, thereby giving propylene. In this route, the C-H β-scission of n-propyl is not dominant because it would rather form ethylene and methyl by C-C β-scission.

Ethylene formation:- The C-C β-scission of n-propyl radical gives methyl and ethylene. The ethyl radical formed via the homolytic scission of propane also can undergo a C-H β-scission to form ethylene. However, the former route is more dominant.

Methane formation:- Both ethylene and propylene formation are linked to the initial decomposition of propane to propyl radicals, hence these are some of the major products. Since methyl radical is also formed in the initial decomposition steps (homolytic scission of propane and C-C β-scission of n-propyl), the eventual methane formed by CH3-assisted abstraction is also a major product. Methyl abstracts from propane, hydrogen, propylene and ethylene majorly.

Benzene formation:- Vinyl radical adds on to butadiene to form hexadienyl radical. This undergoes ring formation and loses a H-atom to form cyclohexadiene. This undergoes H-abstraction and C-H β-scission to form benzene.

Cyclopentadiene formation:- Allyl radicals are formed by hydrogen abstraction of propylene. These allyl radicals recombine to form di-allyl (1,5-hexadiene), which on hydrogen atom addition gives hex-1-en-5-yl radical. This undergoes ring formation to give methyl cyclopentyl which on C-H β-scission gives 3-methyl cyclopentene. 3-methyl cyclopentene preferably loses methyl radical to form resonantly stabilized cyclopentenyl radical, which in turn forms 1,3-cyclopentadiene by C-H β-scission.

Ethane formation:- Ethyl radical formed in the initiation step of propane cracking abstracts a hydrogen atom from substrates like H_2, propane, propylene to give ethane. It is also formed from the recombination of methyl radicals which in turn are formed in the initial decomposition step.

Butadiene formation:- This has 3 major routes. The 1st is from the recombination of methyl and allyl to give 1-butene. This undergoes hydrogen abstraction to give resonantly stabilized butenyl radical, which on C-H β-scission gives 1,3-butadiene. The 2nd route is via C-C β-scission of allylic 1-pentenyl radical. This is formed from the recombination of allyl and ethyl radicals to give 1-pentene which in turn undergoes hydrogen abstraction at the allylic location. The 3rd route is via the addition of methyl radical to propylene to form 2-butyl radical. This on C-H β-scission gives 2-butene. 2-butene undergoes hydrogen abstraction to form allylic butenyl radical, which on C-H β-scission gives 1,3-butadiene.

Hydrogen formation:- H-atom abstracts hydrogen from propane to give the two propyl radicals, thereby forming H_2. H-atom is in turn produced from the 2-propyl radical and ethyl radical via C-H β-scission.

Acetylene formation:- Propylene undergoes hydrogen abstraction to give prop-1-en-1-yl radical. This, on C-C β-scission gives acetylene and methyl radical. Another dominant route is through the hydrogen abstraction of ethylene to form vinyl and subsequent C-H β-scission to give acetylene.

Toluene formation:- Methyl adds on to benzene to give the required structure. The resulting radical loses hydrogen by C-H β-scission to give toluene.

The dominant reaction paths for propane pyrolysis are shown in Figure 2.3.
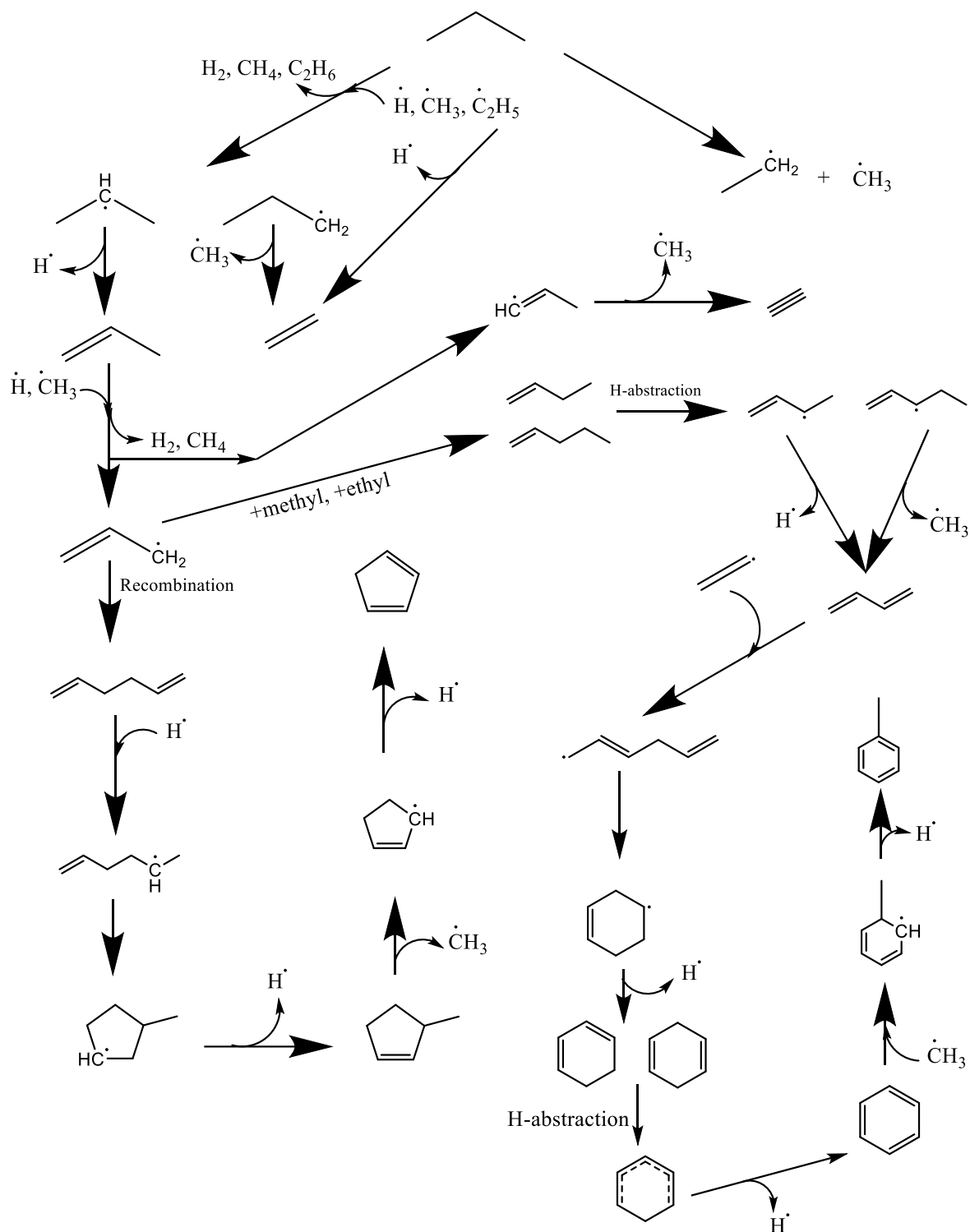
Figure 2.3: Dominant reaction paths in propane pyrolysis

2.3.2 Experimental data and model trends for n-butane pyrolysis

Experimental results of the main products of n-butane pyrolysis and model trends of Genesys, Ranzi[24], CSM[22] and Hefei[12] models are shown in Figures 2.4 and 2.5. For n-butane conversion trends, Genesys, CSM and Aramco mechanisms are the best predictors. Hefei model overpredicts the conversion while Ranzi underpredicts it. Methane trend is predicted well by all models, ethylene too except for Aramco that underpredicts ethylene. Propylene trend is captured by all models but the accuracy is best for Ranzi and Hefei models. Benzene can be considered equally well predicted by all models, while for butadiene, Genesys is the best, followed by Ranzi and then CSM. Hefei and Aramco overpredict butadiene. Acetylene is best predicted by Genesys while Aramco overpredicts it and all others underpredict it. Toluene and cyclopentadiene are best predicted by Genesys. Aramco does not predict these 2 products while Hefei does not predict toluene. A rate of production analysis was carried out to identify the dominant reaction pathways for the different kinetic models. From this analysis the following conclusions can be drawn:
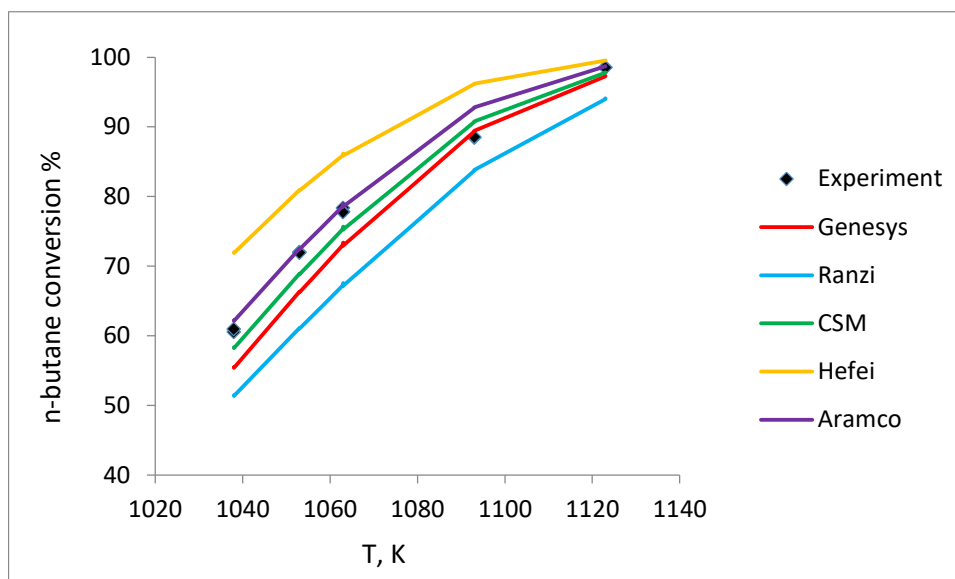
Figure 2.4: n-butane conversion % vs. temperature, K: LCT experiment vs. models (temperature is the average of measured temperature in the isothermal region of reactor temperature profile)
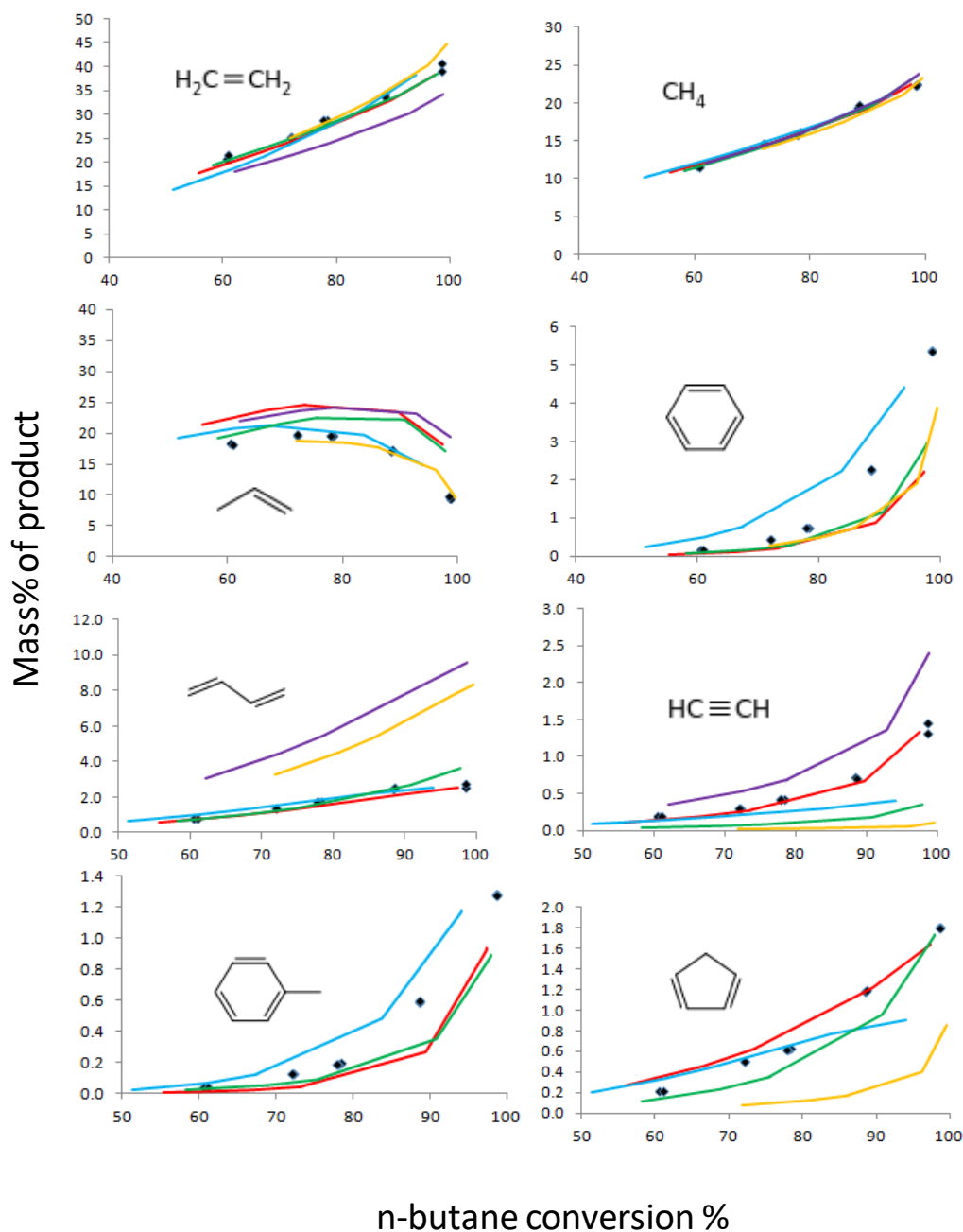
Figure 2.5: LCT experimental trends vs. Model predictions for n-butane pyrolysis. X-axis=n-butane conversion %, Y-axis=product mass%. Legends: ◆ **Experiment,** —— **Genesys,** —— **Ranzi,** —— **CSM,** —— **Hefei,** —— **Aramco**

n-butane conversion routes:- n-butane is converted by H- and CH3-assisted abstraction to i-butyl and n-butyl, followed by homolytic scissions to give 2 ethyl radicals and methyl and propyl radicals. It is to be noted that the hydrogen abstractions take place to preferably form i-butyl instead of n-butyl.

Ethylene formation:- Ethylene is formed by 3 equally dominant routes. The propyl radical that is formed from the homolytic scission of n-butane undergoes C-C β-scission to give ethylene and methyl radical. The other homolytic scission of n-butane which gives ethyl radical is also important, as this ethyl undergoes C-H β-scission to give ethylene. In addition, the H-abstraction of n-butane to form 1-butyl radical is important, as this does a C-C β-scission to give ethylene and ethyl. Since all of these come in the primary decomposition routes, ethylene is one of the major products of n-butane pyrolysis.

Propylene formation:- In the H-abstraction of n-butane, 2-butyl is preferably formed compared to 1-butyl. This 2-butyl undergoes C-C β-scission to give propylene, another major product.

Methane formation:- Methane is formed by the CH_3-assisted hydrogen abstraction. CH_3 is in turn formed in the routes forming ethylene, propylene and decomposing n-butane, as discussed above. Methane, being produced in the primary decomposition is another major product of n-butane pyrolysis.

Butadiene formation:- Initial H-abstraction of n-butane gives 2-butyl radical. C-H β-scission of 2-butyl gives 2-butene (though it is less preferred compared to C-C β-scission leading to propylene). H-abstraction on 2-butene in the allylic position gives allylic butenyl radical. This allylic butenyl radical loses a H-atom by C-H β-scission to form 1,3-butadiene.

Benzene formation:- Vinyl radical is formed by H-abstraction on ethylene. This vinyl radical adds on to butadiene to form hexadienyl radical. This undergoes ring formation and loses a H-atom to form cyclohexadiene. This undergoes H-abstraction and C-H β-scission to form benzene.

Acetylene formation:- Propylene undergoes H-abstraction to form the prop1-en-1-yl radical. This undergoes C-C β-scission to form acetylene. Another dominant route is through the hydrogen abstraction of ethylene to form vinyl and subsequent C-H β-scission to give acetylene.

<u>Cyclopentadiene formation</u>:- Propylene undergoes H-abstraction to preferably form allyl. This allyl adds on to propylene to give hex-1-en-5-yl radical. This undergoes ring formation to give methyl cyclopentyl, which on C-H β-scission forms 3-methyl cyclopentene. This loses the methyl branch to form allylic cyclopentenyl radical. This loses H-atom by C-H β-scission to give 1,3-cyclopentadiene.

<u>Toluene formation</u>:- Toluene formation route is identical to that in propane pyrolysis (by methyl addition to benzene and C-H β-scission).

The dominant reaction paths for n-butane pyrolysis are shown schematically in Figure 2.6.
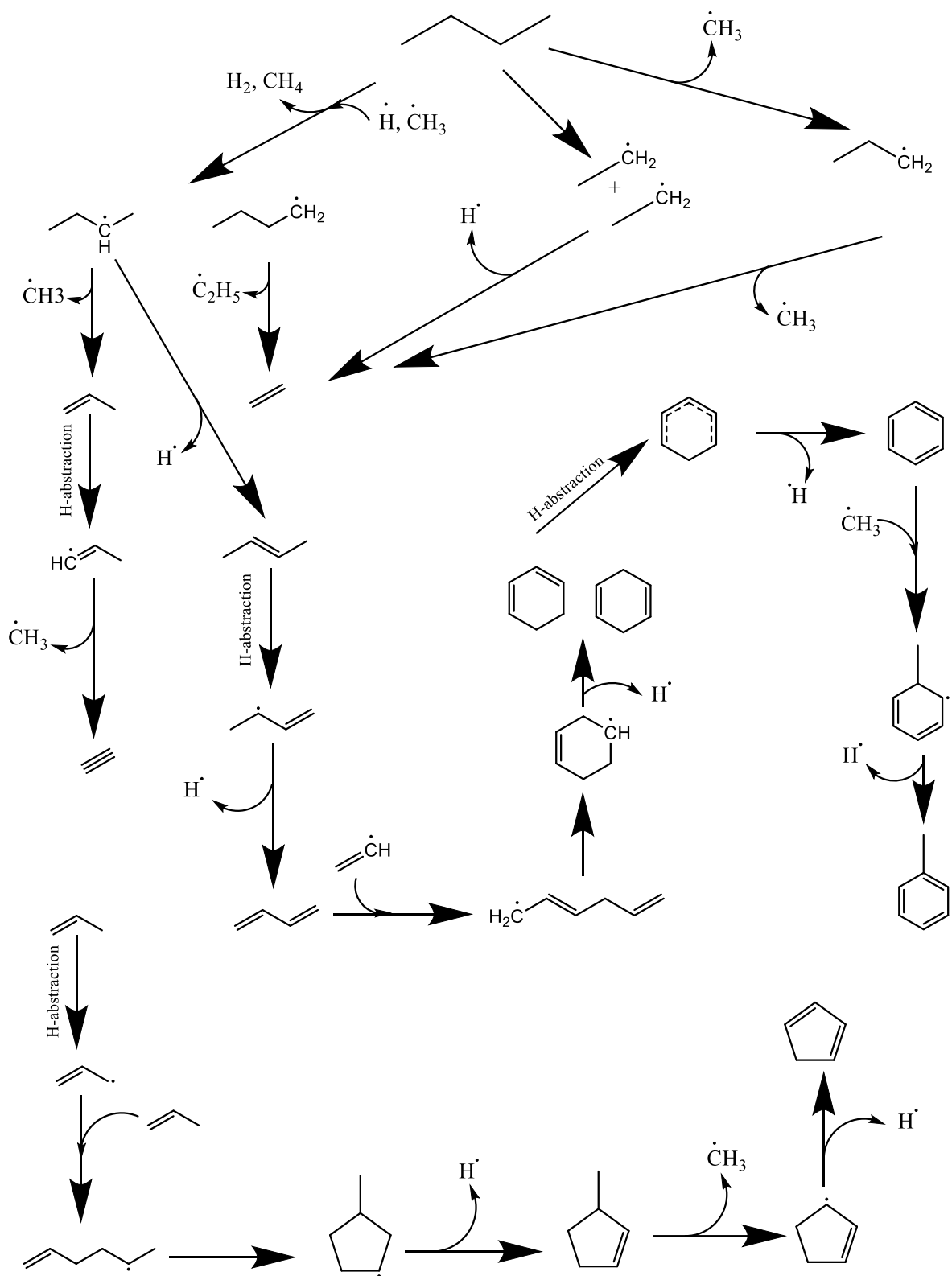
Figure 2.6: Dominant reaction paths in n-butane pyrolysis

2.3.3 Experimental data and model trends for iso-butane pyrolysis

Experimental results of the main products of iso-butane pyrolysis and model trends of Genesys, Ranzi[24], CSM[22] and Hefei[12] models are shown in Figure 2.7 and Figure 2.8. Conversion of iso-butane is best predicted by Aramco and CSM, followed by Genesys.. Ranzi and Hefei's predictions are less accurate than these models. Methane is predicted well by all except Hefei which undepredicts it. Isobutene trend is captured best by Genesys, Ranzi and CSM, while Hefei overpredicts it and Aramco underpredicts it. Ranzi predicts ethylene best while other models underpredict it. For propylene, Ranzi and Genesys are the best while others overpredict it. Benzene and toluene are underpredicted by Genesys for which products, CSm and Ranzi models are better. Genesys gives the best predictions for butadiene, hydrogen, acetylene and cyclopentadiene. A rate of production analysis was carried out to identify the dominant reaction pathways for the different kinetic models. From this analysis the following conclusions can be drawn:
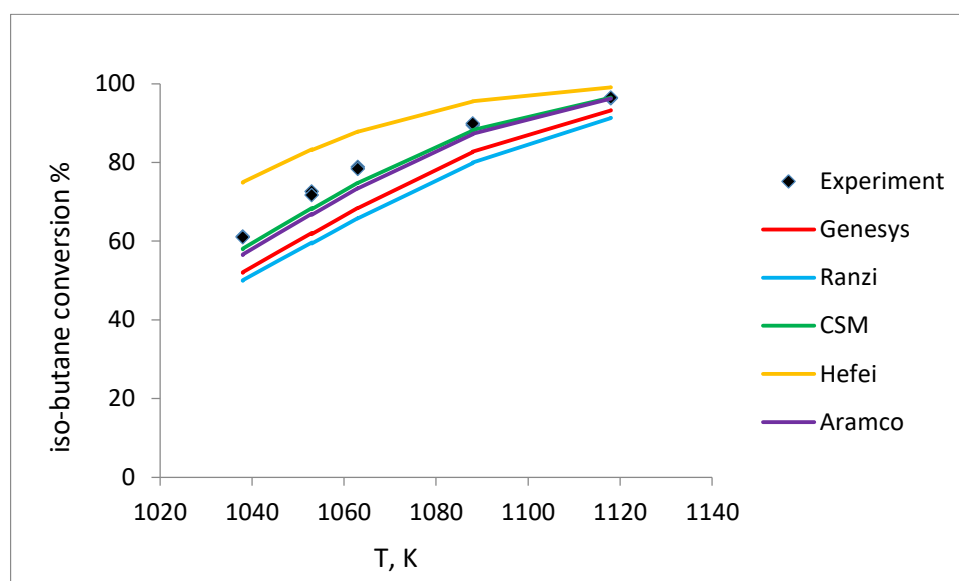
Figure 2.7: iso-butane conversion % vs. temperature, K: LCT experiment vs. models (temperature is the average of measured temperature in the isothermal region of reactor temperature profile)
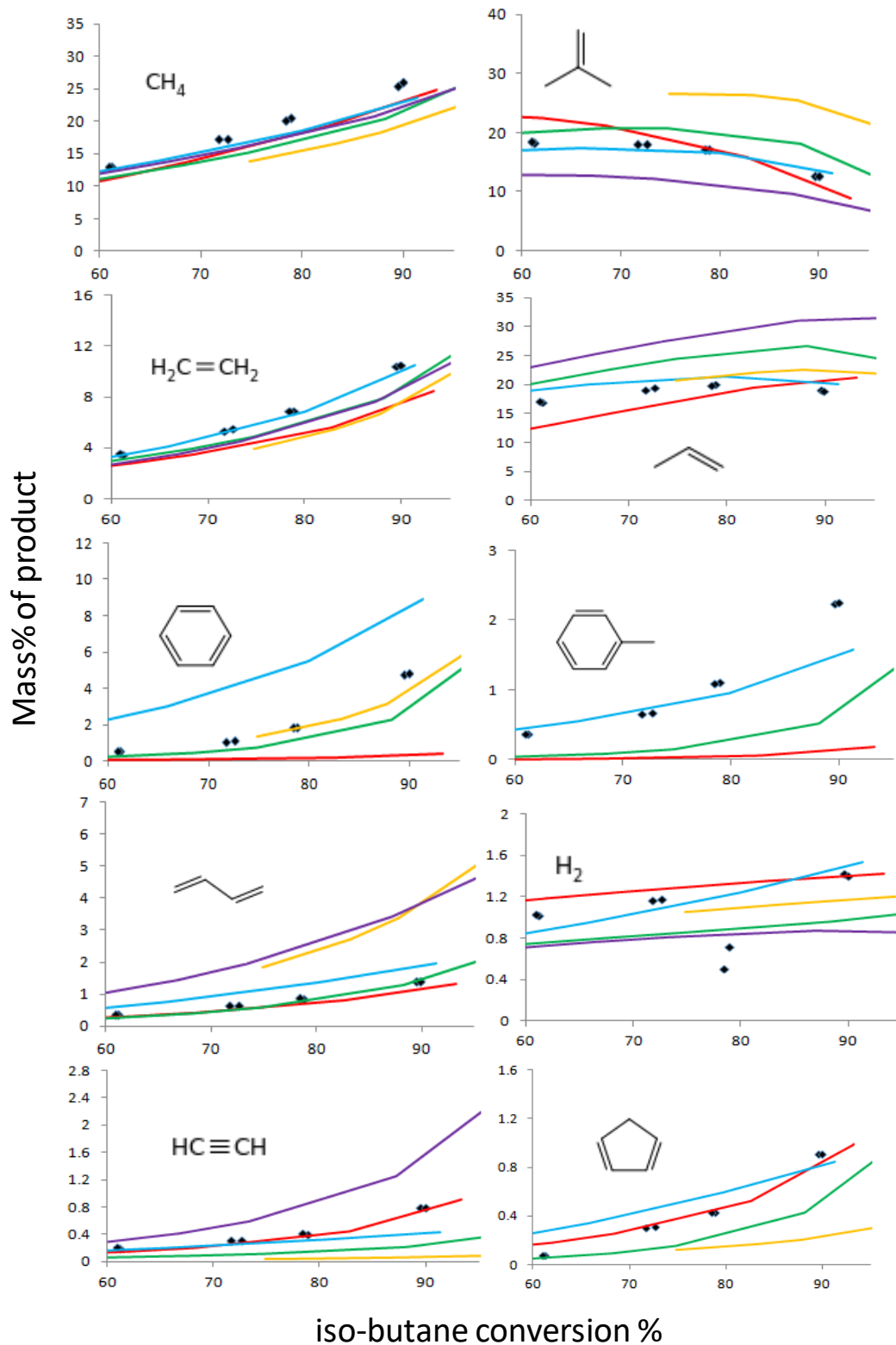
Figure 2.8: LCT experimental trends vs. Model predictions for iso-butane pyrolysis.

X-axis=iso-butane conversion %, Y-axis=product mass%. Legends: ◆ Experiment,

Genesys, Ranzi, CSM, Hefei, Aramco

iso-butane conversion routes:- iso-butane is converted primarily by CH3- and H-assisted abstraction to tertiary and primary isobutyl radicals. Another major route is the homolytic scission of iso-butane to give methyl radical and isopropyl radical. Due to the initial decomposition leading to methyl, isopropyl and isobutyl radicals, the major products are methane, propylene and isobutene.

Ethylene formation:- Ethylene is indirectly formed from propylene. Hydrogen addition to propylene leads to 1-propyl radical, which undergoes C-C β-scission to give ethylene and methyl radical.

Propylene formation:- Propylene is formed by mainly 2 routes. The dominant among these 2 is the C-C β-scission of primary isobutyl radical to give propylene and methyl radical. The other route is by the C-H β-scission of 2-propyl radical formed in the homolytic scission of iso-butane.

Methane formation:- Methane is formed by the CH3-assisted H-abstraction of iso-butane mainly.

Isobutene formation:- Isobutene is mainly formed by the C-H β-scission of tertiary isobutyl radical.

Cyclopentadiene formation:- Due to the large presence of propylene and allyl radicals, addition reaction takes place to form hex-1-en-5-yl radical. This undergoes ring formation to give methyl cyclopentyl radical, and an eventual loss of H-atom to give 3-methyl cyclopentene. This loses the methyl branch and further H-atom by C-H β-scission to give cyclopentadiene (like in the case of n-butane cracking).

Hydrogen formation:- Hydrogen molecule is formed during the H-assisted hydrogen abstractions. H-atom is mainly produced by the C-H β-scission of tertiary iso-butyl. This is because the tertiary is-butyl cannot undergo C-C β-scission.

Benzene formation:- Vinyl radical adds on to butadiene to form hexadienyl radical. This undergoes ring formation and loses a H-atom to form cyclohexadiene. This undergoes H-abstraction and C-H β-scission to form benzene.

Toluene formation:- Toluene is formed in the same way as in n-butane cracking – by the methyl addition of benzene and an eventual H-atom loss by C-H β-scission.

1,3-butadiene formation:- Owing to the excess concentration of methyl and C3 olefinic radicals in the radical pool (as these are produced in the initial stages of iso-butane

decomposition), methyl recombines with allyl to give 1-butene. H-abstraction at the allylic position of 1-butene and an eventual C-H β-scission leads to 1,3-butadiene.

Ethane formation:- Recombination of 2 methyl radicals leads to ethane.

Acetylene formation:- Like in the case of n-butane cracking, H-abstraction of propylene at the 1st double bonded carbon atom and eventual C-C β-scission leads to acetylene. A less dominant route is via C-H β-scission of vinyl radical.

The dominant reaction paths for n-butane pyrolysis are shown in Figure 2.6.
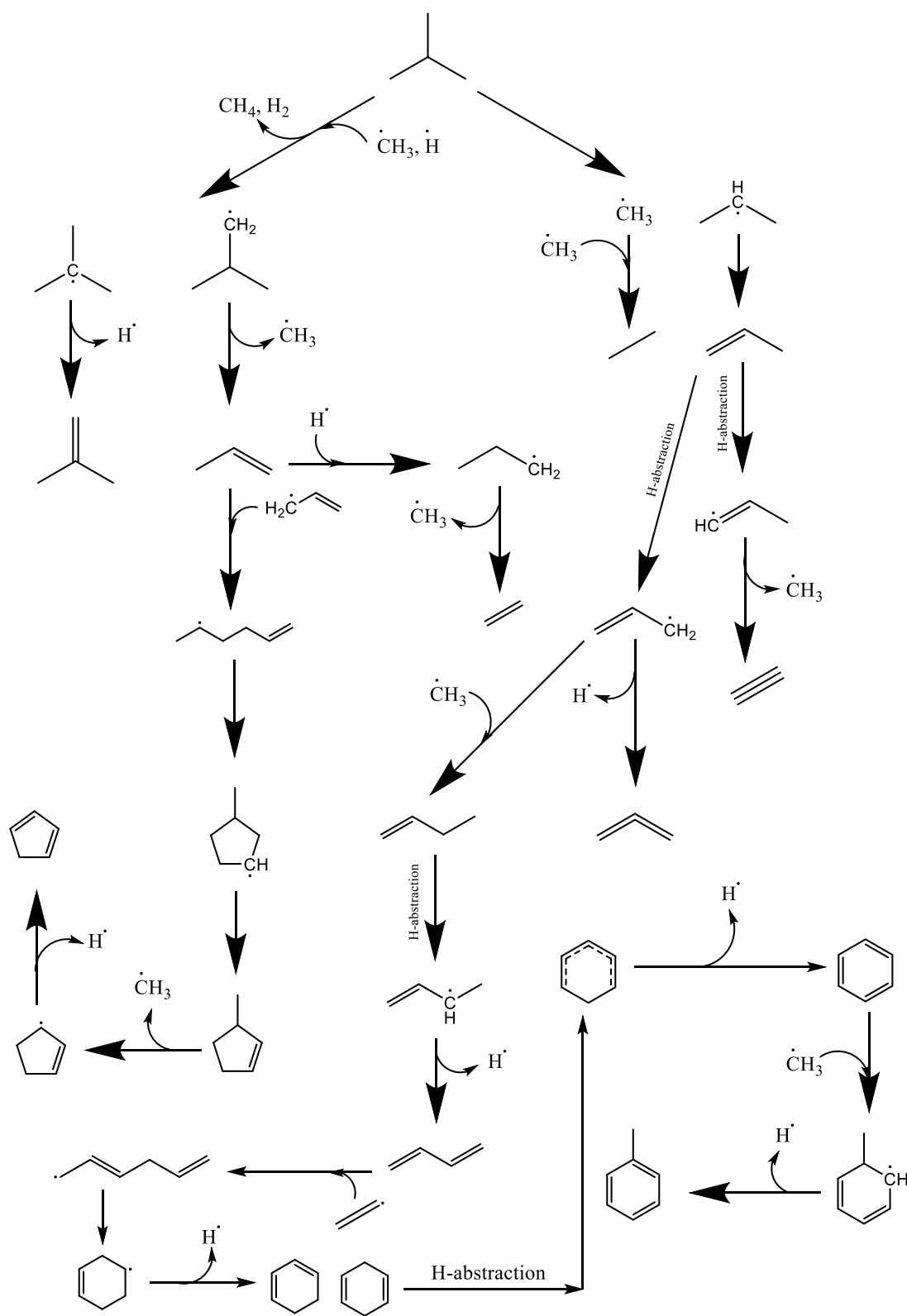
Figure 2.9: Dominant pathways for iso-butane pyrolysis

2.4. Experimental data of Hefei on n-butane and iso-butane pyrolysis

Hefei generated experimental data on n-butane and iso-butane pyrolysis[12] in which the feed hydrocarbon was present at a dilution of 2 mol%. The reactor peak temperature varied from 861 to 1347 K. The feed flow rate was $1.67*10^{-5}$ standard cubic meter per second. The reactor was operated at 3 different pressures – 0.00405 MPa, 0.0203 MPa and 0.1013 MPa. The reactor diameter was 0.007 m and length was 0.225 m. Figure 2.10 shows the experimental conversion trends for both n-butane and iso-butane feeds pyrolysis at the 3 pressures and how the LCT model and other models predict those trends. Figure 2.11 shows the pyrolysis trends for n-butane and Figure 2.12, for iso-butane. It can be seen that the LCT model makes a reasonable prediction for the Hefei trends. The objective here is to check if a high pressure limit model is able to predict the data from another laboratory at a different pressure and temperature and mass% measurement technique. For these experiment predictions by the different models, it can be seen that Ranzi and CSM models do not predict well for most of the cases. Hefei model is the best, followed by Aramco (especially for n-butane) in most of the cases and Genesys in some. Genesys performs well for iso-butane too. However, for conversions, Ranzi and Genesys both are as good as Hefei and Aramco at low pressures, while CSM underpredicts conversion of n-butane and iso-butane. The good predictions of Hefei model can be understood as the model has been developed for these conditions. Aramco mechanism has pressure dependence built into it hence may be performing well at low pressure experiments. Its performance for n-butane is good, but for iso-butane, it grossly misses the trends. Summarizing, for n-butane Hefei experiments, Hefei model is the best followed by Aramco followed by Genesys. For iso-butane Hefei experiments, Hefei model is the best followed by Genesys followed by CSM and Ranzi. Different models perform well at different conditions, but overall, Genesys holds the middle ground – a reasonable model for all cases – all the more appreciable because it is a purely high pressure limit elementary reaction model generated automatically with pure ab-initio kinetics. Hence, we can see here that such a model can compete well with literature optimized global/ pressure dependent/ fine-tuned models.
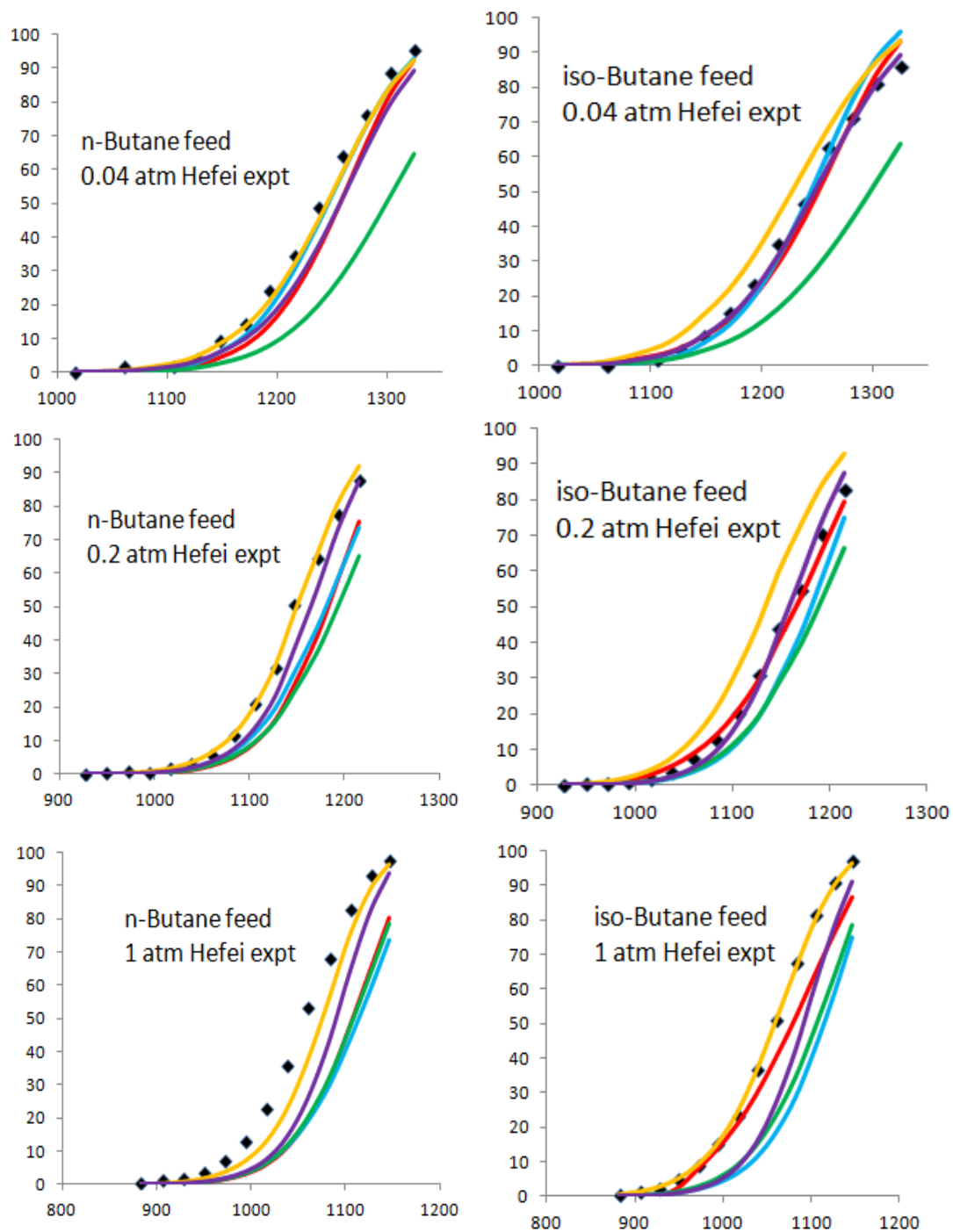
Figure 2.10: Hefei experimental trends vs. Model predictions for n-butane and iso-butane pyrolysis feed conversions at various pressures. X-axis=temperature, K, Y-axis=n-butane/ iso-butane conversion%. Legends: ◆ Hefei experiment, — Genesys, — Ranzi, — CSM, — Hefei, — Aramco
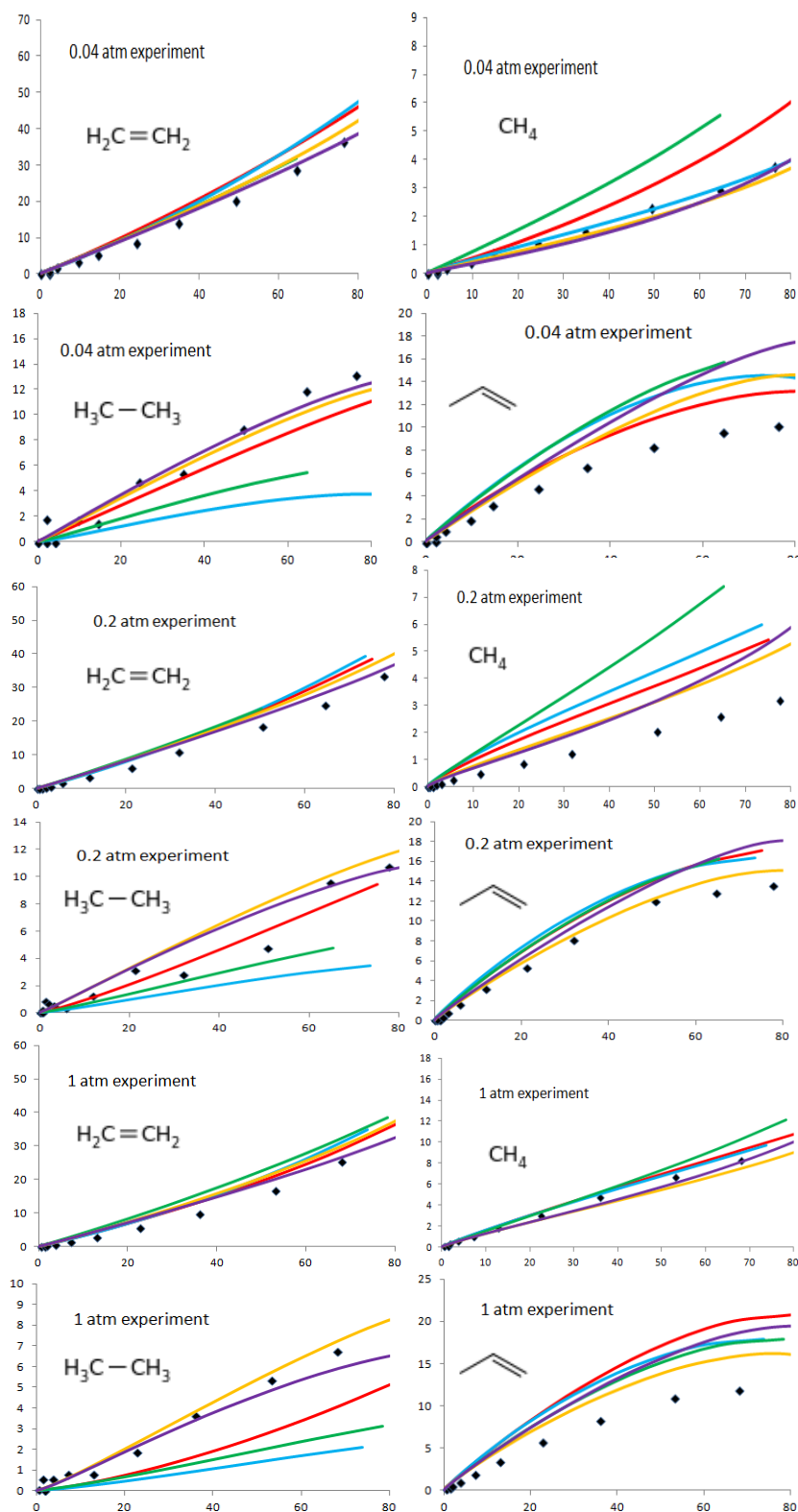
Figure 2.11: Hefei experimental trends vs. Model predictions for n-butane pyrolysis at different pressures. X-axis=n-butane conversion %, Y-axis=product mass%, Legends: ◆ Hefei experiment, — Genesys, — Ranzi, — CSM, — Hefei, — Aramco
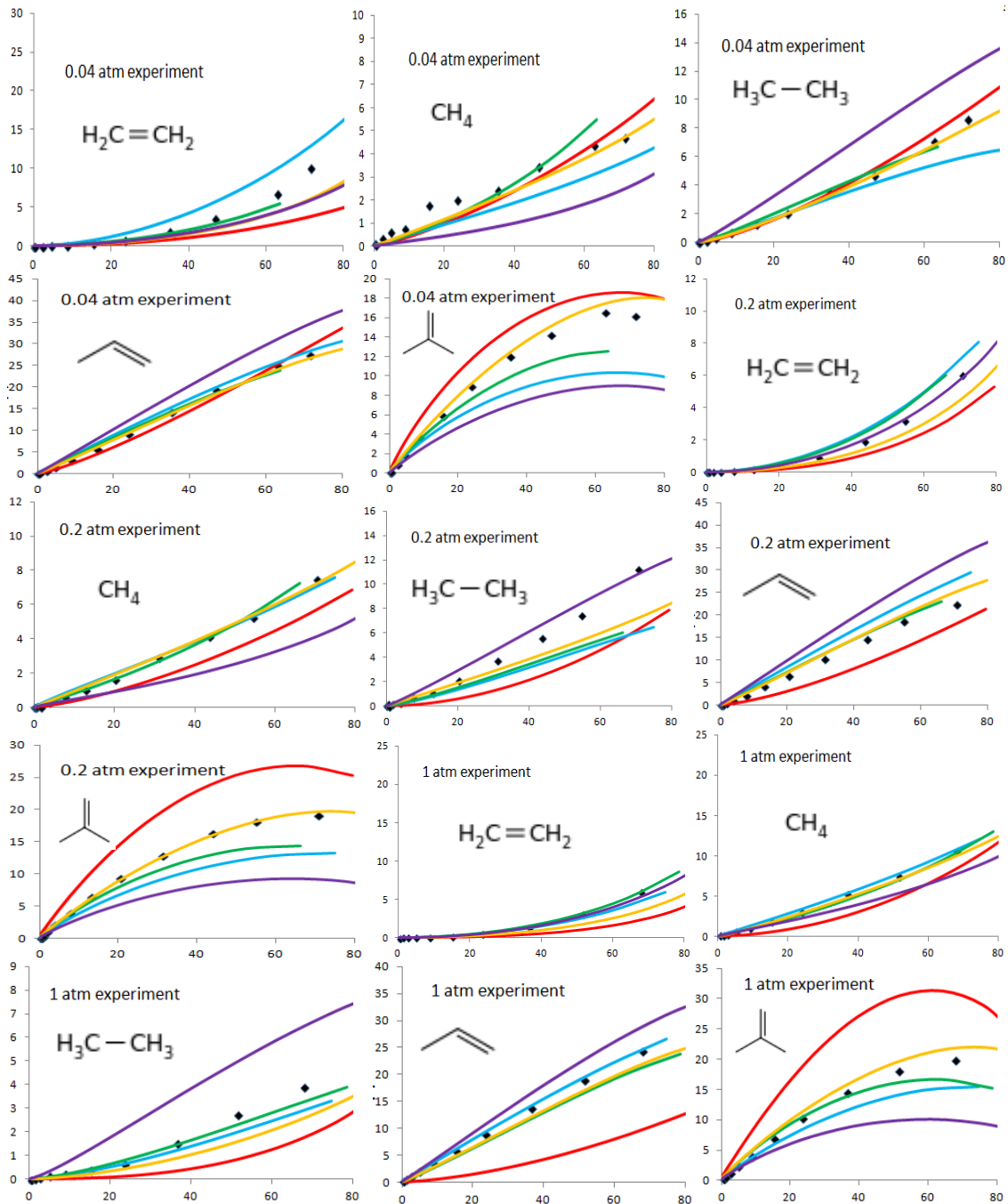
Figure 2.12: Hefei experimental trends vs. Model predictions for iso-butane pyrolysis at different pressures. X-axis=iso-butane conversion %, Y-axis=product mass%, Legends: ◆ Hefei experiment, ── Genesys, ── Ranzi, ── CSM, ── Hefei, ── Aramco

2.5. Conclusions

In this chapter, pyrolysis experimental results were presented for pure propane, n-butane and iso-butane at 1023-1173K, 0.17 MPa, 0.5 s residence time. An automatic reaction mechanism generator software tool - Genesys was used to generate a high pressure limit model to predict pyrolysis of pure feeds propane, n-butane and iso-butane. The model solely consisted of elementary reactions all with ab-initio/group-additive thermodynamics and kinetics with no adjustment of any parameter. This model could make a reasonable prediction of product trends and compared well with other popular optimized literature models – Ranzi, CSM and Hefei models. The new high pressure limit model also performed well for a completely different range of conditions for pyrolysis of n-butane and iso-butane data generated by Hefei lab at 1100-1400K, 0.004 MPa, 50 μ.s residence time. This shows that in spite of not incorporating pressure dependence in the new model, it performs well at extreme ranges of pressure and temperature and residence time, at the same time, it compares well with optimized models from literature. Testing the group additive/ ab-initio automatic mechanism generation methodology for pyrolysis of light gases is a step forward toward convincing the community that this methodology can be reliably extended to more complex systems.

2.6. References

1.Speight, J. G., *Handbook of Industrial Hydrocarbon Processes*. Gulf Professional Publishing: 2010.
2.Van Geem, K. M.; Reyniers, M. F.; Marin, G. B.; Song, J.; Green, W. H.; Matheu, D. M., Automatic reaction network generation using RMG for steam cracking of n-hexane. *Aiche Journal* **2006,** 52, (2), 718-730.
3.Kossiakoff, R., Thermal decomposition of hydrocarbons, resonance stabilisation and isomerization of free radicals. *J Am Chem Soc.* **1943,** 65.
4.Rice, The thermal decomposition of organic compounds from the standpoint of free radicals I. Saturated hydrocarbons. *J Am Chem Soc.* **1931,** 53.
5.Rice, The thermal decomposition of organic compounds from the standpoint of free radicals III. The calculation of the products formed from paraffin hydrocarbons. *J Am Chem Soc.* **1933,** 55.
6.Rice, H., The thermal decomposition of organic compounds from the standpoint of free radicals VI. The mechanism of some chain reactions. *J Am Chem Soc.* **1934**, (56).

7.Clymans, P. J.; Froment, G. F., Computer-generation of reaction paths and rate-equations in the thermal-cracking of normal and branched paraffins. *Comput. Chem. Eng.* **1984,** 8, (2), 137-142.

8.Hillewaert, L. P.; Dierickx, J. L.; Froment, G. F., Computer-generation of reaction schemes and rate-equations for thermal-cracking. *Aiche J.* **1988,** 34, (1), 17-24.

9.Ranzi, E.; Dente, M.; Plerucci, S.; Biardi, G., Initial producr distributions from pyrolysis of normal and branched paraffins. *Industrial & Engineering Chemistry Fundamentals* **1983,** 22, (1), 132-139.

10.Zador, J.; Zsely, I. G.; Turanyi, T.; Ratto, M.; Tarantola, S.; Saltelli, A., Local and global uncertainty analyses of a methane flame model. *J. Phys. Chem. A* **2005,** 109, (43), 9795-9807.

11.Vandewiele, N. M.; Van Geem, K. M.; Reyniers, M. F.; Marin, G. B., Genesys: Kinetic model construction using chemo-informatics. *Chemical Engineering Journal* **2012,** 207, 526-538.

12.Li, W.; Wang, G. Q.; Li, Y. Y.; Li, T. Y.; Zhang, Y.; Cao, C. C.; Zou, J. B.; Law, C. K., Experimental and kinetic modeling investigation on pyrolysis and combustion of n-butane and i-butane at various pressures. *Combustion and Flame* **2018,** 191, 126-141.

13.Djokic, M. R.; Van Geem, K. M.; Cavallotti, C.; Frassoldati, A.; Ranzi, E.; Marin, G. B., An experimental and kinetic modeling study of cyclopentadiene pyrolysis: First growth of polycyclic aromatic hydrocarbons. *Combustion and Flame* **2014,** 161, (11), 2739-2751.

14.Pyl, S. P.; Van Geem, K. M.; Puimege, P.; Sabbe, M. K.; Reyniers, M. F.; Marin, G. B., A comprehensive study of methyl decanoate pyrolysis. *Energy* **2012,** 43, (1), 146-160.

15.Giddings, J. C.; Cortes, H. J., *Multidimensional Chromatography - Techniques and Applications*. Marcel Dekker: New York, 1990.

16.Giddings, J. C., Sample dimensionality - A predictor of order-disorder in component peak distribution in multidimensional separation. *Journal of Chromatography A* **1995,** 703, (1-2), 3-15.

17.Phillips, J. B.; Beens, J., Comprehensive two-dimensional gas chromatography: a hyphenated method with strong coupling between the two dimensions. *Journal of Chromatography A* **1999,** 856, (1-2), 331-347.

18.Dalluge, J.; Beens, J.; Brinkman, U. A. T., Comprehensive two-dimensional gas chromatography: a powerful and versatile analytical tool. *Journal of Chromatography A* **2003,** 1000, (1-2), 69-108.

19.Liu, Z. Y.; Phillips, J. B., Comprehensive 2-dimensional gas chromatography using an on-column thermal modulator interface. *Journal of Chromatographic Science* **1991,** 29, (6), 227-231.

20.Sabbe, M. K.; Van Geem, K. M.; Reyniers, M. F.; Marin, G. B., First Principle-Based Simulation of Ethane Steam Cracking. *Aiche Journal* **2011,** 57, (2), 482-496.

21.Sirjean, B.; Glaude, P. A.; Ruiz-Lopez, M. F.; Fournet, R., Detailed kinetic study of the ring opening of cycloalkanes by CBS-QB3 calculations. *Journal of Physical Chemistry A* **2006,** 110, (46), 12693-12704.

22.Wang, K.; Villano, S. M.; Dean, A. M., Fundamentally-based kinetic model for propene pyrolysis. *Combustion and Flame* **2015,** 162, (12), 4456-4470.

23.Merchant, S. Molecules to Engines: Combustion chemistry of Alcohols and their application to advanced engines. MIT, 2015.

24. Ranzi, E.; Frassoldati, A.; Grana, R.; Cuoci, A.; Faravelli, T.; Kelley, A. P.; Law, C. K., Hierarchical and comparative kinetic modeling of laminar flame speeds of hydrocarbon and oxygenated fuels. Progress in Energy and Combustion Science 2012, 38, (4), 468-501.

25. Y. Li, C-W. Zhou, K.P. Somers, K. Zhang, H.J. Curran The Oxidation of 2-Butene: A High Pressure Ignition Delay, Kinetic Modeling Study and Reactivity Comparison with Isobutene and 1-Butene Proceedings of the Combustion Institute (2017) 36(1) 403–411.

26. Sabbe, M. K.; Vandeputte, A. G.; Reyniers, M. F.; Waroquier, M.; Marin, G. B., Modeling the influence of resonance stabilization on the kinetics of hydrogen abstractions. Physical Chemistry Chemical Physics 2010, 12, (6), 1278-1298.

27. Sabbe, M. K.; Reyniers, M. F.; Van Speybroeck, V.; Waroquier, M.; Marin, G. B., Carbon-centered radical addition and beta-scission reactions: Modeling of activation energies and pre-exponential factors. Chemphyschem 2008, 9, (1), 124-140.

28. Sabbe, M. K.; Reyniers, M. F.; Waroquier, M.; Marin, G. B., Hydrogen Radical Additions to Unsaturated Hydrocarbons and the Reverse beta-Scission Reactions: Modeling of Activation Energies and Pre-Exponential Factors. Chemphyschem 2010, 11, (1), 195-210.
29. Fascella, S.; Cavallotti, C.; Rota, R.; Carra, S., Quantum chemistry investigation of key reactions involved in the formation of naphthalene and indene. Journal of Physical Chemistry A 2004, 108, (17), 3829-3843.
30. Zhang et al., Product Identification and Mass Spectrometric Analysis of n-Butane and i-Butane Pyrolysis at low Pressure. Chinese Journalof Chemical Physics, 2013, 26, 2, 151-156.
31. Pyun et al., Methane and ethylene time-history measurements in n-butane and n-heptane pyrolysis behind reflected shock waves, Fuel, 2013, 108, 557-564
32. Tang et al., Pyrolysis of n-butane investigated using synchrotron threshold photoelectron photoion coincidence spectroscopy, RSC Advances, 2017, 7, 46, 28746-28753
33. Shrestha et al., Fuel pyrolysis in a microflow tube reactor-Measurement and modeling uncertainties of ethane, n-butane, and n-dodecane pyrolysis, Combustion and Flame, 2017, 177, 10-23
34. Vajda, Valko and Turanyi, Principal component analysis of kinetic models, International Journal of Chemical Kinetics, 1985, 55-81

3

Group Additive modeling of Cyclopentane pyrolysis

The pyrolysis of cyclopentane is not well established although it is an abundant compound in typical naphtha feedstocks and can be considered a model compound for cyclic fuels. The studies in literature so far have focused primarily on the initial decomposition of cyclopentane in shock tubes. This chapter therefore explores the pyrolysis of cyclopentane in a continuous flow tubular reactor with pure cyclopentane feed at reactor conditions 0.17MPa, 973 to 1073K, and a residence time of 0.5s. Conversions of 5% to 75% were realized while the product concentrations were quantified using two dimensional gas chromatography. A mechanism composed of elementary high pressure limit reactions has been generated using the automatic network generation tool "Genesys". Kinetics of the reactions originate from high level ab-initio calculations and new group additive values derived from ab-initio kinetic data in literature. Overall the Genesys model outperforms the models available in literature and there is a good agreement between model calculated mass fraction profiles and experimental data for 22 products ranging from hydrogen to naphthalene without any adjustments of the kinetic parameters.. Reaction path analysis reveals that cyclopentane consumption is initiated by the unimolecular isomerization to 1-pentene, but overall dominated by hydrogen abstraction reactions by allyl radicals and hydrogen atoms to give cyclopentyl radicals, whose ring opening and further scissions lead to smaller molecules. Dominant routes for the major products are discussed.

3.1. Introduction

Research in pyrolysis of cyclic hydrocarbons is important for industrial processes like fast pyrolysis and steam cracking [1]. There is a huge pressure on the industry to produce fuels and lower olefins more economically than ever before. This implies more optimal operating conditions and using a cheaper feedstock. There is a limit to which the operating conditions can be optimized within the boundary conditions of metal corrosion and coke deposition [2]. The lucrative knob, which is also the topic of one of the most relevant research areas is to explore a cheaper feedstock. Typically, naphthenes and aromatics are undesirable feed components for pyrolysis, hence petrochemical cuts or other sources containing higher quantities of those components are cheap pyrolysis feeds. The tolerance toward naphthenes is relatively higher than for aromatics because of their lower coking tendency. At the same time, the pyrolysis of naphthenes is a relatively unexplored field compared to their linear and branched counterparts [3]. Among the simplest naphthenes, which are the single ring unsubstituted cycloalkanes, the ones most abundantly found in petrochemical feeds like light naphtha are cyclohexane and cyclopentane [4]. Out of these two, the pyrolysis of cyclohexane is a relatively mature research area [5-8]. Surprisingly, the one molecule whose pyrolysis behavior has not been studied in detail so far is cyclopentane. According to the authors' knowledge, no previous work has been published related to the pyrolysis of cyclopentane, more so at steam cracking conditions.

The few literature studies involving pyrolysis of cyclopentane have focused on experimental investigation of auto-ignition and initial decomposition products in shock tubes [9-11]. In order to explain the ignition delay trends, kinetic models have been developed for cyclopentane oxidation. However, such models, though good for ignition delay time predictions, are generally not ideal for pyrolysis because they tend to focus on extremely short residence times, which implies that primarily the initial decomposition characteristics are well captured. Also, the hydrocarbon feed is highly diluted and this is an unrealistic representation of an industrial pyrolysis reaction as the polycyclic aromatic hydrocarbons are not formed at high dilutions and low residence times to the extent that are usually formed in steam cracking for example. Here we discuss a few relevant studies reported so far.

Around four decades ago, Tsang [11] did experiments to find out initial decomposition rates of cyclopentane in a comparative-rate single-pulse shock-tube. In this,

the initial cyclopentane decomposition rate was established after comparing the experiment with that of a standard reaction whose temperature decay characteristics were well known. This was the well-studied retro-Diels-Alder decomposition of cyclohexene feed giving ethylene and 1,3-butadiene. The residence time in the shock tube reached a maximum of 0.8 milli-second at temperatures 1000K to 1200K and pressures 2 bara to 6 bara with a maximum of 5% cyclopentane in feed. Cyclopentane conversions obtained were in the range of 0.01% to 1%. The main product detected was 1-pentene and based on product yields, the isomerization reaction of cyclopentane to give 1-pentene was hypothesized as the initial dominant decomposition step and a global rate coefficient for the same was proposed. The shock tube experiments also detected cyclopropane and a minor channel forming cyclopropane and ethylene from cyclopentane was proposed with a global rate coefficient, though at the temperatures of interest for steam cracking, the mass yield of cyclopropane was about 100 to 1000 times lower than that of 1-pentene. Tsang proposed a C5 biradical intermediate as the immediate product of cyclopentane decyclization. This biradical was suggested to form majorly 1-pentene through intra-molecular hydrogen abstraction, and minorly cyclopropane and ethylene by C-C beta scission.

About 30 years later, in 2006, Sirjean [12] did high level ab-initio CBS-QB3 calculations on ring opening of cycloalkanes. In that, cyclopentane was studied and a biradical C5 intermediate was envisaged, along the lines of Tsang [11]. Sirjean proposed CBS-QB3 based global rate coefficients for cyclopentane conversion to 1-pentene and that to cyclopropane and ethylene. The rate coefficient of the reaction forming 1-pentene matched well with that proposed by Tsang [11]. Cyclopropane was confirmed to be a minor product and the rate coefficient of the reaction forming cyclopropane and ethylene was about 1% of that forming 1-pentene at 1000K. In this study, ab-initio calculations revealed that the C5 biradical has a bond rotation energy barrier equal to the activation energy for intra-molecular hydrogen abstraction to form 1-pentene. Hence, as soon as the cyclopentane ring opens to form C5 biradical, the C5-biradical undergoes bond rotation and a simultaneous and immediate conversion to 1-pentene. As a practical inference, for a complete cyclopentane pyrolysis model, the initiation step can be represented as a single elementary step isomerization to 1-pentene. Both Tsang [11] and Sirjean [12] studied the initial decomposition of cyclopentane and not its complete decomposition to smaller hydrocarbons and hydrogen nor the molecular growth to polycyclic aromatic hydrocarbons.

Annesley and co-workers measured cyclopentane ring opening kinetics in a Laser-Schlieren apparatus [13,14] at 1500-2000K at low pressures (total pressures 40 to 400 mbar), with cyclopentane partial pressures 0.1-20 mbar. The rate expression for cyclopentane isomerization to 1-pentene was derived from experiment and RRKM theory was applied to extrapolate the same to high pressure limit. Two important conclusions relevant for our present work from Annesley's work are: (1) The rate coefficient at 1050K (temperature of our interest) when calculated by Annesley's rate expression matches the ab-initio value within 8% deviation. (2) According to Annesley, pressure has a minimal effect on the 'k' value for cyclopentane isomerization to 1-pentene. The 'k' at 40 mbar is only about 6% lower than that at high pressure limit. In general, the measured 'k' of cyclopentane ring opening by Annesley agrees with Tsang, Sirjean, the benchmarks so far.

In 2015, Wang [15] proposed a comprehensive ab-initio based kinetic model for propylene pyrolysis with extensive potential energy surface scans of species including cyclopentane. This model predicts another initiation step for cyclopentane decomposition in addition to isomerization – that of C-H homolytic bond scission to give hydrogen atom and cyclopentyl radical. However, the rate coefficient for this reaction was found to be negligible (about 200 times smaller at 1000K) compared to that of isomerization to 1-pentene. The Wang [15] model also contained some reactions involving cyclopentane and cyclopentyl radicals with ab-initio pressure dependent Chebyshev kinetics. Though originally intended for predicting propylene pyrolysis, it has the capability to attempt prediction of cyclopentane pyrolysis too. However, the Wang model uses single-step lumped reactions to form aromatics like benzene, toluene, styrene, indene and naphthalene from 1,3-cyclopentadiene, so it is not a completely elementary reaction model. It has a mixture of pressure dependent kinetics, high pressure limit rate coefficients, for some reactions altered kinetic parameters and global lumped kinetics for aromatics formation. Inspite of these features, it is the most relevant model in literature that comes close to meet our objective of describing the complete pyrolysis of cyclopentane and not just the initial decomposition trends. In addition, this model is also a source of ab-initio kinetic data especially of reactions involving cyclics whose group additive values are not yet reported, and whose rate parameters can be used to derive new group additive values for cyclic reactions. The model is also a source of ab-initio thermodynamics of cyclic species.

The other kinetic and thermodynamic data that may be required for the present study is that involving molecular growth to form aromatics and polycyclic aromatic hydrocarbons. These mechanisms involve many complex species, sometimes bicyclic and tricyclic molecules and may involve reaction families not usually relevant for pyrolysis of simple open chain molecules. It is generally believed that 1,3-cyclopentadiene is the precursor to the formation of aromatics and polyaromatics [16]. Cyclopentane and 1,3-cyclopentadiene being of similar skeletal structure, it is expected that a significant amount of 1,3-cyclopentadiene would be formed during cyclopentane pyrolysis which could in turn trigger aromatics formation and growth. Shamel's model [17] was reported to predict pyrolysis of 1,3-cyclopentadiene and ethylene feed by a model of more than 5000 elementary reactions forming benzene, toluene, styrene, indene and naphthalene. Shamel had done ab-initio investigation of kinetics of the most dominant pathways.

Among other studies on cyclopentane pyrolysis, Sirjean [10] did shock tube experiments with cyclopentane-oxygen-argon mixtures and cyclohexane-oxygen-argon mixtures, both with 0.5 or 1% hydrocarbon at temperatures 1230K to 1840K and pressures 7.3atm to 9.5atm. The purpose was to measure ignition delay times. The residence time in the shock tube was less than 1 milli-second by which time the ignition had already started. Here too, like Tsang [11], the cyclopentane was pyrolyzed at extremely short residence times without allowing complete pyrolysis and formation of polycyclic aromatic hydrocarbons. Also there was no analysis of products like in Tsang's case, as the objectives were different here. In order to explain the ignition delay time measurement, Sirjean formulated a model using EXGAS [18-21] for cyclopentane pyrolysis and oxidation. One important conclusion from Sirjean's study was that cyclopentane is significantly more stable compared to cyclohexane, as the ignition delay times of cyclopentane were 10 times higher than those of cyclohexane.

Tian [9] also measured ignition delay times of cyclopentane/ oxygen mixtures in a shock tube at 1150-1850K and 1-10atm. Tian qualitatively confirmed what Sirjean reported about the stability of cyclopentane. However, in this study, cyclopentane was compared to methyl cyclopentane. In order to explain the ignition delay times, Tian extended the model of JetSurF 2.0 [22] to include cyclopentane pyrolysis initiation kinetics to generate a more complete model than just the initial decomposition reactions. Summarizing, in none of the studies reported in literature was a complete pyrolysis experiment of cyclopentane done

with analysis of full range of products. And none of the models reported had consistently elementary step high pressure limit reactions with ab-initio or ab-initio based (group additive) kinetics without parameter alterations.

In this thesis, for the first time, an experimental and kinetic modeling study of cyclopentane pyrolysis is presented. Experiments have been conducted in a continuous flow reactor at 0.17 MPa, 973 – 1073K and a residence time of 0.5s with pure cyclopentane feed. The in-house model generator tool "Genesys" [23] was used to auto-generate an elementary step high pressure limit kinetic model for cyclopentane pyrolysis having ab-initio/ group additive kinetics and thermodynamics with no adjustment of kinetic parameters. Model trends were compared to the experiment and three other models in literature, all involving one or more global reactions to varying extent[9,10,15]. Reaction path analysis is presented detailing the dominant pathways to the major products.

3.2. Experimental setup and procedure

Cyclopentane pyrolysis experiments were carried out in a bench scale unit which consisted of three main sections – feed section, reactor section and product analysis section. It has been described in detail elsewhere [16,24]. Only the specifics related to this work will be given. Cyclopentane was procured from Sigma-Aldrich (>98% purity). Pure cyclopentane was pumped through a coriolis mass flow controller at 240 g.h^{-1} and fed to an electrically heated tubular reactor made of Incoloy 800HT. The length of the reactor is 1.47m with 6mm internal diameter. No diluent was used, while nitrogen at 20 - 70 g.h^{-1} was added to the reactor effluent and served as an internal standard. The flow rate of cyclopentane was chosen so as to obtain a residence time in the order of 0.5 s. The pressure was maintained at 0.17 MPa using an outlet pressure restriction valve situated at the exit of the effluent line. In all the experiments, the reactor was operated nearly isothermally in the temperature range from 973K to 1073K, i.e. with a steep temperature increase at the reactor inlet and a steep temperature drop at the outlet of the reactor. For carbon balance closure check, after a sample 30 minute experimental run, the reactor was decoked using air at 800 C. During this decoke run, the carbon deposits were burned away and accounted by analyzing CO2. Based on that, it was established that less than 0.1 wt% of carbon in the feed was deposited as coke. Hence, the carbon balance was closed at a minumum of 99.9%

The product analysis section consisted of two different gas chromatographs for a detailed analysis of the reactor effluent: a so-called refinery gas analyzer (RGA) and a GC×GC-FID/TOF-MS. The former enabled analysis of permanent gases and light hydrocarbons ($C_1 - C_4$), while the latter analyzed the whole product spectrum. Response factors for the former were determined by calibration with a synthetically created gas mixture (supplied by Air Liquide, Belgium). The response factors of the C_5+ compounds were determined using the effective carbon number method relative to methane. Every experiment for a given temperature set point was repeated three to five times to establish repeatability. This yielded a relative error of less than 10% on the mass fractions of products.

Separation and analysis using comprehensive two-dimensional gas chromatography (GC×GC) is much more powerful than using one-dimensional gas chromatography (1D-GC). The 2D plane has much higher speed than a 1D retention line; therefore it can accommodate much more complex mixtures [25]. Qualitative analysis is more reliable because each eluent has two identifiers (retention times) rather than one. If proper orthogonal conditions are selected separations are likely to be more structured in the GC×GC leading to recognizable patterns [26,27]. This enables a fast group-type analysis and provisional classifications of unknowns [28]. Moreover, quantification in GC×GC has several potential advantages over 1D-GC such as:

a. Ordering which makes interference due to peak overlap less likely [27,29].
b. Greater sensitivity or detectability due to the high speed of the second column. The resulting peaks are sharper and, therefore, exhibit a higher signal response [27].
c. Reliable presence of a true baseline for peak integration [27].
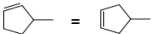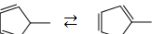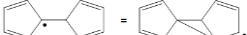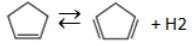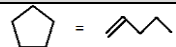
3.3. Kinetic model generation

3.3.1 Reaction families and Mechanism generation

The objective is to create a cyclopentane pyrolysis model consisting of only elementary reversible reactions whose kinetics and thermodynamics are based on ab-initio electronic structure calculations. The first step is to select the relevant reaction families. For ethane cracking [30], Sabbe et al. used the following reaction families: hydrogen

abstraction, hydrogen atom addition, carbon radical addition and recombination (and their reverse reaction families). Based on related literature [12,15,17], the following reaction families and reactions also have been considered: Intra-molecular carbon centered radical addition, Intra-cyclopentadiene hydrogen shift, Intra-molecular hydrogen abstraction, cycloalkane isomerization to 1-alkene, Diels-Alder reaction, H_2 elimination from cyclopentene. Table 3.1 shows the complete list of reaction families considered. With this, we were ready with a hopefully complete list of elementary reaction families to generate a mechanism for cyclopentane pyrolysis.

Table 3.1: Reaction families considered in this work

Reaction family	Description/ Example	Reference
Hydrogen transfer		
Inter-molecular H-abstraction	by C• by H•	[33], In-house
Intra-molecular H-abstraction (acyclics)	C-(C)$_n$-C• $\rightleftarrows$ •C-(C)$_n$-C	[30]
Intra-molecular H-abstraction (cyclics)		[15,17]
Intra-CPD-H-shift		[17]
Addition		
Inter-molecular C-radical addition	C=C + •C $\rightleftarrows$ •C-C-C	[31]
Intra-molecular C-radical addition		[15,17]
Hydrogen atom addition	•C-C-H $\rightleftarrows$ C=C+ •H	[32]
Recombination		
C-C recombination	•C + •C $\rightleftarrows$ C-C	[15,17,30]
C-H recombination	•C + H $\rightleftarrows$ C-H	[15,17,30]
H2 elimination		
Direct release of H2 gas		[17]
Diels-Alder		
Molecular mechanism – rearrangement of double bonds		[17]
Isomerization		
Ring opening of cycloalkanes		[12]

The in-house automatic mechanism generation tool, "Genesys" [23] was used to generate the mechanism for cyclopentane pyrolysis. Genesys does not have pre-defined reaction families, but offers the users flexibility to define the reaction families by creating reaction family recipes in a simple manner. Reaction recipes were created for the families listed in Table 3.1. Figure 3.1 shows an example recipe for intra-cyclopentadiene hydrogen shift having the 1,3-cyclopentadiene moiety. It can be seen that only 6 atoms are part of the recipe: carbon atom numbers 1 to 5 and hydrogen atom number 6. All the 5 carbon atoms

are called reactive centers as all of them are affected by the bond rearrangement. The groups R_1-R_5 are called the nearest neighbors to the reactive centers.
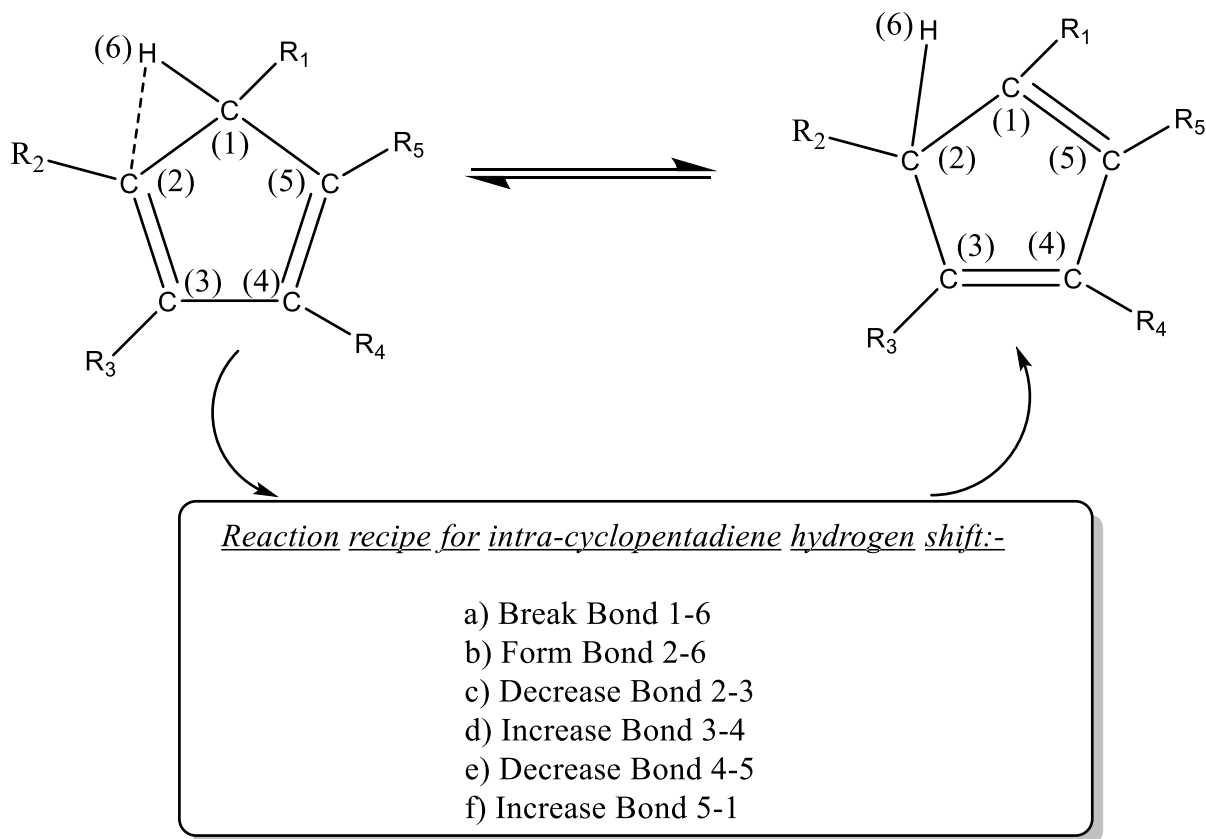
Figure 3.1: A sample reaction recipe in Genesys

The feed molecule to Genesys is cyclopentane. In the first loop of the mechanism generation algorithm, this molecule is tested for possible reactions included in Table 3.1. Accordingly, 1-pentene is generated by isomerization. In the next iteration, both 1-pentene and cyclopentane are checked for possible reactions among the reactions of Table 3.1, and C-C recombination (its reverse reaction) becomes active on 1-pentene to generate new species. This procedure is continued - the list of species present at any iteration being tested for possible reactions to generate further species. In this way, the mechanism grows until it reaches a constraint and there are no more new species generated. The constraint used for the present case was the carbon number of 10 per species based on the idea to stop the molecular growth at naphthalene. Algorithmic details about mechanism generation using Genesys, including schematics can be found in [23].

3.3.2 Kinetics and thermodynamics assignment

After the mechanism generation is complete, Genesys assigns kinetic parameters to the reactions and thermodynamic parameters to the species from user-defined databases. The kinetics databases contain kinetics in the form of standard group additive values (ΔGAV°) of single event Arrhenius pre-exponential factors and activation energies. These ΔGAV°s are defined as a function of groups (molecular fragments/ branches, example R_1-R_5 in Figure 3.1) attached to the reactive centers for a particular reaction family. The ΔGAV°s for a few reaction families have already been reported [31-33], and were used in the Genesys kinetics databases as such. The number of single events, based on symmetry numbers and optical isomers of reactants and transition states is calculated by an auxiliary code of Genesys called SIGMA [34]. For thermodynamics, ab-initio/ group additive parameters exist [15,17,30] in the form of NASA polynomial coefficients. These coefficients were coded into the species thermodynamic database of Genesys so that they are assigned when a particular species is found in the mechanism. For species which are not included in the database, thermodynamics can be estimated by group additivity in Genesys. The ΔGAV° databases of the new reaction families needed for cyclopentane pyrolysis model generation (intra-cyclopentadiene hydrogen shift, intra-molecular carbon radical addition leading to mono, bi and tri-cyclic species and intra-molecular hydrogen abstraction within cyclic species) were completed from literature [15,17]. Tables 3.2 and 3.3 show the ΔGAV°s for the new reaction families: intra-cyclopentadiene hydrogen shift and intra-molecular carbon radical addition.
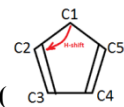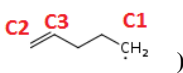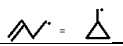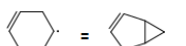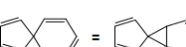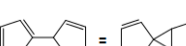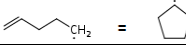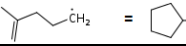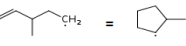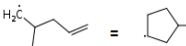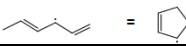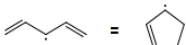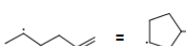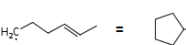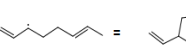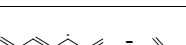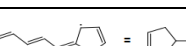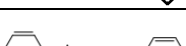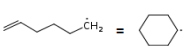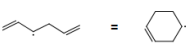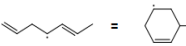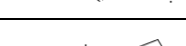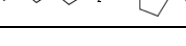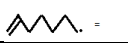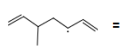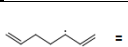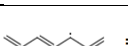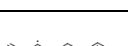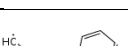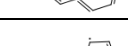
Table 3.2: Group Additive Values for Intra-CPD H-shift reaction family (**)**

Reaction	Group name	$\Delta GAV^\circ[\log(\tilde{A})]$	$\Delta GAV^\circ[E_a]$
REFERENCE REACTION (A, n, Ea) = 4.8×10^{13}, 0, 107.8 kJ, mol, s			
	C1-C	0.317	0.92
	C1-Cd	0.053	-12.59
	C5-C	1.070	14.84
	C5-Cd	0.415	11.97
	C3-C (or C3-Cd)	0.618	8.45
	C1-C.	-0.728	-38.79

Table 3.3: Group Additive Values for Intra-molecular carbon centered radical addition (**)**

Reaction	Group Name	ΔGAV°[log(Ã)]	ΔGAV°[Ea]	Nearest neighbors
		REFERENCE (1.35*10^{12}, 0, 45.5), kJ, mol, s		
		-0.04	-25.7	(C2-Cd)
	C4,exo	0.88	112.4	(C2-Cd) (C1=allyl)
		0.88	112.4	(C2-Cd) (C1=allyl)
		0.23	-4.4	(C2-Cd)(C1=CPDyl)
		REFERENCE (3.09*10^{10}, 0, 69.5), kJ, mol, s		
		0.00	0.0	C5,endo
		0.00	0.0	C5,endo
		0.00	0.0	C5,endo
		0.00	0.0	(C1=allyl)
	C5,endo	0.00	0.0	(C1=allyl)
		0.25	-10.2	(C1-C)
		0.25	-10.2	(C2-C)
		0.25	-10.2	(C2-C) (C1=allyl)
		2.51	90.6	(C2-Cd) (C1=allyl)
		2.51	90.6	(C2-Cd) (C1=allyl)
	C5,exo	REFERENCE (1.79*10^{11}, 0, 67.7), kJ, mol, s		
		0.44	-8.3	(C2-Cd)
		REFERENCE (5.85*10^9, 0, 35), kJ, mol, s		
	C6,endo	0.00	0.0	(C1=allyl)
		0.00	0.0	(C1-C) (C1=allyl)
		2.13	55.7	(C2-C) (C1=CPDyl)
		REFERENCE (2.06*10^{10}, 0, 26.2), kJ, mol, s		
	C6,exo	2.00	6.4	(C2=benzene) (C1d)

		REFERENCE (5.55*10^{10}, 0, 59.3), kJ, mol, s		
		1.17	26.5	(C1=allyl)
		1.17	26.5	(C1=allyl)
	C7,exo	1.17	26.5	(C1=allyl)
		1.17	26.5	(C2-C) (C1=allyl)
		2.72	-10.9	(C2-Cd) (C1d)
		2.58	105.5	(C2-Cd) (C3-C)

In these tables, it can be seen that at some places, only a single reaction leads to a ΔGAV° value. Typically multiple reactions are used to derive a ΔGAV°. However, since the main objective is not derivation of group additive values, the current procedure is sufficient toward generating kinetics of important reactions. The atom labeling for intra-molecular carbon centered radical addition and intra-cyclopentadiene hydrogen shift are shown in Figure 3.2 and Figure 3.3 using illustrative examples.

Valid groups = $C_4(C_d)$ and $C_5(C)$
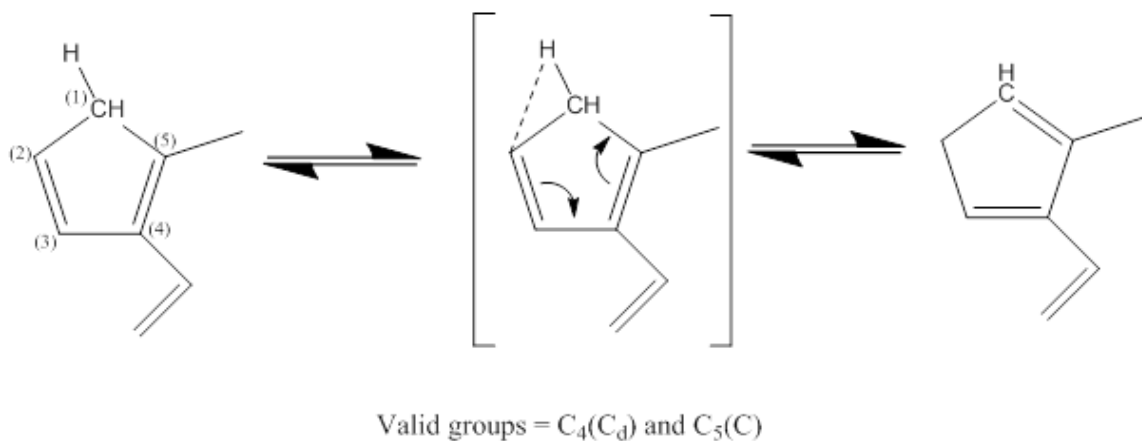
Carbon atom labeling for reactant in intra-cyclopentadiene hydrogen shift

Figure 3.2: Group nomenclature for intra-cyclopentadiene hydrogen shift family
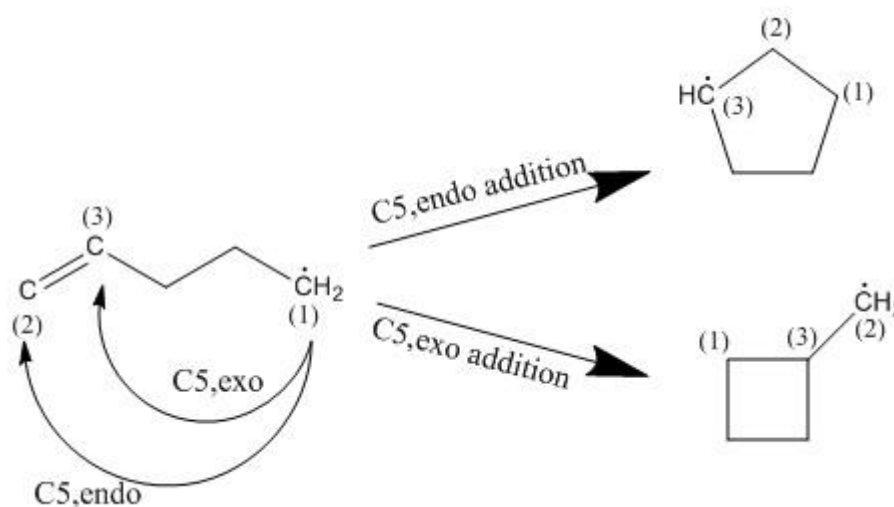
Figure 3.3: Atom labels for endocyclic and exocyclic intra-molecular carbon centered radical addition

In Tables 3.2 and 3.3 the effect of non-nearest neighbors on the rate coefficient is negligible. This is in line with the general philosophy of group additivity that the rate coefficient depends only on the groups attached to the reactive centers and not those far away from the place of action. Based on these input databases, Genesys assigned kinetics to the reactions of the mechanism, yielding an automatically generated group additive model for cyclopentane pyrolysis. Genesys generated the model as a ChemKin [35] readable input file and initial simulations with cyclopentane feed pointed toward a few critical reactions whose kinetics were worthwhile to be checked by a high level CBS-QB3 computation [36] by the method shown next.
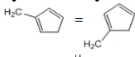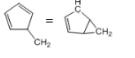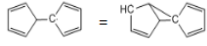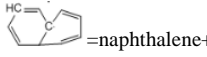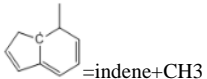
3.3.3 CBS-QB3 computation of rate coefficients of critical reactions

For critical reactions, a CBS-QB3 method [36] was used to compute rate coefficients. The study was performed with the Gaussian 09 revision D suite of programs [37] as implemented on the high-performance supercomputing facility at Ghent University. CBS-QB3 calculations give geometries, external moments of inertia, harmonic oscillator frequencies and the electronic energy at 0 K. The first three properties are used to calculate entropies, heat capacities and thermal contributions to the enthalpy using statistical mechanics calculations. Except for internal rotations, which were treated separately, all internal modes were assumed to behave as harmonic oscillators and a scaling factor of 0.99 was applied. Internal modes that resemble rotations around a single bond were treated

separately by replacing the contributions of the corresponding oscillators to the partition function with numerically calculated partition functions for these hindered rotors. The required hindrance potentials were obtained from scans, in which the dihedral angle defining the rotation was varied from 0 to 360 degrees in steps of 10 degrees while all other molecule parameters were allowed to optimize. The obtained hindrance potential was then expressed as a Fourier series. Together with the reduced moment of inertia calculated at the $I^{(2,3)}$ level as defined by East and Radom [38], the hindrance potential was used to construct the Schrödinger equation for 1-D rotation. The eigenvalues of the solution to this Schrödinger equation represent the energy levels of this mode. They were used to determine the partition function for this mode as a function of temperature. After corrections for symmetry and optical isomers, the total partition function was used to calculate the thermal contribution to the enthalpy, standard entropy and temperature-dependent heat capacity data.

Enthalpies of formation in CBS-QB3 were calculated with the atomization method [39]. Two additional corrections accounting for spin-orbit interactions [36,39,40] and systematic bond additive corrections (BAC) [36] significantly improve these values as has been shown in previous work [41]. However, such corrections are only needed to calculate the thermodynamic properties. All transition state calculations used uncorrected enthalpy data because BACs are not known for transition states. All data were stored as NASA polynomials. The critical reactions are R2-R13 in Table 3.4.

Table 3.4: Most important reactions in the Genesys cyclopentane model - comparison to literature models [9,10,15]

#	Reaction	A	E_a	Source	k(Genesys)	k(Wang)	k(Sirjean)	k(Tian)
	Units/ description:- (blank areas => missing reactions)	m^3, mol, s	kJ/mol	Source of Genesys kinetics	Units of k in m^3, mol, s. k(at T=1050K)			
R1	cyC5H10=1-pentene	$1.3*10^{16}$	355.7	[12]	$2.5*10^{-2}$	$2.5*10^{-2}$	$2.5*10^{-2}$	$2.5*10^{-2}$
R2	1-pentene=allyl+ethyl	$5.1*10^{14}$	273.6	In-house	12	6.6	17	20
R3	cyC5H10+H=cyC5H9+H2	$2.6*10^{8}$	35.6	In-house	$4.4*10^{6}$	$2.2*10^{6}$	$2.3*10^{7}$	$2.3*10^{7}$
R4	cyC5H10+CH3=cyC5H9+CH4	$1.6*10^{7}$	56.7	In-house	$2.4*10^{4}$	$4.5*10^{4}$	$1.0*10^{4}$	$1.0*10^{4}$
R5	cyC5H10+allyl=cyC5H9+C3H6	$5.3*10^{7}$	98.4	In-house	$6.7*10^{2}$	$4.4*10^{3}$	$6.2*10^{2}$	
R6	cyC5H10+C2H5=cyC5H9+C2H6	$1.6*10^{7}$	56.7	In-house	$2.4*10^{4}$	$4.5*10^{4}$	$5.2*10^{4}$	$5.2*10^{4}$
R7	cyC5H9=pent-1-en-5-yl	$1.7*10^{14}$	144.5	In-house	$1.1*10^{7}$	$1.0*10^{6}$	$8.2*10^{6}$	$2.6*10^{4}$
R8	Pent-1-en-5-yl=allyl+C2H4	$1.5*10^{13}$	86.4	In-house	$7.4*10^{8}$	$5.7*10^{7}$	$6.9*10^{8}$	$4.7*10^{5}$
R9	C3H6+H=1-propyl	$6.5*10^{7}$	22.5	In-house	$4.9*10^{6}$	$1.8*10^{5}$		$6.8*10^{5}$
R10	1-propyl=CH3+C2H4	$8.5*10^{13}$	131.1	In-house	$2.5*10^{7}$	$4.3*10^{6}$		$2.9*10^{6}$
R11	C2H4+H=C2H5	$2.1*10^{8}$	18.5	In-house	$2.6*10^{7}$	$3.3*10^{6}$	$2.8*10^{6}$	$7.1*10^{6}$
R12	cyC5H9=cyC5H8+H	$1.9*10^{14}$	154.0	In-house	$4.0*10^{6}$	$2.0*10^{6}$	$1.6*10^{7}$	$1.7*10^{5}$
R13	cyC5H8=cyC5H6+H2	$2.2*10^{13}$	250.8	In-house	7.5	7.4	6.5	7.3
R14	cyC5H6+H=cyC5H5+H2	$8.5*10^{8}$	32.0	[17]	$2.2*10^{7}$	$2.1*10^{6}$	$1.1*10^{7}$	$3.1*10^{6}$
R15	cyC5H5+C2H5=ethyl-CPD	$3.2*10^{7}$	-8.0	[17]	$8.1*10^{7}$			
R16	cyC5H5+cyC5H5=BiCPD	$5.0*10^{7}$	0.0	[17]	$5.0*10^{7}$			
R17	(ring structure) = (ring structure)	$4.9*10^{13}$	174.3	[17]	$1.1*10^{5}$			
R18	(ring structure) = (ring structure)	$1.2*10^{12}$	19.8	[17]	$1.3*10^{11}$			
R19	cyC6H7=benzene+H	$5.5*10^{13}$	125.5	[17]	$3.2*10^{7}$			
R20	(ring structure) = (ring structure)	$2.3*10^{12}$	41.1	[17]	$2.1*10^{10}$			
R21	(ring structure) =naphthalene+H	$2.9*10^{13}$	77.0	[17]	$4.3*10^{9}$			
R22	(ring structure) =indene+CH3	$1.6*10^{14}$	102.1	[17]	$1.3*10^{9}$			

BAC is bond additivity corrections. These corrections are applied to correct for systematic errors in the CBS-QB3 calculations. The correction values are obtained by comparison with experimental data taken mainly from the NIST webbook. Rate coefficients are within a factor of 3 of experimental data [42-44]. All the thermodynamic data have been generated by Genesys. The source of underlying data is in-house and reported CBS-QB3 ab-initio calculations.

Transition state theory expressed in terms of Gibbs free energies was used to calculate the rate coefficients, as shown in equation 1:

$$k_{TST}(T) = \chi(T) \cdot \frac{k_B T}{h} \cdot \left(\frac{RT}{p}\right)^{\Delta n - 1} \cdot e^{-\frac{\Delta G^{\ddagger}}{RT}}$$

$\Delta G^{\ddagger}$ is the Gibbs free energy difference between transition state without the transitional mode and reactant(s), Δn is the molecularity of the reaction (2 for bimolecular and 1 for unimolecular reactions), and $\chi(T)$ accounts for quantum mechanical tunneling. Other

symbols are defined in the list of symbols. The asymmetric Eckart potential is used to estimate tunneling contributions $\chi(T)$. The Gibbs free energies were obtained from the NASA polynomials. Rate coefficients were calculated for the temperature range 300 K to 2500 K in steps of 50 K and the results were regressed to a simple Arrhenius expression. The majority of calculated reaction rate coefficients are believed to be within a factor of 3 of experimental data.

3.3.4 Kinetics evaluation

As stated previously, rate coefficients for the reactions were assigned from existing group additive values and new group additive values derived from available literature data. Ab-initio thermodynamic parameters were assigned to the species. The final model has 220 species (141 radicals, 79 molecules) taking part in 757 reactions.. Based on initial simulations, a few reactions were found to be dominant, and their kinetics were re-calculated in-house at CBS-QB3 level of theory. Leading to the final model. Table 3.4 lists the most important reactions of the model and the source of their kinetics in the Genesys model. It also lists the rate coefficients of the reactions at 1050K for the Genesys model as well as those for the models from literature – Wang [15], Sirjean [10] and Tian [9]. In this Table, reactions R1 to R13 are important reactions for initial decomposition of cyclopentane and propagation leading to the formation of major products with carbon numbers equal to or less than 5. Reactions R14 to R22 are important for the formation of molecular growth leading to aromatics and polycyclic aromatic hydrocarbons. It can be noted that the cyclopentane pyrolysis models in the literature do not have reactions R15 to R22 because these are elementary reactions while the literature models, if at all they form aromatics, do so by global lumped reactions. A few initial decomposition reactions were also missing in the literature models Sirjean [10] and Tian [9], as shown blank. From Table 3.4, it can also be seen that the rate coefficients of important reactions in Genesys are different from those of literature models. At 1050K, the discrepancy is at maximum a factor of 20. Overall, it can be concluded that Genesys model has a more complete reaction list compared to the models in literature. Also, its CBS-QB3 based rate coefficients are different in magnitude from those found in literature models. Moreover, it is the only model that is completely elementary reaction-based and has consistently ab-initio based high

pressure limit rate coefficients with no alteration of kinetic or thermodynamic parameters. In the next section, experimental results and model performance would be discussed.

3.4. Results and discussion

3.4.1 Experimental data

The supporting information of the published article lists the experimental results while Figure 3.4 shows the GC×GC image of the effluent of cyclopentane cracking.
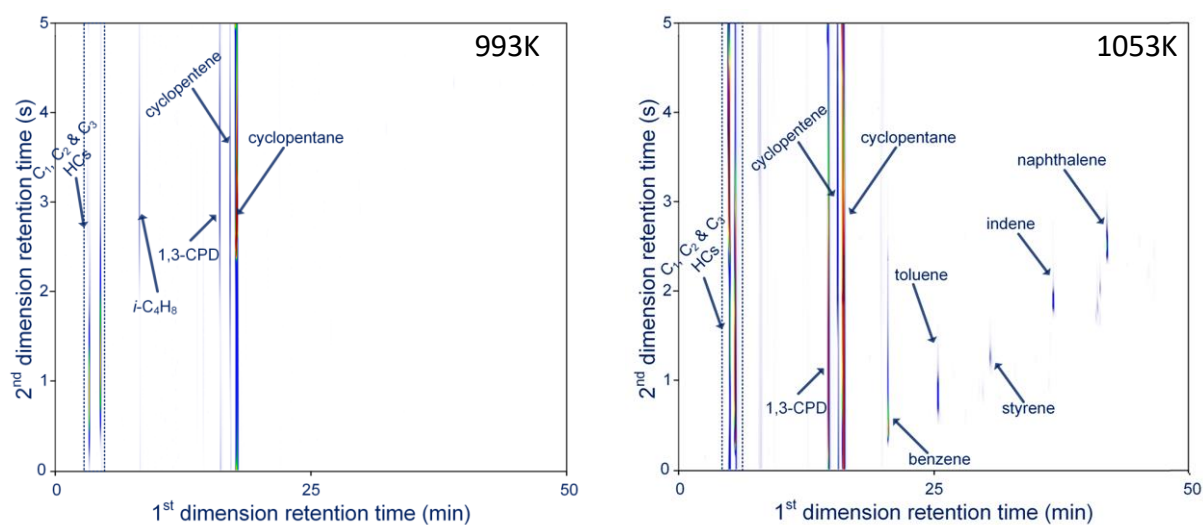
Figure 3.4: GC×GC image of effluent of cyclopentane pyrolysis at 993K (at 240 g.h^{-1} hydrocarbon feed, 20 g.h^{-1} N$_2$ internal standard, 0.17 MPa) and 1053K (at 240 g.h^{-1} hydrocarbon feed, 70 g.h^{-1} N$_2$ internal standard, 0.17 MPa)

Thirty four molecules were detected and quantified in the reactor effluent during experiments spanning six different temperature set points of the reactor between 973K and 1073K, at 20K intervals. Figure 3.5 shows the experimental data (including model trends discussed later) of 9 main products on plots.
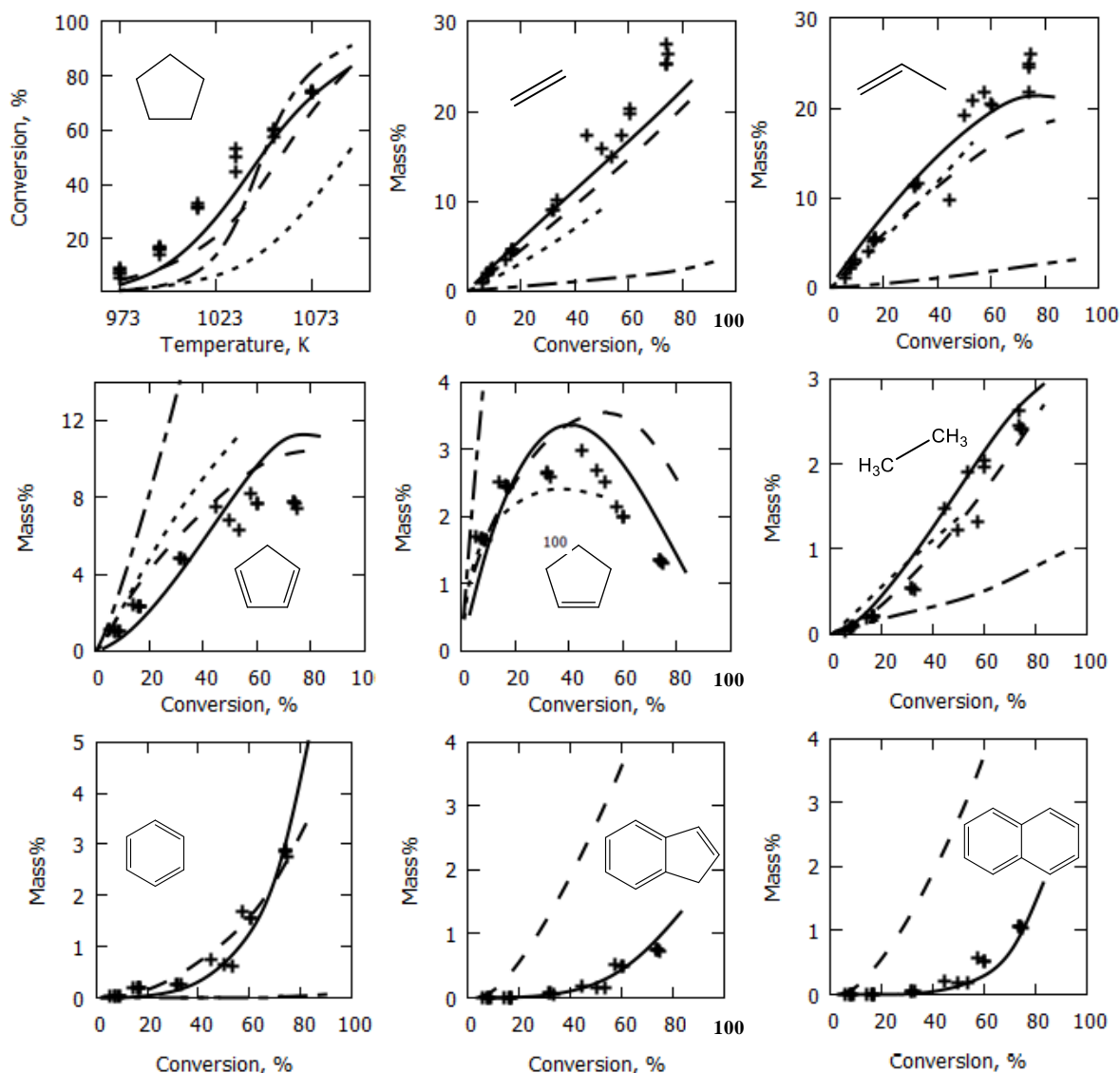
Figure 3.5: Experimental pyrolysis yields and model predictions for 9 main products in continuous flow experiments at 0.5s residence time, 0.17MPa pressure, pure cyclopentane feed (+ Experiment, ———— Genesys, – – – – Wang, ········· Sirjean, —·—·— Tian)

From Figure 3.5, it can be seen that experimental ethylene yield increases monotonically to 25 wt% at the highest temperature, while propylene yield slightly flattens at the conditions. It is to be noted that unlike cyclopentane, for linear alkanes, the propylene yield is a lot lower [30]. For example for ethane cracking, it is about 10 wt% for similar operating conditions. 1,3-Cyclopentadiene product exhibits a maximum of approximately 8 wt% yield at 1053K. Cyclopentene yield has a maximum of 3 wt% at 1013K. Benzene yield increases exponentially with temperature and reaches a maximum of 3 wt%, with

toluene and styrene behaving similarly and both reaching 0.8 wt%. A maximum of 1 wt% each of indene and naphthalene are formed at the highest temperature. A maximum of 2 wt% ethane is formed at the highest temperature while propane yield stays below 1 wt%. Hydrogen data shows some scatter but the trend shows a monotonic increase to 1.5 wt%. A maximum of 4 wt% methane is formed at the highest temperature. These are the 14 products whose maximum experimental yield is more than 0.5 wt%. There are other minor products with lesser than 0.5 wt% maximum yield – like 1- and 2-butenes, acetylene, methyl acetylene, allene (propadiene/ PD), 2-pentene, 1,4-pentadiene and 1,3-butadiene. Carbon balance was closed up to 97% across all experiments, with H/C mole ratio at exit calculated for each temperature. Based on that, the mass balance is excellent for the lower temperatures, while there is some deviation at the high temperatures. At the highest temperature of 1073K, the inlet H/C mole ratio is 2, while the outlet ratio is 2.18.

3.4.2 Kinetic model evaluation

Reactor simulations using the Genesys model were conducted with the CHEMKIN PRO package using the plug flow reactor module [35]. From Figure 3.5, it can be seen that there is quantitative and qualitative agreement between the model and experiments for all plots. The major disagreements are only with some minor products where the maximum experimental yield is less than 0.5 wt%. A reaction path analysis was performed on major products at the experimental reactor temperature set point of 1053K and a schematic showing the dominant reactions of the Genesys mechanism is given in Figure 3.6. Rate of production and sensitivity analyses reveal the following dominant pathways:
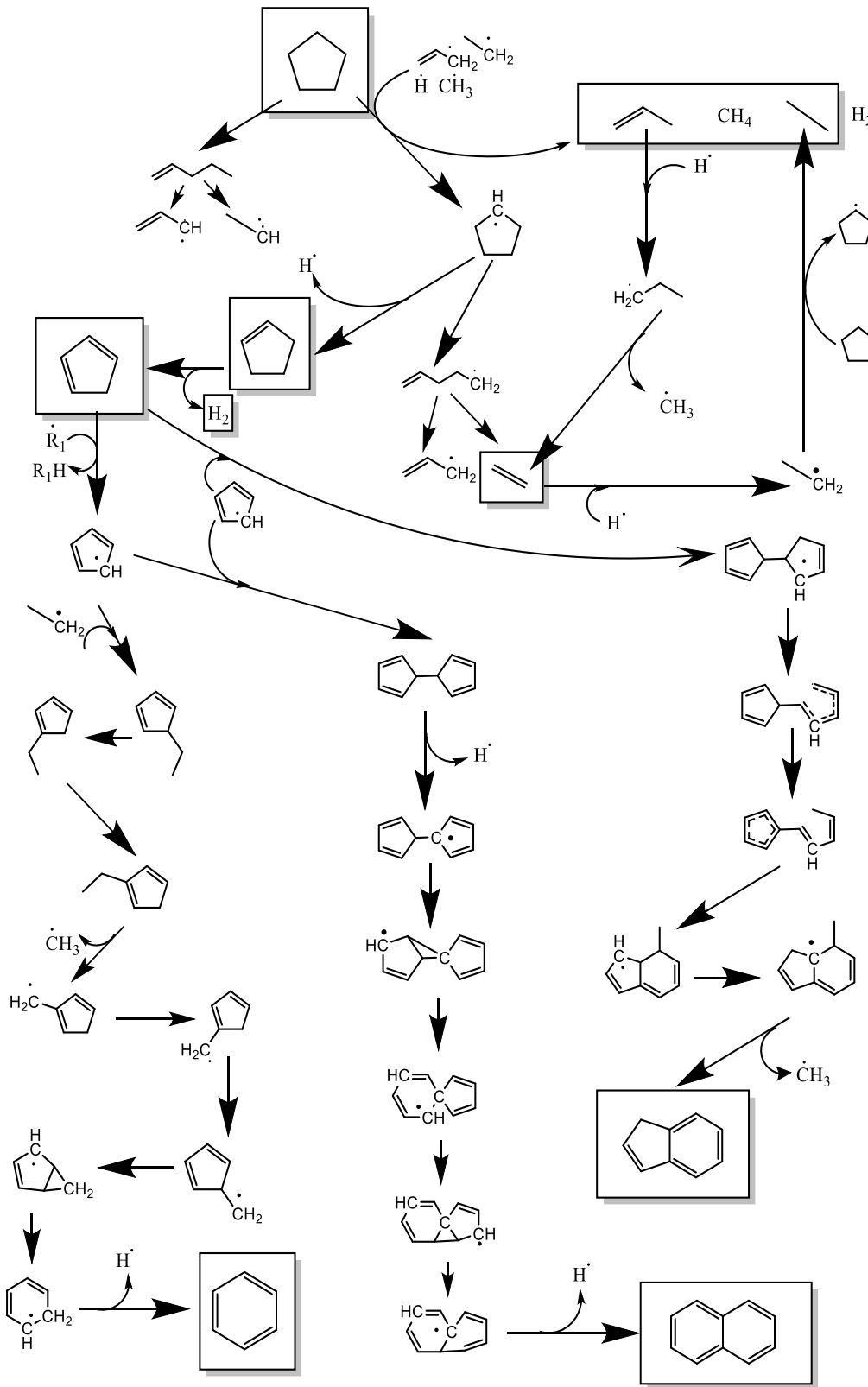
Figure 3.6: Schematic of the dominant reaction pathways in cyclopentane pyrolysis based on Rate of Production Analysis at 1053K, 100 cm reactor length (space time = 0.52 s)

Cyclopentane: Cyclopentane is consumed at the initial temperature ramp majorly by the isomerization reaction to 1-pentene. However, across a substantial part of the reactor, the predominant consumption route is through the hydrogen abstraction by allyl radicals followed by the abstraction by hydrogen atoms. The allyl radical concentration is very high along the reactor length for cyclopentane pyrolysis. The reason for this is - once the isomerization to 1-pentene takes place, 1-pentene undergoes a homolytic C-C scission to give ethyl radicals and allyl radicals. These radicals abstract hydrogen from cyclopentane to give cyclopentyl radical. Cyclopentyl in turn undergoes ring opening to give pent-1-en-5-yl radical. The latter primarily decomposes via a carbon centered beta-scission to give ethylene and a new allyl radical. Since the resonance stabilized allyl radical is produced immediately in the primary decomposition routes of cyclopentane, its concentration is high and hence, the allyl-assisted hydrogen abstraction is the predominant conversion route of cyclopentane. Hydrogen atoms are generated from the C-H beta scission of the cyclopentyl ring giving cyclopentene. This is also released from the ethyl radical produced from 1-pentene decomposition, giving ethylene, hence hydrogen-atom-assisted abstraction is one of the most important consumers of cyclopentane. The rate of consumption and sensitivity plots are shown in Figure 3.7 and Figure 3.8, respectively.
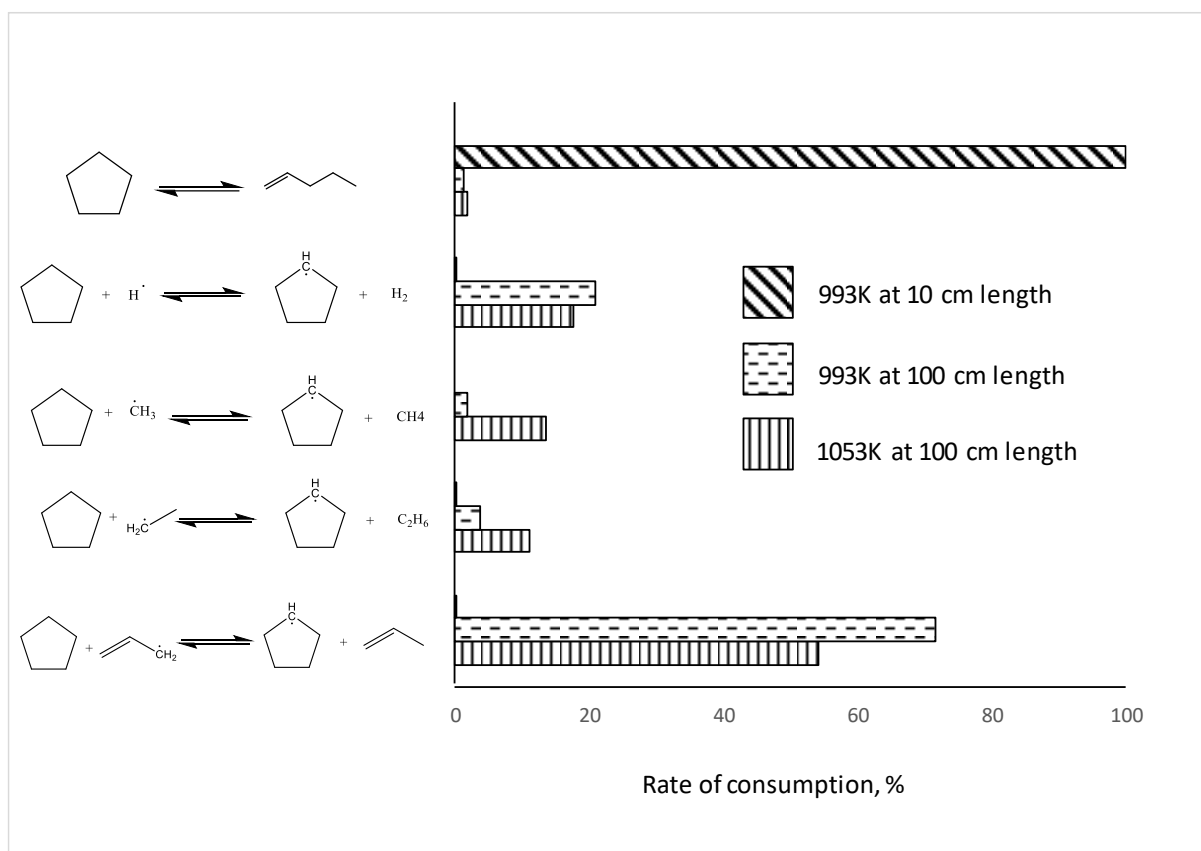
Figure 3.7: Rate of consumption of cyclopentane by various elementary reactions, % at 993K at 10 and 100 cm reactor length and 1053K at 100 cm reactor length
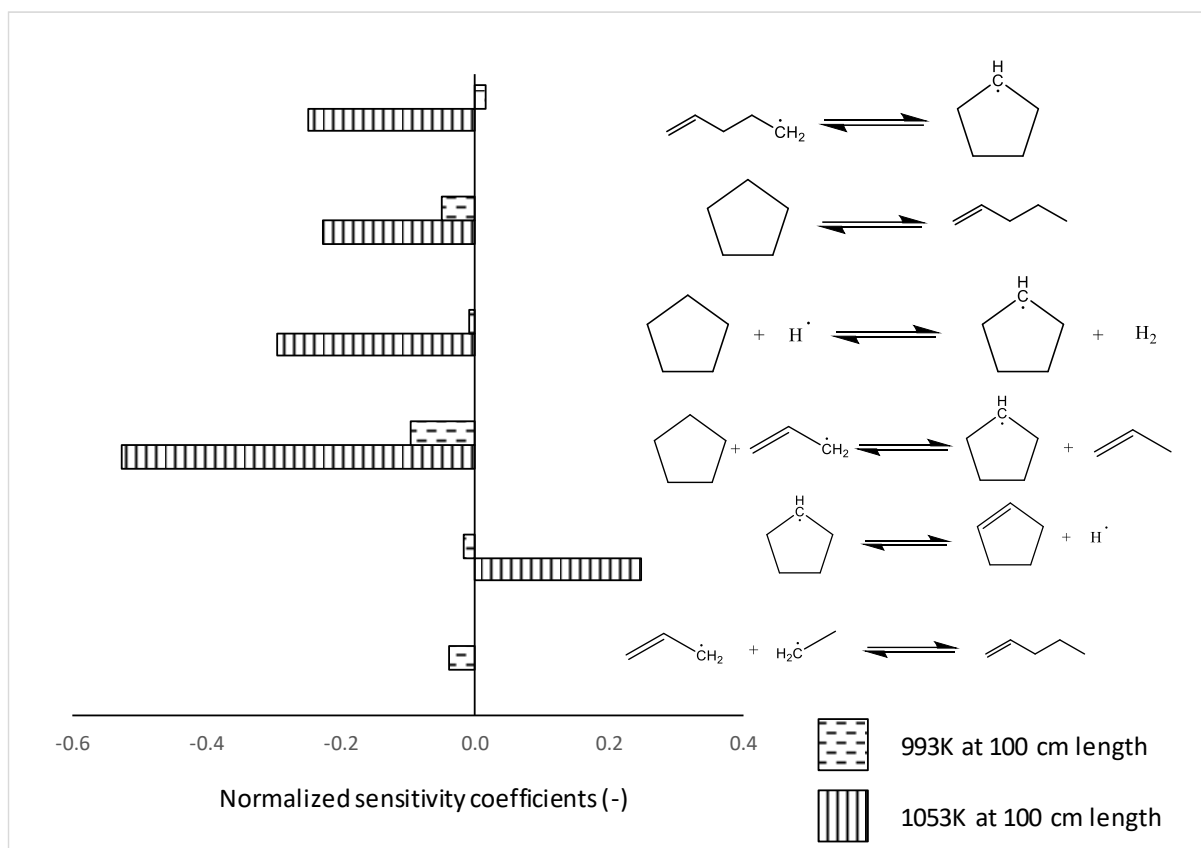
Figure 3.8: Normalized sensitivity coefficients for cyclopentane production at 993K and 1053K at 100 cm reactor length

Ethylene: Ethylene is majorly produced by 2 routes: carbon centered beta scission of pent-1-en-5-yl to give ethylene and allyl radical, and of 1-propyl radical to give ethylene and methyl radical. 1-propyl radical is formed by hydrogen atom addition to propylene. Hence, propylene can be converted to ethylene in this way. As expected, ethylene yield increases monotonically with cyclopentane conversion (Figure 3.5).

Propylene: Across the entire reactor length, propylene is mainly formed by the allyl-assisted hydrogen abstraction of cyclopentane. However, at high concentrations of propylene, it is decomposed by hydrogen atom addition and subsequent conversion to

ethylene and methyl radical. This is the reason why the propylene trend flattens out toward high conversions (Figure 3.5).

Cyclopentene: Cyclopentene is formed mainly by the C-H beta scission of the cyclopentyl radical. The hydrogen atom hence released assists in the further conversion of cyclopentane through hydrogen abstraction. So, we might expect a high conversion of cyclopentane to correspond to a high monotonically increasing yield of cyclopentene. However, it can be seen from Figure 3.5 that the cyclopentene yield goes through a maximum. This is because at high cyclopentene concentrations, there is a molecular mechanism (as opposed to radical mechanism) leading to release of hydrogen gas and 1,3-cyclopentadiene formation, as will be discussed next.

1,3-Cyclopentadiene: Cyclopentene which is formed majorly by the C-H beta-scission of the cyclopentyl radical preferably undergoes a molecular mechanism to form 1,3-cyclopentadiene and hydrogen gas. This is the dominant route of 1,3-cyclopentadiene formation. A minor route from cyclopentene is through the hydrogen abstraction at the allylic position and eventual C-H beta scission to give 1,3-cyclopentadiene. Hence, 1,3-cyclopentadiene is formed at the expense of cyclopentene, giving rise to the maximum feature seen in cyclopentene. However, even 1,3-cyclopentadiene tends to flatten out at the high conversions of cyclopentane. This is because it is the main precursor for the formation of polycyclic aromatic hydrocarbons.

Methane: Methane is formed mainly by the hydrogen abstraction by methyl radicals on cyclopentane. Methyl radicals are in turn generated predominantly by the C-C beta scission of 1-propyl radical which is formed by hydrogen addition to propylene. Hence, there is a trade-off between propylene and methane yields. Hence, it comes as no surprise that while propylene is a bit over-predicted by the model, methane is a bit under-predicted.

Hydrogen: At the initial part of the reactor, hydrogen is mainly generated by 2 routes: hydrogen-atom-assisted hydrogen abstraction of cyclopentane and H_2 gas release from cyclopentene to give 1,3-cyclopentadiene. As the 1,3-cyclopentadiene yield increases at higher conversions, hydrogen is also abstracted from it by hydrogen atoms, releasing H_2 gas. This third route gets activated at high concentrations of 1,3-cyclopentadiene typically towards the end of the reactor.

Ethane: Ethane trend in Figure 3.5 shows a monotonic increase with respect to cyclopentane conversion. This is because the main route forming ethane is the hydrogen

abstraction of cyclopentane by ethyl radical. The ethyl radical is in turn generated by the homolytic C-C scission of 1-pentene to give ethyl and allyl radical. At the start of the reactor where there is excess ethyl produced, on one hand it attacks cyclopentane assisting in its conversion, while on the other hand, it undergoes C-H beta scission to give ethylene.

Propane: Propane is produced predominantly across the reactor by the hydrogen abstraction of cyclopentane by 2-propyl radical. 2-propyl radical is in turn formed by the hydrogen atom addition to propylene. Hydrogen atom addition to propylene can yield 1-propyl as well as 2-propyl. As discussed earlier, 1-propyl leads ultimately to ethylene and methane. However, 2-propyl preferably leads to propane because it cannot undergo a C-C beta scission like 1-propyl due to the positioning of the radical center and a 1-2 radical shift is not energetically favored. Hence, there is a trade-off between propylene and propane.

Benzene: Hydrogen abstraction on 1,3-cyclopentadiene leads to the highly stabilized resonance radical 1,3-cyclopentadien-5-yl. This radical recombines with ethyl radical to give ethyl cyclopentadiene. This molecule undergoes intra-cyclopentadiene hydrogen shifts to give a different location of the ethyl substituent. The ethyl substituent's C-C bond undergoes homolytic C-C scission to give CH2-cyclopentadienyl radical, radical center being at the primary carbon atom, This again undergoes intra-cyclopentadiene hydrogen shifts and then intra-molecular C-C addition (ring formation) to give a six-membered bicyclic radical. This radical undergoes a C-C beta scission to expand the ring from a 5-member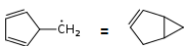ed one to a six membered one: cyclohexadienyl radical. This radical undergoes C-H beta scission to give benzene and hydrogen atom.

Indene and Naphthalene: Indene and naphthalene formation goes by a series of elementary steps starting from 1,3-cyclopentadiene and the resonance stabilized cyclopentadienyl radical.

A detailed discussion of Figure 3.7 and Figure 3.8 along with species concentration profiles can be found in the supporting information. In summary it can be stated that the Genesys model predictions are better than that of the other models for most products. The Wang model [15] is reasonably good for non-polycyclic aromatic hydrocarbon products. As the intention of the other models was not to match pyrolysis data of cyclopentane, it is strictly speaking not a drawback for them, and they may be applicable to their case of interest. However, as an elementary reaction pyrolysis model based consistently on ab-initio derived kinetics, the Genesys developed model is a first.

3.5. Conclusions

The pyrolysis of cyclopentane has been studied for the first time in the temperature range of 973K to 1073K, in a continuous flow reactor. 34 products were identified and quantified using 2 dimensional gas chromatography, ranging from hydrogen to polycyclic aromatic hydrocarbons. A kinetic model has been generated consisting of 757 reactions between 220 species based on mainly CBS-QB3 kinetics and thermodynamics. This compact model predicts the trends of all major products and minor minor products well, significantly better than the currently established models. This is attributed to the use of accurate ab-initio derived kinetics and a more complete kinetic model consisting only of elementary steps. It is to be noted that although the present model performs better than the literature models for cyclopentane pyrolysis, those models were intended for processes like combustion, auto-ignition and pyrolysis of feeds other than cyclopentane. Hence, for those literature models, non-performance with current data is strictly not a measurable drawback. Still, their comparison with the present model was made with the intention to list the models already available in literature, even if remotely applicable. Reaction path analysis reveals the dominant pathways to the most important products such as ethylene, propylene, methane, hydrogen, ethane, cyclopentene, 1,3-cyclopentadiene, benzene, indene and naphthalene. Cyclopentane pyrolysis initiation primarily starts via an isomerization pathway to 1-pentene. However, as the reaction proceeds, radicals are generated by subsequent decomposition which then abstract hydrogen from cyclopentane. This hydrogen abstraction eventually becomes the most dominant conversion route.

3.6. References

[1]   J. Speight, *Handbook of Industrial Hydrocarbon Processes*, Gulf Professional Publishing, 2010, p.

[2]   K.M. Van Geem, M.F. Reyniers, G.B. Marin, J. Song, W.H. Green and D.M. Matheu, *Aiche Journal*, 52, (2006) 718.

[3]   Z. Wang, Z. Cheng, W. Yuan, J. Cai, L. Zhang, F. Zhang, F. Qi and J. Wang, *Combustion and Flame*, 159, (2012) 2243.

[4]   M.K.K. B. R. Nautiyal, R. K. Joshi, B. S. Rawat, S. M. Nanoti, G. Prasad, D. Paul, M. O. Garg, *Separation of cyclopentane from light naphtha fraction*, at: Petrotech, New Delhi, January 9-12,

[5]   Z. Serinyel, O. Herbinet, O. Frottier, P. Dirrenberger, V. Warth, P.A. Glaude and F. Battin-Leclerc, *Combustion and Flame*, 160, (2013) 2319.

[6]   I.G. Zsely, T. Varga, T. Nagy, M. Cserhati, T. Turanyi, S. Peukert, M. Braun-Unkhoff, C. Naumann and U. Riedel, *Energy*, 43, (2012) 85.

[7]   W. Hui, H.F. Yang, X.Q. Ran, Q.Z. Shi and Z.Y. Wen, *Journal of Molecular Structure-Theochem*, 678, (2004) 39.

[8]   H. Wang, H.F. Yang, X.Q. Ran, Q.Z. Shi and Z.Y. Wen, *Journal of Molecular Structure-Theochem*, 581, (2002) 187.

[9]   Z.M. Tian, C.L. Tang, Y.J. Zhang, J.X. Zhang and Z.H. Huang, *Energy & Fuels*, 29, (2015) 428.

[10]   B. Sirjean, F. Buda, H. Hakka, P.A. Glaude, R. Fournet, V. Warth, F. Battin-Leclerc and M. Ruiz-Lopez, *Proceedings of the Combustion Institute*, 31, (2007) 277.

[11]   W. Tsang, *International Journal of Chemical Kinetics*, 10, (1978) 599.

[12]   B. Sirjean, P.A. Glaude, M.F. Ruiz-Lopez and R. Fournet, *Journal of Physical Chemistry A*, 110, (2006) 12693.

[13]   C.J. Annesley, C.F. Goldsmith and R.S. Tranter, *Physical Chemistry Chemical Physics*, 16, (2014) 7241.

[14]   J.B. Randazzo, C.J. Annesley, K. Bell and R.S. Tranter, *Proceedings of the Combustion Institute*, 36, (2017) 273.

[15]   K. Wang, S.M. Villano and A.M. Dean, *Combustion and Flame*, 162, (2015) 4456.

[16]   M.R. Djokic, K.M. Van Geem, C. Cavallotti, A. Frassoldati, E. Ranzi and G.B. Marin, *Combustion and Flame*, 161, (2014) 2739.

[17]   S. Merchant, Molecules to Engines: Combustion chemistry of Alcohols and their application to advanced engines, MIT, 2015,

[18]   V. Warth, N. Stef, P.A. Glaude, F. Battin-Leclerc, G. Scacchi and G.M. Come, *Combustion and Flame*, 114, (1998) 81.

[19]   F. Buda, R. Bounaceur, V. Warth, P. Glaude, R. Fournet and F. Battin-Leclerc, *Combustion and Flame*, 142, (2005) 170.

[20]   S. Touchard, F. Buda, G. Dayma, P.A. Glaude, R. Fournet and F. Battin-Leclerc, *International Journal of Chemical Kinetics*, 37, (2005) 451.

[21]   M. Yahyaoui, N. Djebaili-Chaumeix, C.E. Paillard, S. Touchard, R. Fournet, P.A. Glaude and F. Battin-Leclerc, *Proceedings of the Combustion Institute*, 30, (2005) 1137.

[22]   E.D. H. Wang, B. Sirjean, D. A. Sheen, R. Tango, A. Violi, J. Y. W. Lai, F. N. Egolfopoulos, D. F. Davidson, R. K. Hanson, C. T. Bowman, C. K. Law, W. Tsang, N. P. Cernansky, D. L. Miller, R. P. Lindstedt, in, http://web.stanford.edu/group/haiwanglab/JetSurF/JetSurF2.0/index.html, 2010, p. A high.

[23]   N.M. Vandewiele, K.M. Van Geem, M.F. Reyniers and G.B. Marin, *Chemical Engineering Journal*, 207, (2012) 526.

[24]   S.P. Pyl, K.M. Van Geem, P. Puimege, M.K. Sabbe, M.F. Reyniers and G.B. Marin, *Energy*, 43, (2012) 146.

[25]   J.C. Giddings and H.J. Cortes, *Multidimensional Chromatography - Techniques and Applications*, Marcel Dekker, New York, 1990, p.

[26]   J.C. Giddings, *Journal of Chromatography A*, 703, (1995) 3.

[27]   J.B. Phillips and J. Beens, *Journal of Chromatography A*, 856, (1999) 331.

[28]   J. Dalluge, J. Beens and U.A.T. Brinkman, *Journal of Chromatography A*, 1000, (2003) 69.

[29]   Z.Y. Liu and J.B. Phillips, *Journal of Chromatographic Science*, 29, (1991) 227.

[30]   M.K. Sabbe, K.M. Van Geem, M.F. Reyniers and G.B. Marin, *Aiche Journal*, 57, (2011) 482.

[31]   M.K. Sabbe, M.F. Reyniers, V. Van Speybroeck, M. Waroquier and G.B. Marin, *Chemphyschem*, 9, (2008) 124.

[32]   M.K. Sabbe, M.F. Reyniers, M. Waroquier and G.B. Marin, *Chemphyschem*, 11, (2010) 195.

[33]   M.K. Sabbe, A.G. Vandeputte, M.F. Reyniers, M. Waroquier and G.B. Marin, *Physical Chemistry Chemical Physics*, 12, (2010) 1278.

[34]   R. Van de Vijver, N.M. Vandewiele, A.G. Vandeputte, K.M. Van Geem, M.F. Reyniers, W.H. Green and G.B. Marin, *Chemical Engineering Journal*, 278, (2015) 385.

[35]   in, Reaction Design, San Diego, 2013.

[36]   G.A. Petersson, D.K. Malick, W.G. Wilson, J.W. Ochterski, J.A. Montgomery and M.J. Frisch, *Journal of Chemical Physics*, 109, (1998) 10570.

[37]   G.W.T. M. J. Frisch, H. B. Schlegel, G. E. Scuseria, M. A. Robb, J. R. Cheeseman, G. Scalmani, V. Barone, B. Mennucci, G. A. Petersson, H. Nakatsuji, M. Caricato, X. Li, H. P. Hratchian, A. F. Izmaylov, J. Bloino, G. Zheng, J. L. Sonnenberg, M. Hada, M. Ehara, K. Toyota, R. Fukuda, J. Hasegawa, M. Ishida, T. Nakajima, Y. Honda, O. Kitao, H. Nakai, T. Vreven, J. A. Montgomery, Jr., J. E. Peralta, F. Ogliaro, M. Bearpark, J. J. Heyd, E. Brothers, K. N. Kudin, V. N. Staroverov, R. Kobayashi, J. Normand, K. Raghavachari, A. Rendell, J. C. Burant, S. S. Iyengar, J. Tomasi, M. Cossi, N. Rega, J. M. Millam, M. Klene, J. E. Knox, J. B. Cross, V. Bakken, C. Adamo, J. Jaramillo, R. Gomperts, R. E. Stratmann, O. Yazyev, A. J. Austin, R. Cammi, C. Pomelli, J. W. Ochterski, R. L. Martin, K. Morokuma, V. G. Zakrzewski, G. A. Voth, P. Salvador, J. J. Dannenberg, S. Dapprich, A. D. Daniels, Ö. Farkas, J. B. Foresman, J. V. Ortiz, J. Cioslowski, and D. J. Fox, in, Wallingford CT, 2009.

[38]   A.L.L. East and L. Radom, *Journal of Chemical Physics*, 106, (1997) 6655.

[39]   L.A. Curtiss, K. Raghavachari, P.C. Redfern and J.A. Pople, *Journal of Chemical Physics*, 106, (1997) 1063.

[40]   L.A. Curtiss, K. Raghavachari, P.C. Redfern, V. Rassolov and J.A. Pople, *Journal of Chemical Physics*, 109, (1998) 7764.

[41]   M.K. Sabbe, M. Saeys, M.F. Reyniers, G.B. Marin, V. Van Speybroeck and M. Waroquier, *Journal of Physical Chemistry A*, 109, (2005) 7466.

[42]   H.H. Carstensen and A.M. Dean, *International Journal of Chemical Kinetics*, 44, (2012) 75.

[43]   H.H. Carstensen and A.M. Dean, *Journal of Physical Chemistry A*, 113, (2009) 367.

[44]   H.H. Carstensen, C.V. Naik and A.M. Dean, *Journal of Physical Chemistry A*, 109, (2005) 2264.

4

An experimental and kinetic modeling study of cyclohexane pyrolysis

The pyrolysis of undiluted cyclohexane has been studied in a continuous flow tubular reactor at temperatures from 913 to 1073K, inlet feed flow rates in the range 288-304 g.h-1 at 0.17 MPa reactor pressure with average reactor residence time of 0.5 s calculated based on the pressure in the reactor, the temperature profile along the reactor and the molar flow rate along the reactor estimated by the logarithmic average of the inlet and outlet molar flows. The reactions lead to conversions between 2% and 95%. 49 products were identified and quantified using two dimensional gas chromatography equipped with TCD and FID detectors. The products with molecular weights between those of hydrogen and naphthalene constitute more than 99 mass% of the total products. A kinetic mechanism composed exclusively of elementary step reactions with high pressure limit rate coefficients has been generated with the automatic network generation tool "Genesys". The kinetic parameters for the reactions originate either directly from high level ab-initio calculations or from reported group additive values which were derived from ab-initio calculations. The Genesys model performs well when compared to five models available in the literature and its predictions agree well with the experimental data for 15 products without any adjustments of the kinetic parameters. Reaction path analysis shows that cyclohexane consumption is initiated by the unimolecular isomerization to 1-hexene but is overall dominated by hydrogen abstraction reactions by hydrogen atoms and methyl radicals. Dominant pathways to major products predicted with the new model are discussed and compared to other well performing models in literature.

4.1. Introduction

Petrochemical feedstocks and derived liquid fuels are complex mixtures composed of various molecule classes such as paraffins, olefins, naphthenes and aromatics. Whether used for pyrolytic or combustion applications, the thermal decomposition chemistry of cyclic compounds plays a central role in the prediction of product yields from biomass fast pyrolysis [1], waste fractions [2], scram jet modelling [3-6], naphtha steam cracking [7] and autoignition of gasoline [8-10]. Therefore the pyrolysis chemistry of hydrocarbons has been the subject of research for many years. While the gas-phase chemistry of open-chain hydrocarbons is very well understood, the knowledge of pyrolysis reaction of cyclic hydrocarbons is less matured [10, 11]. This is even true for the simplest cycloalkanes, such as cyclopentane and cyclohexane.

Thermal decomposition of cyclohexane has been studied for more than 100 years and many publications exist on this topic [10-26]. Only some selected studies will be briefly reviewed in the following paragraphs. The single pulse shock tube experiments between 1000K to 1200K reported by Tsang [27] in 1978 were the first study to provide important mechanistic insight as it showed that cyclohexane is directly converted to 1-hexene. This result together with the overall decomposition rates were later confirmed experimentally by Kiefer [28] using a shock tube setup with laser-schlieren analysis at 1300K to 2000K. Kiefer analyzed this data with a Master equation approach accounting for pressure fall-off behavior. An ab initio study by Sirjean et al. [29] further supported these experimental results.

Tubular and annular stainless steel flow reactor experiments conducted by Aribike, Susu and Ogunye [30-33] at atmospheric pressure and residence times in the range of 0.16 to 0.48 s used gas chromatography to measure effluent product distributions as a function of temperature (1003K to 1133K) and conversions between 23% to 70%. The authors noted differences in the results depending on the reactor type used and concluded that the reactor material is catalytically active. The products measured were hydrogen, methane, ethane, ethylene, propylene, propane, acetylene, butadiene and butenes. Higher molecular weight compounds such as cyclopentadiene, benzene and polycyclic aromatic hydrocarbons could not be detected. A non-elementary molecular mechanism was put together using mainly estimated rate parameters. Using pulse injections into a pyrolysis GC, Zamostny et al [34] studied the relative pyrolytic behavior of various families of chemicals including

cycloalkanes. Given the uncertainties in temperature profile, residence time, concentrations, the results are only of qualitative value and not suitable for kinetic modeling. Pyrolysis experiments on pure and substituted cyclohexanes at super-critical conditions were reported by Lai and Song [35]. These batch experiments at 723K required a reaction time of 480 minutes for sufficient conversion, monitored via pressure increase. Comprehensive product analyses were done including aromatics and the most important conclusion from this study is that long chains attached to the cycloalkane have a significant impact on the reactivity as these side chains react faster than ring opening.

Besides the earlier studies by Tsang and Kiefer, more recent shock tube studies on cyclohexane pyrolysis have been reported by Peukert et al [36, 37]. The focus of the studies was on hydrogen atom generation and hydrogen atom reactions with cyclohexane. Wang et al. [38] reported plug flow pyrolysis experiments at very low cyclohexane partial pressure (< 1 mbar). The study was done using the advanced synchrotron light source in Hefei for SVUV-PIMS detection. Extensive product spectra as a function of temperature between 950 and 1520 K were recorded and a kinetic model was developed to explain the experimental data.

A few kinetic models exist which can be used to predict the product distribution of cyclohexane pyrolysis experiments although not all are applicable for all reaction conditions of interest. The list includes: JetSurF [39], POLIMI[40-43] gas phase model, a cyclohexane mechanism developed in Nancy [10] and the aforementioned Hefei mechanism by Wang et al. [38]. Furthermore, Wang et al. proposed a comprehensive ab-initio based kinetic model (CSM) for propylene pyrolysis[44] which includes cyclohexane chemistry and some limited single-step lumped reactions to form aromatics like benzene, toluene, styrene, indene and naphthalene from 1,3-cyclopentadiene.

Despite the large literature and availability of several kinetic models, there are still important open questions on cyclohexane pyrolysis, which motivated the current study. First, only very limited experimental data is available that relate to technically relevant, e.g., steam-cracking, conditions. Therefore experiments are conducted in an isothermal plug flow reactor covering cyclohexane conversions from 2 to 95%. Second, the available kinetic models are tested against this new data to explore the accuracy of their predictions. Third, a new kinetic model based solely on elementary step reactions, a first of its kind, is developed with the aid of an pautomated mechanism generating tool. Here the objective is

to test if such automatically generated models can compete with optimized models from the literature. Finally, the most important reaction pathways will be analyzed for steam cracking conditions.

4.2. Methodology

4.2.1. Experimental setup and procedure

The experimental bench scale unit consists of three main sections – feed section, reactor section and product analysis section. It has been described in detail elsewhere[45, 46]. Only the specifics related to this work will be given. The length of the reactor is 1.47m with 6mm internal diameter, made of Incoloy 800HT (Ni, 30-35; Cr, 19-23; and Fe, >39.5 wt %). The reactor is placed vertically in a rectangular furnace, where it is heated to a preset temperature. In all experiments, the reactor is operated nearly isothermally, i.e. with a steep temperature increase at the reactor inlet and a steep temperature drop at the outlet of the reactor. Thermocouples monitor the process gas temperature at eight axial positions. The pressure in the reactor is controlled by an outlet pressure restriction valve. Two manometers, situated at the inlet and outlet of the reactor, allow measuring the coil inlet pressure (CIP) and the coil outlet pressure (COP), respectively. The pressure drop over the reactor was found to be negligible, with the pressure remaining constant in the reactor at 0.17 MPa. In all the experiments, the reactor was operated nearly isothermally from 913K to 1073K. In the setup, Type K thermocouples are used for which the manufacturer calibrated accuracy is ±2.2K or 0.75% of the reading in °C whichever is greater, valid for the temperature range 273-1523K (0-1250°C). For example, for 800K the accuracy is ±6K[47]. Cyclohexane was pumped through a coriolis mass flow controller at 288 - 304 g.h^{-1} and fed to an electrically heated tubular reactor made of Incoloy 800HT. No diluent was used, however nitrogen was added to the reactor effluent serving as an internal standard. For each experiment, the nitrogen set point was constant and in the range of 20 - 50 gh^{-1}. The flow rate of cyclohexane was chosen such that an average residence time of 0.5 s in the heated zone is obtained. Reactor temperature was varied between 913 and 1073K, with reactor pressure at 0.17 MPa. The average reactor residence time was calculated based on the pressure in the reactor, the temperature profile along the reactor and the molar flow rate along the reactor estimated by the logarithmic average of the inlet and outlet molar flows.

The reactor effluent is sampled on-line, and at high temperature (625 K) to avoid condensation [48]. Even after 8 hours of operation, there was no change in pressure drop across the reactor and the H/C ratio of the outlet stream matched that of the inlet stream. In addition, during several hours of maintaining the constant operating conditions, the acquired and analyzed product effluent had a stable composition indicating no effect of either the wall or coke on gas phase reactions. If the coke deposit or the reactor wall had any effect on the gas kinetics, this should be noticed in the mass fraction profiles of the products species. The product analysis section consisted of two different gas chromatographs for a detailed analysis of the reactor effluent: a so-called refinery gas analyzer (RGA) and a GC×GC-FID/TOF-MS. The former enabled analysis of permanent gases and light hydrocarbons (H_2 – C_4), while the latter analyzed the whole product spectrum. Response factors for the former were determined by calibration with a known gas mixture [7, 45, 46, 48] supplied by Air Liquide, Belgium. The response factors of the C_{5+} compounds were determined using the effective carbon number method relative to methane. GC×GC is an arrangement of 2 GC columns in series situated in a single oven with programmable temperature profile. The first GC column typically separates compounds based on volatility and the second GC column based on polarity. This enables a fast group-type analysis and provisional classifications of unknowns [49]. Quantification in GC×GC has several advantages over 1D-GC such as:

    a. Ordering which makes interference due to peak overlap less likely [50, 51].

    b. Greater sensitivity or detectability due to the high speed of the second column. The resulting peaks are sharper and, therefore, exhibit a higher signal response [51].

    c. Reliable presence of a true baseline for peak integration [51].

The relative error on the mass fractions of products was less than 10% based on prior experience[42, 44]. The mass balance closure was checked using the internal standard method, i.e. nitrogen being continuously added to the reactor effluent to serve as an internal standard. Based on the determined reactor effluent composition, the elemental outlet flows of carbon and hydrogen were calculated. The latter was compared to the feedstock and in

the case of the cyclohexane pyrolysis experiments, both, the carbon and hydrogen balances were within 5% at all experimental conditions.

4.2.2. Kinetic model generation

4.2.2.1 CBS-QB3 computation of rate coefficients

For critical reactions, the CBS-QB3 method [52] was used to compute rate coefficients. The study was performed with the Gaussian 09 revision D suite of programs [53] as implemented on the high-performance supercomputing facility at Ghent University. CBS-QB3 calculations give geometries, external moments of inertia, harmonic oscillator frequencies and the electronic energy at 0 K. The first three properties are used to calculate entropies, heat capacities and thermal contributions to the enthalpy using statistical mechanics calculations. Except for internal rotations, which were treated separately, all internal modes were assumed to behave as harmonic oscillators and a scaling factor of 0.99 was applied. Internal modes that resemble rotations around a single bond were treated separately by replacing the contributions of the corresponding oscillators to the partition function with numerically calculated partition functions for these hindered rotors. The required hindrance potentials were obtained from scans, in which the dihedral angle defining the rotation was varied from 0 to 360 degrees in steps of 10 degrees while all other molecule parameters were allowed to optimize. The obtained hindrance potential was then expressed as a Fourier series. Together with the reduced moment of inertia calculated at the $I^{(2,3)}$ level as defined by East and Radom [54], the hindrance potential was used to construct the Schrödinger equation for 1-D rotation. The eigenvalues of the solution to this Schrödinger equation represent the energy levels of this mode. They were used to determine the corresponding partition function as a function of temperature. After corrections for symmetry and optical isomers, the total partition function was used to calculate the thermal contribution to the enthalpy, standard entropy and temperature-dependent heat capacity data.

Enthalpies of formation in CBS-QB3 were calculated with the atomization method [55]. Two additional corrections accounting for spin-orbit interactions [52, 55, 56] and systematic Bond Additive Corrections (BAC) [52] significantly improve these values as have been

shown in previous work [57]. However, such corrections are only needed to calculate the thermodynamic properties. All transition state calculations used uncorrected enthalpy data because BACs are not known for transition states. All thermodynamic data are stored as NASA polynomials.

Transition state theory expressed in terms of Gibbs free energies was used to calculate the rate coefficients, as shown in equation 1:

$$k_{TST}(T) = \chi(T) \cdot \frac{k_B T}{h} \cdot \left(\frac{RT}{p}\right)^{\Delta n - 1} \cdot e^{-\frac{\Delta G^{\ddagger}}{RT}}$$

$\Delta G^{\ddagger}$ is the Gibbs free energy difference between transition state without the transitional mode and reactant(s), Δn is the molecularity of the reaction (2 for bimolecular and 1 for unimolecular reactions), and $\chi(T)$ accounts for quantum mechanical tunneling. Other symbols are defined in the list of symbols. The asymmetric Eckart potential is used to estimate tunneling contributions $\chi(T)$. The Gibbs free energies were obtained from the NASA polynomials. Rate coefficients were calculated for the temperature range 300 K to 2500 K in steps of 50 K and the results between 800 K and 1200 K were regressed to an Arrhenius expression (Table 4.2). The majority of calculated reaction rate coefficients are believed to be within a factor of 3 of the correct value.

The CBS-QB3 method used here was the same as that used by Vermeire et al.[58] and Paraskevas et al.[59] who established the uncertainty in calculated enthalpy of formation at 298 K to be generally within 4kJ/mole and entropies are expected to be well reproduced. This uncertainty was further supported by Villano et al[60]. Carstensen and Dean[61] studied the hydrogen abstraction reaction from methane by a hydrogen atom at the CBS-QB3 level of theory. For this case study, the deviation between the theoretical and experimental rate coefficient was within a factor 2. Vandeputte et al.[62] assessed the reliability of two composite methods and two density functional theory methods for the determination of kinetic parameters. Also the influence the internal hindered rotor treatment and the effect of tunneling is studied. The best agreement with experimental data is obtained with the CBS-QB3 level of theory combined with 1D-HIR corrections and Eckart tunneling. With this approach, the uncertainty on the kinetic data between 600 and 1000 K is below a factor of 3.

4.2.2.2. Reaction families and Mechanism generation

The objective is to create a cyclohexane pyrolysis model consisting of only elementary reversible reactions whose kinetics and thermodynamics are based on ab-initio electronic structure calculations. The first step is to select the relevant reaction families. For ethane cracking [63], Sabbe et al. used the following reaction families: hydrogen abstraction, hydrogen atom addition, carbon radical addition and recombination (and their reverse reaction families). Based on related literature [29, 44, 64, 65], the following reaction families and reactions also have been considered: Intra-molecular carbon centered radical addition, hydrogen shift, Intra-molecular hydrogen abstraction, cycloalkane isomerization to 1-alkene, Diels-Alder reaction, direct H_2 elimination. Table 4.1 shows the complete list that was used to generate a mechanism for cyclohexane pyrolysis.

Table 4.1: Reaction families considered in this work

Reaction family	Description/ Example	Reference for kinetics
Hydrogen transfer		
Inter-molecular H-abstraction	by C• by H•	[74], In-house
Intra-molecular H-abstraction (acyclics)	$C\text{-}(C)_n\text{-}C\bullet \rightleftarrows \bullet C\text{-}(C)_n\text{-}C$	[63], In-house
Intra-molecular H-abstraction (cyclics)		[44, 64]
Intra-CPD-H-shift		[64]
Addition		
Inter-molecular C-radical addition	$C=C + \bullet C \rightleftarrows \bullet C\text{-}C\text{-}C$	[72]
Intra-molecular C-radical addition		[44, 64]
Hydrogen atom addition	$\bullet C\text{-}C\text{-}H \rightleftarrows C=C + \bullet H$	[73]
Recombination		
C-C recombination	$\bullet C + \bullet C \rightleftarrows C\text{-}C$	[44, 63, 64]
C-H recombination	$\bullet C + H \rightleftarrows C\text{-}H$	[44, 63, 64]
H2 elimination		
Direct release of H2 gas		[64, 65]
Diels-Alder		
Molecular mechanism – rearrangement of double bonds		[64]
Isomerization		
Ring opening of cycloalkanes		[29]

The in-house automatic mechanism generation tool, "Genesys" [66] was used to generate the mechanism for cyclohexane pyrolysis. The C_0-C_4 base chemistry has been completely generated in-house using Genesys. Genesys contains large databases of thermodynamic and kinetic parameters and uses these as primary source for the assignment of parameters during the kinetic model generation. If no entry is present in these databases for thermodynamic properties or kinetics, these are estimated by group additivity methods[57, 67-69]. A detailed example of how these group additive methods work are given in the work by Khandavilli et al.[47]. Hence, the C_0-C_4 base mechanism is incorporated in one of databases of Genesys and it is primarily based on in-house high level ab initio calculations. The aromatics chemistry is based on various literature sources. The ethane pyrolysis model of Sabbe et al.[63] contains ab-initio kinetics of elementary reactions leading to benzene formation starting from 1,3-butadiene and vinyl radical. Merchant's model for the pyrolysis of a cyclopentadiene-ethene mixture[64] has the kinetics for H-shift reactions and many reactions of intra-molecular carbon radical addition from which group additive values were derived and made part of Genesys databases[47]. These groups of reactions play an important role in ring formation and ring expansion, ultimately leading to the formation of aromatics higher than benzene like toluene, styrene, indene and naphthalene. In Genesys, the size of the kinetic model is controlled by a rule based termination criterion. In Genesys, starting from the user-defined reaction families and the initial feed molecules, an exhaustive mechanism is generated which is terminated by user-defined constraints on product species, e.g. constraints on the maximum carbon number, and constraints on the reaction families, e.g. limiting the size of the abstracting and adding species. The reaction families are defined by the user in Genesys by supplying a reaction recipe, the possible reactive center by the user-friendly SMARTS language and constraints on the appearance of the reaction family or the products formed by this reaction family. Reaction recipes were created for the families listed in Table 4.1. Example recipes are shown in[47]. The feed molecule to Genesys in this work is cyclohexane. In the first loop of the mechanism generation algorithm, this molecule is tested for possible reactions included in Table 4.1. Accordingly, 1-hexene is generated by isomerization. In the next iteration, both 1-hexene and cyclohexane act as input species for possible reactions among those in Table 4.1, and C-C recombination (its reverse reaction) becomes active on 1-hexene to generate allyl and 1-propyl radicals. In the next iteration, these radicals abstract hydrogen from cyclohexane, among other possibilities.

This procedure is continued - the list of species presented is at any iteration tested for possible reactions to generate new species. In this way, the mechanism grows until it reaches a certain constraint and there are no more new species generated. The constraint used for the present case was the carbon number of 10 based on the idea to stop the molecular growth at naphthalene. Algorithmic details about mechanism generation using Genesys, including schematics can be found in [66, 70, 71].

4.2.2.3. Kinetics and thermodynamics assignment

After the mechanism generation is completed, Genesys assigns kinetic parameters to the reactions and thermodynamic parameters to the species from user-defined databases. The kinetics databases contain kinetics in the form of standard group additive values ($\Delta GAV°$) of single event Arrhenius pre-exponential factors and activation energies. These $\Delta GAV°$s are defined as a function of groups (molecular fragments/ branches) attached to the reactive centers for a particular reaction family. The $\Delta GAV°$s have already been reported[47, 72-74], and were used in the Genesys kinetics databases as such. The number of single events, based on symmetry numbers and optical isomers of reactants and transition states is calculated by an auxiliary code of Genesys called SIGMA [75]. The reference[47] shows how kinetic rate parameters are calculated using the group additive values. For thermodynamics, ab-initio/ group additive parameters exist [44, 63, 64] in the form of NASA polynomial coefficients. These coefficients were coded into the species thermodynamic database of Genesys so that they are assigned when a particular species is found in the mechanism. For species which are not included in the database, thermodynamics can be estimated by group additivity in Genesys. Based on these input databases, Genesys assigned kinetics to the reactions of the mechanism, yielding an automatically generated group additive model for cyclohexane pyrolysis. Genesys generated the model as a ChemKin [76] readable input file. Initial simulations with cyclohexane feed pointed toward a few critical reactions whose kinetics were worthwhile to be refined by a high level CBS-QB3 computation [52].

4.3. Results and discussion

4.3.1 Experimental data

Forty molecules were detected and quantified in the reactor effluent during experiments at temperatures between 913K and 1073K in 20K intervals. Out of the 40 molecules detected, 21 were detected with peak quantities above 0.5 wt% and 15 of those have maximum mass fractions above 0.8 wt%. The profiles of these 15 are shown in Figures 4.1-4.4.
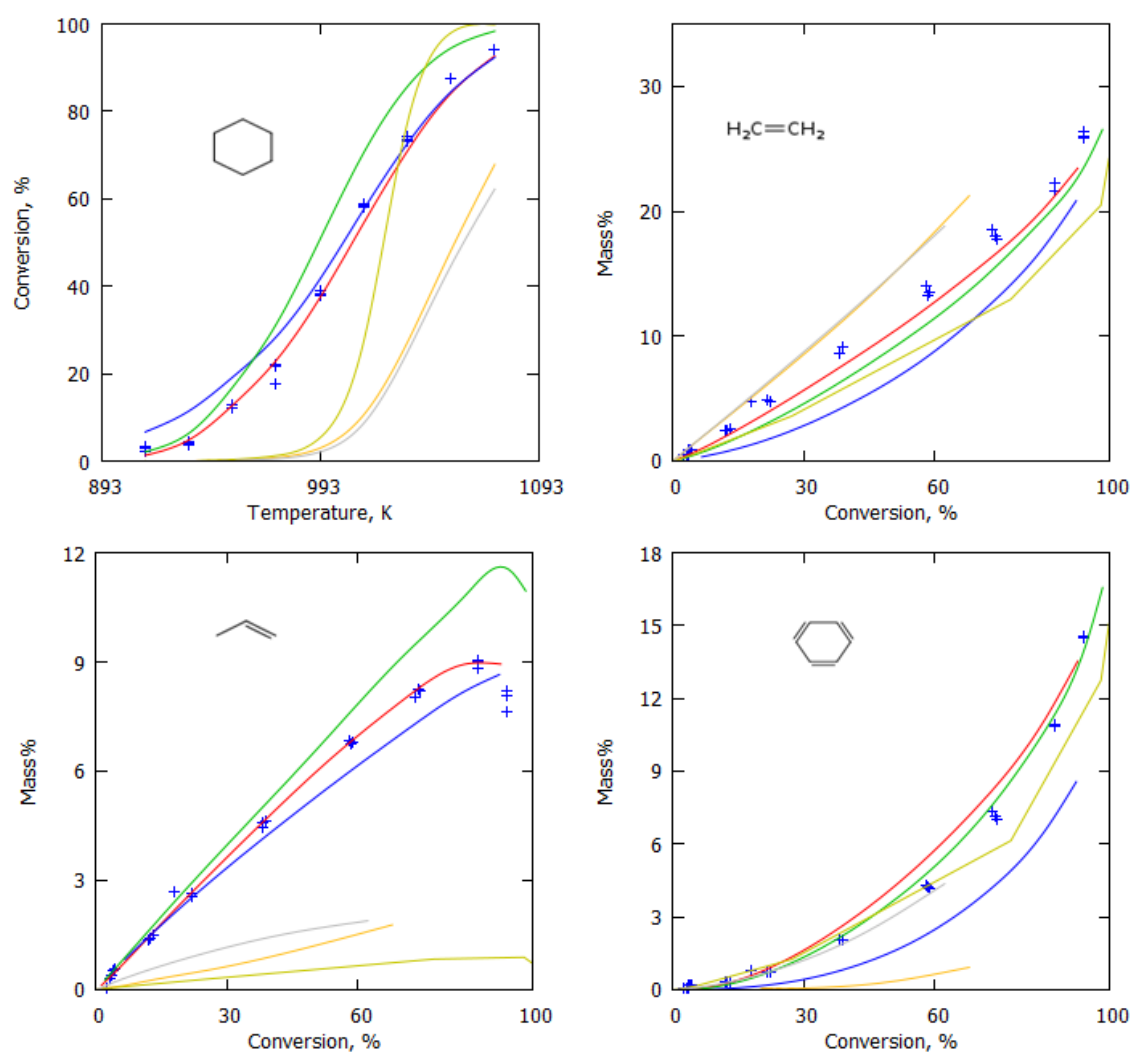
Figure 4.1: Experimental data and model predictions for cyclohexane conversion, mass % of ethylene, propylene and benzene in cyclohexane pyrolysis in continuous flow experiments, 0.17 MPa pressure at 0.5s average residence time (+ Experiment, ▬▬ Genesys, ▬▬ POLIMI, ▬▬ CSM, ▬▬ Hefei, ▬▬ Nancy, ▬▬ JetSurF)
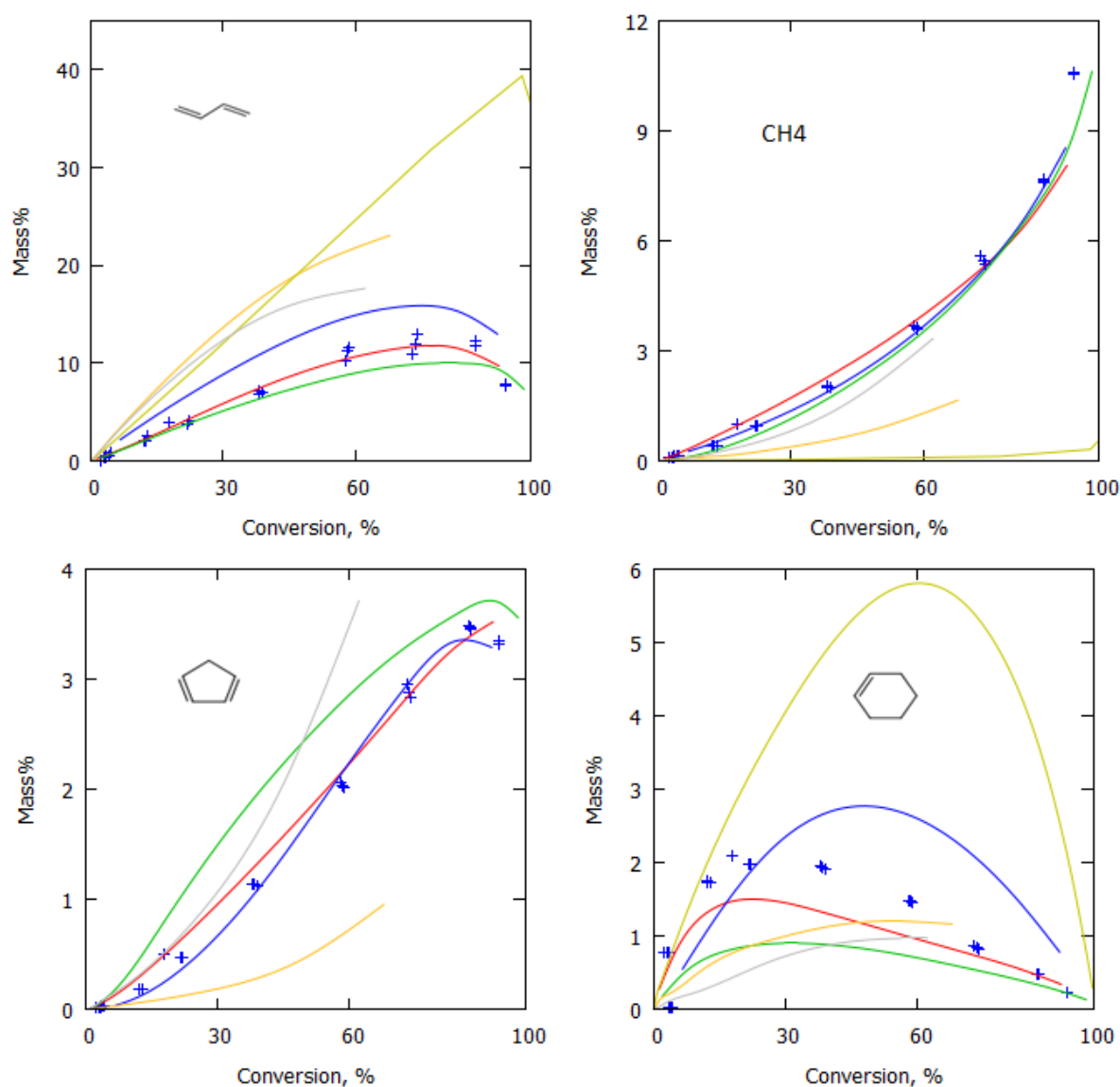
Figure 4.2: Experimental data and model predictions for mass % of 1,3-butadiene, methane, 1,3-cyclopentadiene and cyclohexene in cyclohexane pyrolysis in continuous flow experiments, 0.17 MPa pressure at 0.5s average residence time (+ Experiment, ▬ Genesys, ▬ POLIMI, ▬ CSM, ▬ Hefei, ▬ Nancy, ▬ JetSurF)
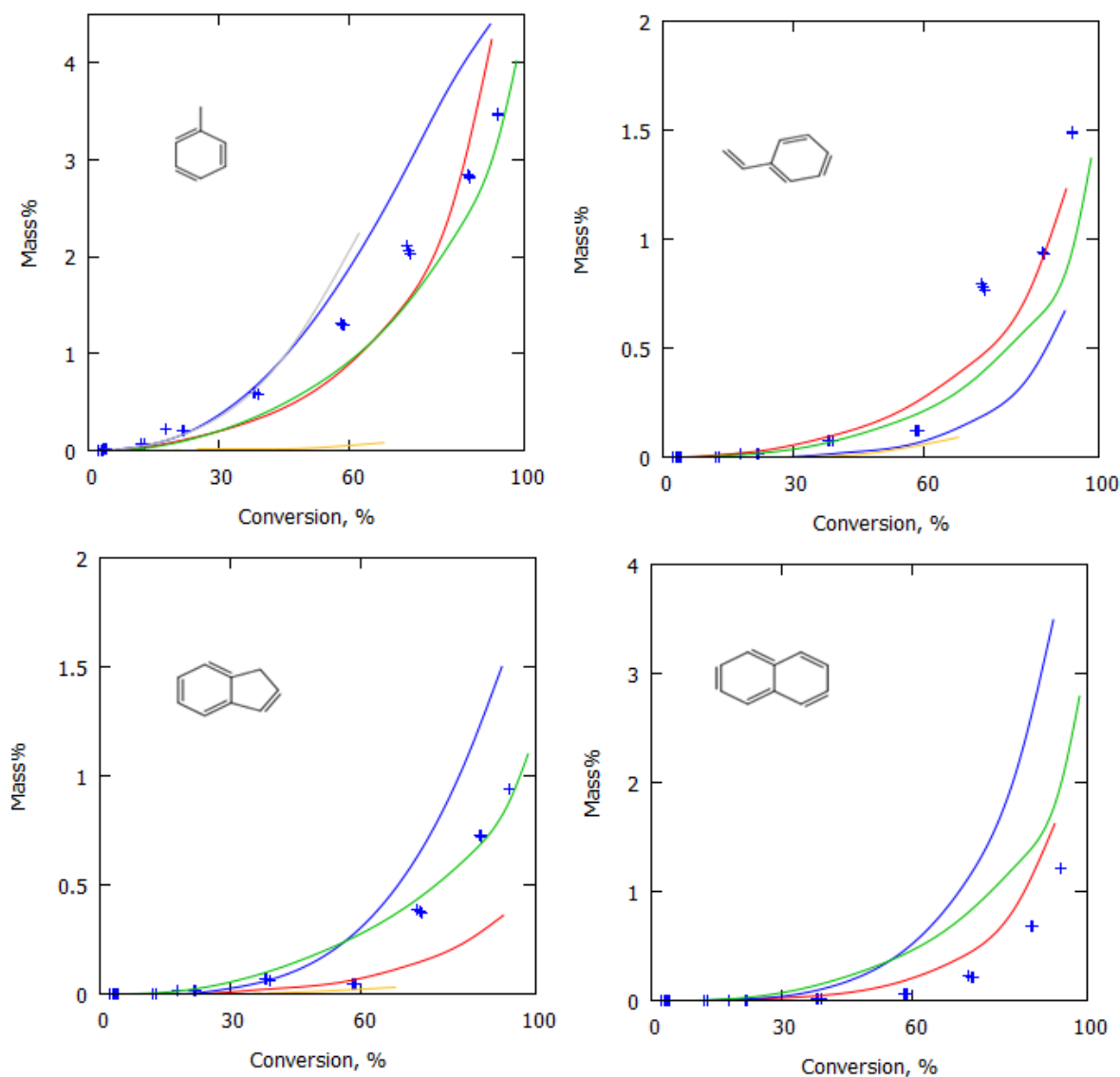
Figure 4.3: Experimental data and model predictions for mass % of toluene, styrene, indene and naphthalene in cyclohexane pyrolysis in continuous flow experiments, 0.17 MPa pressure at 0.5s average residence time (+ Experiment, ▬▬ Genesys, ▬▬ POLIMI, ▬▬ CSM, ▬▬ Hefei, ▬▬ Nancy, ▬▬ JetSurF)
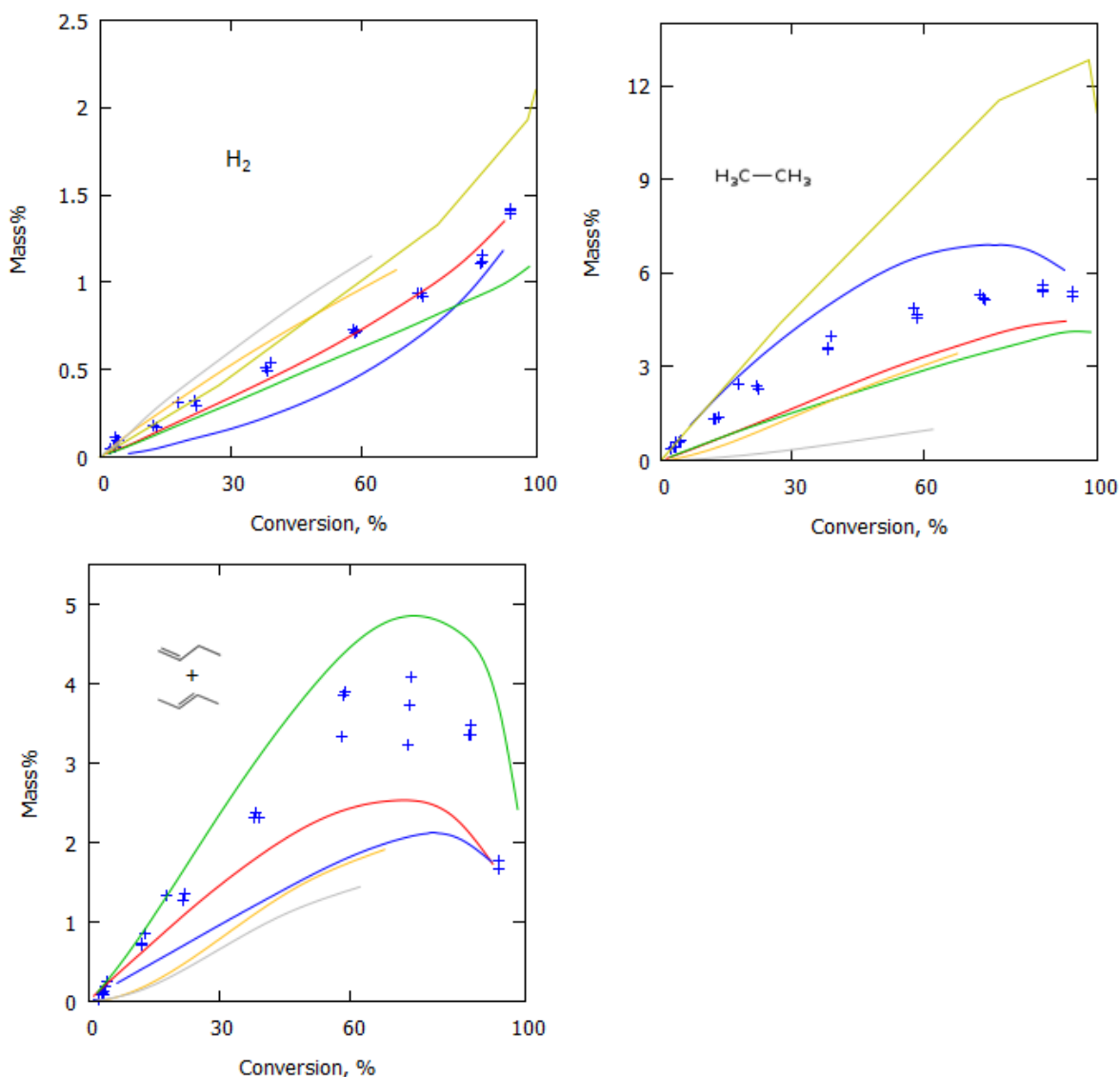
Figure 4.4: Experimental data and model predictions for mass % of hydrogen, ethane and butenes in cyclohexane pyrolysis in continuous flow experiments, 0.17 MPa pressure at 0.5s average residence time (+ Experiment, ——— Genesys, ——— POLIMI, ——— CSM, ——— Hefei, ——— Nancy, ——— JetSurF)

It can be seen that the experimental ethylene yield increases monotonically to 25 wt% at the highest temperature, while propylene yield plateaus at around 9 wt%. Benzene yield increases exponentially with the temperature and reaches a maximum of 15 wt%, while 1,3-butadiene shows a maximum of more than 10 wt%. Ethane goes up to 6 wt% while 1,3-cyclopentadiene reaches a maximum of less than 4 wt%. Methane increases monotonically to 9 wt% while hydrogen stays below 1.5 wt%. n-butenes are below 4 wt% while cyclohexene undergoes a maximum at less than 3 wt%. Among aromatics other than

benzene, toluene increases to 4 wt% while styrene, indene and naphthalene stay below 1.5 wt%.

4.3.2. Performance of literature models on the new experimental data

Five popular models from literature were tested against the new experimental data: POLIMI[40-43], CSM[44], Hefei[38], Nancy[10] and JetSurF[39]. The POLIMI model was originally intended to predict the laminar flame speeds of fuel/ air mixtures. The POLIMI model is a combination of many sub-mechanisms, a sub-mechanism for cyclohexane being one too. Hence, the POLIMI model has been tested for the new experimental data. For the case of cyclohexane/ air flames, the temperatures tested were 298K and 353K with respect to experimental data reported in 1998. More recently, the POLIMI model was extended to predict cyclopentadiene pyrolysis[45]. The POLIMI model has been generated automatically by the MAMA program which creates lumped species and reactions. The main objective there was to create a compact model which is applicable to a wide range of feeds. However, due to lumping, the underlying elementary reactions and their kinetics are no longer transparent to the user. Also, many of the reactions are not listed as reversible reactions. Some examples of lumped reactions in the POLIMI model are shown in Figure 4.5.
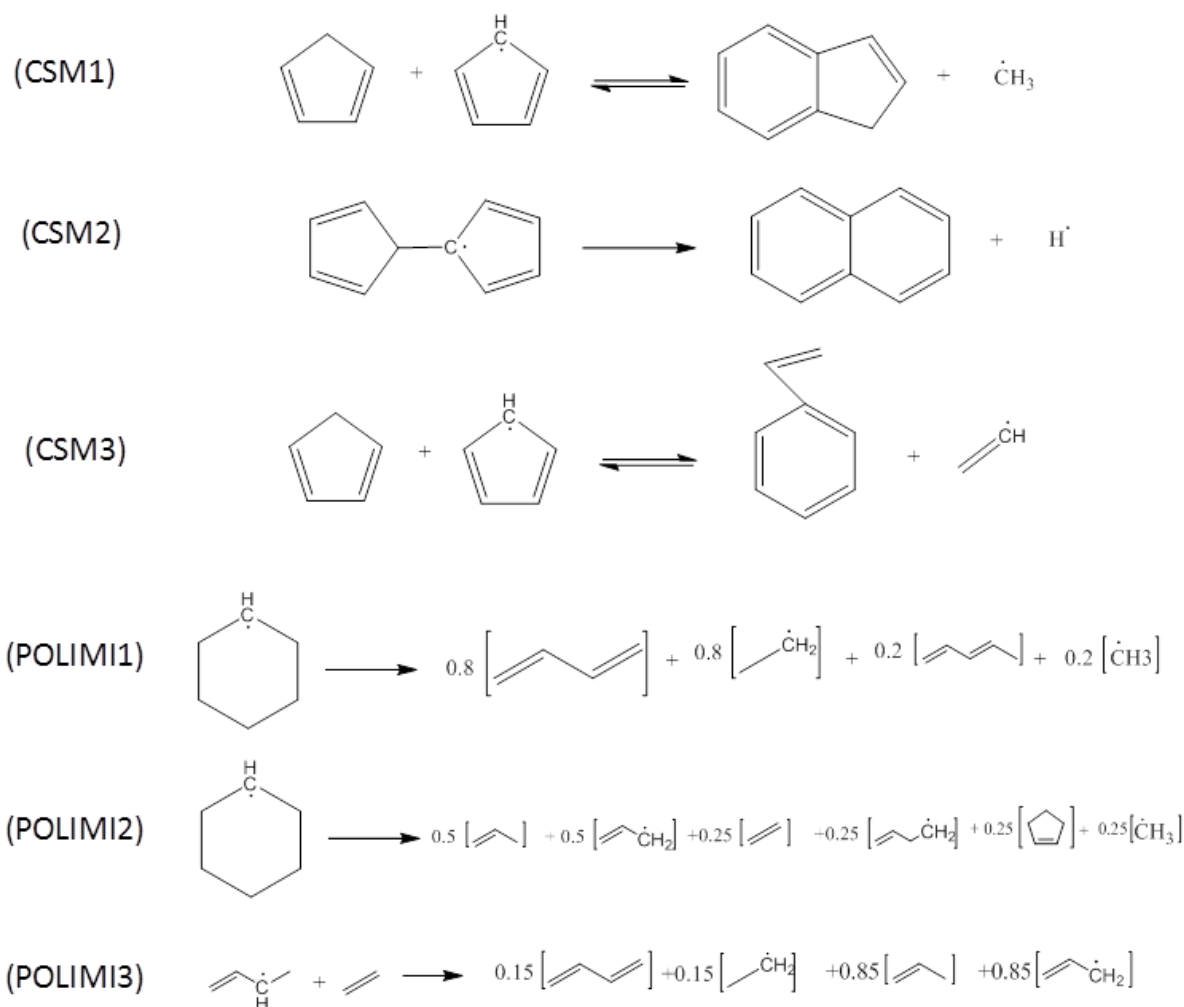
Figure 4.5: Dominant reactions discussed in the text toward the formation of indene, naphthalene, styrene, butadiene, propylene and ethylene in the CSM and POLIMI models

The CSM model has been developed for propylene pyrolysis, but this model, which is largely based on CBS-QB3 ab initio calculations, includes a sub-mechanism for cyclohexane pyrolysis. The Hefei model was developed to model cyclohexane pyrolysis experiments at low pressure (0.004 MPa), 5 micro second space time and 1100 – 1600 K temperature range. These conditions are very different from that of the new experimental data reported here and thus the question arises how the Hefei model performs for the current data. The Nancy model was developed to predict ignition delay times of cyclohexane-oxygen-argon mixtures in the temperature range 1230K to 1840K, 0.73-0.95 MPa pressure and up to 1% cyclohexane content in feed. It has many reactions that are irreversible. Since pyrolysis reactions play an important role in combustion processes, it

should be able to predict the current experimental data as well. Finally, the JetSurF model has a wide range of applicability, though it is claimed to be work in progress. For cyclohexane, it is suggested to be used for high temperature applications. The predictions of the five literature models are shown in Figures 4.1 – 4.4. The POLIMI and CSM models show the best predictions among the five literature models, but even these do not predict all experimental product trends well. This is not surprising as a common feature of these five models is that they are optimized for their respective application.

The following profiles that deviate significantly from the experimental data are discussed: The POLIMI model underpredicts ethylene and benzene trends. The Hefei, Nancy and JetSurF models underpredict feed conversion and propylene but overpredict 1,3-butadiene. In addition, the Nancy model underpredicts the methane yields. The CSM model overpredicts the feed conversion. These trends were investigated using reaction path analysis.

In the POLIMI model, 3 reactions predominantly affect ethylene formation (from ROP and sensitivity analysis): Hydrogen addition to ethylene produces an ethyl radical, the retro-Diels-Alder reaction of cyclohexene produces ethylene and butadiene and a lumped reaction (POLIMI 2 reaction in Figure 4.5) describing the decomposition of cyclohexyl radicals.

For the first reaction, Sabbe[73] reports CBS-QB3 high pressure limit kinetics of hydrogen addition to ethylene. At 1000 K, its rate coefficient is $2.3*10^{13}$ $cm^3.mol^{-1}.s^{-1}$ which itself is a factor of 1.5 lower than experimental measured value, as discussed in the Table 4.2 of the article of Sabbe[73]. POLIMI's high pressure limit rate coefficient is a factor of 2 lower than the CBS-QB3 high pressure limit rate coefficient. This could contribute to the underprediction of ethylene by the POLIMI model. The second dominant reaction for ethylene formation, the retro Diels-Alder reaction also has different kinetics in POLIMI model versus later evaluations[77]. The POLIMI model has a rate coefficient at 1000 K of 2.3 s^{-1}, while in their latest evaluations, Tsang et al. from NIST [77] evaluated in 2015 historical data on the kinetics of retro-Diels Alder reaction for the decomposition of cyclohexene. For the conditions of our interest, at 1000K, the rate coefficient is 9.4 s^{-1}. As the rate coefficient of the POLIMI model is about 4 times lower, this again could contribute to lower ethylene predictions by the POLIMI model. The third reaction stated above is a

lumped reaction and cannot be interpreted easily, though it is a minor channel to produce ethylene.

The Hefei, Nancy and JetSurF models underpredict cyclohexane conversion. A reaction path analysis with the Hefei model points to two main reactions for cyclohexane conversion: hydrogen abstraction from cyclohexane by hydrogen atom and methyl radical, respectively. At 1000K, the Hefei and JetSurF model rate coefficients of abstraction by H-atom are about half that of the ab-initio value calculated in-house, while that by methyl radical is strikingly only about 10% of the ab-initio value calculated in-house. For the latter reaction, Sway et al.[78] report an experiment done in a shock tube at atmospheric pressure at 420K. Their experimental rate coefficient at 420 K is 21 $m^3.mol^{-1}s^{-1}$. This experimental rate coefficient lies closer to the in-house ab-initio CBS-QB3 value at 420K (4 $m^3.mol^{-1}s^{-1}$) than to the Hefei/ JetSurF values (0.16 $m^3.mol^{-1}s^{-1}$). The smaller rate coefficient for the abstraction by methyl radical causes the Hefei and JetSurF models to underpredict cyclohexane conversion. In the Nancy model[10], the high pressure limit rate coefficient of hydrogen abstraction on cyclohexane by hydrogen atom is twice the ab-initio value while that by methyl radical is only 2.5% of the ab-initio value at 1000 K. Hence, the experimental rate coefficient of methyl abstraction on cyclohexane, at $1.1*10^4$ $m^3.mol^{-1}s^{-1}$ at 1000K, is much closer to the ab-initio calculated rate expression used in the current model ($3*10^4$ $m^3.mol^{-1}s^{-1}$) than to the Nancy model value ($2.5*10^2$ $m^3.mol^{-1}s^{-1}$).

The propylene profile is underpredicted by the Hefei model. Reaction path analysis reveals that very fast propylene consumption by addition of vinyl radical causes this underprediction. The vinyl radical is produced by ring opening of the cyclohexyl radical followed by two successive C-C beta scissions. The Hefei model has a rate coefficient of $1.6*10^7$ $m^3.mol^{-1}.s^{-1}$ for this addition reaction at 1000K. However, this value is around 4500 times that of the CBS-QB3 value. There is no direct experimental data for this reaction for comparison, but Vandeputte et al[62] report that in general ab-initio rate coefficients of carbon radical addition reactions to unsaturated hydrocarbons are reliable. Hence, it can be understood why the Hefei model underpredicts propylene yields .

1,3-butadiene is overpredicted by the Nancy, Hefei and JetSurF models. In the Nancy model, there are a number of irreversible reactions producing 1,3-butadiene, most dominant being the C-C beta scission of allylic hex-1-en-yl radical to form 1,3-butadiene and ethyl radical. The reverse reaction is not listed. This leads to a direct forward reaction

forming 1,3-butadiene with no reverse reaction listed, which could explain its overprediction. The reverse reaction is important at our conditions because when the same is removed from the well predicting CSM model, the butadiene trend is overpredicted. There is no experimental data for this reaction.

In the CSM model, for the isomerization reaction of cyclohexane giving 1-hexene, the activation energy has been modified to a lower value than that proposed by Tsang. This modification gives a rate coefficient 33 times higher than the ab-initio value[29]. Hence, the conversions are over-predicted by the CSM model.

Although the POLIMI and CSM models generally perform well and could easily be further optimized using the experimental data of this study, an alternative approach was selected, which is to generate a new kinetic model automatically using Genesys software. The goal is to develop a model with comparable or improved predictive capabilities that is solely based on group additivity thermochemical information stored in the databases of Genesys. Such a kinetic model is thermodynamically consistent as reverse rate expressions are calculated with the help of the equilibrium constant. It is also kinetically consistent because all rate expressions for reactions belonging to the same reaction class are the same. Besides describing cyclohexane pyrolysis chemistry, the new model also serves as validation of the Genesys databases if the prediction are acceptable. To address questions of transferability, the new model will also be applied to the experimental data reported by the Hefei group.

4.3.3. Genesys kinetic model evaluation

As stated previously, rate coefficients for the reactions were assigned from existing group additive values. Ab-initio thermodynamic parameters were assigned to the species. In total, there were 806 reactions between 241 species in the model. Based on initial simulations, a few reactions (all are included in Table 4.2) were found to be dominant, and their kinetics were re-calculated at the CBS-QB3 level of theory, leading to the final model. Table 4.2 lists the most important reactions of the model and the source of their kinetics in the Genesys model. For comparison, it also lists the rate coefficients of those reactions at 1050K for the Genesys model versus two literature models : CSM [38] and POLIMI [40-43]. It is to be noted that the CSM model forms aromatics via lumped reactions, so the elementary reactions pertaining to those are missing.

Table 4.2: Most important reactions in the Genesys cyclohexane model - comparison to best performing literature models (CSM, POLIMI) [43, 44]. Blank areas indicate missing reactions

#	Reaction	A	E_a	k(Genesys)	k(CSM)	k(POLIMI)
	Elementary reaction	m^3, mol, s	kJ/mol	k(at T=1050K), units in m3, mol, s	
R1	cyC6H12=1-hexene	1.25×10^{18}	389.9	5.03×10^{-2}	1.67	0.105
R2	1-hexene=allyl+1-propyl	7.94×10^{15}	295.7	15.5	15.5	
R3	1-propyl=C2H4+CH3	8.46×10^{13}	131.1	2.54×10^7	4.29×10^6	2.22×10^6
R4	H+cyC6H12=H2+cyC6H11	1.14×10^9	39.4	1.25×10^7	1.15×10^7	4.80×10^6
R5	CH3+cyC6H12=CH4+cyC6H11	4.90×10^7	59.4	5.42×10^4	6.98×10^4	5.01×10^4
R6	cyC6H11=cyC6H10+H	2.06×10^{14}	153.8	4.58×10^6	6.45×10^5	1.55×10^6
R7	hex-1-en-6-yl=cyC6H11	5.85×10^9	35.0	1.06×10^8	1.54×10^7	
R8	hex-1-en-6-yl=C2H4+but-1-en-4-yl	7.05×10^{13}	128.5	2.85×10^7	2.87×10^7	
R9	but-1-en-4-yl=C2H4+C2H3	1.47×10^{14}	156.6	2.39×10^6	6.05×10^5	3.13×10^5
R10	C2H4+H=ethyl	2.13×10^8	18.5	6.21×10^6	1.88×10^7	2.15×10^6
R11	C3H6+H=1-propyl	6.46×10^7	22.5	4.91×10^6	1.61×10^5	2.15×10^6
R12	hex-1-en-6-yl=hex-1-en-3-yl	1.77×10^{11}	70.3	5.65×10^7	1.22×10^7	
R13	hex-1-en-3-yl=1,3-C4H6+C2H5	3.88×10^{14}	154.7	7.82×10^6	1.94×10^6	
R14	but-1-en-3-yl=1,3-C4H6+H	2.52×10^{14}	202.5	2.13×10^4	6.65×10^2	4.96×10^3
R15	cyC6H12+but-1-en-3-yl=cyC6H11+2-butene	1.74×10^7	97.8	2.37×10^2	4.27×10^2	
R16	2-butene+H=2-butyl	1.35×10^8	20.1	1.35×10^7	3.25×10^5	
R17	C3H6+CH3=2-butyl	1.83×10^6	41.7	1.54×10^4	2.12×10^3	1.96×10^4
R18	hexa-1,4-dien-6-yl=C2H3+1,3-C4H6	1.71×10^{15}	188.5	7.15×10^5	2.17×10^5	
R19	hexa-1,4-dien-6-yl=hexa-1,4-dien-3-yl	1.84×10^{12}	130.7	5.79×10^5	3.31×10^5	
R20	Me-cy(CC.C=CC)=CY13PD+CH3	5.73×10^{15}	184.8	3.69×10^6	1.93×10^6	

cyC6H12=cyclohexane, cyC6H11=cyclohexyl, 1,3-C4H6=1,3-butadiene, Me-cy(CC.CC=CC)=4-Methyl cyclopentene, CY13PD=1,3-cyclopentadiene

The POLIMI model in general is a lumped model, so many elementary reactions are only indirectly included as lumped reactions. It can be seen that the rate coefficients of some important reactions in Genesys differ from those of these 2 literature models. The most striking example is the critical reaction R1, for which a factor of 33 difference between the Genesys and CSM rate coefficients is observed. While Genesys uses the CBS-QB3 result for this reaction, the CSM value is an altered one from the CBS-QB3 ab-initio 'k' [29]. The CBS-QB3 value which Genesys uses has been reported by Sirjean[29] which itself agrees well with the value of Tsang[27]. Hence, the Genesys model is the only model that is completely elementary reaction-based and has consistently ab-initio based high pressure

limit rate coefficients with no alteration of kinetic or thermodynamic parameters. In the next section, experimental results and model performance will be discussed.

From Figures 4.1-4.4, it can be seen that for most species there is qualitative and quantitative agreement between the Genesys model and the experimental data. A reaction path analysis was performed on major products at the experimental reactor temperature set point of 1053K and a schematic showing the dominant reactions of the Genesys mechanism is given in Figure 4.6. Rate of production and sensitivity analyses reveal the dominant pathways.
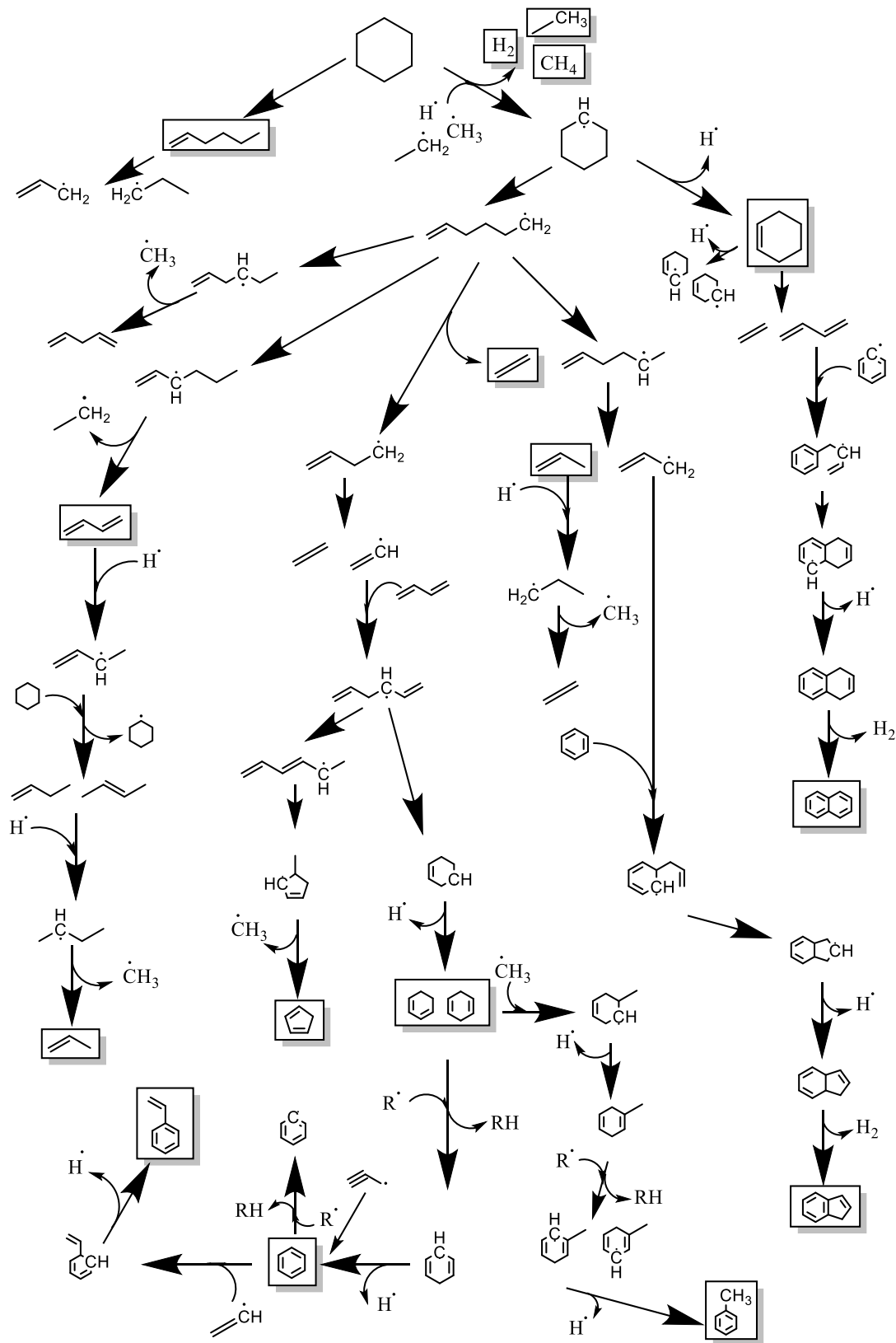
Figure 4.6: Dominant reaction pathways in cyclohexane pyrolysis

Cyclohexane: Cyclohexane initially isomerizes to form 1-hexene which upon homolytic C-C scission gives allyl and 1-propyl radicals. 1-propyl radical on C-C beta scission gives ethylene and methyl radical. The allyl and methyl radicals in turn abstract hydrogen from cyclohexane to form cyclohexyl radical. Cyclohexyl can either form cyclohexene, releasing a hydrogen atom by C-H beta scission, or open the ring to form hex-1-en-6-yl radical. In the largest part of the reactor, the primary route of consumption of cyclohexane is by hydrogen abstraction by hydrogen atom and methyl radical. Hydrogen radical is generated by numerous C-H beta scission reactions that present the dominant pathways for formation of the major products such as ethylene, benzene, 1,3-cyclopentadiene, toluene, indene and naphthalene. Methyl is primarily produced by hydrogen addition to 2-butene and the C-C beta scission to give methyl and propylene. 2-butene is in turn formed by the reaction between hydrogen atom and 1,3-butadiene, as discussed later. Figure 4.7 shows the rate of consumption for cyclohexane with respect to various elementary reactions in the Genesys model.
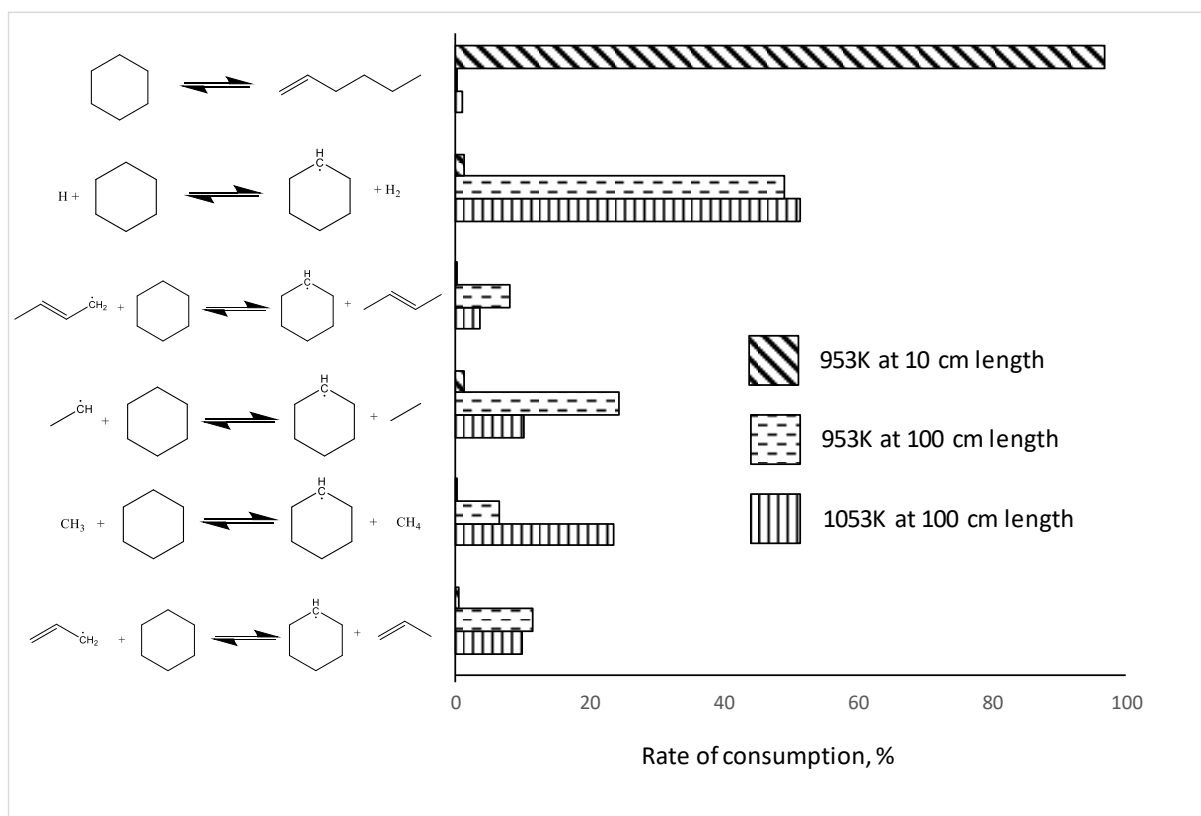
Figure 4.7: Rate of consumption of cyclohexane by various elementary reactions, % at 953K at 10 and 100 cm reactor length and 1053K at 100 cm reactor length

It can be seen that near the inlet of the reactor (10 cm) for the lower temperature experiment (953 K), isomerization to 1-hexene is the major route of consumption of cyclohexane. The reason is, at an early stage in the reactor, radical chemistry is not yet important owing to the low radical concentration. This is due to the decomposition progress still being in its initial stages. At 100 cm, for the 953 K experiment, one of the important reactions is the hydrogen migration of 6-hexenyl to form 3-hexenyl which gives 1,3-butadiene and ethyl radical. Due to this abundant presence of ethyl radicals, hydrogen abstraction on cyclohexane by ethyl radical is one of the dominant reactions in the 953 K experiment. Methyl radicals are not produced at this stage. They are produced much later, during the formation of propylene from butadiene as explained in the propylene formation routes. As the formation of methyl radicals is preferred at higher temperatures, their attack on cyclohexane leading to hydrogen abstraction is the dominant route of cyclohexane consumption at the higher temperatures (1053 K). At both lower and higher temperatures, hydrogen abstraction from cyclohexane by hydrogen atom is the most dominant route at 100 cm reactor axial length. This is because of two reasons: Firstly, hydrogen atom is produced in many important reactions of the mechanism, all along the reactor. Secondly, the rate coefficient of hydrogen abstraction by hydrogen atom is faster than that by other radicals, for example, at 1053 K, it is 230 times faster than that by methyl. Hence, This explains the dominant reactions of cyclohexane consumptions at low and high temperatures across the reactor axis.

Cyclohexene: Cyclohexene is formed through C-H beta scission reactions of the cyclohexyl radical. It mainly decomposes via retro-Diels-Alder reaction to give ethylene and 1,3-butadiene. Hydrogen abstractions from cyclohexene and subsequent beta scission reactions are not the most dominant pathways to benzene formation.

Ethylene: The cyclohexyl radical ring-opens to form hex-1-en-6-yl radical, which upon C-C beta scission gives ethylene and but-1-en-4-yl radical. The but-1-en-4-yl radical again undergoes C-C beta scission to give yet another ethylene molecule and a vinyl radical. Ethylene is also produced by the hydrogen atom addition to propylene and the subsequent C-C beta scission of 1-propyl.

1,3-butadiene: Hex-1-en-6-yl undergoes intra-molecular hydrogen abstraction to form the resonantly stabilized hex-1-en-3-yl radical. This radical undergoes C-C beta scission to form 1,3-butadiene and ethyl radical. 1,3-butadiene is also formed by the retro-Diels-Alder

reaction of cyclohexene giving 1,3-butadiene and ethylene, another important route for ethylene formation.

Propylene: The hex-1-en-6-yl radical formed by ring opening of cyclohexyl can undergo intra-molecular hydrogen abstraction to form hex-1-en-5-yl radical. This radical undergoes C-C beta scission to form propylene and allyl radical. The allyl radical in turn abstracts hydrogen atom from cyclohexane to again form propylene. However, the most dominant route of propylene formation is via the decomposition of 1,3-butadiene. Upon hydrogen atom addition, 1,3-butadiene forms the allylic butenyl radical. Latter abstracts a hydrogen atom from cyclohexane to form 2-butene. 2-butene in turn undergoes hydrogen addition to form 2-butyl radical, which after C-C beta scission gives propylene and methyl radical.

Methane: Methyl radical abstracts hydrogen from cyclohexane to give methane. Methyl radical is in turn dominantly produced, along with propylene from the C-C beta scission of 2-butyl radical, which in turn is derived from the major product 1,3-butadiene as discussed in the propylene formation routes.

Hydrogen: Hydrogen atom abstracts hydrogen from cyclohexane to form H_2 gas and cyclohexyl. Hydrogen atom is in turn produced by the many C-H beta scissions taking place in the mechanism, like that of ethyl, cyclohexyl, cyclohexenyl, cyclohexadienyl and cyclopentenyl to form products ethylene, cyclohexene, cyclohexadiene, benzene and cyclopentadiene. These are shown Figures 4.1-4.4

Ethane: Ethane is produced by the H-abstraction from cyclohexane by ethyl radical. Ethyl radical is produced during the formation of 1,3-butadiene by the C-C beta scission of hex-1-en-3-yl.

Butenes: 1-butene and 2-butene are formed by the hydrogen atom addition to 1,3-butadiene to form allylic butenyl radical and its subsequent hydrogen abstraction from cyclohexane.

1,3-Cyclopentadiene: Vinyl radical, which is produced by the 2-times C-C beta scission of hex-1-en-6-yl radical, adds to 1,3-butadiene to form hexadienyl radical. This radical undergoes intra-molecular hydrogen abstraction and exocyclic intra-molecular carbon centered radical addition to form 4-methyl cyclopent-1-en3-yl. This radical undergoes C-C beta scission to cut off the methyl branch thereby forming 1,3-cyclopentadiene and methyl radical.

Benzene: Vinyl and 1,3-butadiene add to form hexadienyl radical. This undergoes endo cyclization to form cyclohex-1-en-4-yl, which after C-H beta scission gives 1,4-

cyclohexadiene. Hydrogen abstraction from 1,4-cyclohexadiene leads to doubly resonance stabilized cyclohexadienyl radical, which upon C-H beta scission gives benzene.

Toluene: Toluene is formed by methyl addition to benzene and subsequent C-H beta scission. It is also formed by methyl addition to 1,4-cyclohexadiene and subsequent C-H beta scission, hydrogen abstraction to form di-allylic methyl cyclohexadiene and its C-H beta scission.

Styrene: When vinyl radical adds on to benzene followed by a C-H beta scission, styrene is formed. Vinyl is formed in the initial decomposition mechanism by the C-C beta scission of hex-1-en-6-yl and then of but-1-en-4-yl. It is also important in the formation of benzene by addition to 1,3-butadiene, a major product.

Indene: Allyl radical addition to benzene and subsequent ring formation leads to a double ring intermediate (3a,7a-dihydro-1H-indene), which on loosing hydrogen forms indene.

Naphthalene: Since benzene and 1,3-butadiene are 2 of the major products of cyclohexane pyrolysis, naphthalene is formed from these sources. Butadiene and phenyl radical add, as do butadienyl and benzene, to form phenyl butenyl radical. This upon ring formation gives 1,8a-dihydronaphthalene which loses hydrogen to form naphthalene.

Based on prediction capability, the Genesys model overall performs better than others reported in literature. An additional advantage of the Genesys model is that the chemistry is more transparent because exclusively elementary reactions have been incorporated.

Comparison to cyclopentane pyrolysis: The model developed for cyclopentane[47] pyrolysis is a sub-set of that for cyclohexane. The most important reactions for cyclopentane pyrolysis are shown in chapter 4. It is to be noted that the routes to major products are quite different between cyclohexane and cyclopentane pyrolysis. In both feeds, the ring opening of the corresponding cycloalkyl radical leads to the respective primary olefinic radicals which preferably undergo C-C beta scission. However, the C5 and C6 radicals give rise to different radical pools. C5 decomposes into C2 and C3 species while C6 gives rise to C2 and C4 species. Understandably, in cyclopentane pyrolysis, more propylene and less 1,3-butadiene is formed compared to that in cyclohexane pyrolysis. The excess C2 and C4 species produced in cyclohexane pyrolysis initiate benzene formation via vinyl addition to butadiene and ring formation. However, as cyclopentane pyrolysis leads to a substantial formation of 1,3-cyclopentadiene without ring opening, this cyclopentadiene combines with methyl radical and expands the ring to form benzene. 1,3-cyclopentadiene is a major

intermediate in cyclopentane pyrolysis but less important in cyclohexane pyrolysis where it is formed via molecular weight growth chemistry of smaller species.

4.3.4 Model performance on experimental data from literature

In the recent literature, one of the most comprehensive cyclohexane pyrolysis experiments was reported by Wang et al. [38] in 2012. Though their setup was also a continuous flow reactor experiment, the reaction conditions were substantially different from those considered in the present study. Wang et al. realized zero to complete cyclohexane conversions and analyzed an extensive product spectrum at reactor conditions of 800 to 1300 ^{0}C, 0.004 MPa total pressure (<0.0001 MPa cyclohexane partial pressure diluted with Ar at inlet), and 5 microseconds residence time. They also developed a kinetic model and compared its predictions against their experimental data. Figures 4.1-4.4 show that predictions with their model (Hefei) deviate clearly from the experimental data of the current study, however this is not unexpected because their model was designed for the low-pressure conditions. This raises the question how the current Genesys model containing solely high-pressure rate expressions performs when used on the Hefei experimental data. As seen in Figure 4.8, the Genesys model actually performs fairly well for most of the products.
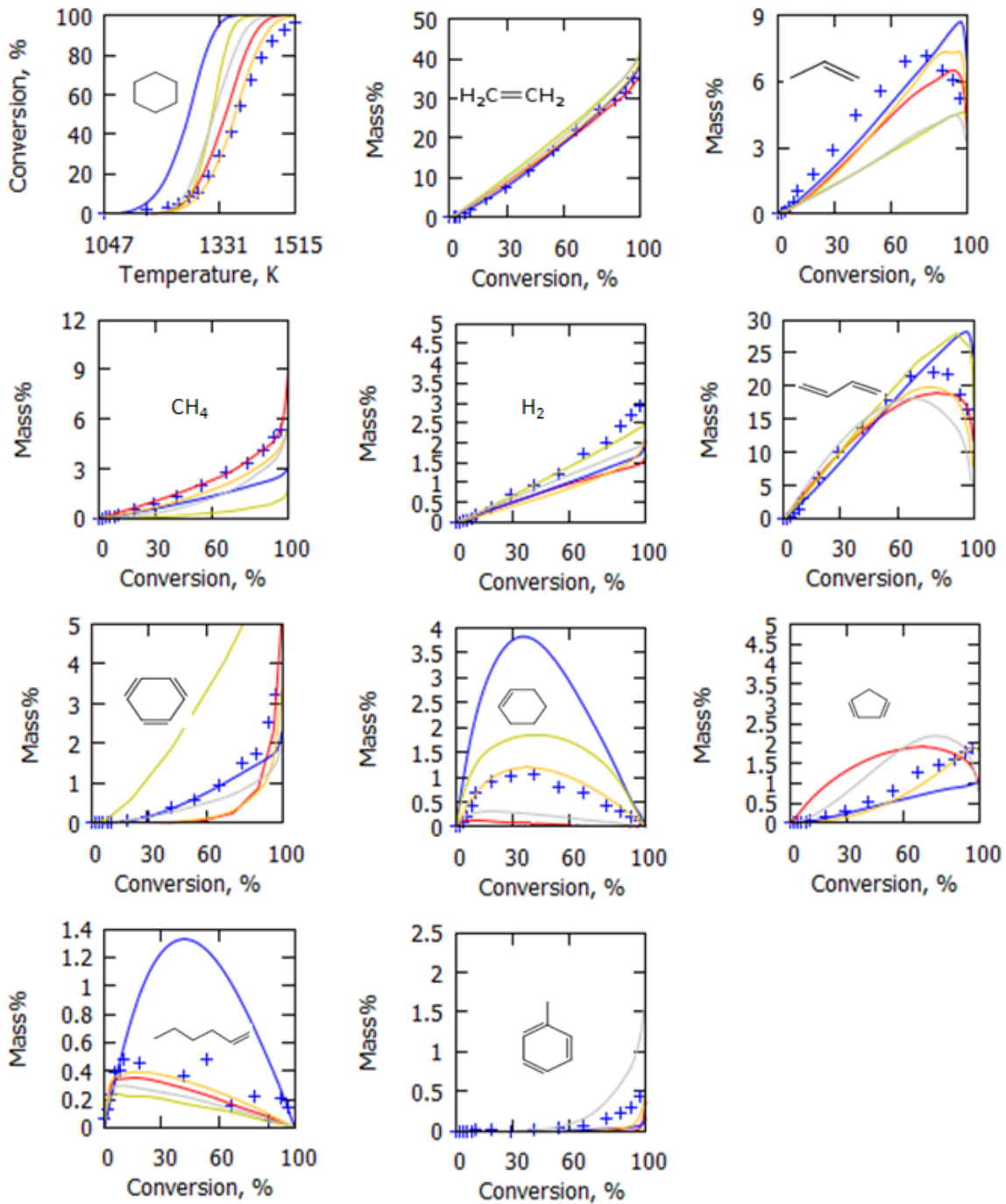
Figure 4.8: Model predictions (with completely high pressure limit Genesys model) on Hefei cyclohexane pyrolysis experimental data at 1047-1515K, 0.004 MPa, 5 micro second average residence time, 98% Argon dilution (+ Hefei Experiment, ▬▬ Genesys, ▬▬ POLIMI, ▬▬ CSM, ▬▬ Hefei, ▬▬ Nancy, ▬▬ JetSurF)

Conversion of cyclohexane is well captured across the wide temperature range by the Genesys model, although it preforms slightly worse than the Hefei model but better than all other literature models. The Genesys model also captures the monotonic rise of ethylene yields and the maxima in the propylene profile. It predicts the methane data better than the Hefei model. The Genesys model underpredicts hydrogen. It reproduces the trend of butadiene yields fairly well. The benzene profile is underpredicted at lower temperatures. 1-hexene is well predicted while toluene is underpredicted. It is to be noted that a high pressure limit ab-initio model has been able to predict well the cyclohexane pyrolysis experiment at close to atmospheric pressure and fairly well the experiment at very low pressure and combustion range temperatures. Hence, this widens the applicability of the Genesys model to processes covering low to combustion level temperatures and low to atmospheric pressures at varying residence times. Cyclohexene is underpredicted in Figure 4.8, owing to the effect of pressure dependency of retro-Diels-Alder reaction. Further, the high-pressure limited rate expression for the retro-Diels Alder reaction was converted to a pressure dependent rate coefficient represented in Chebyshev format. The method used for this conversion is stated in the article [41]. This improved the predictions of cyclohexene for the very low pressure experiment, as seen in Figure 4.9. It is to be noted that only a single elementary reaction in the LCT model was converted from high pressure limit to a pressure-dependent format just for trial purpose in Figures 4.8 and 4.9. The actual LCT model however has completely high pressure limit reactions.
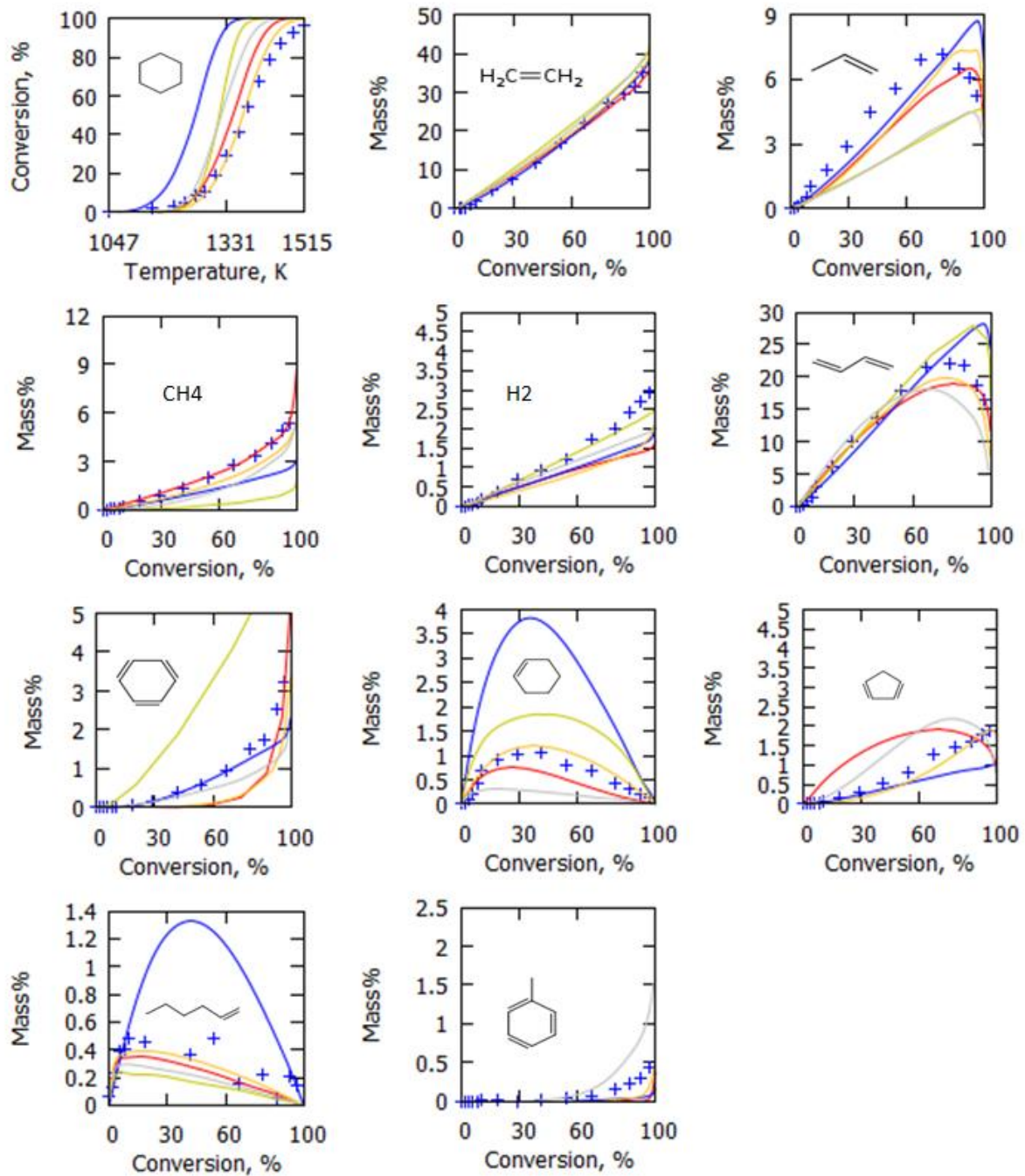
Figure 4.9: Model predictions (Genesys model with only 1 pressure-dependent reaction – retro-Diels-Alder) on Hefei cyclohexane pyrolysis experimental data at 1047-1515K, 0.004 MPa, 5 micro second average residence time, 98% Argon dilution dilution (+ Hefei Experiment, —— Genesys, —— POLIMI, —— CSM, —— Hefei, —— Nancy, —— JetSurF)

This case is an example for which pressure dependency plays an important role for the product distribution. This may also be partly the reason why the Hefei model, developed for low pressures, does not predict well the atmospheric pyrolysis data. Accounting for pressure dependency in the Genesys high pressure limit model may lead to a better prediction of some other species too apart from cyclohexene in the Hefei experimental data, however this investigation is outside the scope of the current work. Wang also conducted a high temperature experiment (1100K-1350K) at 1 atm for cyclohexane pyrolysis[79]. The Genesys and Hefei model predictions for the pyrolysis products are shown in the original article based on this chapter. The Hefei model predicts the conversion and product trends well as does the Genesys model. Conversion of cyclohexane at temperatures lower than 1180K is slightly underpredicted both by Hefei and Genesys models, while at higher temperatures, it is overpredicted. Ethylene trend shows a monotonic increase in mass% reaching up to 31 mass% at 80% feed conversion, and is well captured by both models, though Hefei model shows a slightly better prediction. Propylene mass % trend shows a maxima and this is captured by both models, though the Genesys model shows a better prediction. Butadiene trend also shows a maxima, and the Genesys model captures the trend more closely than the Hefei model. Benzene and hydrogen trends are better predicted by the Hefei model, while methane trend is captured closely by Genesys model.

4.4. Conclusions

The pyrolysis of cyclohexane has been studied in a continuous approximately isothermal flow reactor in the temperature range 913 K to 1073 K. 49 products were identified and quantified using 2 dimensional gas chromatography. The product spectrum ranges from hydrogen to polycyclic aromatic hydrocarbons. A kinetic model has been generated consisting of 806 reactions between 241 species. This compact model, which has also been applied successfully to cyclopentane pyrolysis, predicts the trends of 15 major products significantly better than currently established models. This is attributed to the use of accurate ab-initio derived thermochemical data and a more complete kinetic model consisting only of elementary step reactions. Reaction path analysis shows the dominant pathways to the most important products such as ethylene, propylene, methane, hydrogen, ethane, cyclohexene, 1,3-cyclopentadiene, 1,3-butadiene, n-butenes, benzene, indene,

toluene, styrene, naphthalene and cyclohexane feed conversion. Cyclohexane pyrolysis is initiated by isomerization to 1-hexene. 1-hexene contains a weak allylic bond which upon scission quickly generates a radical pool leading to a dominance of radical chemistry as the reaction proceeds. Unlike in cyclopentane pyrolysis, butadiene is found to be an important intermediate responsible for the formation of propylene, cyclopentadiene and benzene.

4.5. References

1.Djokic, M. R.; Dijkmans, T.; Yildiz, G.; Prins, W.; Van Geem, K. M., Quantitative analysis of crude and stabilized bio-oils by comprehensive two-dimensional gas-chromatography. *Journal of Chromatography A* **2012,** 1257, 131-140.

2.Vargas, D. C.; Alvarez, M. B.; Portilla, A. H.; Van Geem, K. M.; Streitwieser, D. A., Kinetic Study of the Thermal and Catalytic Cracking of Waste Motor Oil to Diesel-like Fuels. *Energy & Fuels* **2016,** 30, (11), 9712-9720.

3.Vandewiele, N. M.; Magoon, G. R.; Van Geem, K. M.; Reyniers, M. F.; Green, W. H.; Marin, G. B., Kinetic Modeling of Jet Propellant-10 Pyrolysis. *Energy & Fuels* **2015,** 29, (1), 413-427.

4.Vandewiele, N. M.; Magoon, G. R.; Van Geem, K. M.; Reyniers, M. F.; Green, W. H.; Marin, G. B., Experimental and Modeling Study on the Thermal Decomposition of Jet Propellant-10. *Energy & Fuels* **2014,** 28, (8), 4976-4985.

5.Gascoin, N.; Abraham, G.; Gillard, P., Synthetic and jet fuels pyrolysis for cooling and combustion applications. *Journal of Analytical and Applied Pyrolysis* **2010,** 89, (2), 294-306.

6.Yang, Q. C.; Chetehouna, K.; Gascoin, N.; Bao, W., Experimental study on combustion modes and thrust performance of a staged-combustor of the scramjet with dual-strut. *Acta Astronautica* **2016,** 122, 28-34.

7.Pyl, S. P.; Schietekat, C. M.; Reyniers, M. F.; Abhari, R.; Marin, G. B.; Van Geem, K. M., Biomass to olefins: Cracking of renewable naphtha. *Chemical Engineering Journal* **2011,** 176, 178-187.

8.Buda, F.; Bounaceur, R.; Warth, V.; Glaude, P.; Fournet, R.; Battin-Leclerc, F., Progress toward a unified detailed kinetic model for the autoignition of alkanes from C-4 to C-10 between 600 and 1200 K. *Combustion and Flame* **2005,** 142, (1-2), 170-186.

9.Buda, F.; Glaude, P. A.; Battin-Leclerc, F.; Porter, R.; Hughes, K. J.; Griffiths, J. F., Use of detailed kinetic mechanisms for the prediction of autoignitions. *Journal of Loss Prevention in the Process Industries* **2006,** 19, (2-3), 227-232.

10.Sirjean, B.; Buda, F.; Hakka, H.; Glaude, P. A.; Fournet, R.; Warth, V.; Battin-Leclerc, F.; Ruiz-Lopez, M., The autoignition of cyclopentane and cyclohexane in a shock tube. *Proceedings of the Combustion Institute* **2007,** 31, 277-284.

11.Serinyel, Z.; Herbinet, O.; Frottier, O.; Dirrenberger, P.; Warth, V.; Glaude, P. A.; Battin-Leclerc, F., An experimental and modeling study of the low- and high-temperature oxidation of cyclohexane. *Combustion and Flame* **2013,** 160, (11), 2319-2332.

12.Hui, W.; Yang, H. F.; Ran, X. Q.; Shi, Q. Z.; Wen, Z. Y., Pyrolysis mechanism of carbon matrix precursor cyclohexane(V) - formation process of benzene from C-4 species. *Journal of Molecular Structure-Theochem* **2004,** 678, (1-3), 39-48.

13.Liu, X. B.; Li, W. Z.; Xu, H. Y.; Chen, Y. X., A comparative study of non-oxidative pyrolysis and oxidative cracking of cyclohexane to light alkenes. *Fuel Processing Technology* **2004,** 86, (2), 151-167.

14. Wang, H.; Yang, H. F.; Chuang, W.; Ran, X. Q.; Shi, Q. Z.; Wen, Z. Y., Pyrolysis mechanism of carbon matrix precursor cyclohexane - The formation of condensed-ring aromatics and the growing process of molecules. *Journal of Molecular Graphics & Modelling* **2007,** 25, (6), 824-830.

15. Wang, H.; Yang, H. F.; Ran, X. Q.; Shi, Q. Z.; Wen, Z. Y., Pyrolysis mechanism of carbon matrix precursor cyclohexane. II. Pyrolysis process of intermediate 1,3-butadiene. *Journal of Molecular Structure-Theochem* **2002,** 581, 187-194.

16. Wang, H.; Yang, H. F.; Ran, X. Q.; Shi, Q. Z.; Wen, Z. Y., Pyrolysis mechanism of carbon matrix precursor cyclohexane(III) - pyrolysis process of intermediate 1-hexene. *Journal of Molecular Structure-Theochem* **2004,** 710, (1-3), 179-191.

17. Wang, H.; Yang, H. F.; Ran, X. Q.; Shi, Q. Z.; Wen, Z. Y., Pyrolysis mechanism of carbon matrix precursor cyclohexane(I). *Journal of Molecular Structure-Theochem* **2001,** 571, 115-131.

18. Yang, H. F.; Wang, H.; Ran, X. Q.; Shi, Q. Z.; Wen, Z. Y., Pyrolysis mechanism of carbon matrix precursor cyclohexane(IV)-formation process of intermediates C4HX (X=3,4,5). *Journal of Molecular Structure-Theochem* **2002,** 618, (3), 209-217.

19. Zhao, Y. X.; Shen, B.; Wei, F., Quantitative interpretation to the chain mechanism of free radical reactions in cyclohexane pyrolysis. *Journal of Natural Gas Chemistry* **2011,** 20, (5), 507-514.

20. Zsely, I. G.; Varga, T.; Nagy, T.; Cserhati, M.; Turanyi, T.; Peukert, S.; Braun-Unkhoff, M.; Naumann, C.; Riedel, U., Determination of rate parameters of cyclohexane and 1-hexene decomposition reactions. *Energy* **2012,** 43, (1), 85-93.

21. Woebcke, H. N.; Korosi, A.; Virk, P. S., Pyrolysis of unsubstituted mono-cycloalkanes, di-cycloalkanes and tri-cycloalkanes. *Abstracts of Papers of the American Chemical Society* **1978,** 175, (MAR), 27-27.

22. Jones, D. T., CLXXVII. - The thermal decomposition of hydrogenated aromatic hydrocarbons. *Journal of the Chemical Society, Transactions* **1915,** 107, 1582-1588.

23. Frolich, P. K.; Simard, R.; White, A., Formation of Butadience by Cracking of Hydrocarbons1. *Industrial & Engineering Chemistry* **1930,** 22, (3), 240-241.

24. Egloff, G.; Bollman, H. T.; Levinson, B. L., Thermal reactions of cycloparaffins and cycloölefins. *Journal of Physical Chemistry* **1931,** 35, (12), 3489-3552.

25. Pease, R. N.; Morton, J. M., Kinetics of dissociation of typical hydrocarbon vapors. *Journal of the American Chemical Society* **1933,** 55, (8), 3190-3200.

26. Levush, S. S.; Abadzhev, S. S.; Shevchuk, V. U., Pyrolysis of cyclohexane. *Petroleum Chemistry* **1969,** 9, (3), 185-&.

27. Tsang, W., Thermal stability of cyclohexane and 1-hexene. *International Journal of Chemical Kinetics* **1978,** 10, (11), 1119-1138.

28. Kiefer, J. H.; Gupte, K. S.; Harding, L. B.; Klippenstein, S. J., Shock Tube and Theory Investigation of Cyclohexane and 1-Hexene Decomposition. *Journal of Physical Chemistry A* **2009,** 113, (48), 13570-13583.

29. Sirjean, B.; Glaude, P. A.; Ruiz-Lopez, M. F.; Fournet, R., Detailed kinetic study of the ring opening of cycloalkanes by CBS-QB3 calculations. *Journal of Physical Chemistry A* **2006,** 110, (46), 12693-12704.

30. Aribike, D. S.; Susu, A. A., Kinetics of the pyrolysis of cyclohexane using the pulse technique. *Industrial & Engineering Chemistry Research* **1988,** 27, (6), 915-920.

31. Aribike, D. S.; Susu, A. A.; Ogunye, A. F., Mechanistic and mathematical modeling of the thermal decomposition of cyclohexane. *Thermochimica Acta* **1981,** 51, (2-3), 113-127.

32. Aribike, D. S.; Susu, A. A.; Ogunye, A. F., Kinetics of the thermal decomposition of cyclohexane. *Thermochimica Acta* **1981,** 47, (1), 1-14.

33. Susu, A. A.; Ogunye, A. F., Selective naphthene pyrolysis for ethylene with hydrogen as diluent. *Thermochimica Acta* **1979,** 34, (2), 197-210.

34. Zamostny, P.; Belohlav, Z.; Starkbaumova, L.; Patera, J., Experimental study of hydrocarbon structure effects on the composition of its pyrolysis products. *Journal of Analytical and Applied Pyrolysis* **2010,** 87, (2), 207-216.

35. Lai, W. C.; Song, C. S., Pyrolysis of alkylcyclohexanes in or near the supercritical phase. Product distribution and reaction pathways. *Fuel Processing Technology* **1996,** 48, (1), 1-27.

36. Peukert, S.; Naumann, C.; Braun-Unkhoff, M.; Riedel, U., The reaction of cyclohexane with H-atoms: A shock tube and modeling study. *International Journal of Chemical Kinetics* **2012,** 44, (2), 130-146.

37. Peukert, S.; Naumann, C.; Braun-Unkhoff, M.; Riedel, U., Formation of H-Atoms in the Pyrolysis of Cyclohexane and 1-Hexene: A Shock Tube and Modeling Study. *International Journal of Chemical Kinetics* **2011,** 43, (3), 107-119.

38. Wang, Z.; Cheng, Z.; Yuan, W.; Cai, J.; Zhang, L.; Zhang, F.; Qi, F.; Wang, J., An experimental and kinetic modeling study of cyclohexane pyrolysis at low pressure. *Combustion and Flame* **2012,** 159, (7), 2243-2253.

39. H. Wang, E. D., B. Sirjean, D. A. Sheen, R. Tango, A. Violi, J. Y. W. Lai, F. N. Egolfopoulos, D. F. Davidson, R. K. Hanson, C. T. Bowman, C. K. Law, W. Tsang, N. P. Cernansky, D. L. Miller, R. P. Lindstedt *JetSurF*, 2.0; http://web.stanford.edu/group/haiwanglab/JetSurF/JetSurF2.0/index.html, 2010.

40. Granata, S.; Faravelli, T.; Ranzi, E., A wide range kinetic modeling study of the pyrolysis and combustion of naphthenes. *Combustion and Flame* **2003,** 132, (3), 533-544.

41. Cavallotti, C.; Rota, R.; Faravelli, T.; Ranzi, E., Ab initio evaluation of primary cyclo-hexane oxidation reaction rates. *Proceedings of the Combustion Institute* **2007,** 31, 201-209.

42. Ciajolo, A.; Tregrossi, A.; Mallardo, M.; Faravelli, T.; Ranzi, E., Experimental and kinetic modeling study of sooting atmospheric-pressure cyclohexane flame. *Proceedings of the Combustion Institute* **2009,** 32, 585-591.

43. Ranzi, E.; Frassoldati, A.; Grana, R.; Cuoci, A.; Faravelli, T.; Kelley, A. P.; Law, C. K., Hierarchical and comparative kinetic modeling of laminar flame speeds of hydrocarbon and oxygenated fuels. *Progress in Energy and Combustion Science* **2012,** 38, (4), 468-501.

44. Wang, K.; Villano, S. M.; Dean, A. M., Fundamentally-based kinetic model for propene pyrolysis. *Combustion and Flame* **2015,** 162, (12), 4456-4470.

45. Djokic, M. R.; Van Geem, K. M.; Cavallotti, C.; Frassoldati, A.; Ranzi, E.; Marin, G. B., An experimental and kinetic modeling study of cyclopentadiene pyrolysis: First growth of polycyclic aromatic hydrocarbons. *Combustion and Flame* **2014,** 161, (11), 2739-2751.

46. Pyl, S. P.; Van Geem, K. M.; Puimege, P.; Sabbe, M. K.; Reyniers, M. F.; Marin, G. B., A comprehensive study of methyl decanoate pyrolysis. *Energy* **2012,** 43, (1), 146-160.

47. Khandavilli, M. V.; Vermeire, F. H.; Van de Vijver, R.; Djokic, M.; Carstensen, H. H.; Van Geem, K. M.; Marin, G. B., Group additive modeling of cyclopentane pyrolysis. *Journal of Analytical and Applied Pyrolysis* **2017,** 128, 437-450.

48. Steven P. Pyl, C. M. S., Kevin M. Van Geem, Marie-Françoise Reyniers, Joeri Vercammen, Jan Beens,Guy B. Marin, *J. Chrom. A.* **2011,** 1218, 3217-3223.

49. Dalluge, J.; Beens, J.; Brinkman, U. A. T., Comprehensive two-dimensional gas chromatography: a powerful and versatile analytical tool. *Journal of Chromatography A* **2003,** 1000, (1-2), 69-108.

50. Liu, Z. Y.; Phillips, J. B., Comprehensive 2-dimensional gas chromatography using an on-column thermal modulator interface. *Journal of Chromatographic Science* **1991,** 29, (6), 227-231.

51. Phillips, J. B.; Beens, J., Comprehensive two-dimensional gas chromatography: a hyphenated method with strong coupling between the two dimensions. *Journal of Chromatography A* **1999,** 856, (1-2), 331-347.

52. Petersson, G. A.; Malick, D. K.; Wilson, W. G.; Ochterski, J. W.; Montgomery, J. A.; Frisch, M. J., Calibration and comparison of the Gaussian-2, complete basis set, and density functional methods for computational thermochemistry. *Journal of Chemical Physics* **1998,** 109, (24), 10570-10579.

53. M. J. Frisch, G. W. T., H. B. Schlegel, G. E. Scuseria, M. A. Robb, J. R. Cheeseman, G. Scalmani, V. Barone, B. Mennucci, G. A. Petersson, H. Nakatsuji, M. Caricato, X. Li, H. P. Hratchian, A. F. Izmaylov, J. Bloino, G. Zheng, J. L. Sonnenberg, M. Hada, M. Ehara, K. Toyota,

R. Fukuda, J. Hasegawa, M. Ishida, T. Nakajima, Y. Honda, O. Kitao, H. Nakai, T. Vreven, J. A. Montgomery, Jr., J. E. Peralta, F. Ogliaro, M. Bearpark, J. J. Heyd, E. Brothers, K. N. Kudin, V. N. Staroverov, R. Kobayashi, J. Normand, K. Raghavachari, A. Rendell, J. C. Burant, S. S. Iyengar, J. Tomasi, M. Cossi, N. Rega, J. M. Millam, M. Klene, J. E. Knox, J. B. Cross, V. Bakken, C. Adamo, J. Jaramillo, R. Gomperts, R. E. Stratmann, O. Yazyev, A. J. Austin, R. Cammi, C. Pomelli, J. W. Ochterski, R. L. Martin, K. Morokuma, V. G. Zakrzewski, G. A. Voth, P. Salvador, J. J. Dannenberg, S. Dapprich, A. D. Daniels, Ö. Farkas, J. B. Foresman, J. V. Ortiz, J. Cioslowski, and D. J. Fox *Gaussian, Inc.*, Wallingford CT, 2009.

54. East, A. L. L.; Radom, L., Ab initio statistical thermodynamical models for the computation of third-law entropies. *Journal of Chemical Physics* **1997,** 106, (16), 6655-6674.

55. Curtiss, L. A.; Raghavachari, K.; Redfern, P. C.; Pople, J. A., Assessment of Gaussian-2 and density functional theories for the computation of enthalpies of formation. *Journal of Chemical Physics* **1997,** 106, (3), 1063-1079.

56. Curtiss, L. A.; Raghavachari, K.; Redfern, P. C.; Rassolov, V.; Pople, J. A., Gaussian-3 (G3) theory for molecules containing first and second-row atoms. *Journal of Chemical Physics* **1998,** 109, (18), 7764-7776.

57. Sabbe, M. K.; Saeys, M.; Reyniers, M. F.; Marin, G. B.; Van Speybroeck, V.; Waroquier, M., Group additive values for the gas phase standard enthalpy of formation of hydrocarbons and hydrocarbon radicals. *Journal of Physical Chemistry A* **2005,** 109, (33), 7466-7480.

58. Vermeire, F. H.; Carstensen, H. H.; Herbinet, O.; Battin-Leclerc, F.; Marin, G. B.; Van Geem, K. M., Experimental and modeling study of the pyrolysis and combustion of dimethoxymethane. *Combustion and Flame* **2018,** 190, 270-283.

59. Paraskevas, P. D.; Sabbe, M. K.; Reyniers, M. F.; Papayannakos, N.; Marin, G. B., Group Additive Values for the Gas-Phase Standard Enthalpy of Formation, Entropy and Heat Capacity of Oxygenates. *Chemistry-a European Journal* **2013,** 19, (48), 16431-16452.

60. Villano, S. M.; Huynh, L. K.; Carstensen, H. H.; Dean, A. M., High-Pressure Rate Rules for Alkyl + O-2 Reactions. 1. The Dissociation, Concerted Elimination, and Isomerization Channels of the Alkyl Peroxy Radical. *Journal of Physical Chemistry A* **2011,** 115, (46), 13425-13442.

61. Carstensen, H. H.; Dean, A. M., Rate Constant Rules for the Automated Generation of Gas-Phase Reaction Mechanisms. *Journal of Physical Chemistry A* **2009,** 113, (2), 367-380.

62. Vandeputte, A. G.; Sabbe, M. K.; Reyniers, M. F.; Van Speybroeck, V.; Waroquier, M.; Marin, G. B., Theoretical study of the thermodynamics and kinetics of hydrogen abstractions from hydrocarbons. *Journal of Physical Chemistry A* **2007,** 111, (46), 11771-11786.

63. Sabbe, M. K.; Van Geem, K. M.; Reyniers, M. F.; Marin, G. B., First Principle-Based Simulation of Ethane Steam Cracking. *Aiche Journal* **2011,** 57, (2), 482-496.

64. Merchant, S. Molecules to Engines: Combustion chemistry of Alcohols and their application to advanced engines. MIT, 2015.

65. Fascella, S.; Cavallotti, C.; Rota, R.; Carra, S., Quantum chemistry investigation of key reactions involved in the formation of naphthalene and indene. *Journal of Physical Chemistry A* **2004,** 108, (17), 3829-3843.

66. Vandewiele, N. M.; Van Geem, K. M.; Reyniers, M. F.; Marin, G. B., Genesys: Kinetic model construction using chemo-informatics. *Chemical Engineering Journal* **2012,** 207, 526-538.

67.   Benson, S. W., *Thermochemical Kinetics*. Wiley: New York, 1968.

68. Benson, S. W.; Buss, J. H., Additivity rules for the estimation of molecular properties - thermodynamic properties. *Journal of Chemical Physics* **1958,** 29, (3), 546-572.

69. Saeys, M.; Reyniers, M. F.; Marin, G. B.; Van Speybroeck, V.; Waroquier, M., Ab initio group contribution method for activation energies for radical additions. *Aiche Journal* **2004,** 50, (2), 426-444.

70. Vandewiele, N. Kinetic model construction using chemoinformatics. Universiteit Gent, Universiteit Gent, Belgium, 2014.

71. Vijver, R. V. d. Automatic ab-initio calculations for kinetic model generation of gas phase processes. Universiteit Gent, Universiteit Gent, Belgium, 2017.

72.Sabbe, M. K.; Reyniers, M. F.; Van Speybroeck, V.; Waroquier, M.; Marin, G. B., Carbon-centered radical addition and beta-scission reactions: Modeling of activation energies and pre-exponential factors. *Chemphyschem* **2008,** 9, (1), 124-140.

73.Sabbe, M. K.; Reyniers, M. F.; Waroquier, M.; Marin, G. B., Hydrogen Radical Additions to Unsaturated Hydrocarbons and the Reverse beta-Scission Reactions: Modeling of Activation Energies and Pre-Exponential Factors. *Chemphyschem* **2010,** 11, (1), 195-210.

74.Sabbe, M. K.; Vandeputte, A. G.; Reyniers, M. F.; Waroquier, M.; Marin, G. B., Modeling the influence of resonance stabilization on the kinetics of hydrogen abstractions. *Physical Chemistry Chemical Physics* **2010,** 12, (6), 1278-1298.

75.Van de Vijver, R.; Vandewiele, N. M.; Vandeputte, A. G.; Van Geem, K. M.; Reyniers, M. F.; Green, W. H.; Marin, G. B., Rule-based ab initio kinetic model for alkyl sulfide pyrolysis. *Chemical Engineering Journal* **2015,** 278, 385-393.

76.   *CHEMKIN-PRO 15131*, Reaction Design: San Diego, 2013.

77.Tsang, W.; Rosado-Reyes, C. M., Unimolecular Rate Expression for Cyclohexene Decomposition and Its Use in Chemical Thermometry under Shock Tube Conditions. *Journal of Physical Chemistry A* **2015,** 119, (28), 7155-7162.

78.Sway, Kinetics of abstraction reactions of methyl radicals with alkanes in gas phase. *Indian J. Chem.* **1990**, (29).

79.Zhandong, W. Experimental and Kinetic Modeling Study of Cyclohexane and Its Mono-alkylated Derivatives Combustion. University of Science and Technology of China,Hefei

5

Microkinetic modeling of methyl-cyclohexane pyrolysis

In this chapter, a mechanism is generated for the pyrolysis of methyl-cyclohexane, using the automatic mechanism generator tool, "Genesys". The mechanism is composed of high pressure limit elementary reactions whose kinetics originate from ab-initio calculations without any alterations. The mechanism is validated using the SVUV-PIMS experimental data of 2014 from Zhandong Wang et al. at Hefei, China, in which a feed of 2 mol% methyl-cyclohexane in Argon is continuously fed to a tubular reactor maintained at a maximum temperature of 1000 to 1300K at pressures 1013, 200, 40 mbara, respectively. One objective of this chapter is to check if an automatically generated elementary reaction model with uniformly ab-initio based unaltered kinetics can predict methyl-cyclohexane pyrolysis well compared to literature optimized/ tuned/ global/ lumped models. Three popular models from literature were compared – Hefei (2014), JetSurF 2.0 (2010) and Orme (2006) et al. Another objective is to check if the high pressure limit model can predict species concentrations at different pressures. Overall, the Genesys model (LCT model) allows a reasonable prediction of the product yields compared to other models, and the best prediction for feed conversion for all the pressures. JetSurF model performs the worst, while Hefei and Orme models perform as well as the LCT model for species other than methyl-cyclohexane. Reaction path analysis shows the dominant pathways toward major products. The homolytic scission of the methyl-cyclohexyl bond dominates in the conversion of methyl-cyclohexane. Another important route is the hydrogen abstraction by hydrogen and methyl radicals at the 3- and 2- positions on the ring, followed by ring opening and subsequent beta scissions. The effect of pressure on experimental trends is also analyzed by plotting their mass % against feed conversion for the different pressures, and it is realized that pressure has a negligible effect on the yields of major products in the range of 1013-40 mbara.

5.1. Introduction

Petrochemical feedstocks and derived liquid fuels are complex mixtures composed of various molecule classes such as paraffins, olefins, naphthenes and aromatics. Whether used for pyrolytic or combustion applications, the thermal decomposition chemistry of cyclic compounds plays a central role in the prediction of product yields from biomass fast pyrolysis[1], waste fractions[2], scram jet modelling[3-6], naphtha steam cracking[7] and undesired auto ignition of gasoline[8-10]. Therefore the pyrolysis chemistry of hydrocarbons has been the subject of research for many years. While the gas-phase chemistry of open-chain hydrocarbons is well understood, the knowledge of the pyrolysis chemistry of cyclic hydrocarbons is less understood[10, 11]. This is even true for the simplest cycloalkanes, such as cyclopentane and cyclohexane. In chapters 4 and 5, the pyrolysis of unsubstituted cyclopentane and cyclohexane has been discussed. The simplest alkylated cyclohexane is methyl-cyclohexane, whose study is the subject of this chapter.

Recently, pyrolysis of cycloalkanes have received increasing attention because of their high concentrations in real-life feedstocks such as North American diesel fuel, where their content is 20-40%[12, 13]. Diesel itself has a higher carbon number range than C5 or C6. Hence, the naphthenic content of such fuels is more likely to contain methyl- and ethyl-cyclohexanes rather than unsubstituted cyclopentane and cyclohexane. Methyl-cyclohexane is an important component of fuel surrogate for naphtha[21], especially naphthenic naphtha whose carbon number range is C5-C9, so a C7 molecule falls midway. Naphtha is one of the ideal liquid feedstocks for pyrolysis processes to yield ethylene, propylene and other lower olefins, which themselves are raw materials for poly-olefin industry as well as other chemicals and pharmaceuticals. A naphtha feed has many compounds, sometimes hundreds, hence making it difficult to understand its detailed pyrolytic mechanism. Hence, usually a surrogate/ representative molecule is studied experimentally and theoretically to grasp its chemistry. In this respect, a detailed kinetic modeling study of methyl-cyclohexane would help to understand the pyrolytic behavior of the methyl cycloalkane cut of naphtha, in turn extending our knowledge of pyrolysis chemistry.

There have been some prior studies on methyl-cyclohexane pyrolysis – like of very low pressure pyrolysis[14], pyrolysis of methyl-cyclohexane in a turbulent flow reactor[15], ignition time delay in rapid compression machine[16, 17] and in shock tubes[18, 19]. More recently,

Bounaceur et al[20] developed a kinetic model to describe thermal cracking of methyl-cyclohexane which focused on identification of dominant pathways to aromatics formation. However, the most comprehensive recent pyrolysis study is by Zhandong Wang et al[21]., in Hefei, China, who performed pyrolysis experiments on methyl-cyclohexane feed in their SVUV-PIMS (Synchrotron Vacuum Ultra Violet - Photo Ionization Mass Spectrometry) setup. They fed 2 mol% of methyl-cyclohexane in Argon to the reactor maintained at a maximum temperature of 1000 to 1300K at 1013, 200 and 40 mbara, respectively. They also developed a model to calculate the product spectrum.

In this chapter, a mechanism is generated for the pyrolysis of methyl-cyclohexane, using the automatic mechanism generator tool, "Genesys". The mechanism is composed of high pressure limit elementary reactions whose kinetics originate from ab-initio calculations without any alterations. The mechanism is validated using the SVUV-PIMS experimental data from Zhandong Wang et al. at Hefei, China, in which a feed of 2 mol% methyl-cyclohexane in Argon is continuously fed to a tubular reactor maintained at a maximum temperature of 1000 to 1300K at 1013, 200 and 40 mbara, respectively. One objective of this chapter is to check if an automatically generated elementary reaction model with uniformly ab-initio based unaltered kinetics can predict methyl-cyclohexane pyrolysis well compared to literature optimized/ tuned/ global/ lumped models. Three popular models from literature were compared – Hefei[21], JetSurF 2.0[22] and Orme[23] et al. Finally, the most important reaction pathways will be analyzed for pyrolysis conditions. Another objective is to verify if the high pressure limit model can predict species concentrations at different pressures.

5.2. Methodology

5.2.1. Experimental setup and procedure

The experiments were performed by Wang et al.[21] in the National Synchrotron Radiation Laboratory, Hefei, China (referred to simply has "Hefei" henceforth). The reactor is a furnace made of sintered alumina, with a 6.8mm inner diameter, 229 mm length, mounted in a pressure chamber. The pressure is controlled by a MKS throat valve at 1013, 200 and 40 mbara, respectively. The heated zone is 150 mm long. Methyl-cyclohexane was procured from Aladdin, Shanghai with 99 wt% purity. It was vaporized using Argon to create a mixture of 2 mol% methyl-cyclohexane and 98 mol% Argon. The temperature

profiles showed a maxima in the heated zone, and the maximum temperatures achieved were in the range 1000K-1300K. The feed flow rate was maintained at 1 Nl/min at 273 K corresponding to nominal residence times in the range 0.007 – 0.2s. Mole fractions of pyrolysis products were calculated from the photo-ionization cross sections, which are available in literature. For those molecules where PICs photo-ionization cross sections (PICs) are not available, they are estimated from similar molecules. The setup has been described in more detail in their publication[21].
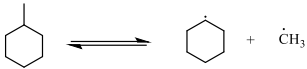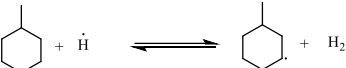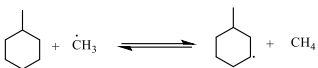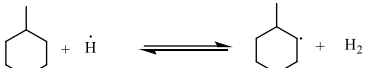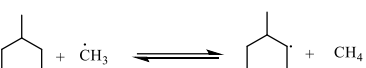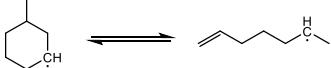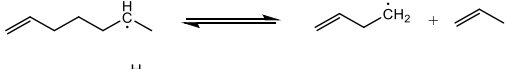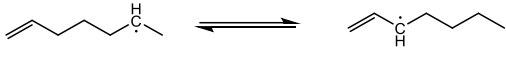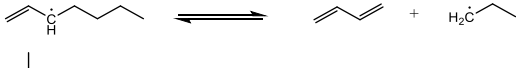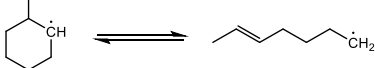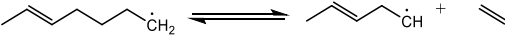
5.2.2. Kinetic model generation

5.2.2.1 CBS-QB3 computation of rate coefficients

Genesys was used to automatically generate the reaction mechanism for the pyrolysis of methyl-cyclohexane. The input reaction families for Genesys were the same as those given in Table 4.1 of chapter 4. The primary decomposition mechanism of methyl-cyclohexane involves reactions such as scission of methyl branch to give cyclohexyl radical. The mechanism of the subsequent ring opening of cyclohexyl was already present in the cyclohexane pyrolysis sub-mechanism. Methyl-cyclohexane conversion also takes place dominantly by hydrogen abstractions at various carbon sites of methyl-cyclohexane to form methyl-cyclohexyl radical. Subsequent ring opening of the cyclohexyl moiety forms an open chain alkenyl radical. This could subsequently undergo a C-C beta scission reaction or an intra-molecular hydrogen abstraction reaction (radical isomerization) to form an allylic alkenyl radical. The source of some of the kinetics was the CBS-QB3 values calculated by Zhandong Wang et al.[21] (elaborated in Table 5.1) for the primary decomposition reactions of methyl-cyclohexane, using the Gaussian 09 suite of programs. ChemKin-PRO was used to do a reaction path analysis to find the dominant routes to major products. The rate coefficients for the most important reactions involved in the pyrolysis of methyl-cyclohexane for all the 4 models are shown in Table 5.1.

Table 5.1: Most important reactions in the pyrolysis of methyl-cyclohexane - comparison of rate coefficients of 4 models – LCT, Hefei, JetSurF, Orme

#	Reaction	k(LCT)	k(Hefei)	k(JetSurF)	k(Orme)
	Elementary reaction	k(at T=1050K), units in cm3, mol, s			
R1	1-propyl=C2H4+CH3	2.54E+07 (origin=LCT)	1.31E+07	9.57E+06	6.18E+06
R2	C2H4+H=ethyl	6.21E+12 (origin=LCT)	5.17E+12	1.88E+13	3.02E+12
R3	C3H6+H=1-propyl	4.91E+12 (origin=LCT)	2.8E+12	2.79E+12	1.03E+13
R4		2.91E-01 (origin=Hefei)	2.91E-01	3.77E-02	2.57E-01
R5		2.41E+12 (origin=Hefei)	2.41E+12	2.74E+12	5.45E+12
R6		2.26E+09 (origin=Hefei)	2.26E+09	2.26E+09	6.22E+09
R7		2.07E+12 (origin=Hefei)	2.07E+12	2.24E+12	5.45E+12
R8		1.41E+09 (origin=Hefei)	1.41E+09	1.41E+09	6.22E+09
R9		5.20E+06 (origin=LCT)	5.20E+06	1.20E+07	6.69E+08
R10		3.65E+07 (origin=LCT)	3.65E+07	3.65E+07	1.10E+04
R11		3.19E+07 (origin=LCT)	3.19E+07	3.19E+07	3.72E+07
R12		6.53E+06 (origin=LCT)	6.53E+06	6.53E+06	1.10E+04
R13		4.16E+06 (origin=LCT)	4.16E+06	1.20E+07	6.08E+08
R14		1.71E+07 (origin=LCT)	1.71E+07	1.71E+07	1.10E+04

The kinetics of the most important reactions involved in the primary decomposition of methyl-cyclohexane have been plotted as ln(k) vs. 1000/T. A comparison is also made with the kinetics of simpler analogous reactions (indicated as "Reference" in the Figures 5.1 to 5.11) involving smaller, simpler molecules. The kinetics of these simpler analogous reactions originate from LCT CBS-QB3 calculations.
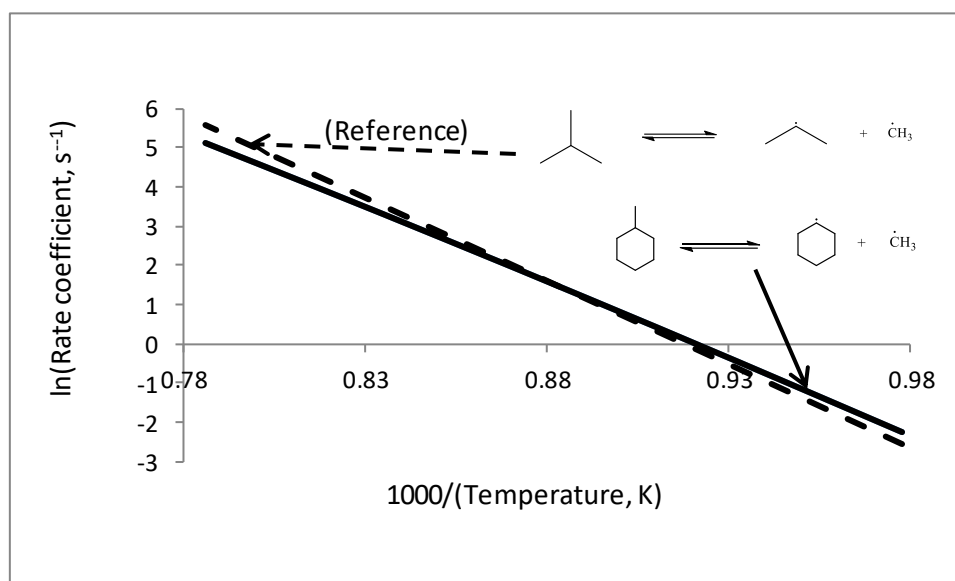
Figure 5.1: Kinetics of scission of methyl group

As shown in Figure 5.1, scission of methyl group is faster for isobutane than for methyl-cyclohexane in the temperature range of interest. Hence, it seems the C6-ring tends to stabilize the methyl substituent.
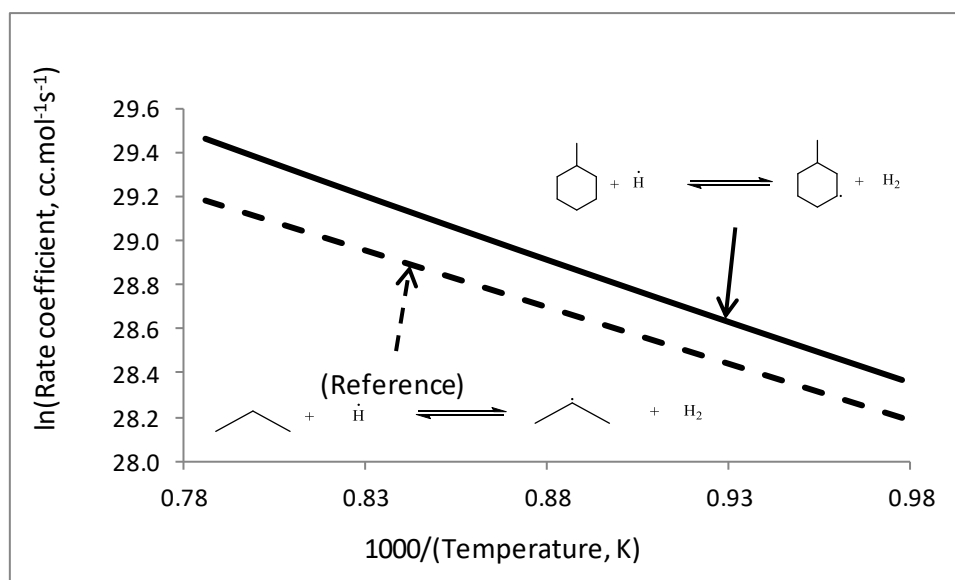
Figure 5.2: Kinetics of hydrogen abstraction by H-atom

As shown in Figure 5.2, rate coefficient of hydrogen abstraction by H-atom (at the 3-yl position) is higher for methyl-cyclohexane than for propane to 2-propyl radical. This could be attributed to the stereochemistry of methyl-cyclohexane and the relative ease of availability of the hydrogen for abstraction at the 3-yl position. The hydrogen at the 2nd carbon of propane probably faces more steric hindrance owing to the more obtuse angle, hence this trend.
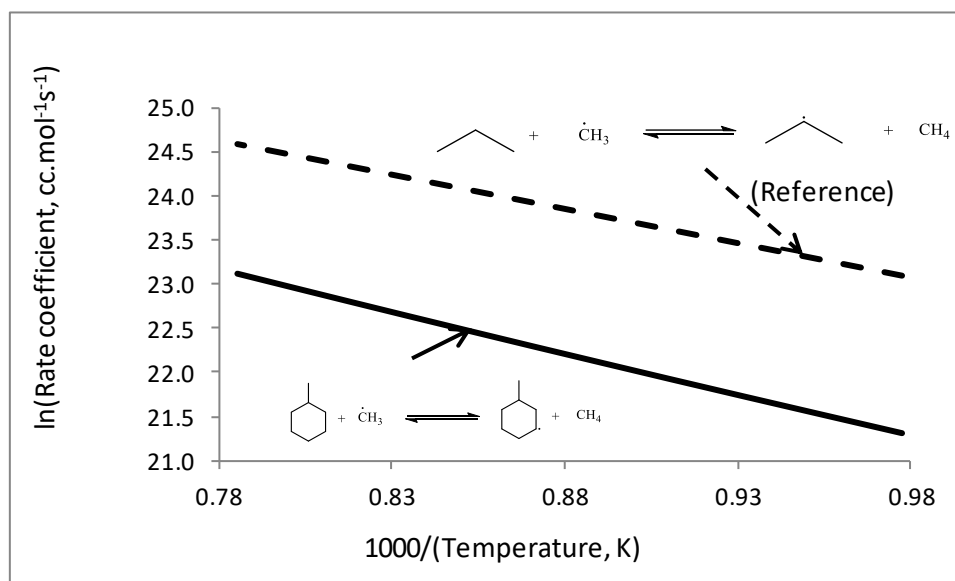
Figure 5.3: Kinetics of hydrogen abstraction by methyl radical

As shown in Figure 5.3, hydrogen abstraction at the 3-yl position by methyl radical is slower than the propane counterpart. This could be due to the specific steric hindrance caused by the attacking methyl group on the 2 reactants.
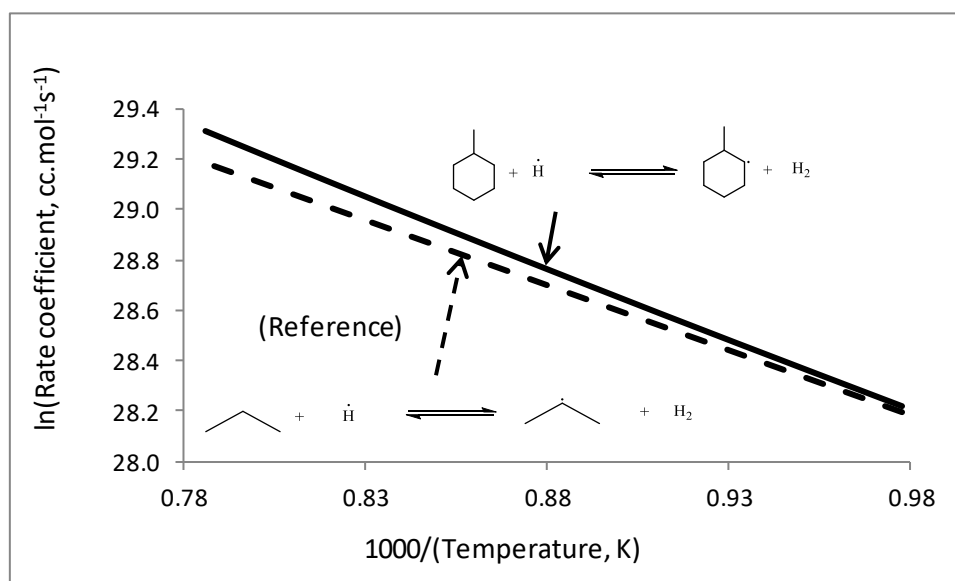
Figure 5.4: Kinetics of hydrogen abstraction by H-atom

As shown in Figure 5.4, the rate coefficient of hydrogen abstraction by H-atom (at the 2-yl position) is higher for methyl-cyclohexane than for propane to 2-propyl radical. This could be attributed to the stereochemistry of methyl-cyclohexane and the relative ease of availability of the hydrogen for abstraction at the 2-yl position. The hydrogen at the 2nd carbon of propane probably faces more steric hindrance owing to the more obtuse angle, hence this trend.
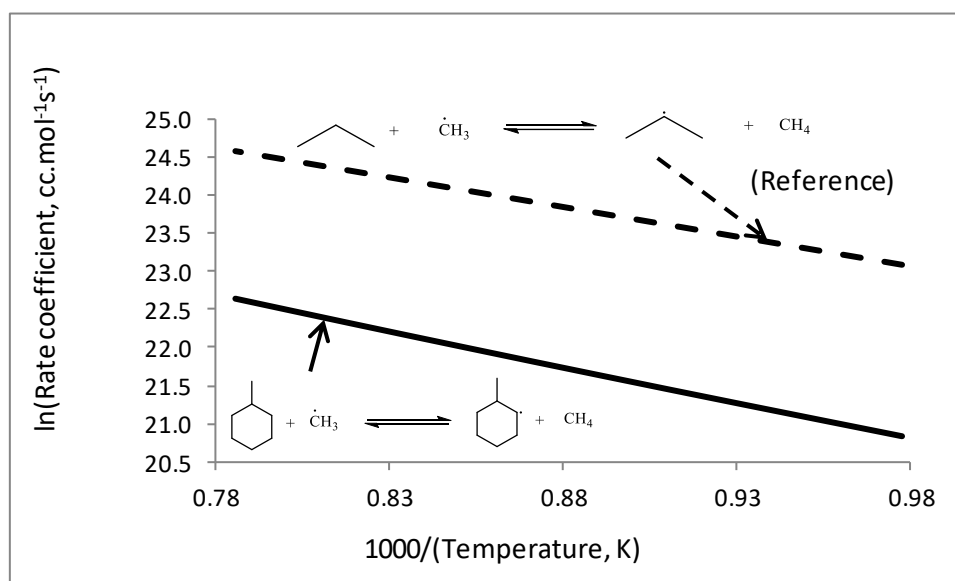
Figure 5.5: Kinetics of hydrogen abstraction by methyl radical

Similar to the 3-yl case, hydrogen abstraction at the 2-yl position by methyl radical is slower than for the propane counterpart (Figure 5.5). This could be due to the specific steric hindrance caused by the attacking methyl group on the 2 reactants.
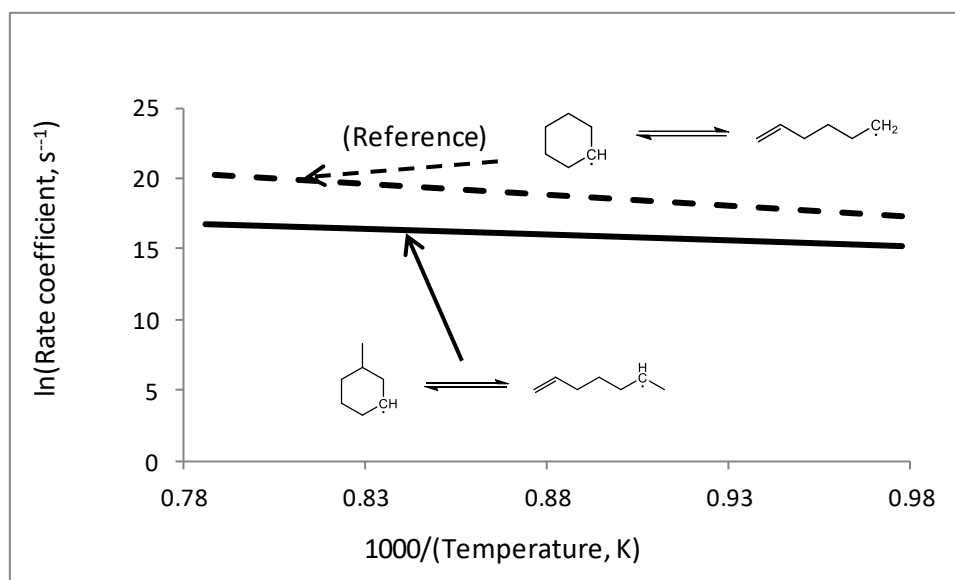
Figure 5.6: Kinetics of ring opening of cyclohexyl moeity

As shown in Figure 5.6, Methyl cyclohex-3-yl radical ring opening is slower than the ring opening of cyclohexyl. The reason is not immediately clear.
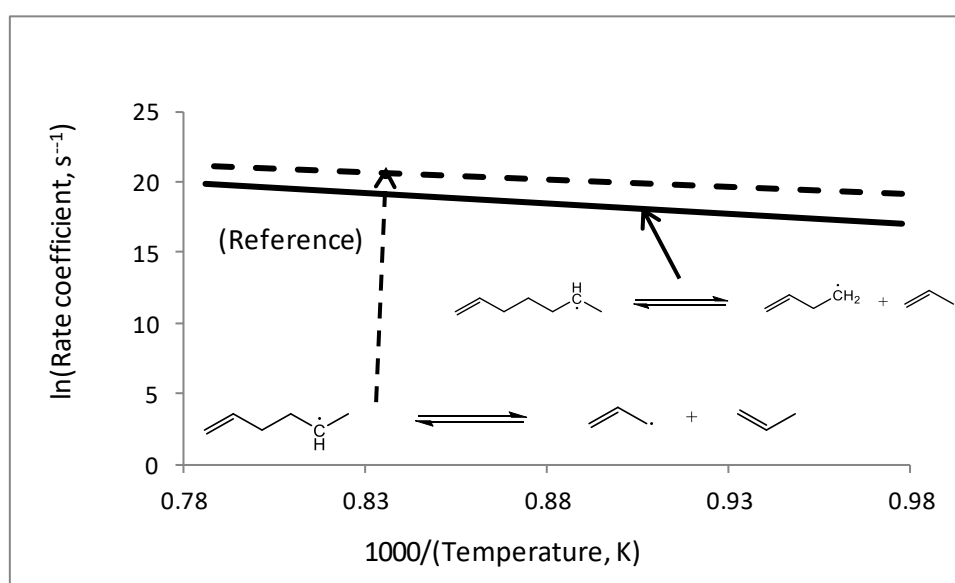
Figure 5.7: Kinetics of C-C beta scission of alkenyl radicals

C-C beta scission of hept-1-en-6-yl is slower than that of hex-1-en-5-yl radical (Figure 5.7). The reason could be the formation of resonance stabilized allyl radical in case of hex-1-en-5-yl. Hept-1-en-6-yl does not form any resonance stabilized radical.
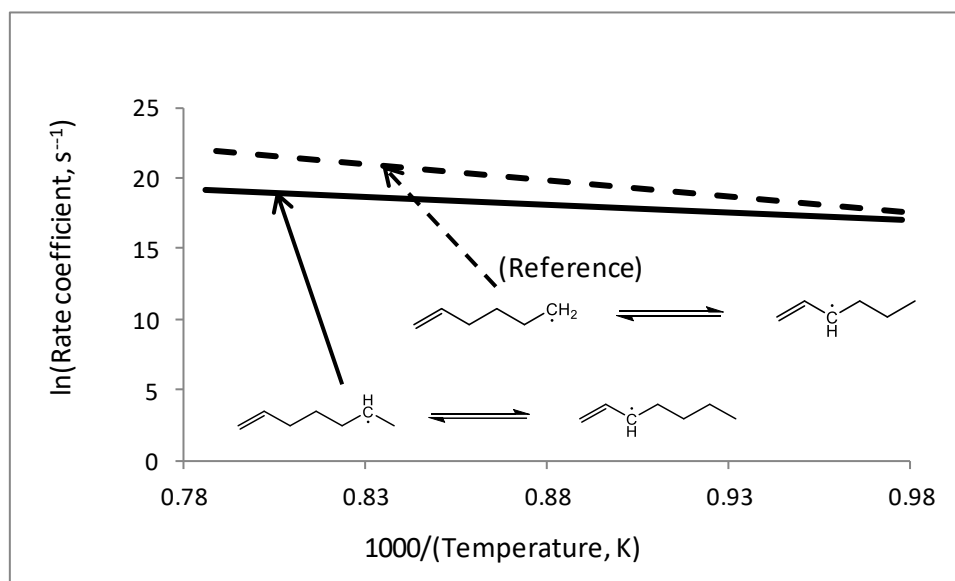
Figure 5.8: Kinetics of intra-molecular hydrogen abstraction (radical isomerization) to form allylic alkenyl radical

As a precursor to 1,3-butadiene formation, alk-1-en-6-yl radicals isomerize to the resonance stabilized alk-1-en-3-yl radicals. Figure 5.8 shows that the C7 chain has slower kinetics than the C6 chain. This could be attributed to the relative stability of a secondary radical as opposed to a primary radical.
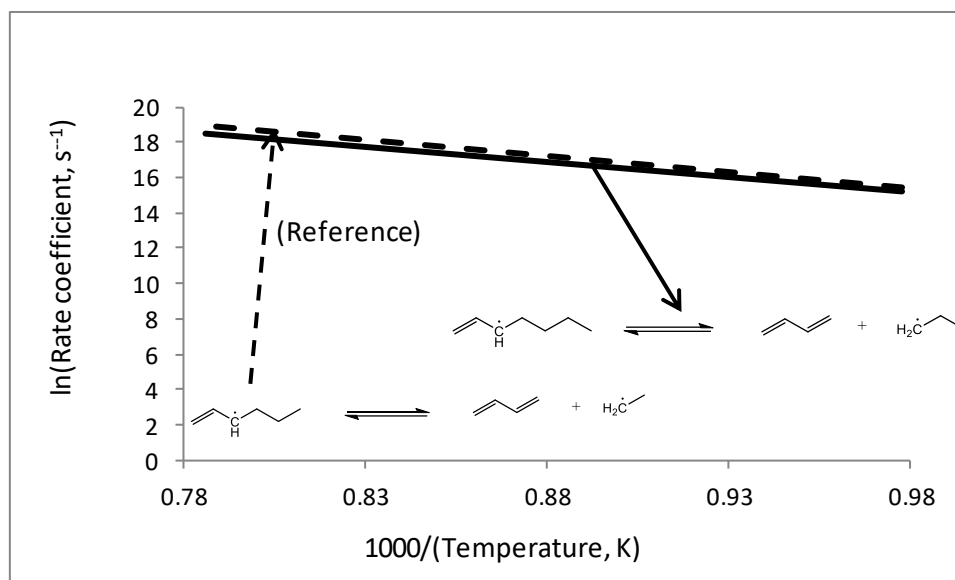
Figure 5.9: Kinetics of C-C beta scission of allylic alkenyl radicals

Alk-1-en-3-yl radicals undergo C-C beta scission to give 1,3-butadiene. Here the C7 chain has slower kinetics than the C6 chain (Figure 5.9). It seems the formation of ethyl radical is preferred over formation of 1-propyl radical.
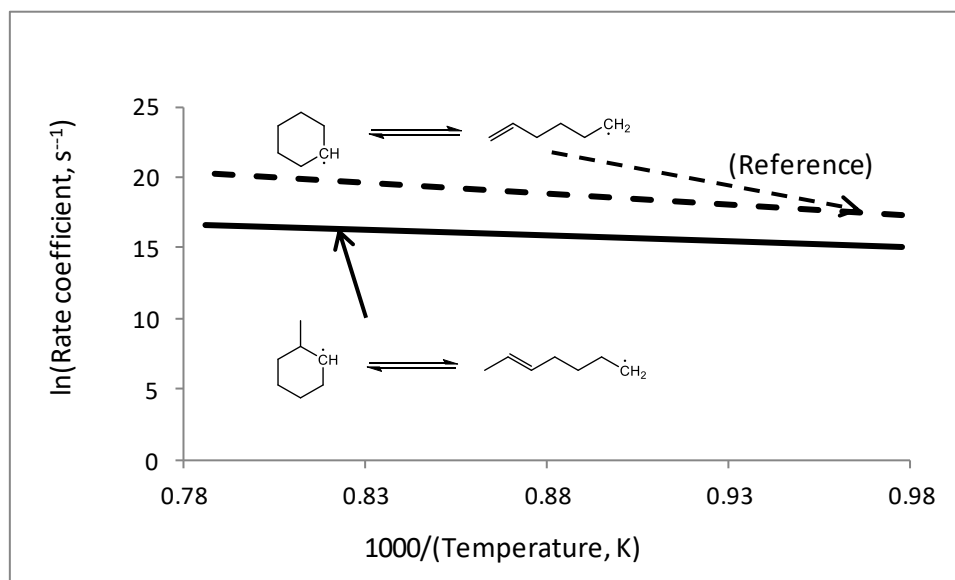
Figure 5.10: Kinetics of ring opening of cyclohexyl moeity

Ring opening of cyclohexyl to hex-1-en-6-yl is faster than that of methyl cyclohex-2-yl to form hept-2-en-7-yl (Figure 5.10). Both the open chain radicals have the general structure

of alk-1-en-6-yl. Hence it seems the unsubstituted double bonded carbon is preferred over the substituted species.
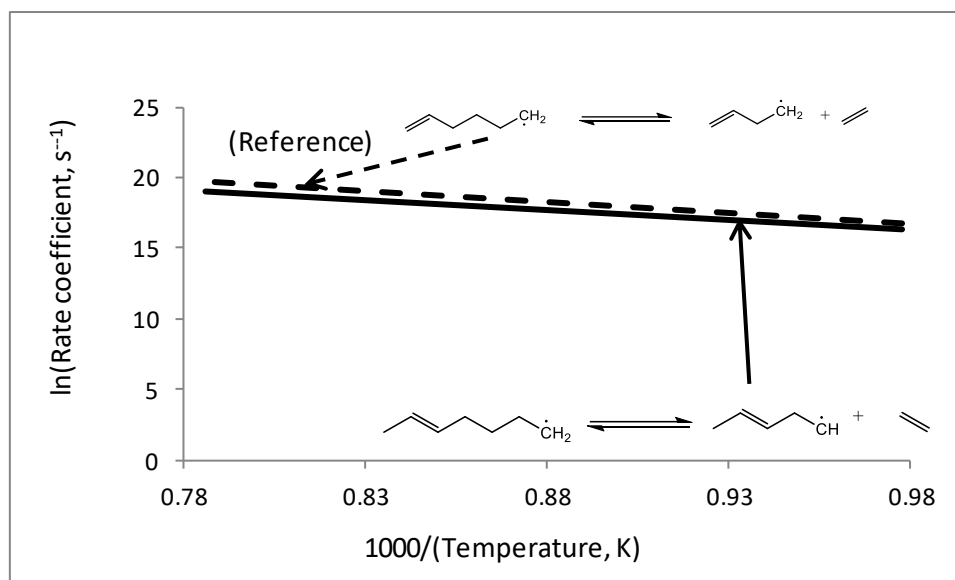
Figure 5.11: Kinetics of C-C beta scission of alkenyl radicals

As shown in Figure 5.11, alk-1-en-6-yl moiety undergoes C-C beta scission to form ethylene and alk-1-en-4-yl moiety. Here too, consistent with Figure 5.10, the formation of unsubstituted double bonded carbon is preferred over substituted species.

5.3. Results and discussion

5.3.1 Experimental data and model analysis

Experimental results of the main products of methyl-cyclohexane pyrolysis are discussed here. Also discussed are the 4 model trends- LCT, Hefei, JetSurF and Orme. Figure 5.12 shows the conversion of methyl-cyclohexane in Hefei experiments done at 1013, 200 and 40 mbara, respectively, and the 4 model predictions for the same. The experiment at 1013 mbara realizes high methyl-cyclohexane conversions, reaching a maximum of 90% at 1275 K. At 200 mbara, the conversion is about 60% at the same temperature, while at 40 mbara, it is 20%. This trend is understandable because the low gas concentrations in the low pressure experiments will lead to low reaction rates, and thereby conversion. It can be seen that the conversion predictions of the LCT model are better than

the other models. LCT is followed by Hefei, followed by Orme model. The conversion predictions of JetSurF model are the worst.
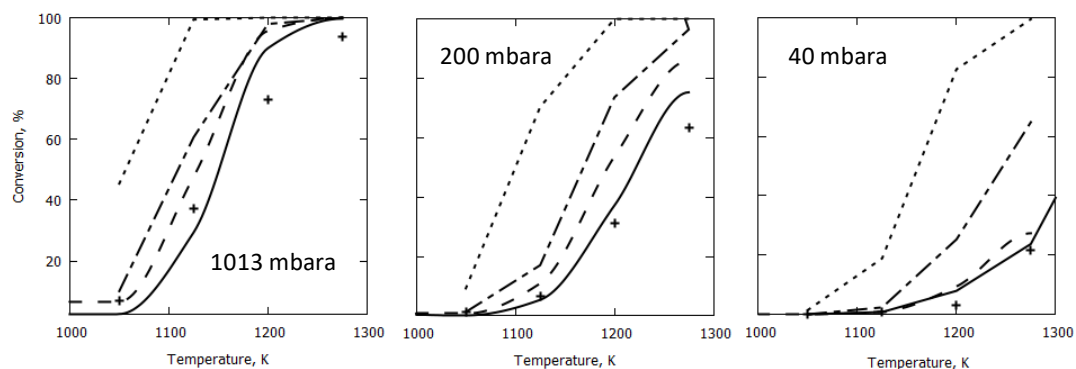
Figure 5.12: Hefei experimental trends vs. model predictions for methyl-cyclohexane pyrolysis feed conversions at various pressures. X-axis=temperature, K, Y-axis=methyl-cyclohexane conversion%. Legends: + Hefei experiment, ——— LCT, − − − − Hefei ·········JetSurF 2.0, − · — · − Orme

The bad performance of JetSurF model for methyl-cyclohexane conversion is investigated for further understanding, by comparing its ROP analysis with that of the LCT model. Figure 5.13 shows the Rate of Production Analysis for the conversion of methyl-cyclohexane using the LCT model:
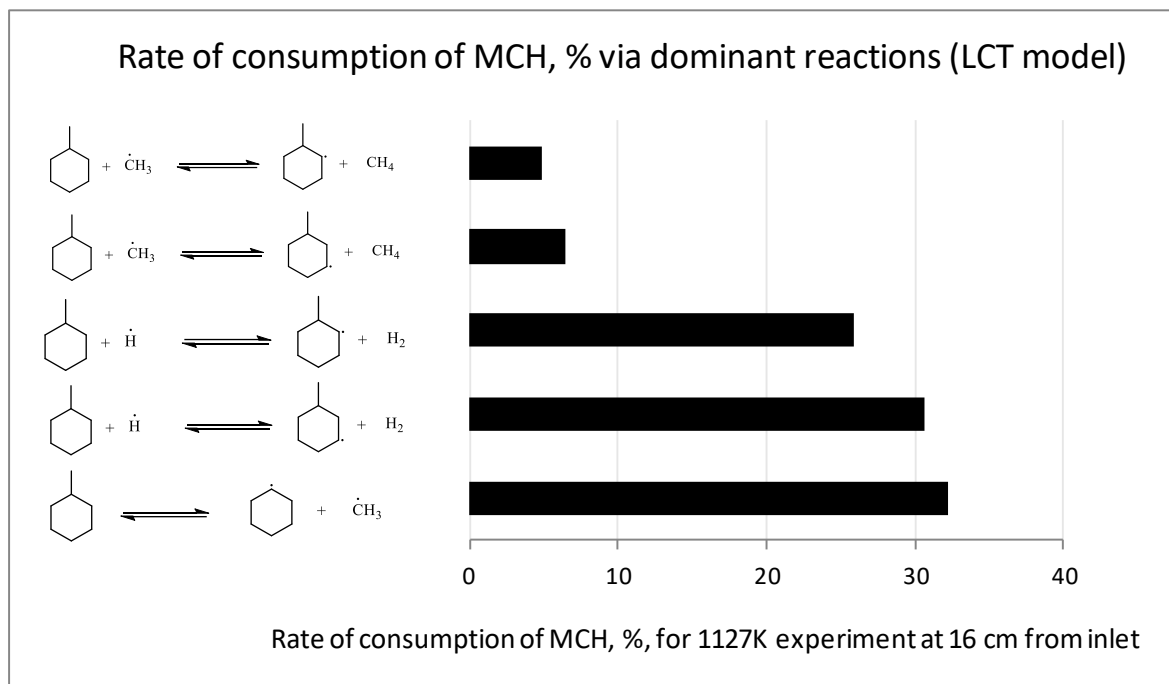
Figure 5.13: Rate of Production analysis, 1123K experiment at 16 cm from reactor inlet, 1013 mbara pressure - dominant routes for methyl-cyclohexane (MCH) consumption using LCT model

The above figure shows that homolytic scission of the methyl-cyclohexyl bond is the most dominant mechanism, followed by hydrogen abstractions using H-atom and then by methyl radical. This finding seems reasonable based on prior experience, and is in line with the Hefei model too. However, the JetSurF model has a different set of dominant reactions, as shown in Figure 5.14.
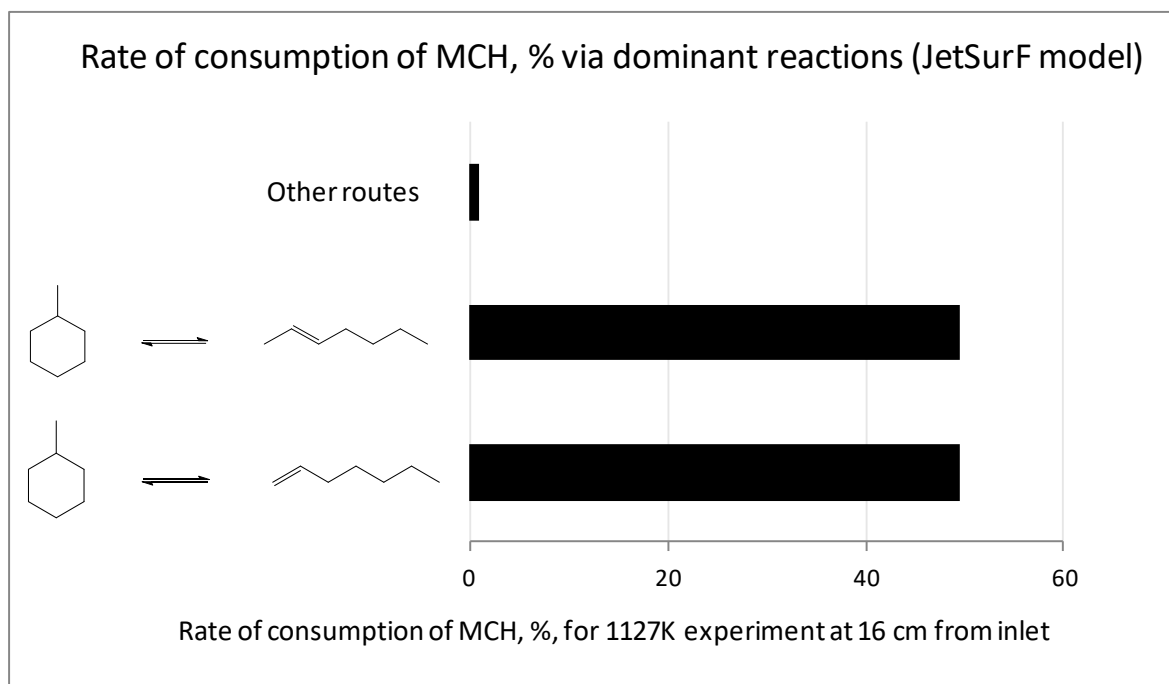
Figure 5.14: Rate of Production analysis, 1123K experiment at 16 cm from reactor inlet, 1013 mbara pressure - dominant routes for methyl-cyclohexane (MCH) consumption using JetSurF model

     The dominant reactions in the JetSurF model that contribute to about 99% of methyl-cyclohexane conversion are:- isomerization to 1-heptene and 2-heptene, respectively. The rate coefficient of these 2 reactions are identical   in the JetSurF model and amount to 7.17 s^{-1} at 1050K. An analogous reaction for which a CBS-QB3 rate coefficient exists is the isomerization of cyclohexane to 1-hexene[24]. For this reaction, the rate coefficient is 0.014 s^{-1} at 1050K. Figure 5.15 shows the pictorial representation of these three rate coefficients on a logarithmic scale. Hence, not only are the rate coefficients in JetSurF for methyl-cyclohexane isomerizations to 1-heptene and 2-heptene equal, they are about 500 times higher than that of cyclohexane to 1-hexene. This could be an indicator that these particular kinetics in JetSurF are not reliable. Since the kinetics are so fast, the extremely overpredicted conversions by JetSurF model are understandable.
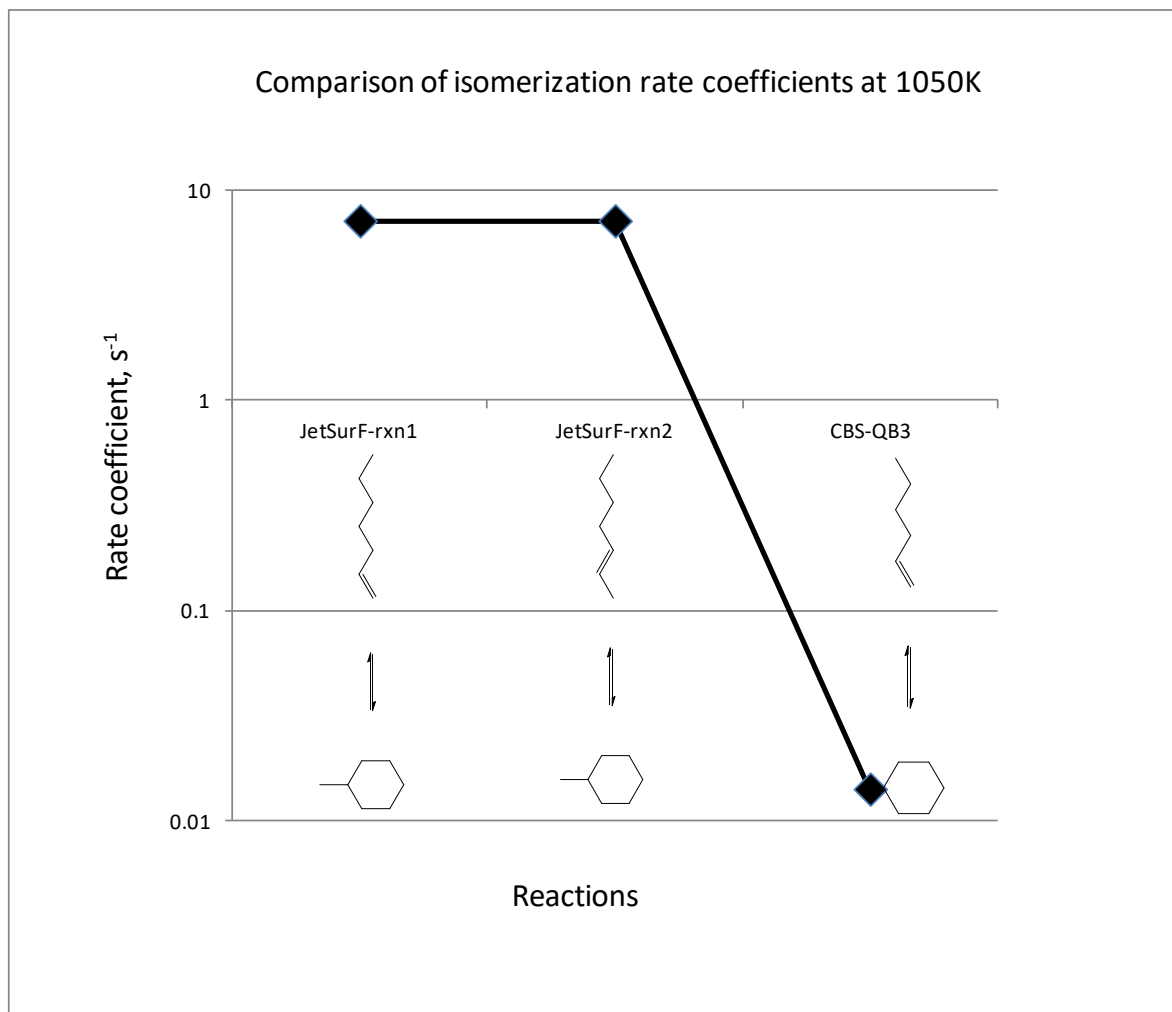
Figure 5.15: Rate coefficients of the two JetSurF isomerizations to 1- and 2-heptenes, and CBS-QB3 rate coefficient of cyclohexane isomerization to 1-hexene, all at 1050K
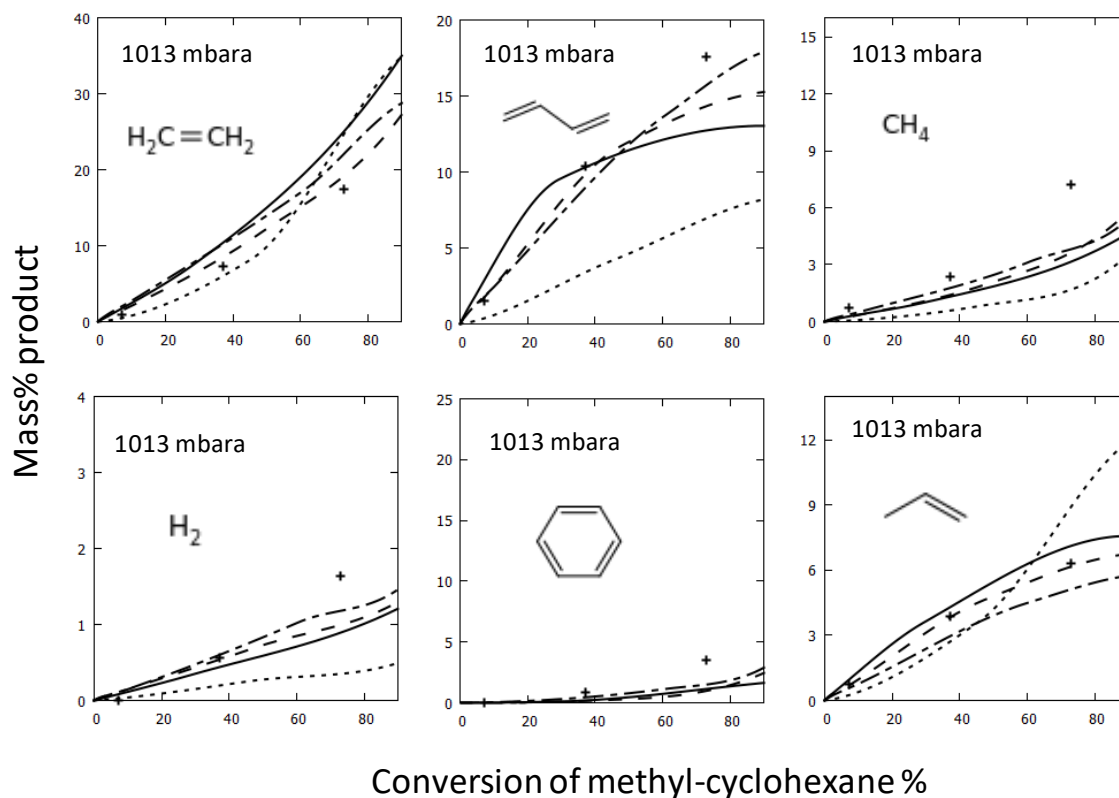
Figure 5.16: Hefei experimental trends vs. model predictions at 1013 mbara, X-axis=methyl-cyclohexane conversion %, Y-axis=mass% of product, Legends: **+** **Hefei experiment,** —————— **LCT,** − − − − **Hefei** ·········**JetSurF 2.0,** − · — · — **Orme**

Figure 5.16 shows the 1013 mbara experiment plot of product mass% vs. methyl-cyclohexane feed conversion. It can be seen that the product yield trends are predicted well by all the models except for JetSurF model. JetSurF model grossly underpredicts butadiene and overpredicts propylene. Hydrogen and methane are also underpredicted. The dominant routes leading to butadiene and propylene for LCT and JetSurF models are investigated using the reaction path analysis and are shown pictorially in Figure 5.17. In the LCT model, propylene and butadiene originate from the hydrogen abstraction of methyl-cyclohexane, which seems reasonable. Methyl cyclohex-3-yl opens the ring to form hept-1-en-6-yl. The latter undergoes C-C beta scission to give propylene and but-1-en-4-yl. This route to propylene seems reasonable. In contrast, according to the JetSurF model (Figure 5.18), propylene and butadiene originate from the isomerization of methyl-cyclohexane to 1- and 2- heptenes, whose kinetics are not reliable, according to the above discussion. 1-Heptene undergoes homolytic scission to give allyl and 1-butyl radicals. Allyl instead of abstraction

to directly give propylene, recombines with methyl to give 1-butene. 1-butene then combines with hydrogen atom to give propylene and methyl. This last step is listed as a lumped high pressure limit reaction in JetSurF model. This route to propylene seems unreasonable based on prior experience with different feedstocks. In LCT model, 1,3-butadiene originates from the methyl cyclohex-2-yl radical. It opens the ring to form hept-2-en-7-yl. The latter undergoes C-C beta scission to give ethylene and pent-2-en-5-yl. Pent-2-en-5-yl undergoes radical isomerization to give allylic pentenyl radical followed by C-C beta scission to give 1,3-butadiene. In JetSurF model, 1,3-butadiene originates from 2-heptene, whose homolytic scission gives allylic butenyl radical and 1-propyl radical. Allylic butenyl radical undergoes C-H beta scission to give 1,3-butadiene. Overall, the dominant routes of Hefei and Orme models are in line with the LCT model. Hence, qualitatively, the LCT, Hefei and Orme models are similar, and different and better than the JetSurF model.
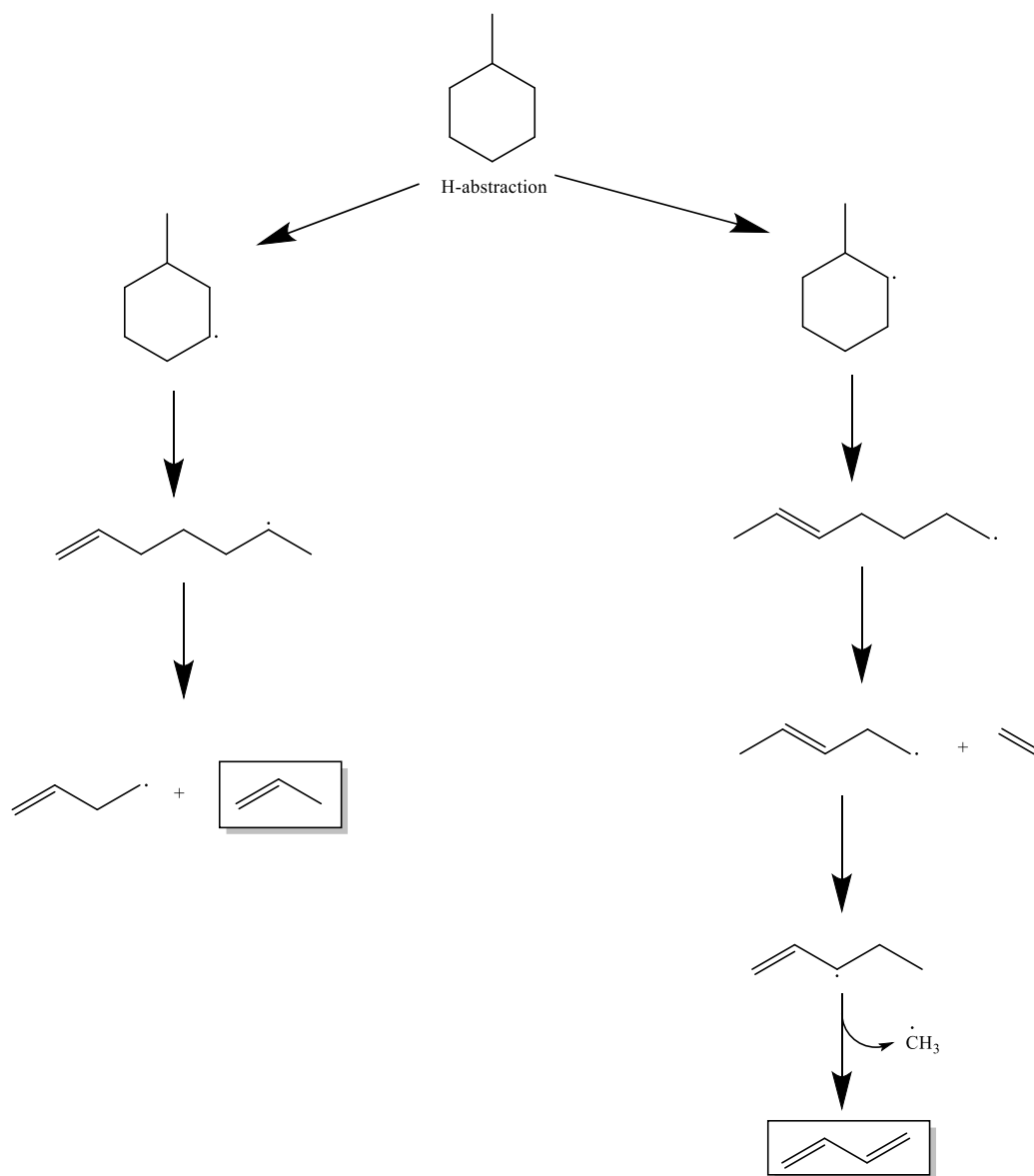
Figure 5.17: Dominant pathways toward formation of propylene and 1,3-butadiene by LCT, Hefei and Orme models
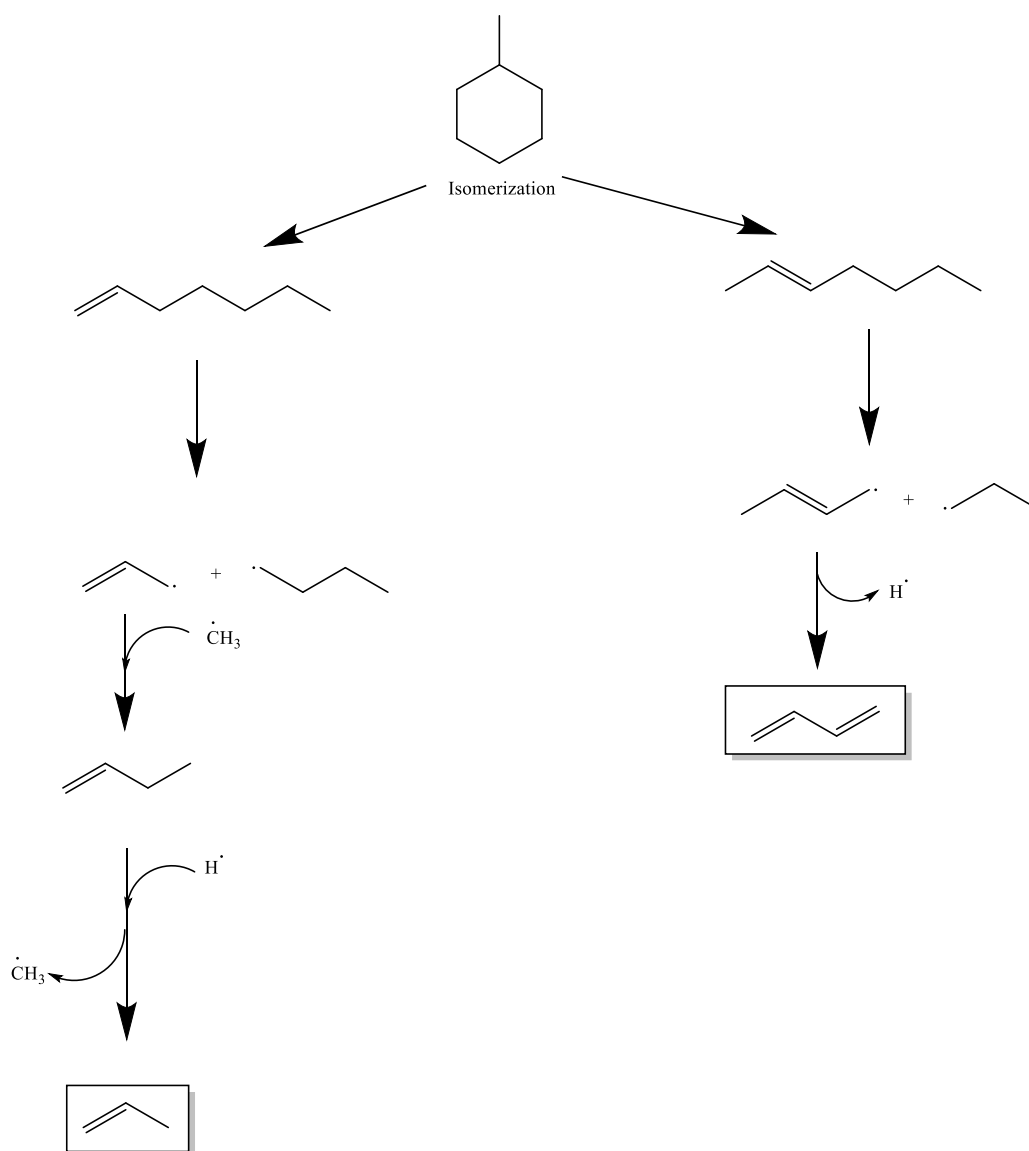
Figure 5.18: Dominant pathways toward formation of propylene and 1,3-butadiene by JetSurF model

Another species which is predicted well by the LCT model and underpredicted by JetSurF is methane. Figures 5.19 and 5.20 show the different dominant routes to methane for these two models. Methane is mainly formed by the hydrogen abstraction by methyl radical in both the models. However, the routes to formation of methyl radical are different. In the LCT model, one of the dominant routes of methyl formation is by the homolytic scission of the CH_3-cyclohexyl bond of methyl-cyclohexane. Another dominant route is related to the formation of ethylene and 1,3-butadiene. Hydrogen abstraction of methyl-cyclohexane by H-atom leads to the formation of methyl cyclohex-2-yl. Its ring opening leads to hept-2-en-

7-yl radical, which undergoes C-C beta scission to form ethylene and pent-2-en-5-yl. Pent-2-en-5-yl undergoes radical isomerization to form pent-1-en-3-yl, which upon C-C beta scission gives 1,3-butadiene and methyl radical. In contrast, in the JetSurF model, methyl radical is formed during the formation of ethylene, propylene and propyne. Especially the formation of propyne from allylic butenyl is listed as a high pressure limit reaction and seems to indicate a lumped non-elementary reaction. Overall, the routes of LCT model seem more reasonable, in line with prior experience.
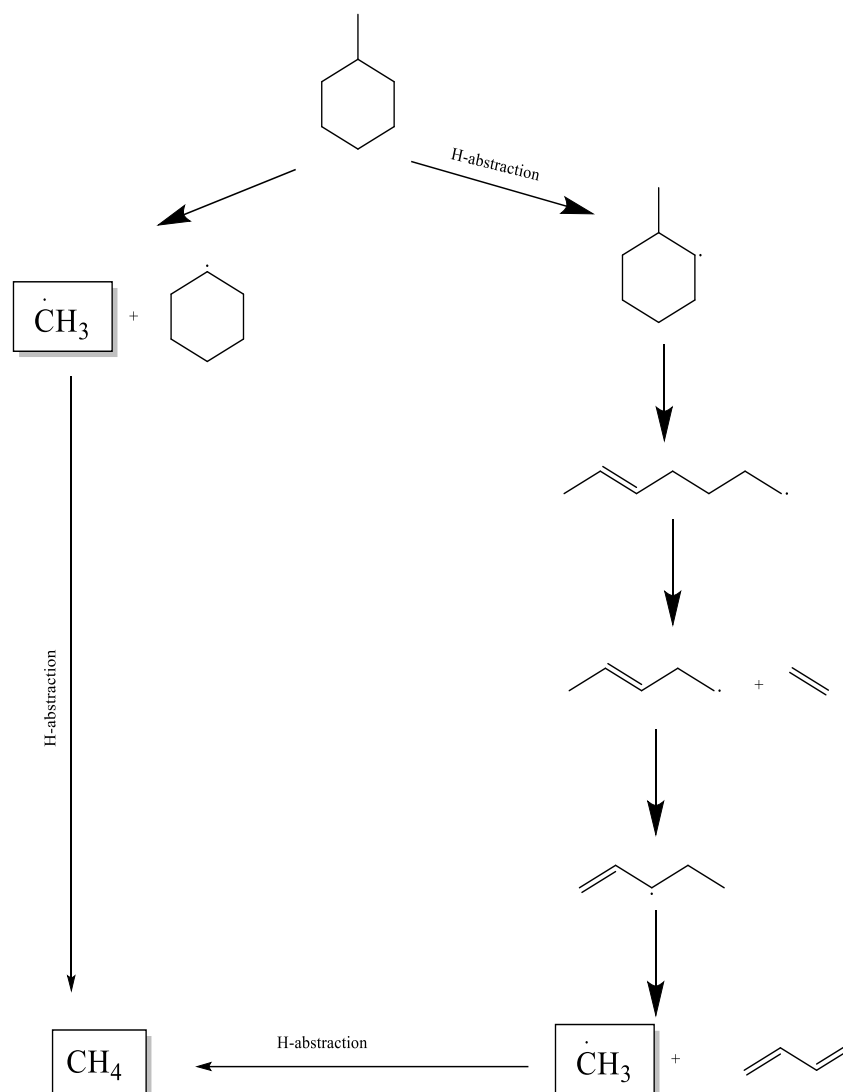
Figure 5.19: Dominant pathways toward formation of methane by LCT, Hefei and Orme models
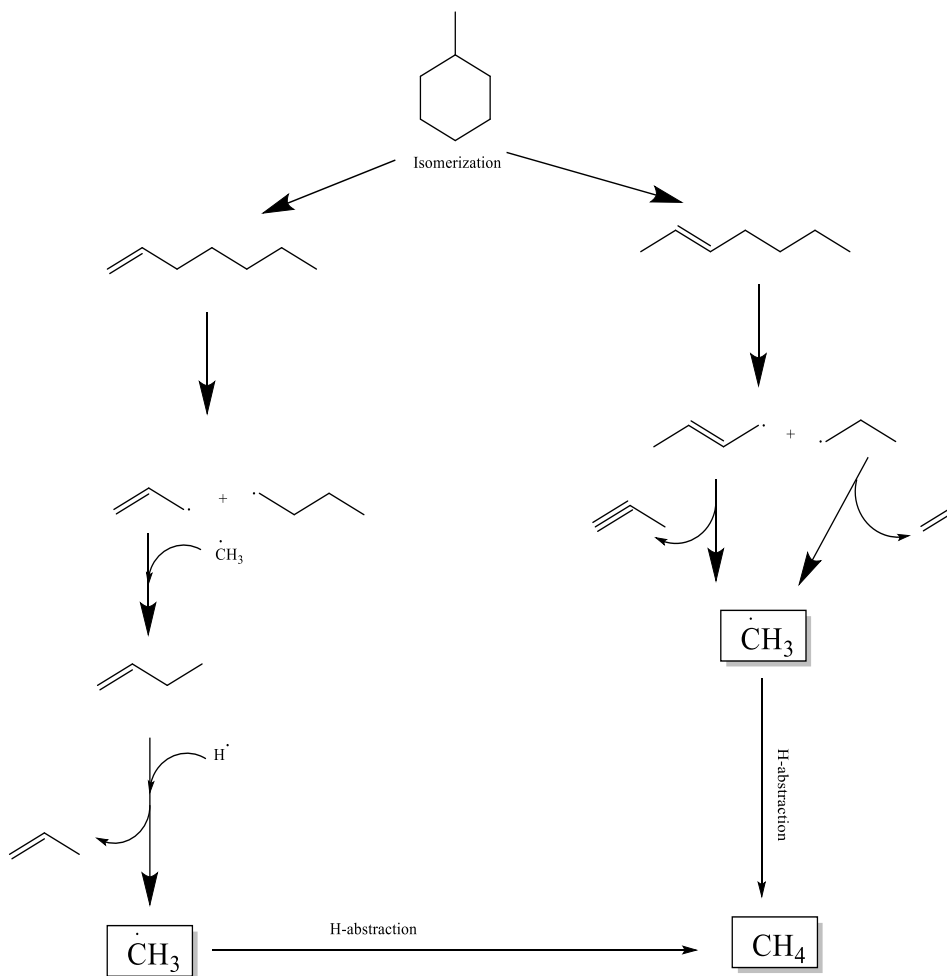
Figure 5.20: Dominant pathways toward formation of methane by JetSurF model

Figure 5.21 shows the product trends for the 200 mbara experiment. The LCT model captures the monotonic trend of ethylene, though it overpredicts it compared to other models. However, the 1,3-butadiene yield is very well captured by the LCT model, better than the other models. Methane, hydrogen, benzene are underpredicted and propylene is better than other models.
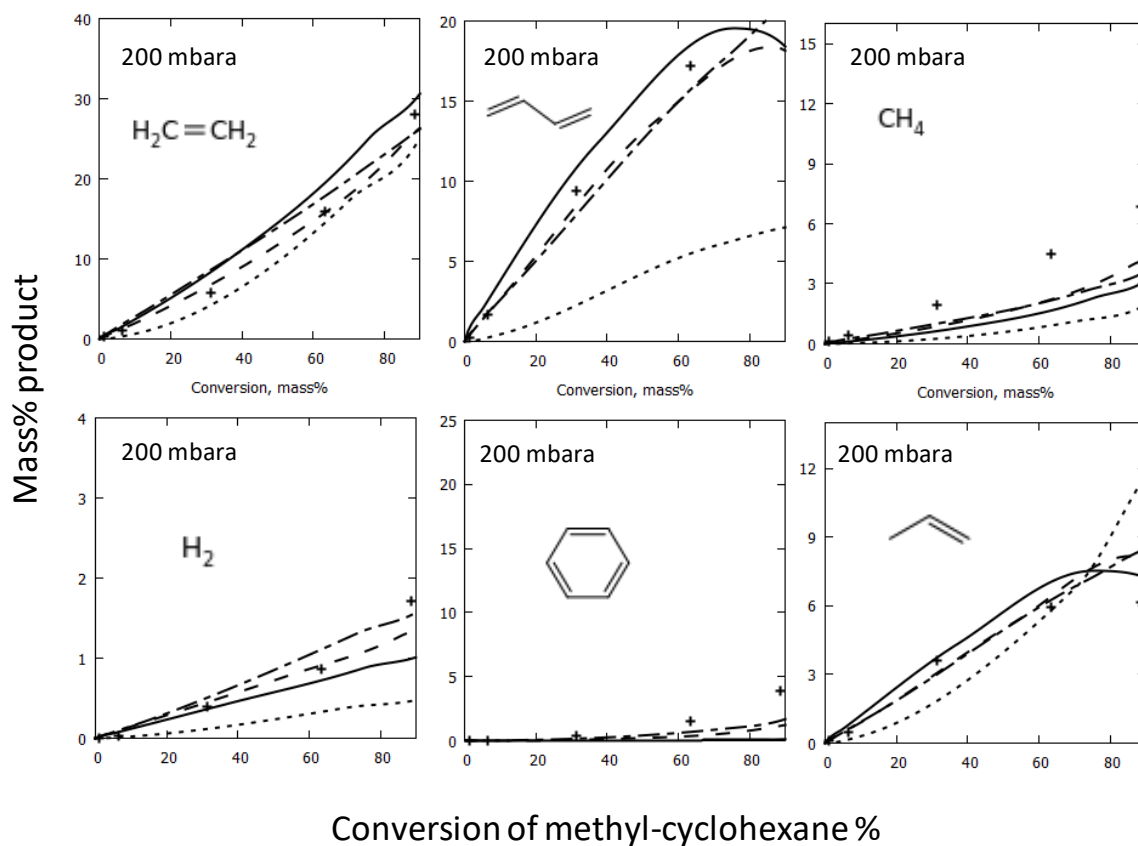
Figure 5.21: Hefei experimental trends vs. model predictions at 200 mbara, X-axis=methyl-cyclohexane conversion %, Y-axis=mass% of product, Legends: + Hefei experiment, ——— LCT, - - - - Hefei ········JetSurF 2.0, —·—·— Orme

Figure 5.22 shows the product trends for the 40 mbara experiment. The LCT model captures the trends of ethylene, butadiene, methane and propylene better than other models, while it underpredicts hydrogen and benzene.
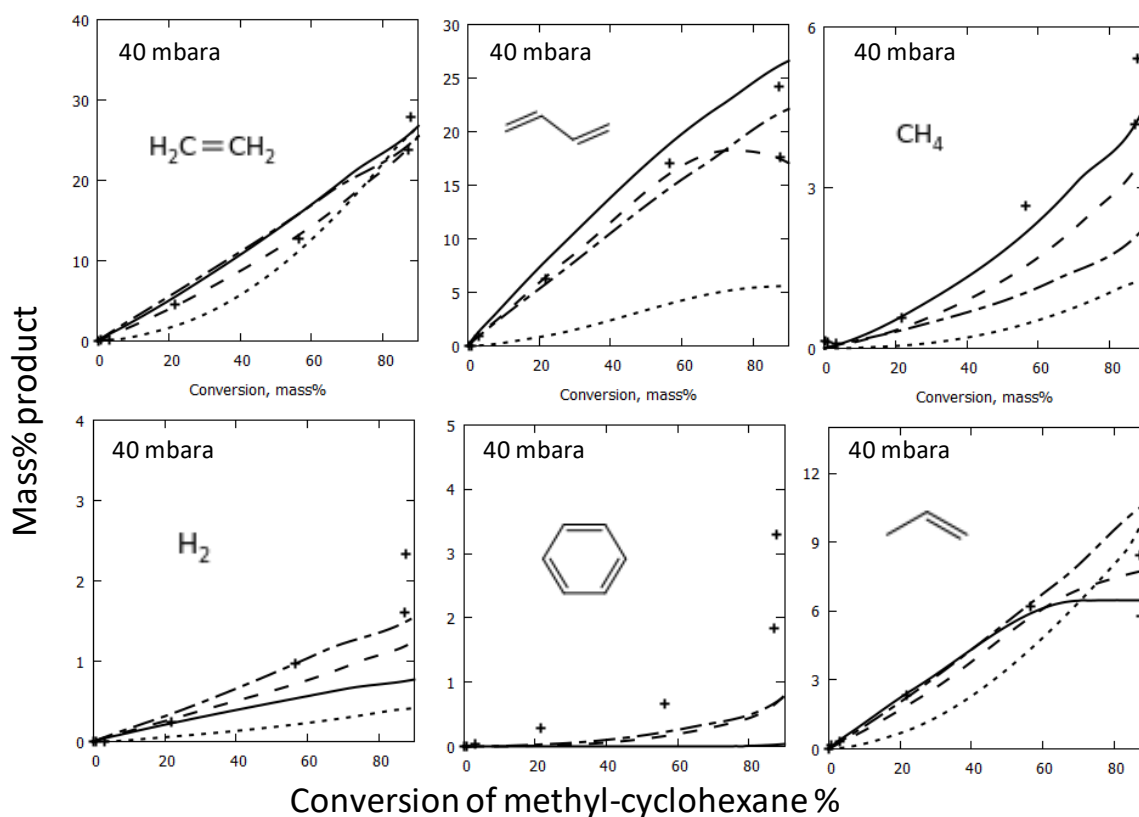
Figure 5.22: Hefei experimental trends vs. model predictions at 40 mbara, X-axis=methyl-cyclohexane conversion %, Y-axis=mass% of product, Legends: ✚ Hefei experiment, ———— LCT, – – – – Hefei ········JetSurF 2.0, — ·— ·— Orme

Overall, the methyl-cyclohexane conversion shows an "S"-type of trend and the higher pressure experiments yield higher conversion than lower pressure experiments for the same temperature. LCT model seems to best predict the conversion trends at all the pressures, followed by Hefei model. Orme and JetSurF models overpredict the conversions, in particular at lower pressures. Ethylene experimental mass % shows a monotonic increase for all pressures and its mass% is in the range of 25-35% at 90% methyl-cyclohexane conversion, the 35 mass% obtained at 40 mbara. All the models perform reasonably well for ethylene prediction, with Orme model being slightly better than the rest. Propylene undergoes a maximum at 7 mass%, obtained at about 80% methyl-cyclohexane conversion at all pressures. LCT model predicts propylene the best and JetSurF shows maximum deviation. 1,3-Butadiene also shows a maximum at 18 mass% butadiene obtained at 80% methyl-cyclohexane conversion. At lower pressures, more butadiene is formed, showing a maximum at 25 mass% for the same conversion at 40 mbara. LCT and Orme models

perform the best for predicting butadiene, followed by Hefei model. JetSurF shows large overpredictions at 1013 and 200 mbara pressures. Methane shows a monotonic increase to 12 mass% at 90% methyl-cyclohexane conversion, though its yield decreases at lower pressures. Hefei and LCT models perform the best for methane. Hydrogen shows a decrease at lower pressures, as does benzene. Hence, Hefei experimental data shows more yield of ethylene and butadiene at lower pressures as compared to higher pressure experiments. Propylene seems to be neutral to pressure, while methane, hydrogen and benzene and methyl-cyclohexane conversion are lower at lower pressures. Benzene is underpredicted by all the models, possibly due to unknown reaction families that are not accounted for. In particular, benzene is underpredicted by the trends of the LCT model for the 200 and 40 mbara experiments (but not for the 1013 mbara trend). This may lead us to believe that the experimental product benzene is actually pressure dependent hence not properly predicted by the high pressure limit LCT model. This will be investigated next.

5.3.2 Effect of pressure

Figure 5.12 shows that the conversion of methyl-cyclohexane is influenced by pressure. In 1013 mbara experiment, methyl-cyclohexane achieves almost 90% conversion at 1275K. In the 200 mbara experiment, about 60% conversion is achieved at the same temperature, while in 40 mbara experiment, the conversion is about 20%. This trend is as expected because the gas concentration of methyl-cyclohexane in the reactor at low pressure experiment is low, hence the decomposition reactions proceed slowly, leading to low conversions. However, what would be interesting would be to see the effect of pressure on product mass% when plotted against feed conversion, when the effect of low gas concentration plays a level field for all the reactions and species with methyl-cyclohexane as the feed.
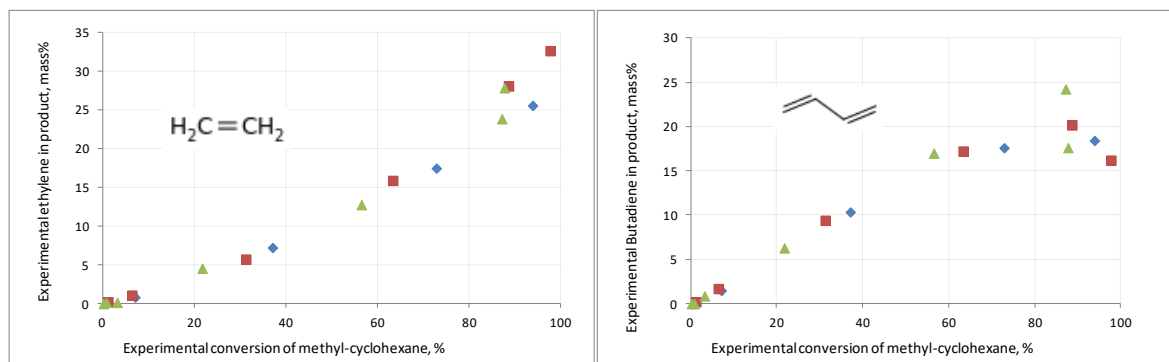
Figure 5.23: Experimental ethylene and butadiene mass % vs feed conversion, ◆ **1013 mbara,** ■ **200 mbara,** ▲ **40 mbara**

Figure 5.23 shows the experimental product mass% of ethylene and 1,3-butadiene plotted against experimental conversion % of methyl-cyclohexane for all the 3 pressures – 1013, 200 and 40 mbara. Ethylene can be seen to increase monotonically while butadiene undergoes a maxima. However, there does not seem to be any observable effect of pressure on these trends. This is an interesting observation from the Hefei experiment which the original article does not report, since it plots the mass% of products against reactor temperature and not against feed conversion.
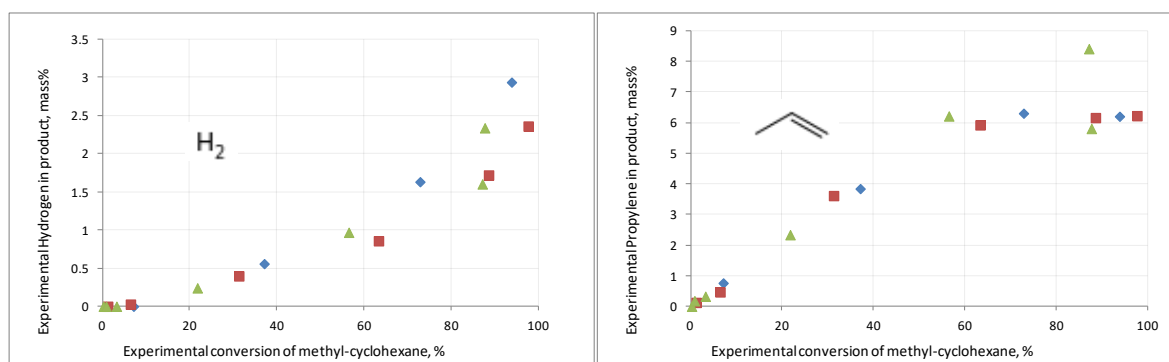
Figure 5.24: Experimental hydrogen and propylene mass % vs feed conversion, ◆ **1013 mbara,** ■ **200 mbara,** ▲ **40 mbara**

Figure 5.24 shows the experimental product mass% of hydrogen and propylene plotted against experimental conversion % of methyl-cyclohexane for all the 3 pressures – 1013, 200 and 40 mbara. Hydrogen can be seen to increase monotonically while propylene

undergoes a maxima. Here too, there does not seem to be any observable effect of pressure on these trends.
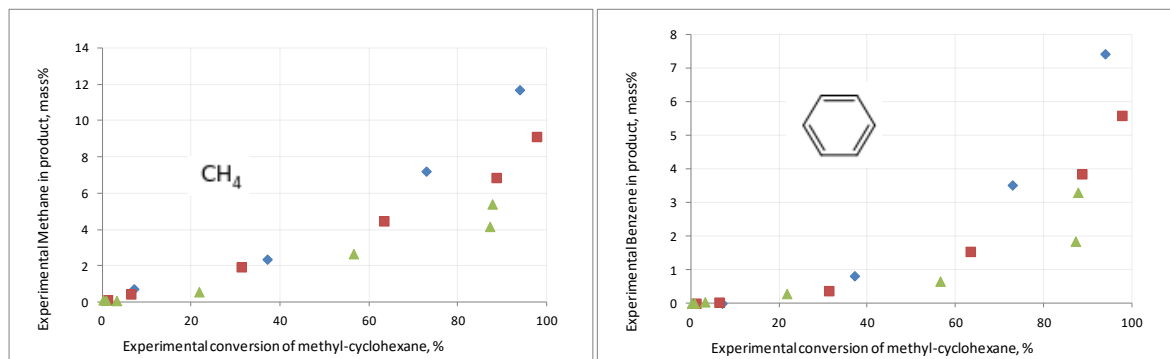
Figure 5.25: Experimental methane and benzene mass % vs feed conversion, ◆ **1013 mbara,** ■ **200 mbara,** ▲ **40 mbara**

Figure 5.25 shows the experimental product mass% of methane and benzene plotted against experimental conversion % of methyl-cyclohexane for all the 3 pressures – 1013, 200 and 40 mbara. There seems to be a trend here. For the same amount of feed conversion, the mass% of methane and benzene at 1013 mbara seems to be higher than that at 200 mbara, which itself is higher than that at 40 mbara.

The above discussion shows the importance of plotting product mass% against feed conversion as opposed to temperature, so that the real effect of pressure dependence of rates is captured rather than the effect of varying gas concentrations. In this particular case of methyl-cyclohexane, it seems pressure does not play a major role for the dominant products. Probably that explains why a high pressure limit model like that of LCT holds good even for a 40 mbara experiment.

5.3.3 LCT kinetic model evaluation

As seen in Figure 5.12, LCT model captures the experimental trends of methyl-cyclohexane pyrolysis at the 3 pressures – 1013, 200 and 40 mbara, respectively, better than other 3 models especially in the conversions predictions and mass% of products propylene and butadiene. The Hefei model captures the experimental trends, but the objective here was to verify if an ab-initio based elementary reaction model generated automatically can perform well compared to optimized models in literature. From that respect, the LCT model seems to be predicting sufficiently accurate. JetSurF 2.0 and Orme models are not as good as

Hefei and LCT models in terms of predictions. The following section explains the routes of formation of important products according to LCT model based on Reaction Path Analysis using ChemKin-PRO. Figure 5.26 shows the dominant routes schematically.

Methyl-cyclohexane conversion routes:- In the Hefei experiment set point 1123K, 1013 mbara pressure at 15 cm reactor length, methyl-cyclohexane cracking in SVUV-PIMS, in the isothermal region, there are 3 dominant routes of methyl-cyclohexane conversion: (a) Scission of the methyl branch to give cyclohexyl radical, (b) Hydrogen abstraction by H-atom and methyl radical to give methyl cyclohex-3-yl radical and (c) Hydrogen abstraction by H-atom and methyl radical to give methyl cyclohex-2-yl radical. Figure 5.13 shows the relative rate of consumption of methyl-cyclohexane by different reactions. Scission of methyl group from methyl-cyclohexane is a major contributor, followed by H-atom assisted abstraction at 3-yl and 2-yl positions followed by the same by methyl radical.

Ethylene formation:- Methyl cyclohex-2-yl radical undergoes ring opening to form hept-2-en-7-yl radical. This radical undergoes C-C beta scission to give ethylene and pent-2-en-5-yl radical. This is the most dominant route to form ethylene from methyl-cyclohexane. The next most dominant route to ethylene is from C-C beta scission of but-1-en-4-yl to form ethylene and vinyl radical. But-1-en-4-yl radical is formed in the primary decomposition of methyl-cyclohexane. Hydrogen abstraction of methyl-cyclohexane gives methyl cyclohex-3-yl radical, which on C-C beta scission gives hept-1-en-6-yl, which on further C-C beta scission gives but-1-en-4-yl radical and propylene. This is also the dominant route for propylene formation. The next dominant routes are those known to cyclohexane cracking discussed in the previous chapter: C-H beta scission of ethyl radical, C-C beta scission of 1-propyl radical and C-C beta scission of hex-1-en-6-yl radical which is formed by the ring opening of cyclohexyl radical which in turn is formed by the methyl loss from methyl-cyclohexane. Retro-Diels Alder contributes to ethylene formation though to a smaller extent.

Propylene formation:- As discussed in the ethylene formation section above, the most dominant route for propylene formation is by the C-C beta scission of hept-1-en-6-yl radical.

1,3-Butadiene formation:- Isomerization of hept-1-en-6-yl leads to the resonance stabilized allylic hept-1-en-3-yl radical. This on C-C beta scission gives 1,3-butadiene and 1-propyl

radical. Another dominant route originates from methyl cyclohex-2-yl radical, which on ring opening gives hept-2-en-7-yl radical as discussed in the ethylene formation section. On C-C beta scission, this gives ethylene and pent-2-en-5-yl radical. Pent-2-en-5-yl radical on isomerization leads to the allylic pent-1-en-3-yl radical. This on C-C beta scission gives 1,3-butadiene and releases methyl radical. This route is also the main source of methyl radicals. Another dominant route originates from cyclohexyl radical, which has been discussed in the chapter on cyclohexane pyrolysis.

Methane and Hydrogen formation:- Methyl radicals and hydrogen atom abstract hydrogen from methyl-cyclohexane substrate mainly to form methane and hydrogen gas.

Benzene formation:- Benzene formation originates from the C-C addition of 1,3-butadiene and vinyl radical and subsequent ring formation and hydrogen loss. This is because of the excess presence of vinyl and 1,3-butadiene in the species pool as both of these are formed preferably in the primary decomposition of methyl-cyclohexane.
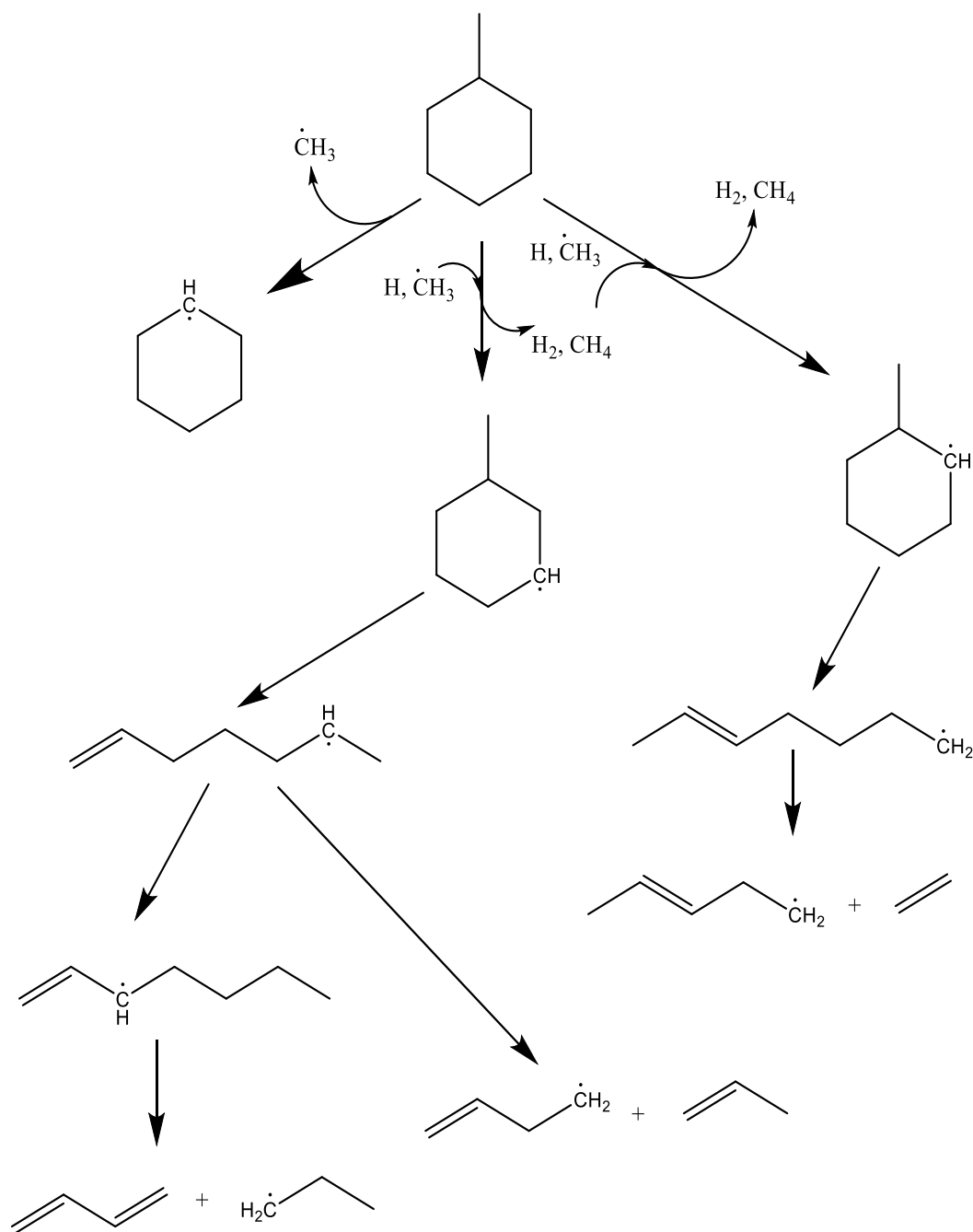
Figure 5.26: Dominant pathways of methyl-cyclohexane pyrolysis at 1123K, 1013 mbara pressure at 15 cm reactor length, 16% conversion, LCT model

5.4. Conclusions

An ab-initio based elementary reaction mechanism has been generated automatically using Genesys for the pyrolysis of methyl-cyclohexane. It has been validated with experimental data from the SVUV-PIMS apparatus at Hefei, China. The conditions were 1000-1300K,

0.007-0.2 s residence time, 1 SLM gas feed flow, where the feed is 2 mol% methyl-cyclohexane and 98 mol% Argon. The predictions capture the experimental trends of major products. Rate of consumption analysis shows that methyl-cyclohexane is consumed mainly by homolytic scission of methyl groups and almost equally strongly by hydrogen abstraction by H-atoms at the 3-yl, followed by 2-yl position. In this chapter, it is realized that a high pressure limit model, elementary in nature with ab-initio based kinetics with no fine-tuning of parameters, generated automatically using an automatic mechanism generation tool can compete well with literature optimized/ lumped/ global/ pressure dependent models. The LCT model generated by Genesys makes reasonable predictions of methyl-cyclohexane pyrolysis at 1013, 200 and 40 mbara pressures. As a path forward, benzene predictions need to be improved. For methyl-cyclohexane pyrolysis, all the models seem to underpredict benzene, so new routes need to be evaluated.

5.5. References

1.Djokic, M. R.; Dijkmans, T.; Yildiz, G.; Prins, W.; Van Geem, K. M., Quantitative analysis of crude and stabilized bio-oils by comprehensive two-dimensional gas-chromatography. *Journal of Chromatography A* **2012,** 1257, 131-140.

2.Vargas, D. C.; Alvarez, M. B.; Portilla, A. H.; Van Geem, K. M.; Streitwieser, D. A., Kinetic Study of the Thermal and Catalytic Cracking of Waste Motor Oil to Diesel-like Fuels. *Energy & Fuels* **2016,** 30, (11), 9712-9720.

3.Vandewiele, N. M.; Magoon, G. R.; Van Geem, K. M.; Reyniers, M. F.; Green, W. H.; Marin, G. B., Kinetic Modeling of Jet Propellant-10 Pyrolysis. *Energy & Fuels* **2015,** 29, (1), 413-427.

4.Vandewiele, N. M.; Magoon, G. R.; Van Geem, K. M.; Reyniers, M. F.; Green, W. H.; Marin, G. B., Experimental and Modeling Study on the Thermal Decomposition of Jet Propellant-10. *Energy & Fuels* **2014,** 28, (8), 4976-4985.

5.Gascoin, N.; Abraham, G.; Gillard, P., Synthetic and jet fuels pyrolysis for cooling and combustion applications. *Journal of Analytical and Applied Pyrolysis* **2010,** 89, (2), 294-306.

6.Yang, Q. C.; Chetehouna, K.; Gascoin, N.; Bao, W., Experimental study on combustion modes and thrust performance of a staged-combustor of the scramjet with dual-strut. *Acta Astronautica* **2016,** 122, 28-34.

7.Pyl, S. P.; Schietekat, C. M.; Reyniers, M. F.; Abhari, R.; Marin, G. B.; Van Geem, K. M., Biomass to olefins: Cracking of renewable naphtha. *Chemical Engineering Journal* **2011,** 176, 178-187.

8.Buda, F.; Bounaceur, R.; Warth, V.; Glaude, P.; Fournet, R.; Battin-Leclerc, F., Progress toward a unified detailed kinetic model for the autoignition of alkanes from C-4 to C-10 between 600 and 1200 K. *Combustion and Flame* **2005,** 142, (1-2), 170-186.

9.Buda, F.; Glaude, P. A.; Battin-Leclerc, F.; Porter, R.; Hughes, K. J.; Griffiths, J. F., Use of detailed kinetic mechanisms for the prediction of autoignitions. *Journal of Loss Prevention in the Process Industries* **2006,** 19, (2-3), 227-232.

10.Sirjean, B.; Buda, F.; Hakka, H.; Glaude, P. A.; Fournet, R.; Warth, V.; Battin-Leclerc, F.; Ruiz-Lopez, M., The autoignition of cyclopentane and cyclohexane in a shock tube. *Proceedings of the Combustion Institute* **2007,** 31, 277-284.

11.Serinyel, Z.; Herbinet, O.; Frottier, O.; Dirrenberger, P.; Warth, V.; Glaude, P. A.; Battin-Leclerc, F., An experimental and modeling study of the low- and high-temperature oxidation of cyclohexane. *Combustion and Flame* **2013,** 160, (11), 2319-2332.

12. Guthrie, F., Sabourin, *Gasoline and Diesel: Fuel Survey*. 2003.

13. Grumman, N., Diesel Fuel Oils. **2003**.

14.Brown, T. C.; King, K. D., Bery low-pressure pyrolysis (VLPP) of methyl-cyclopentanes and ethynyl-cyclopentanes and cyclohexanes. *International Journal of Chemical Kinetics* **1989,** 21, (4), 251-266.

15.Zeppieri, S.; Brezinsky, K.; Glassman, I., Pyrolysis studies of methylcyclohexane and oxidation studies of methylcyclohexane and methylcyclohexane/toluene blends. *Combustion and Flame* **1997,** 108, (3), 266-286.

16.Pitz, W. J.; Naik, C. V.; Mhaolduin, T. N.; Westbrook, C. K.; Curran, H. J.; Orme, J. P.; Simmie, J. M., Modeling and experimental investigation of methylcyclohexane ignition in a rapid compression machine. *Proceedings of the Combustion Institute* **2007,** 31, 267-275.

17.Mittal, G.; Sung, C. J., Autoignition of methylcyclohexane at elevated pressures. *Combustion and Flame* **2009,** 156, (9), 1852-1855.

18.Orme, J. P.; Curran, H. J.; Simmie, J. M., Experimental and modeling study of methyl cyclohexane pyrolysis and oxidation. *Journal of Physical Chemistry A* **2006,** 110, (1), 114-131.

19.Vasu, S. S.; Davidson, D. F.; Hanson, R. K., OH time-histories during oxidation of n-heptane and methylcyclohexane at high pressures and temperatures. *Combustion and Flame* **2009,** 156, (4), 736-749.

20.Bounaceur, R.; Burkle-Vitzthum, V.; Marquaire, P. M.; Fusetti, L., Mechanistic modeling of the thermal cracking of methylcyclohexane near atmospheric pressure, from 523 to 1273 K: Identification of aromatization pathways. *Journal of Analytical and Applied Pyrolysis* **2013,** 103, 240-254.

21.Wang, Z. D.; Ye, L. L.; Yuan, W. H.; Zhang, L. D.; Wang, Y. Z.; Cheng, Z. J.; Zhang, F.; Qi, F., Experimental and kinetic modeling study on methylcyclohexane pyrolysis and combustion. *Combustion and Flame* **2014,** 161, (1), 84-100.

22. H. Wang, E. D., B. Sirjean, D. A. Sheen, R. Tango, A. Violi, J. Y. W. Lai, F. N. Egolfopoulos, D. F. Davidson, R. K. Hanson, C. T. Bowman, C. K. Law, W. Tsang, N. P. Cernansky, D. L. Miller, R.   P.   Lindstedt   JetSurF,   2.0; http://web.stanford.edu/group/haiwanglab/JetSurF/JetSurF2.0/index.html, 2010.

23. Orme, Curran and Simmie, Experimental and Modeling Study of Methyl Cyclohexane Pyrolysis and Oxidation, J. Phys Chem A, 2006, 110(1), 114-131.

24. Sirjean, B.; Glaude, P. A.; Ruiz-Lopez, M. F.; Fournet, R., Detailed kinetic study of the ring opening of cycloalkanes by CBS-QB3 calculations. Journal of Physical Chemistry A 2006, 110, (46), 12693-12704.

6

Microkinetic modeling of ethyl-cyclohexane pyrolysis

In this chapter, a mechanism is generated for the pyrolysis of ethyl-cyclohexane using the automatic mechanism generator tool, "Genesys". The mechanism is composed of high pressure limit elementary reactions whose kinetics originate from ab-initio calculations without any alterations. The mechanism is validated using the SVUV-PIMS experimental data of 2015 from Zhandong Wang et al. at Hefei, China, in which a feed of 2 mol% ethyl-cyclohexane in Argon is continuously fed to a tubular reactor maintained at a maximum temperature of 1000 to 1300K at pressures 1013, 200, 40 mbara, respectively. One objective of this chapter is to check if an automatically generated elementary reaction model with uniformly ab-initio based unaltered kinetics can predict ethyl-cyclohexane pyrolysis well compared to literature optimized/ tuned/ global/ lumped models. Two models from literature were compared – Hefei (2015) and JetSurF 2.0 (2010). Another objective is to check if the high pressure limit model can predict species concentrations at different pressures. Overall, the Genesys model (LCT model) allows a reasonable prediction of the product yields compared to other models, and the best prediction for feed conversion at different pressures. The JetSurF model performs the worst, while the Hefei model performs as well as the LCT model. Reaction path analysis shows the dominant pathways toward major products. Additionally, experimental trends of ethyl-cyclohexane are compared with those of methyl-cyclohexane, cyclohexane and cyclopentane to understand the effect of substituent and ring size. The experimental trends of feeds having the cyclohexane moiety are qualitatively similar and quantitatively closer to each other than those of cyclopentane trends.

6.1. Introduction

Petrochemical feedstocks and derived liquid fuels are complex mixtures composed of various molecule classes such as paraffins, olefins, naphthenes and aromatics. Whether used for pyrolytic or combustion applications, the thermal decomposition chemistry of cyclic compounds plays a central role in the prediction of product yields from biomass fast pyrolysis[1], waste fractions[2], scram jet modelling[3-6], naphtha steam cracking[7] and undesired auto ignition of gasoline[8-10]. Therefore the pyrolysis chemistry of hydrocarbons has been the subject of research for many years. While the gas-phase chemistry of open-chain hydrocarbons is well understood, the knowledge of the pyrolysis chemistry of cyclic hydrocarbons is less understood[10, 11]. This is even true for the simplest cycloalkanes, such as cyclopentane and cyclohexane. In chapters 4 and 5, the pyrolysis of unsubstituted cyclopentane and cyclohexane has been discussed. In chapter 6, the pyrolysis of the simplest alkylated cyclohexane, methyl-cyclohexane was studied. Pyrolysis of ethyl-cyclohexane is the subject of this chapter.

Recently, pyrolysis of cycloalkanes have received increasing attention because of their high concentrations in real-life feedstocks such as North American diesel fuel, where their content is 20-40%[12, 13]. Diesel itself has a higher carbon number range than C5 or C6. Hence, the naphthenic content of such fuels is more likely to contain methyl- and ethyl-cyclohexanes rather than unsubstituted cyclopentane and cyclohexane. Ethyl-cyclohexane is an important component of fuel surrogate for naphtha, especially naphthenic naphtha whose carbon number range is C5-C9. Naphtha is one of the ideal liquid feedstocks for pyrolysis processes to yield ethylene, propylene and other lower olefins, which themselves are raw materials for poly-olefin industry as well as other chemicals and pharmaceuticals. A naphtha feed contains many compounds, sometimes hundreds, hence making it difficult to understand its detailed pyrolytic mechanism. Hence, usually a surrogate/ representative molecule is studied experimentally and theoretically to grasp its chemistry. In this respect, a detailed kinetic modeling study of ethyl-cyclohexane would help to understand the pyrolytic behavior of the naphthenic C_8-cut of naphtha, in turn extending our knowledge of pyrolysis chemistry.

There have been some prior studies on ethyl-cyclohexane pyrolysis – like that of low and intermediate temperature oxidation in a jet stirred reactor by Husson et al[14], ignition studies

on ethyl-cyclohexane and 2 isomers by Kang et al[15], shock tube ignition delay times at pressures 10-50 atm by Vanderover and Oehlschlaeger[16], and Tian et al[17, 18]. These studies focus on oxidation and combustion of ethyl-cyclohexane while none focus on non-oxidative pyrolysis. The first experimental study to conduct a non-oxidative pyrolysis of ethyl-cyclohexane was by Zhandong Wang et al[19], in Hefei, China, in which ethyl-cyclohexane is the feed in their SVUV-PIMS (Synchrotron Vacuum Ultra Violet - Photo Ionization Mass Spectrometry) setup. They fed 2 mol% of ethyl-cyclohexane in Argon to the reactor maintained at a maximum temperature of 1000 to 1300K at 1013, 200 and 40 mbara, respectively. They also developed a model to calculate the product spectrum.

In this chapter, a mechanism is generated for the pyrolysis of ethyl-cyclohexane, using the automatic mechanism generator tool, "Genesys"[20]. The mechanism is composed of high pressure limit elementary reactions whose kinetics originate from ab-initio calculations without any alterations. The mechanism is validated using the SVUV-PIMS experimental data from Zhandong Wang et al. at Hefei, China[19], in which a feed of 2 mol% ethyl-cyclohexane in Argon is continuously fed to a tubular reactor maintained at a maximum temperature of 1000 to 1300K at 1013, 200 and 40 mbara, respectively. One objective of this chapter is to check if an automatically generated elementary reaction model with uniformly ab-initio based unaltered kinetics can predict ethyl-cyclohexane pyrolysis well compared to literature optimized/ tuned/ global/ lumped models. Two models from literature were compared – Hefei[19] and JetSurF 2.0[21]. Finally, the most important reaction pathways are analyzed for pyrolysis conditions. Another objective is to verify if the high pressure limit model can predict species concentrations at different pressures. A final objective would be to observe for any trend in the experimental data of pyrolysis of cyclohexane[22, 23], methyl-cyclohexane[24], ethyl-cyclohexane[19] and cyclopentane[25].

6.2. Methodology

6.2.1. Experimental setup and procedure

The experiments were performed by Wang et al[19] in the National Synchrotron Radiation Laboratory, Hefei, China (referred to simply has "Hefei" henceforth). The reactor is a

furnace made of sintered alumina, with a 6.8mm inner diameter, 229 mm length, mounted in a pressure chamber. The pressure is controlled by a MKS throat valve at 1013, 200 and 40 mbara, respectively. The heated zone is 150 mm long. Ethyl-cyclohexane was procured from Aladdin, Shanghai with 99 wt% purity. It was vaporized using Argon to create a mixture of 2 mol% ethyl-cyclohexane and 98 mol% Argon. The temperature profiles showed a maxima in the heated zone, and the maximum temperatures achieved were in the range 1000K-1300K. The feed flow rate was maintained at 1 Nl/min at 273 K corresponding to nominal residence times in the range 0.007 – 0.2s. Mole fractions of pyrolysis products were calculated from the photo-ionization cross sections, which are available in literature. For those molecules where PICs photo-ionization cross sections (PICs) are not available, they are estimated from similar molecules. The setup is described below.
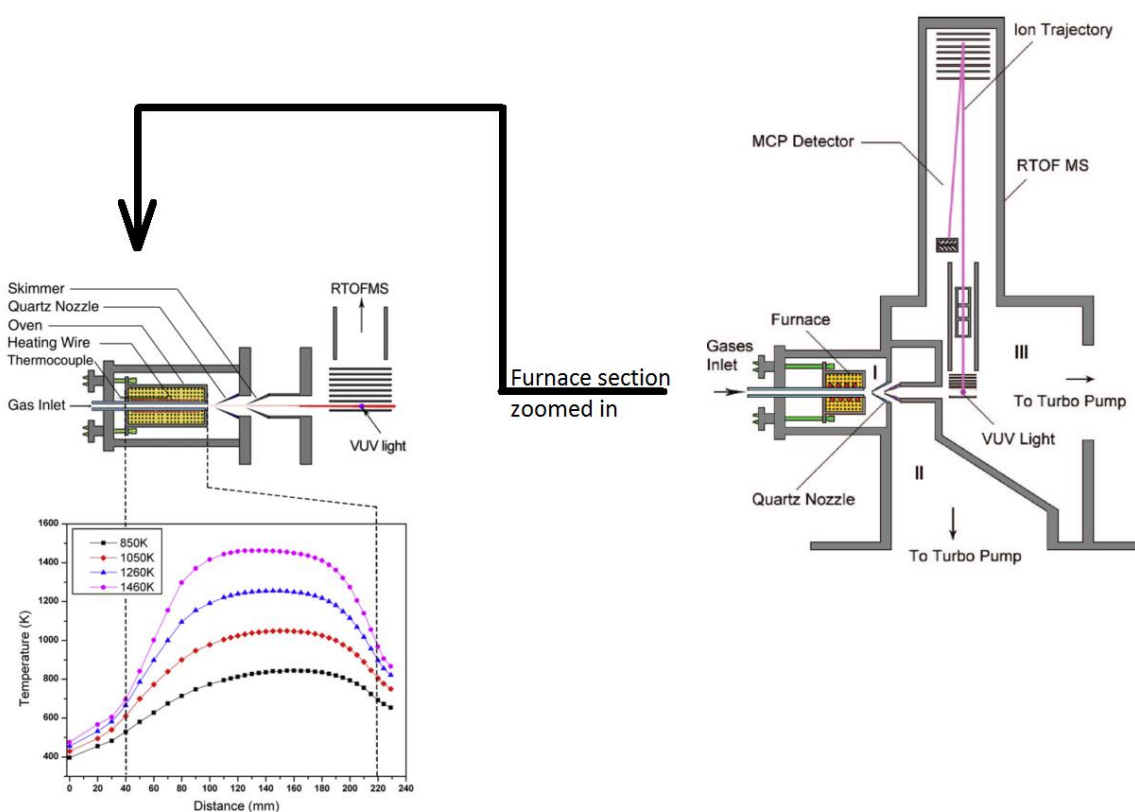
Figure 6.1: Schematic diagram of synchrotron vacuum ultra-violet photo-ionization mass spectrometer (SVUV-PIMS) at Hefei[28]

As shown in Figure 6.1, the experimental setup consists of three sections - a pyrolysis chamber with a high temperature furnace (I), a differentially pumped chamber with a

molecular-beam sampling system (II) and a photoionization chamber with a reflectron time-of-flight mass spectrometer (III). The differential chamber is pumped by a turbomolecular pump at speed 1500 L/s, while the photoionization chamber is pumped by a turbomolecular pump at speed 600 L/s. A quartz cone-like nozzle with a 500 μm orifice at the tip is used to sample the pyrolysis species. The sampled species form a molecular beam in the differentially pumped chamber and pass on to the photo-ionization chamber through a nickel skimmer. Then the molecular beam is crossed by the tunable synchrotron VUV light in the ionization region. Depending on the photon energy, the species are ionized. If the photon energy is too low, the species would be ionized. If it is too high, then there would be fragmentation of the species. These 2 thresholds are specific to each species. So, the photon energy is maintained in the boundary of these 2 overall thresholds for all the species. This is done through initial trials for any new system. For ethyl-cyclohexane system, the typical range of photon energy is 9.5 to 11.8 eV. Once the species are ionized, they are drawn out of the photo-ionization region by a pulse-extraction field triggered by a pulse generator. The ions are then detected by a micro-channel plate detector. The ion signal is amplified and recorded by a multiscaler. For a given pyrolysis species, by varying the photon energy, different relative photo-ion intensities can be obtained for a specific pyrolysis temperature set point, as shown in Figure 6.2. This is called the photo-ionization efficiency spectrum.
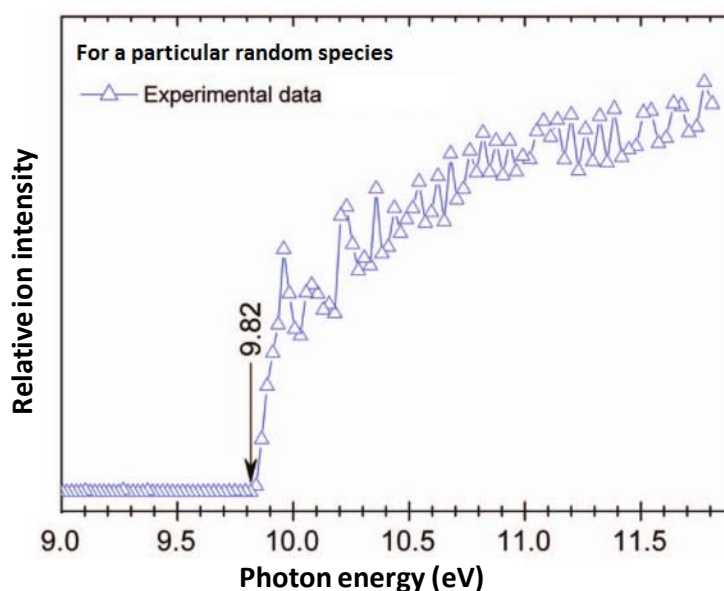
Figure 6.2: Photo-ionization efficiency (PIE) spectrum for a random species[28]

The PIE spectrum contains the precise information of the ionization energies of the particular species. In order to understand the source of error, there is a cooling effect when the molecular beam enters the photo-ionization chamber. The error due to this on the PIE spectrum positioning is within 0.05 eV. Figure 6.2 also depicts the onset of ionization for a particular species at 9.82 eV. This is called the photo-ionization cross section (PIC). This data is available in standard databases in literature for various species. Figure 6.3 shows how the mass spectrum of the pyrolysis effluent sample changes with respect to photon energy. The X-axis shows the molecular weight of the species, and the Y-axis, the relative intensity.
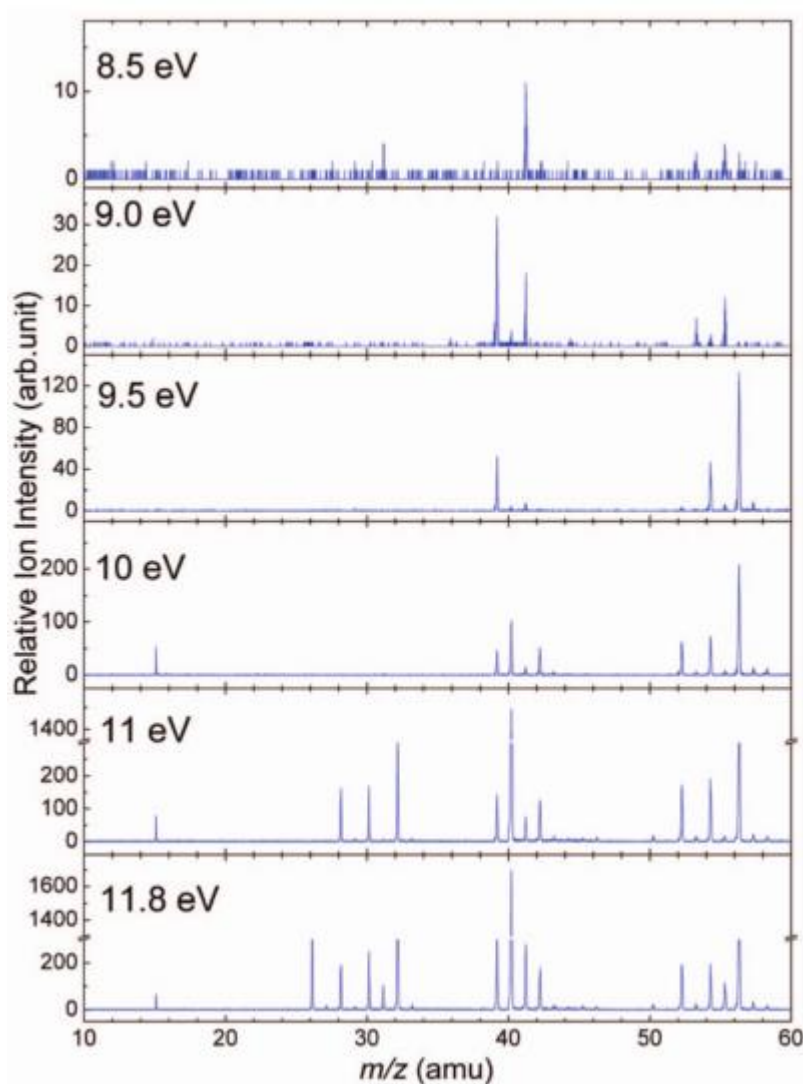
Figure 6.3: Mass spectra at various photon energies, but at constant pyrolysis conditions[28]

In Figure 6.3, only the photon energy is varied. All the other operating parameters of pyrolysis remain the same, like temperature, pressure, flow rates. However, in order to calculate the mole fractions of the pyrolysis species for different reactor temperature set points, we would ideally need to freeze the photon energy at a particular value (typically at the higher threshold value in order to obtain high intensities of photo-ions) and vary the temperature to obtain the mass spectra. This is shown in Figure 6.4.
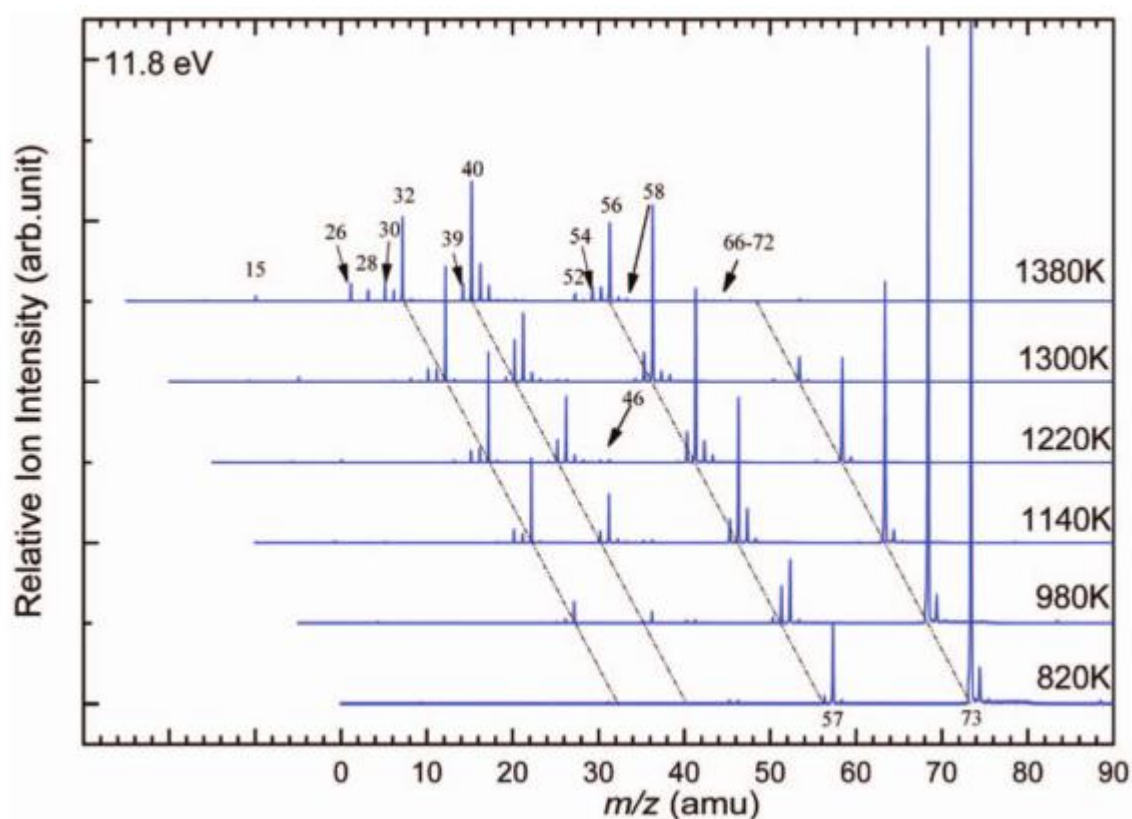
Figure 6.4: Mass spectra at various pyrolysis temperatures, at 11.8 eV photon energy[28]
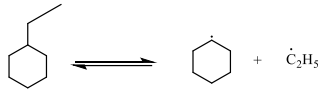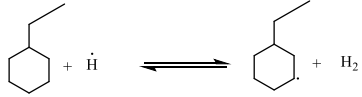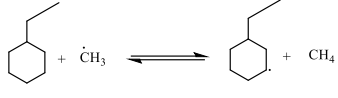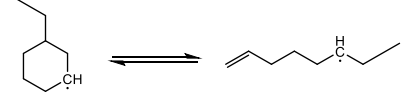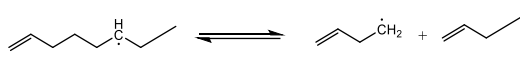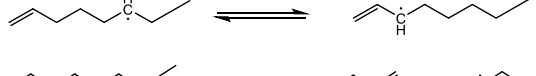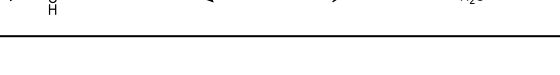
Figure 6.4 shows the mass spectra at various pyrolysis temperatures, at a fixed photon energy of 11.8 eV. The intensities of the spectra are normalized in order to obtain the mole fraction of each species as a function of temperature. Based on the errors expected in the three chambers – furnace chamber, differential pumping chamber and the photo-ionization chamber, the experimental error expected on mole fraction of a species is up to 10%.

6.2.2. Kinetic model generation

6.2.2.1 CBS-QB3 computation of rate coefficients

Genesys[20] was used to automatically generate the reaction mechanism for the pyrolysis of methyl-cyclohexane. The input reaction families for Genesys were the same as those given in Table 4.1 of chapter 4. The primary decomposition mechanism of ethyl-cyclohexane involves reactions such as scission of ethyl branch to give cyclohexyl radical. The mechanism of the subsequent ring opening of cyclohexyl was already present in the cyclohexane pyrolysis sub-mechanism. Ethyl-cyclohexane conversion also takes place dominantly by hydrogen abstractions at various carbon sites of ethyl-cyclohexane to form ethyl-cyclohexyl radical. Subsequent ring opening of the cyclohexyl moiety forms an open chain alkenyl radical. This could subsequently undergo a C-C beta scission reaction or an intra-molecular hydrogen abstraction reaction (radical isomerization) to form an allylic alkenyl radical. The source of some of the kinetics was the CBS-QB3 values calculated by Zhandong Wang et al[19] (elaborated in Table 6.1) for the primary decomposition reactions of ethyl-cyclohexane, using the Gaussian 09 suite of programs[26]. ChemKin-PRO[27] was used to do a reaction path analysis to find the dominant routes to major products. The rate coefficients for the most important reactions involved in the pyrolysis of ethyl-cyclohexane for the 3 models are shown in Table 6.1.

Table 6.1: Most important reactions in the pyrolysis of ethyl-cyclohexane - comparison of rate coefficients of 3 models – LCT, Hefei, JetSurF

#	**Reaction** k(at T=1050K), units in cm3, mol, s	k(LCT)	k(Hefei)	k(JetSurF)
	Elementary reaction			
R1	1-propyl=C2H4+CH3	2.54E+07 (origin=LCT)	1.31E+07	9.57E+06
R2	C2H4+H=ethyl	6.21E+12 (origin=LCT)	5.17E+12	1.88E+13
R3	C3H6+H=1-propyl	4.91E+12 (origin=LCT)	2.8E+12	2.79E+12
R4		2.91E-01 (origin=Hefei)	2.91E-01	3.77E-02
R5		2.41E+12 (origin=Hefei)	2.41E+12	2.74E+12
R6		2.26E+09 (origin=Hefei)	2.26E+09	2.26E+09
R7		2.07E+12 (origin=Hefei)	2.07E+12	2.24E+12
R8		1.41E+09 (origin=Hefei)	1.41E+09	1.41E+09
R9		5.20E+06 (origin=LCT)	5.20E+06	1.20E+07
R10		3.65E+07 (origin=LCT)	3.65E+07	3.65E+07
R11		3.19E+07 (origin=LCT)	3.19E+07	3.19E+07
R12		6.53E+06 (origin=LCT)	6.53E+06	6.53E+06

6.3. Results and discussion

6.3.1 Experimental data and model analysis

Experimental results of the main products of ethyl-cyclohexane pyrolysis are discussed here. Also discussed are the 3 model trends- LCT, Hefei and JetSurF. Figure 6.5 shows the conversion of ethyl-cyclohexane in Hefei experiments at 1013 and 200 mbara, and the 3 model predictions for the same. The experiment at 1013 mbara realizes high ethyl-cyclohexane conversions, reaching a maximum of 90% at 1200 K. At 200 mbara, the

conversion is about 50% at the same temperature. This trend is understandable because the low gas concentrations in the low pressure experiments will lead to low reaction rates, and thereby conversion. It can be seen that the conversion predictions of the LCT model are better than the other models. LCT is followed by Hefei, followed by JetSurF, which over-predicts it.
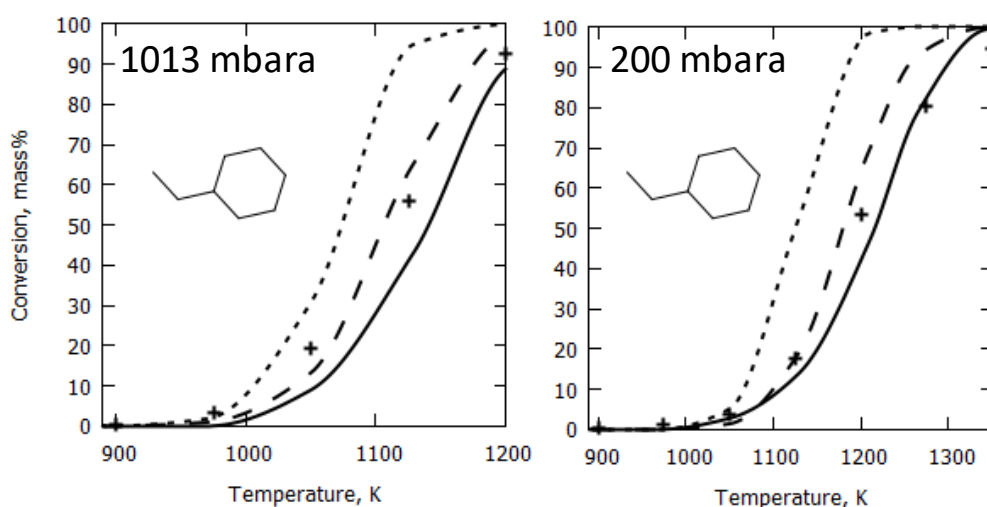
Figure 6.5: Hefei experimental trends vs. model predictions for ethyl-cyclohexane pyrolysis (ECH) feed conversions at 1013 and 200 mbara. X-axis=temperature, K, Y-axis=ethyl-cyclohexane (ECH) conversion%. Legends: ✚ Hefei experiment, ——— LCT, − − − − Hefei, ········ JetSurF 2.0

Figure 6.6 shows the Rate of Production Analysis for the conversion of ethyl-cyclohexane using the LCT model. It shows that hydrogen abstraction by H-atom at the 3-yl position is the most dominant route, followed by the homolytic scission of the ethyl branch to give cyclohexyl, followed by the hydrogen abstraction by methyl radical at the 3-yl position.
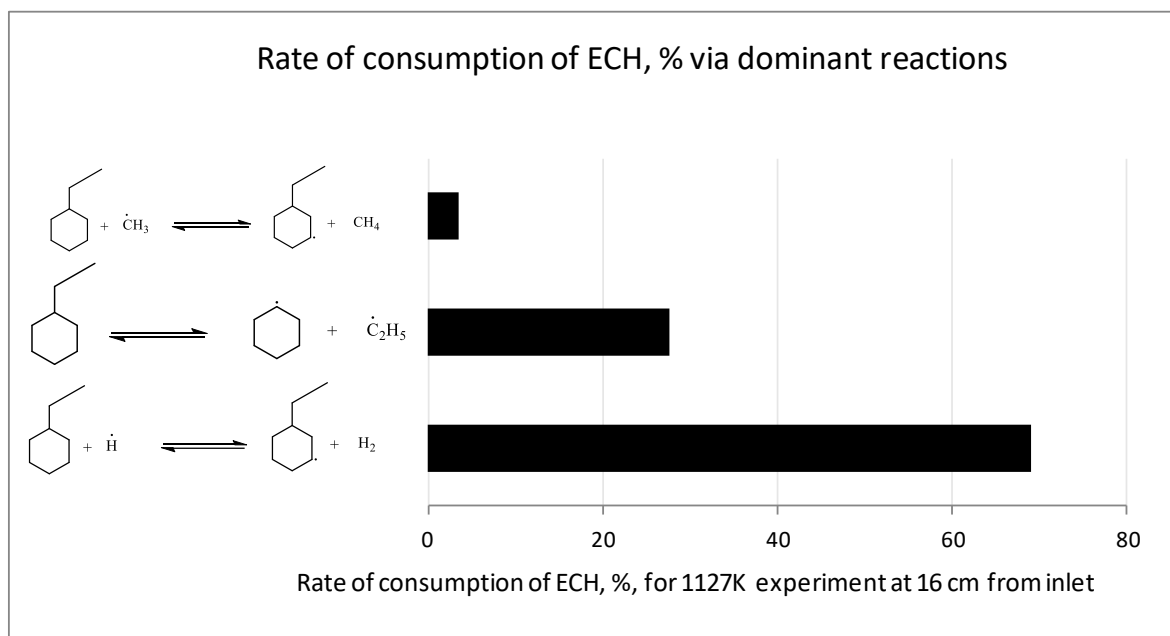
Figure 6.6: Rate of Production analysis, 1123K experiment at 16 cm from reactor inlet, 1013 mbara pressure - dominant routes for ethyl-cyclohexane (ECH) consumption using LCT model
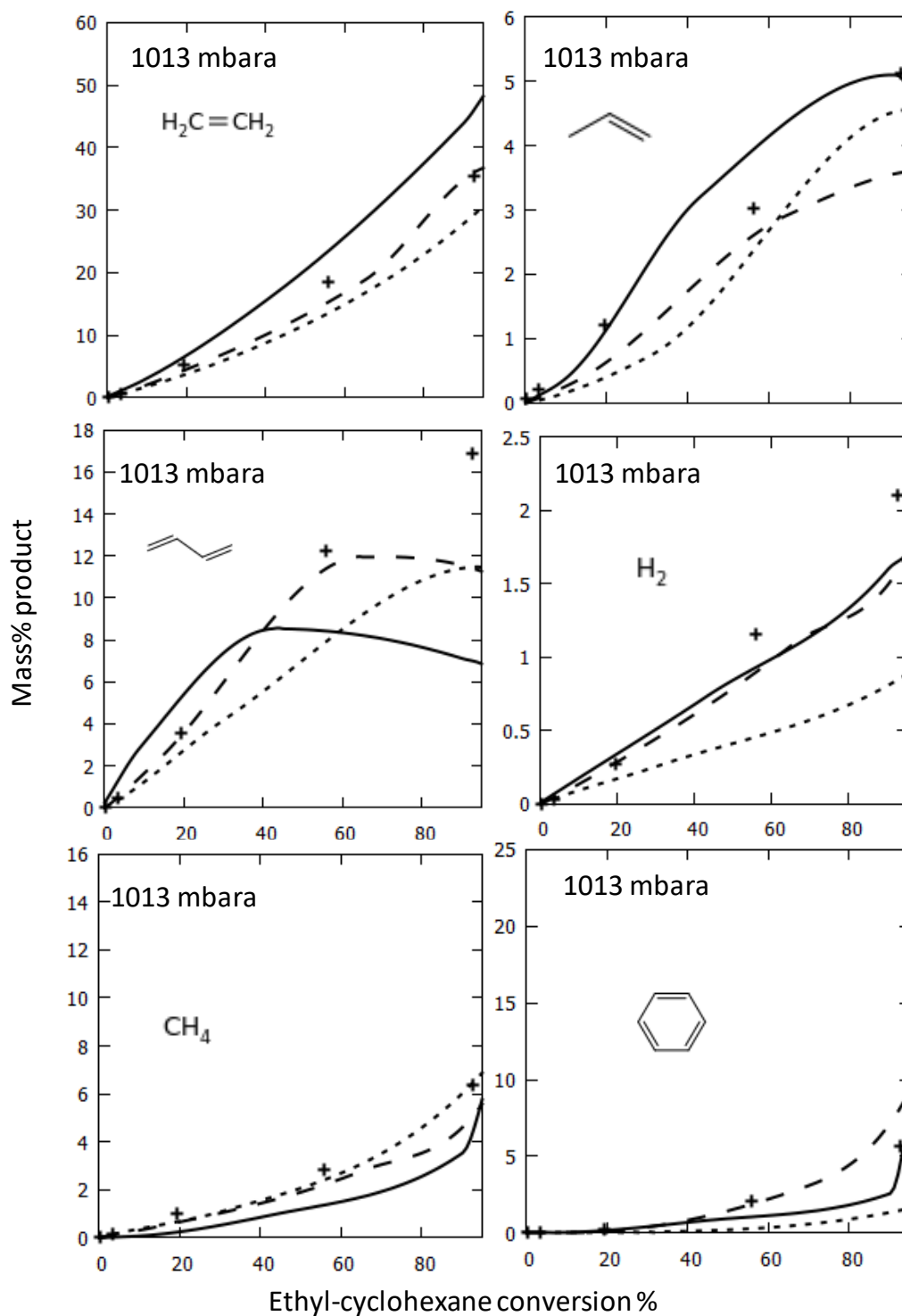
Figure 6.7: Hefei experimental trends vs. model predictions at 1013 mbara, X-axis=ethyl-cyclohexane conversion %, Y-axis=mass% of product, Legends: **✚** **Hefei experiment,** ——— **LCT,** − − − − **Hefei,** ········· **JetSurF 2.0**

Figure 6.7 shows the 1013 mbara experiment plot of product mass% vs. ethyl-cyclohexane feed conversion. It can be seen that the product yield trend of ethylene is predicted best by Hefei model, followed by LCT model and then by JetSurF, while for propylene, LCT is the best, followed by Hefei and then by JetSurF. Butadiene predictions of JetSurF seem to be better than Hefei and LCT models, while the hydrogen is best predicted by both LCT and Hefei and worst by JetSurF. Methane is best predicted by JetSurF, followed by Hefei and then by LCT, while for benzene, the predictions of LCT are better than that of Hefei and JetSurF.

Figure 6.8 shows the product trends for the 200 mbara experiment. The LCT model captures the monotonic trend of ethylene the best compared to the other 2 models, especially at lower conversions. Propylene trend is overpredicted by LCT though qualitatively it is the best model for it. For butadiene and hydrogen trends, LCT is next to Hefei and better than JetSurF. Methane is predicted equally well by all the models while LCT model underpredicts benzene, in line with the previous chapter.
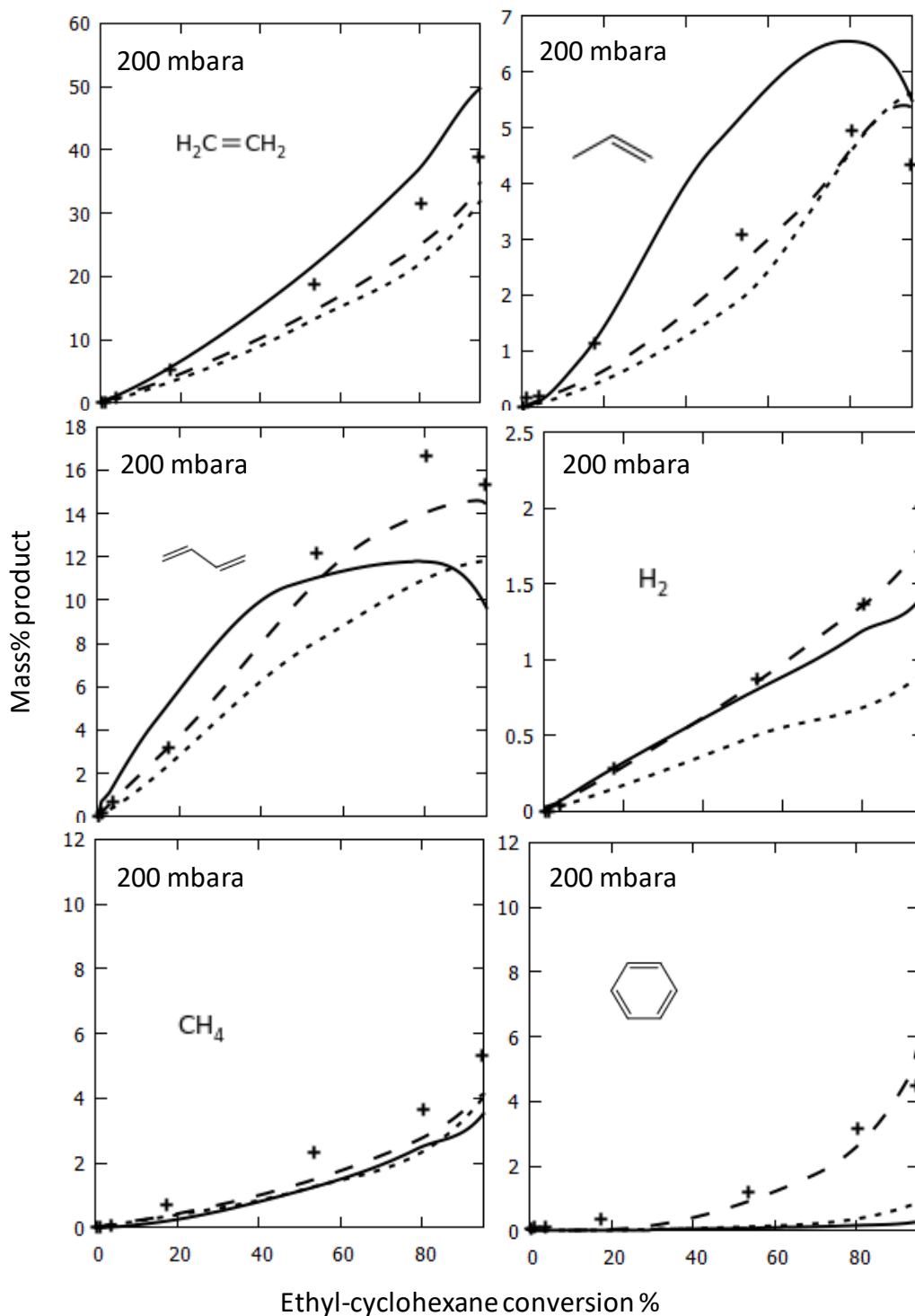
Figure 6.8: Hefei experimental trends vs. model predictions at 200 mbara, X-axis=ethyl-cyclohexane conversion %, Y-axis=mass% of product, Legends: + Hefei experiment, ——— LCT, − − − − Hefei, ·········· JetSurF 2.0

6.3.2 Effect of pressure, ring size and substituent

Figure 6.9 shows that the conversion of ethyl-cyclohexane is influenced by pressure. In 1013 mbara experiment, ethyl-cyclohexane achieves almost 90% conversion at 1200K. In the 200 mbara experiment, about 50% conversion is achieved at the same temperature. Also shown are the experimental data of methyl-cyclohexane at 1013 mbara and 200 mbara and cyclohexane experiment of Hefei at 1013 mbara. The Hefei experiments were conducted under the same conditions for cyclohexane[22], methyl-[24] and ethyl-[19] cyclohexane, respectively. Figure 6.9 shows that for the same temperature and pressure, ethyl-cyclohexane conversions are higher than that of methyl-cyclohexane, which itself is higher than that of cyclohexane. This could be understandable since the bigger the molecule, the more sites would available for conversion. Unsubstituted cylohexane would have limited routes of conversion compared to substituted cyclohexane moiety.

Figure 6.10 shows the experimental product mass% of pyrolysis plotted against feed conversion (where feed could be cyclohexane, methyl-cyclohexane or ethyl-cyclohexane). With respect to pressure, it can be seen that, like for the case of methyl-cyclohexane, ethyl-cyclohexane pyrolysis products: benzene and methane seem to depend on pressure, while ethylene, hydrogen, propylene and butadiene trends are independent of pressure.

In this particular case of ethyl-cyclohexane, it seems pressure does not play a major role for the dominant products. Probably that explains why a high pressure limit model like that of LCT holds even for pyrolysis of ethyl-cyclohexane at 200 mbara.
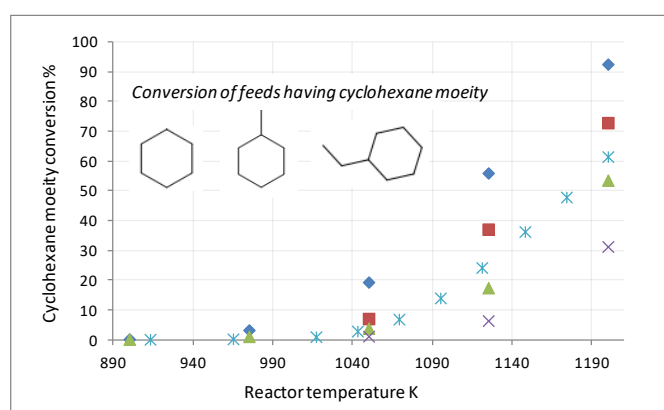
Figure 6.9: Experimental conversion of cyclohexane moiety vs. reactor temperature for 5 different experiments: ◆ **Hefei experiment on ethyl-cyclohexane pyrolysis at 1013 mbara,** ▲ **Hefei experiment on ethyl-cyclohexane pyrolysis at 200 mbara,** ■ **Hefei experiment on methyl-cyclohexane pyrolysis at 1013 mbara,** ✕ **Hefei experiment on methyl-cyclohexane pyrolysis at 200 mbara,** ✳ **Hefei experiment on cyclohexane pyrolysis at 1013 mbara**
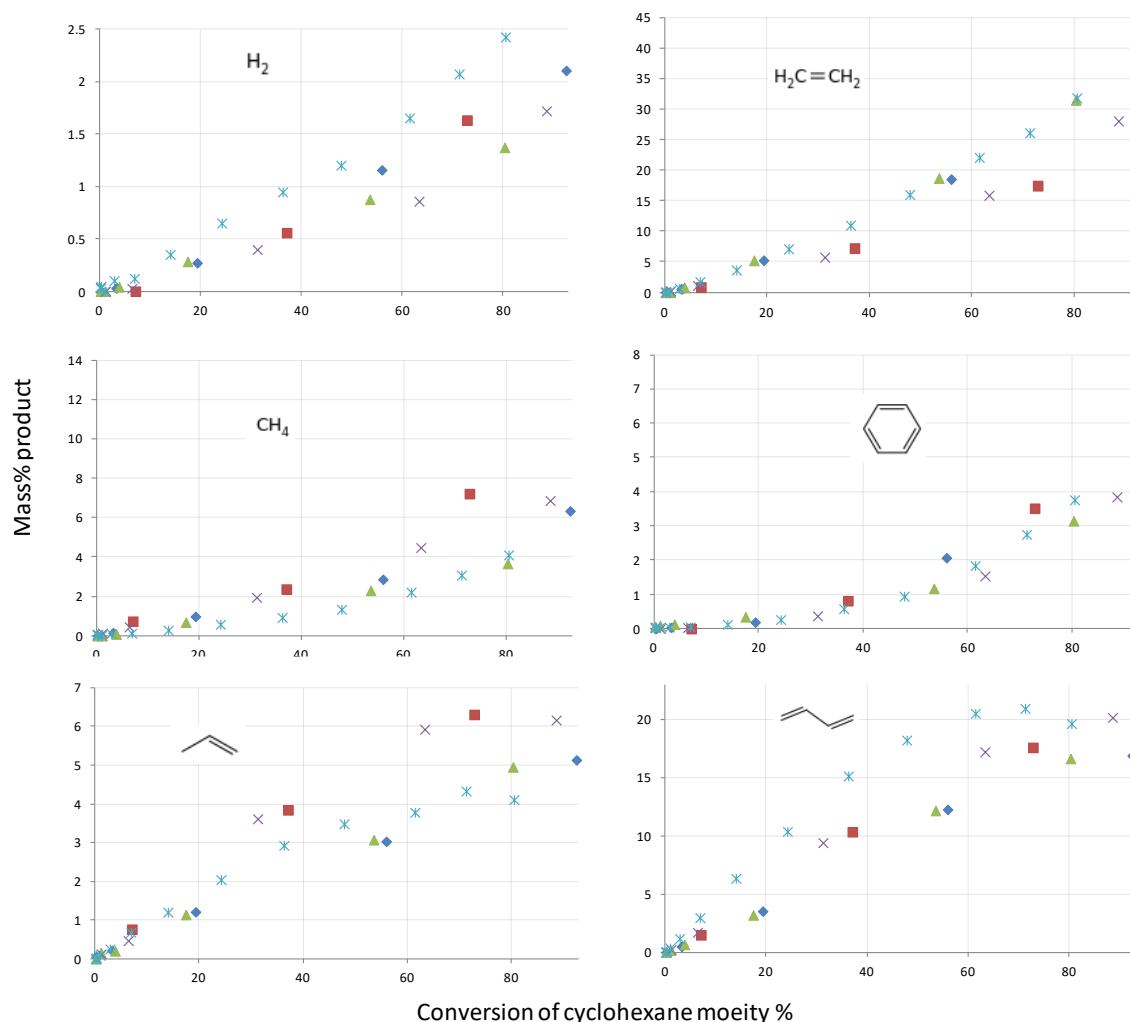
Figure 6.10: Experimental trends of mass% of pyrolysis product vs. conversion of cyclohexane moiety for 5 different experiments: ◆ **Hefei experiment on ethyl-cyclohexane pyrolysis at 1013 mbara,** ▲ **Hefei experiment on ethyl-cyclohexane pyrolysis at 200 mbara,** ■ **Hefei experiment on methyl-cyclohexane pyrolysis at 1013 mbara,** ✕ **Hefei experiment on methyl-cyclohexane pyrolysis at 200 mbara,** ✳ **Hefei experiment on cyclohexane pyrolysis at 1013 mbara**

The above discussion and plots also reveal that the experimental trends of the 1013 mbara pyrolysis experiments of cyclohexane, methyl-cyclohexane and ethyl-cyclohexane are qualitatively the same, and quantitatively close. In order to add another dimension in our understanding of the effect of ring size and laboratory data from another lab at different conditions, 2 extra trends have been added: LCT experimental data on cyclopentane

pyrolysis[25] and LCT experimental data on cyclohexane pyrolysis[23]. The LCT experiments have been conducted at 1700 mbara, somewhat close to the 1013 mbara pressure of Hefei. However, LCT experiments had undiluted feed, whereas Hefei had 2 mol% feed in 98 mol% Argon at higher temperature and lower residence time. Figure 6.11 (a) shows three Hefei experiments at 1013 mbara – with feeds ethyl-cyclohexane, methyl-cyclohexane and cyclohexane, and two LCT experiments at 1700 mbara, with cyclohexane and cyclopentane feeds. Experimental data shows that Hefei conversion trends of cyclohexane, methyl-cyclohexane and ethyl-cyclohexane are qualitatively similar and quantitatively close. As expected, the conversion of LCT cyclohexane is higher than that of Hefei for the same temperature because of higher pressure, undiluted feed and higher residence time. LCT cyclohexane conversion is higher than LCT cyclopentane conversion because comparatively, more sites are available in cyclohexane for hydrogen abstraction compared to cyclopentane. So, Figure 6.11 (a) is understandable. Figure 6.11 (b) shows that LCT model is able to capture the effect of substituent and ring size, in line with experimental observations. It would be interesting to plot these pyrolysis data as mass% product vs. feed conversion. This is shown in Figures 6.12(i) and 6.12(ii).
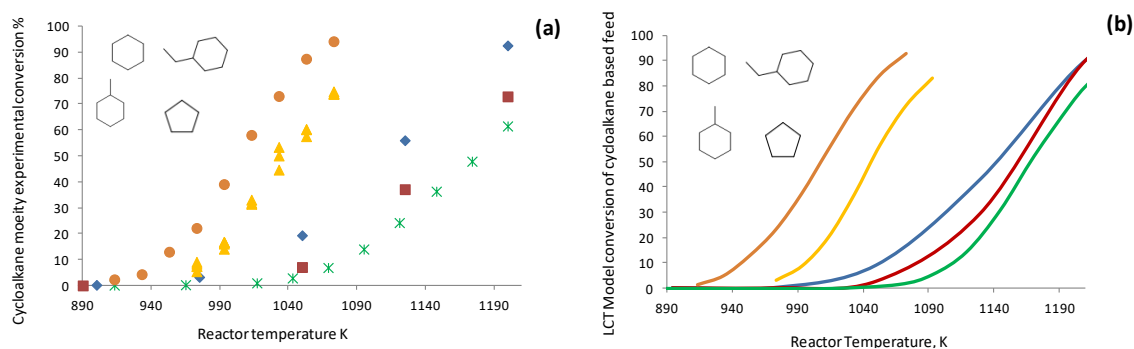
Figure 6.11: Conversion of cycloalkane moiety vs. reactor temperature for 5 different experiments: Experiment shown by dots (a), LCT model simulation shown by lines (b): ◆ —— **Hefei experiment on ethyl-cyclohexane pyrolysis at 1013 mbara,** ■ —— **Hefei experiment on methyl-cyclohexane pyrolysis at 1013 mbara,** ✳ —— **Hefei experiment on cyclohexane pyrolysis at 1013 mbara,** ● —— **LCT experiment on cyclohexane pyrolysis at 1700 mbara,** ▲ —— **LCT experiment on cyclopentane pyrolysis at 1700 mbara**
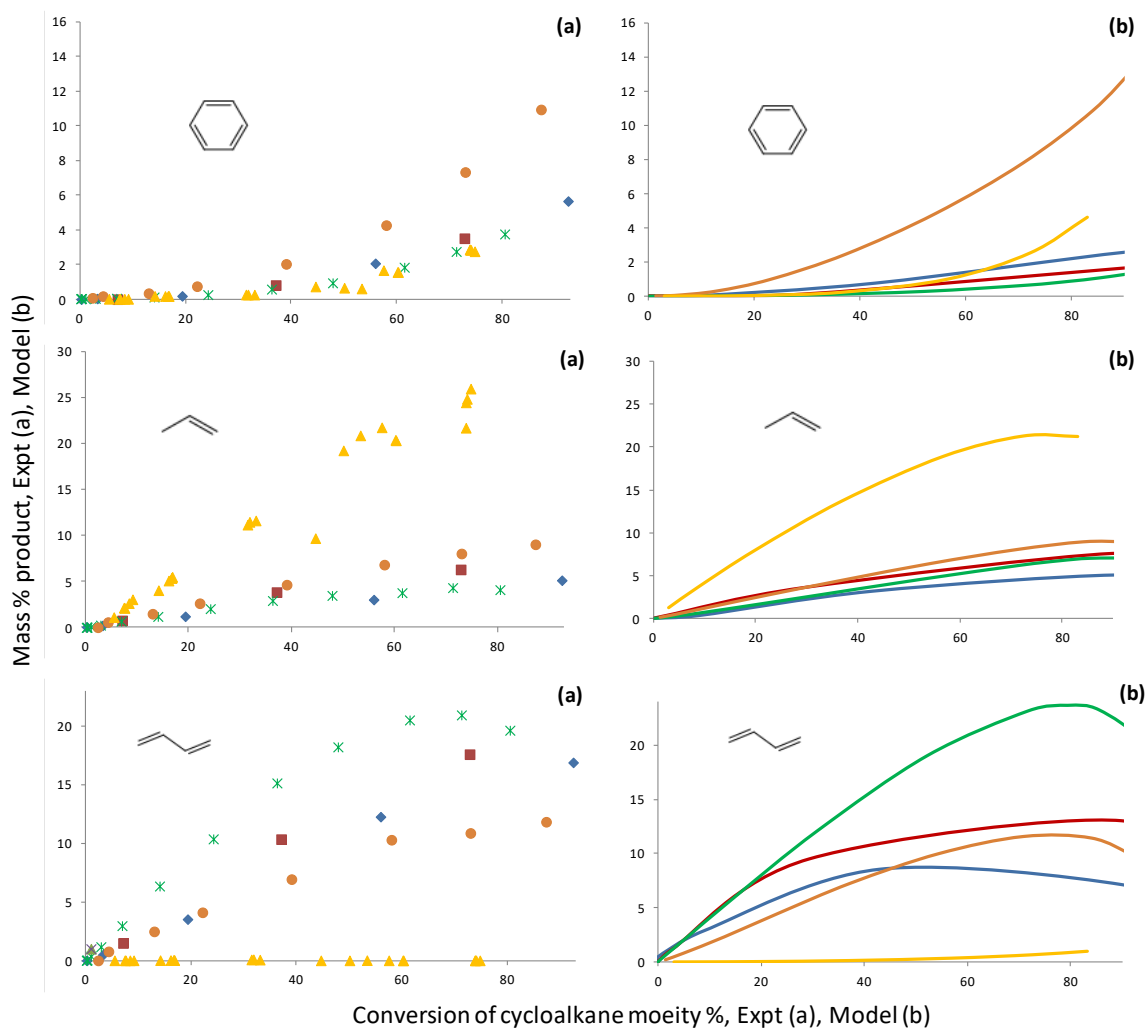
Figure 6.12(i): Product mass% vs. conversion of cycloalkane moiety% for 5 different experiments: Experiment shown by dots (a), LCT model simulation shown by lines (b): ♦ ── **Hefei experiment on ethyl-cyclohexane pyrolysis at 1013 mbara,** ■ ── **Hefei experiment on methyl-cyclohexane pyrolysis at 1013 mbara,** ✳ ── **Hefei experiment on cyclohexane pyrolysis at 1013 mbara,** ● ── **LCT experiment on cyclohexane pyrolysis at 1700 mbara,** ▲ ── **LCT experiment on cyclopentane pyrolysis at 1700 mbara**
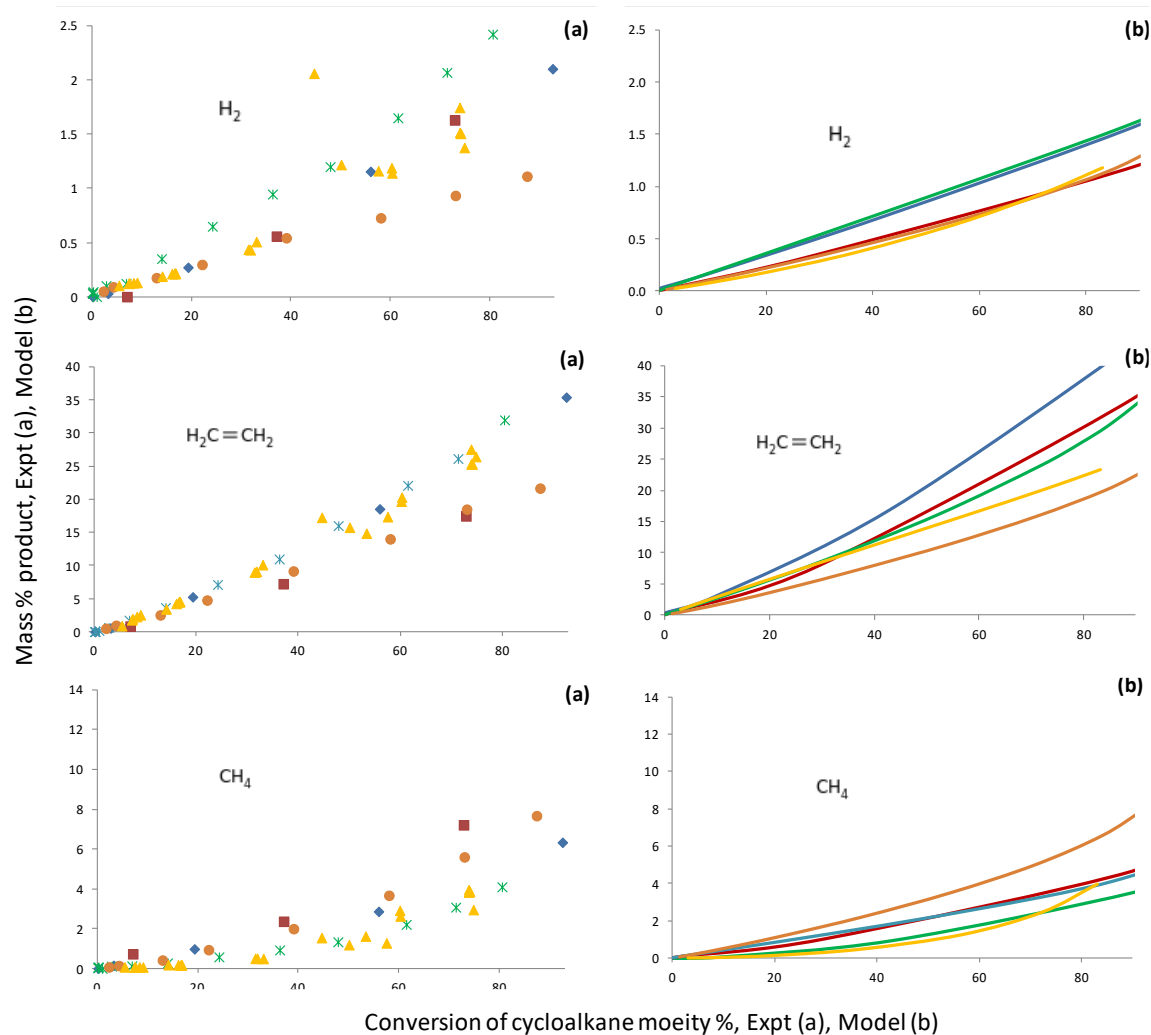
Figure 6.12(ii): Product mass% vs. conversion of cycloalkane moiety% for 5 different experiments: Experiment shown by dots (a), LCT model simulation shown by lines (b): ◆ —— Hefei experiment on ethyl-cyclohexane pyrolysis at 1013 mbara, ■ —— Hefei experiment on methyl-cyclohexane pyrolysis at 1013 mbara, ✳ —— Hefei experiment on cyclohexane pyrolysis at 1013 mbara, ● —— LCT experiment on cyclohexane pyrolysis at 1700 mbara, ▲ —— LCT experiment on cyclopentane pyrolysis at 1700 mbara

From Figures 6.12(i) and (ii), it can be seen that the Hefei experiment trends of cyclohexane, methyl-cyclohexane and ethyl-cyclohexane are qualitatively similar and quantitatively close for all the products. These are in turn close to the LCT experimental trend of cyclohexane, despite it being at a widely different operating condition. However, the trend is very different for LCT cyclopentane pyrolysis, especially for propylene and butadiene, as seen in Figure 6.12(i). Cyclopentane pyrolysis gives relatively more

propylene and less butadiene compared to cyclohexane based feeds. This discussion shows the effect of ring moiety and substituent on experimental product yield trends and model simulations for the same. From the above sections, it can be seen that the LCT model is able to capture the effect of pressure, ring size and substituent for cycloalkane feeds.

6.3.3 LCT kinetic model evaluation

As seen in Figures 6.5, 6.7, 6.8, LCT model captures the experimental trends of ethyl-cyclohexane pyrolysis at 1013 and 200 mbara, respectively, on par or better than other 2 models especially in the conversions predictions and mass% of products propylene and ethylene. The Hefei model captures the experimental trends, but the objective here was to verify if an ab-initio based elementary reaction model generated automatically can perform well compared to optimized models in literature. From that respect, the LCT model seems to be predicting sufficiently accurate. JetSurF 2.0 model is not as good as Hefei and LCT models in terms of predictions. The following section explains the routes of formation of important products according to LCT model based on Reaction Path Analysis using ChemKin-PRO. Figure 6.13 shows the dominant routes schematically.

Ethyl cyclohexane conversion routes:- According to Figure 6.6, hydrogen abstraction by H-atom at the 3-yl position is the most dominant route, followed by the homolytic scission of the ethyl branch to give cyclohexyl, followed by the hydrogen abstraction by methyl radical at the 3-yl position.

Ethylene formation:- Ethyl cyclohex-3-yl radical undergoes ring opening to form oct-1-en-6-yl radical, which on C-C beta scission gives 1-butene and but-1-en-4-yl radical. But-1-en-4-yl undergoes C-C beta scission to give ethylene and vinyl radical. Apart from this, cyclohexyl leads to formation of ethylene as discussed in the cyclohexane pyrolysis chapter, as shown in Figure 6.14.

Propylene formation:- Unlike in the case of methyl cyclohexane pyrolysis, propylene is not formed in the primary decomposition of ethyl cyclohexane. It is formed by the smaller molecules. Understandably, its mass% is low in the product as compared to ethylene.

1,3-butadiene formation:- As discussed in the section on ethylene formation, ethyl cyclohex-3-yl radical undergoes ring opening to form oct-1-en-6-yl radical. This isomerizes to the allylic oct-1-en-3-yl radical. This on C-C beta scission gives 1,3-butadiene and 1-

butyl radical as shown in Figure 6.13. The other dominant route for 1,3-butadiene formation is via the cyclohexyl radical as discussed in the chapter on cyclohexane pyrolysis.

Methane and Hydrogen formation:- Methyl radicals and hydrogen atoms abstract hydrogen from ethyl cyclohexane to form methane and hydrogen gas.

Benzene formation:- Benzene formation originates from the C-C addition of 1,3-butadiene and vinyl radical and subsequent ring formation and hydrogen loss, as shown in Figure 6.15. This is because of the excess presence of vinyl and 1,3-butadiene in the species pool as both of these are formed preferably in the primary decomposition of ethyl cyclohexane.
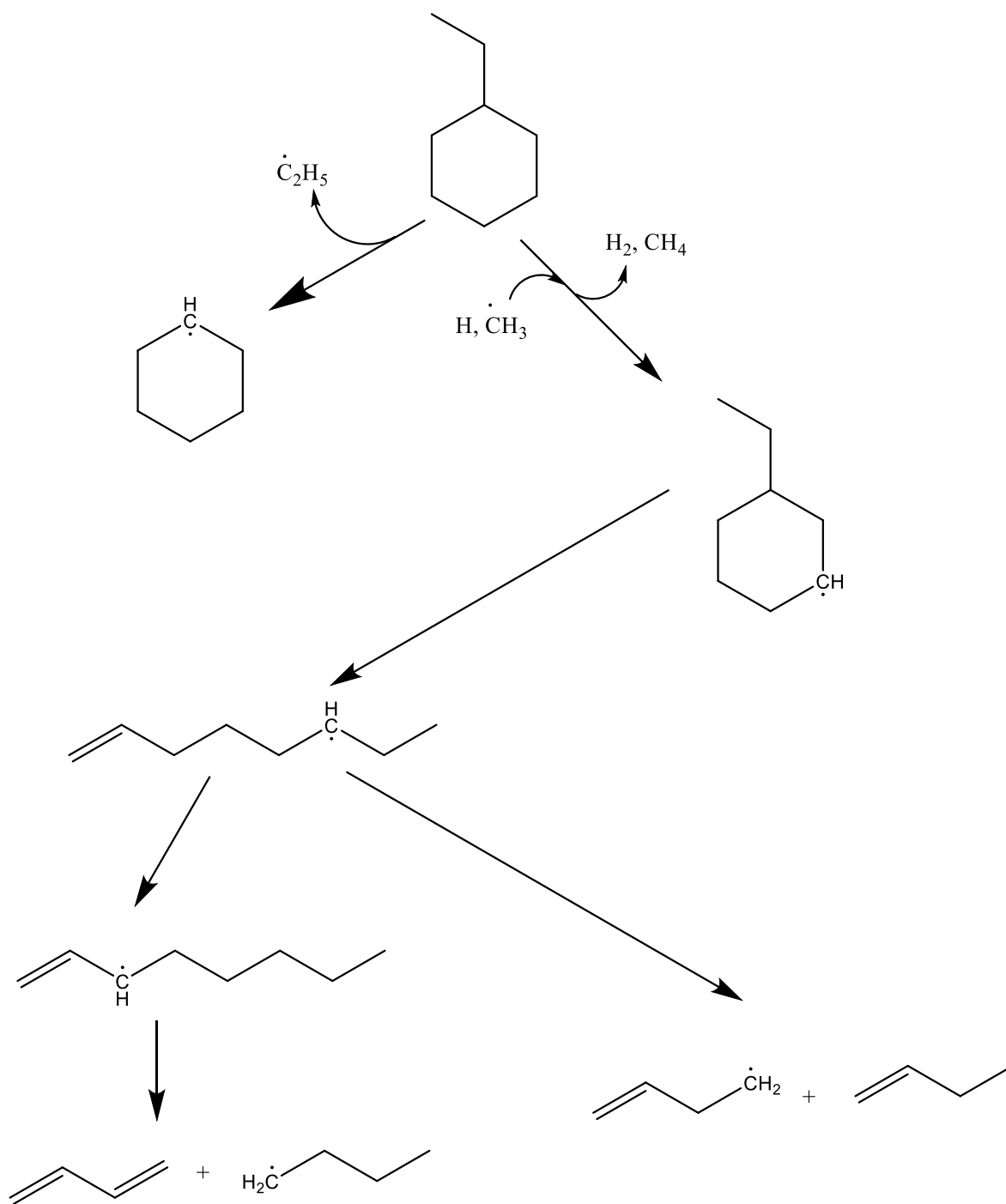
Figure 6.13: Dominant pathways of ethyl-cyclohexane pyrolysis at 1123K, 1013 mbara pressure at 15 cm reactor length, 16% conversion, LCT model
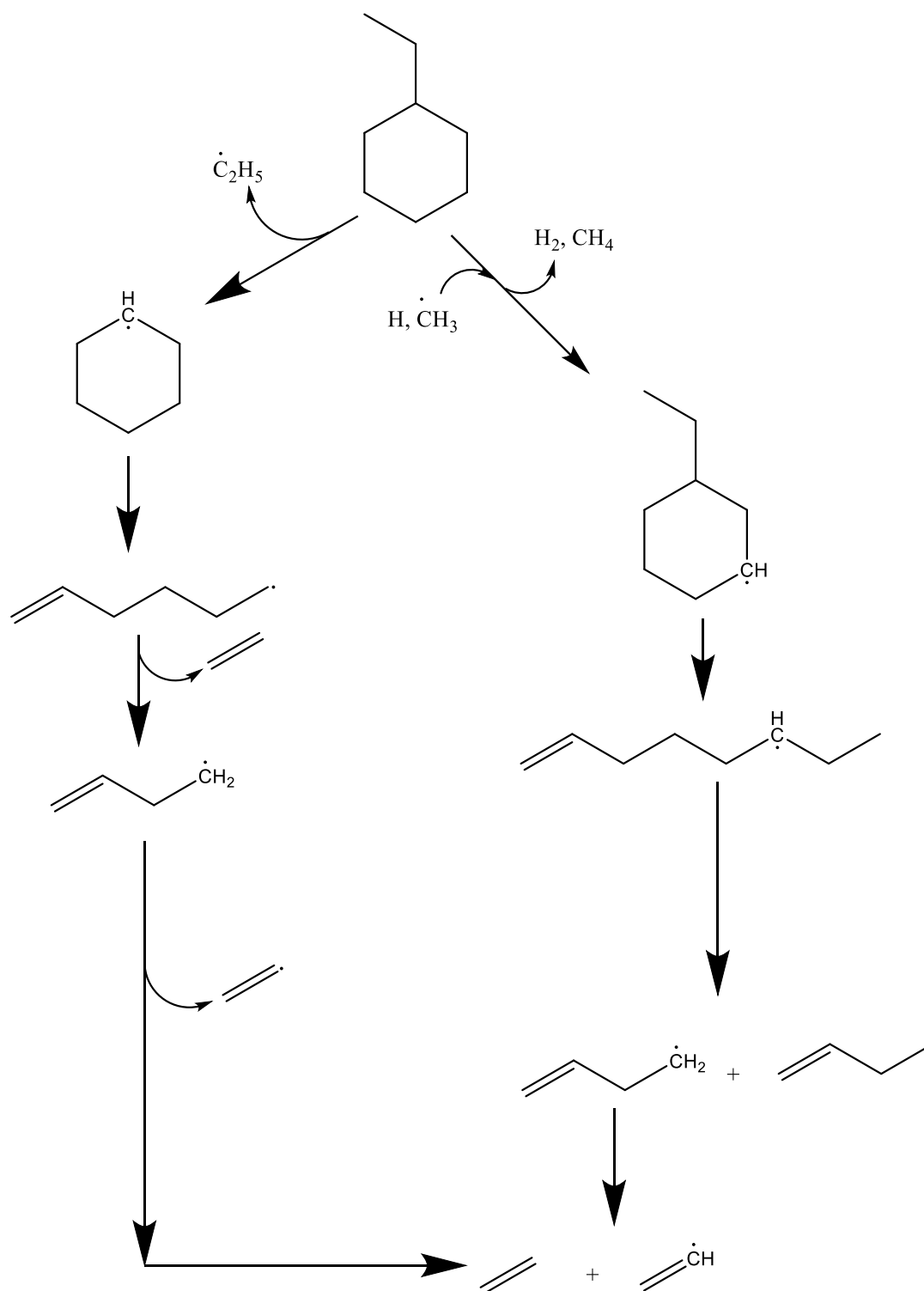
Figure 6.14: Dominant pathways of ethylene formation from ethyl-cyclohexane pyrolysis at 1123K, 1013 mbara pressure at 15 cm reactor length, 16% conversion, LCT model
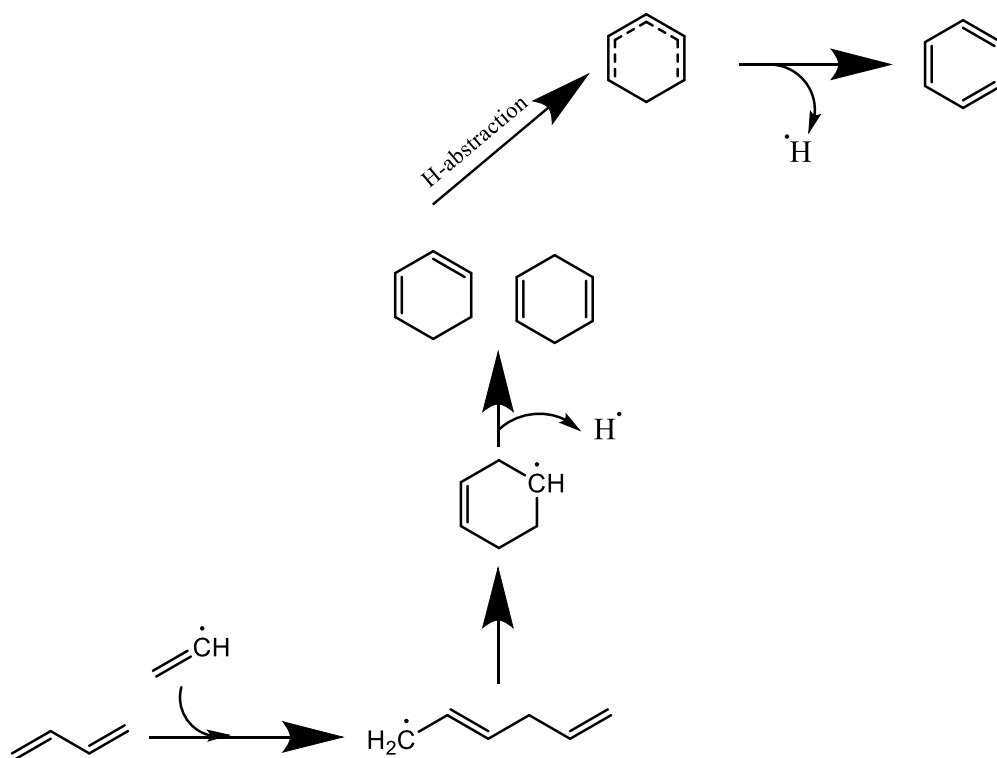
Figure 6.15: Dominant pathway of benzene formation from ethyl-cyclohexane pyrolysis at 1123K, 1013 mbara pressure at 15 cm reactor length, 16% conversion, LCT model

6.4. Conclusions

An ab-initio based high pressure limit elementary reaction mechanism without any alterations has been generated automatically using Genesys for the pyrolysis of ethyl-cyclohexane. It has been validated with experimental data from the SVUV-PIMS apparatus at Hefei, China, whose conditions were 1000-1300K, 0.007-0.2 s residence time, 1 SLM gas feed flow, where the feed is 2 mol% ethyl-cyclohexane and 98 mol% Argon. The model predictions capture the experimental trends of major products at 1013 and 200 mbara, showing that the high pressure limit model can predict the pyrolysis trends even at low pressure. Rate of consumption analysis shows that ethyl-cyclohexane is consumed mainly by hydrogen abstraction by H-atom at the 3-yl position, followed by homolytic scission of the ethyl group and then by the hydrogen abstraction by methyl radical at the 3-yl position. The automatically generated, high pressure limit, unaltered LCT model performs well compared to literature optimized/ lumped/ global/ pressure dependent models – JetSurF and

Hefei. Additionally, the experimental trends of ethyl-cyclohexane are compared with those of methyl-cyclohexane, cyclohexane and cyclopentane. It is realized that pressure has a negligible effect on the experimental mass% of major products when plotted against feed conversions showing why the high pressure limit model predicts well low pressure experiments as well. Also, it is realized that the experimental trends of feeds having the cyclohexane moiety are qualitatively similar and quantitatively closer to each other than those of cyclopentane trends. The effect of pressure, ring size and substituent on cycloalkane pyrolysis feeds is captured by the LCT model.

6.5. References

1.Djokic, M. R.; Dijkmans, T.; Yildiz, G.; Prins, W.; Van Geem, K. M., Quantitative analysis of crude and stabilized bio-oils by comprehensive two-dimensional gas-chromatography. *Journal of Chromatography A* **2012,** 1257, 131-140.

2.Vargas, D. C.; Alvarez, M. B.; Portilla, A. H.; Van Geem, K. M.; Streitwieser, D. A., Kinetic Study of the Thermal and Catalytic Cracking of Waste Motor Oil to Diesel-like Fuels. *Energy & Fuels* **2016,** 30, (11), 9712-9720.

3.Vandewiele, N. M.; Magoon, G. R.; Van Geem, K. M.; Reyniers, M. F.; Green, W. H.; Marin, G. B., Kinetic Modeling of Jet Propellant-10 Pyrolysis. *Energy & Fuels* **2015,** 29, (1), 413-427.

4.Vandewiele, N. M.; Magoon, G. R.; Van Geem, K. M.; Reyniers, M. F.; Green, W. H.; Marin, G. B., Experimental and Modeling Study on the Thermal Decomposition of Jet Propellant-10. *Energy & Fuels* **2014,** 28, (8), 4976-4985.

5.Gascoin, N.; Abraham, G.; Gillard, P., Synthetic and jet fuels pyrolysis for cooling and combustion applications. *Journal of Analytical and Applied Pyrolysis* **2010,** 89, (2), 294-306.

6.Yang, Q. C.; Chetehouna, K.; Gascoin, N.; Bao, W., Experimental study on combustion modes and thrust performance of a staged-combustor of the scramjet with dual-strut. *Acta Astronautica* **2016,** 122, 28-34.

7.Pyl, S. P.; Schietekat, C. M.; Reyniers, M. F.; Abhari, R.; Marin, G. B.; Van Geem, K. M., Biomass to olefins: Cracking of renewable naphtha. *Chemical Engineering Journal* **2011,** 176, 178-187.

8.Buda, F.; Bounaceur, R.; Warth, V.; Glaude, P.; Fournet, R.; Battin-Leclerc, F., Progress toward a unified detailed kinetic model for the autoignition of alkanes from C-4 to C-10 between 600 and 1200 K. *Combustion and Flame* **2005,** 142, (1-2), 170-186.

9.Buda, F.; Glaude, P. A.; Battin-Leclerc, F.; Porter, R.; Hughes, K. J.; Griffiths, J. F., Use of detailed kinetic mechanisms for the prediction of autoignitions. *Journal of Loss Prevention in the Process Industries* **2006,** 19, (2-3), 227-232.

10.Sirjean, B.; Buda, F.; Hakka, H.; Glaude, P. A.; Fournet, R.; Warth, V.; Battin-Leclerc, F.; Ruiz-Lopez, M., The autoignition of cyclopentane and cyclohexane in a shock tube. *Proceedings of the Combustion Institute* **2007,** 31, 277-284.

11.Serinyel, Z.; Herbinet, O.; Frottier, O.; Dirrenberger, P.; Warth, V.; Glaude, P. A.; Battin-Leclerc, F., An experimental and modeling study of the low- and high-temperature oxidation of cyclohexane. *Combustion and Flame* **2013,** 160, (11), 2319-2332.

12.Guthrie, F., Sabourin, *Gasoline and Diesel: Fuel Survey*. 2003.

13.Grumman, N., Diesel Fuel Oils. **2003**.

14.Husson, B.; Herbinet, O.; Glaude, P. A.; Ahmed, S. S.; Battin-Leclerc, F., Detailed Product Analysis during Low- and Intermediate-Temperature Oxidation of Ethylcyclohexane. *Journal of Physical Chemistry A* **2012,** 116, (21), 5100-5111.

15.Kang, D.; Lilik, G.; Dillstrom, V.; Agudelo, J.; Lapuerta, M.; Al-Qurashi, K.; Boehman, A. L., Impact of branched structures on cycloalkane ignition in a motored engine: Detailed product and conformational analyses. *Combustion and Flame* **2015,** 162, (4), 877-892.

16.Vanderover, J.; Oehlschlaeger, M. A., Ignition Time Measurements for Methylcylcohexane- and Ethylcyclohexane-Air Mixtures at Elevated Pressures. *International Journal of Chemical Kinetics* **2009,** 41, (2), 82-91.

17.Tian, Z. M.; Zhang, Y. J.; Pan, L.; Zhang, J. X.; Yang, F. Y.; Jiang, X.; Huang, Z. H., Shock-Tube Study on Ethylcyclohexane Ignition. *Energy & Fuels* **2014,** 28, (8), 5505-5514.

18.Tian, Z. M.; Zhang, Y. J.; Yang, F. Y.; Pan, L.; Jiang, X.; Huang, Z. H., Comparative Study of Experimental and Modeling Autoignition of Cyclohexane, Ethylcyclohexane, and n-Propylcyclohexane. *Energy & Fuels* **2014,** 28, (11), 7159-7167.

19.Wang, Z. D.; Zhao, L.; Wang, Y.; Bian, H. T.; Zhang, L. D.; Zhang, F.; Li, Y. Y.; Sarathy, S. M.; Qi, F., Kinetics of ethylcyclohexane pyrolysis and oxidation: An experimental and detailed kinetic modeling study. *Combustion and Flame* **2015,** 162, (7), 2873-2892.

20.Vandewiele, N. M.; Van Geem, K. M.; Reyniers, M. F.; Marin, G. B., Genesys: Kinetic model construction using chemo-informatics. *Chemical Engineering Journal* **2012,** 207, 526-538.

21.H. Wang, E. D., B. Sirjean, D. A. Sheen, R. Tango, A. Violi, J. Y. W. Lai, F. N. Egolfopoulos, D. F. Davidson, R. K. Hanson, C. T. Bowman, C. K. Law, W. Tsang, N. P. Cernansky, D. L. Miller, R. P. Lindstedt *JetSurF*, 2.0; http://web.stanford.edu/group/haiwanglab/JetSurF/JetSurF2.0/index.html, 2010.

22.Zhandong, W. Experimental and Kinetic Modeling Study of Cyclohexane and Its Mono-alkylated Derivatives Combustion. University of Science and Technology of China,Hefei

23.Khandavilli, M. V.; Djokic, M.; Vermeire, F. H.; Carstensen, H. H.; Van Geem, K. M.; Marin, G. B., Experimental and Kinetic Modeling Study of Cyclohexane Pyrolysis. *Energy & Fuels* **2018,** 32, (6), 7153-7168.

24.Wang, Z. D.; Ye, L. L.; Yuan, W. H.; Zhang, L. D.; Wang, Y. Z.; Cheng, Z. J.; Zhang, F.; Qi, F., Experimental and kinetic modeling study on methylcyclohexane pyrolysis and combustion. *Combustion and Flame* **2014,** 161, (1), 84-100.

25.Khandavilli, M. V.; Vermeire, F. H.; Van de Vijver, R.; Djokic, M.; Carstensen, H. H.; Van Geem, K. M.; Marin, G. B., Group additive modeling of cyclopentane pyrolysis. *Journal of Analytical and Applied Pyrolysis* **2017,** 128, 437-450.

26.M. J. Frisch, G. W. T., H. B. Schlegel, G. E. Scuseria, M. A. Robb, J. R. Cheeseman, G. Scalmani, V. Barone, B. Mennucci, G. A. Petersson, H. Nakatsuji, M. Caricato, X. Li, H. P. Hratchian, A. F. Izmaylov, J. Bloino, G. Zheng, J. L. Sonnenberg, M. Hada, M. Ehara, K. Toyota, R. Fukuda, J. Hasegawa, M. Ishida, T. Nakajima, Y. Honda, O. Kitao, H. Nakai, T. Vreven, J. A. Montgomery, Jr., J. E. Peralta, F. Ogliaro, M. Bearpark, J. J. Heyd, E. Brothers, K. N. Kudin, V. N. Staroverov, R. Kobayashi, J. Normand, K. Raghavachari, A. Rendell, J. C. Burant, S. S. Iyengar, J. Tomasi, M. Cossi, N. Rega, J. M. Millam, M. Klene, J. E. Knox, J. B. Cross, V. Bakken, C. Adamo, J. Jaramillo, R. Gomperts, R. E. Stratmann, O. Yazyev, A. J. Austin, R. Cammi, C. Pomelli, J. W. Ochterski, R. L. Martin, K. Morokuma, V. G. Zakrzewski, G. A. Voth, P. Salvador, J. J. Dannenberg, S. Dapprich, A. D. Daniels, Ö. Farkas, J. B. Foresman, J. V. Ortiz, J. Cioslowski, and D. J. Fox *Gaussian, Inc.*, Wallingford CT, 2009.

27.*CHEMKIN-PRO 15131*, Reaction Design: San Diego, 2013.

28.Zhang, et al., Pyrolysis of MTBE. 1. Experimental study with molecular-beam mass spectrometry and tunable synchrotron VUV photoionization, *J. Phys. Chem A*, **2008**, 112, 10487-10494.

7

Conclusions and Perspectives

7.1. Conclusions

The current gradual shift in the petrochemical industry from fossil fuels to renewable fuels like those derived from biomass is the key driver for innovation in the 21st century. The chemical industry faces many challenges in terms of evaluation of new feedstocks and estimation of product spectrum for new sets of operating conditions. Experiments are not possible for each scenario and are neither fully scalable many a time. Hence, detailed kinetic modeling of the feedstocks from first principles is employed by researchers. This way, there are no extrapolations or adjustment of kinetic parameters and the reaction chemistry is built into a truly predictive model rather than a calculated model and separated from and independent of the reactor model. In industrial steam cracking, a naphtha feedstock may contain majorly paraffins and isoparaffins. However, a bio-derived naphtha may contain mainly cycloalkanes. These could be substituted and unsubstituted cyclopentanes and cyclohexanes. Pyrolysis of paraffins and isoparaffins is relatively well understood as compared to cycloalkanes. In this thesis, pyrolysis of cycloalkanes is modeled for four important species – cyclopentane, cyclohexane, methyl-cyclohexane and ethyl-cyclohexane. This is done by automatic generation of a high pressure limit elementary reaction model with ab-initio based/ group additive kinetics with no adjustments done to the parameters. The model has been generated using the automatic mechanism generation tool, 'Genesys'[1, 2]. It has been validated by in-house and external laboratory data. The Genesys model (LCT model) has also been compared to seven other literature models – AramcoMech[3], CSM[4], POLIMI[5], Nancy[6], JetSurF[7], Tian[8] and Hefei[9-11]. The experimental

and model trends of open chain alkanes may still be comparable to some cycloalkanes. It is shown here. Figure 7.1 shows the experimental and LCT model trends for the conversion of seven molecules modeled in this thesis – propane, n-butane, iso-butane, cyclopentane, cyclohexane, methyl-cyclohexane and ethyl-cyclohexane.
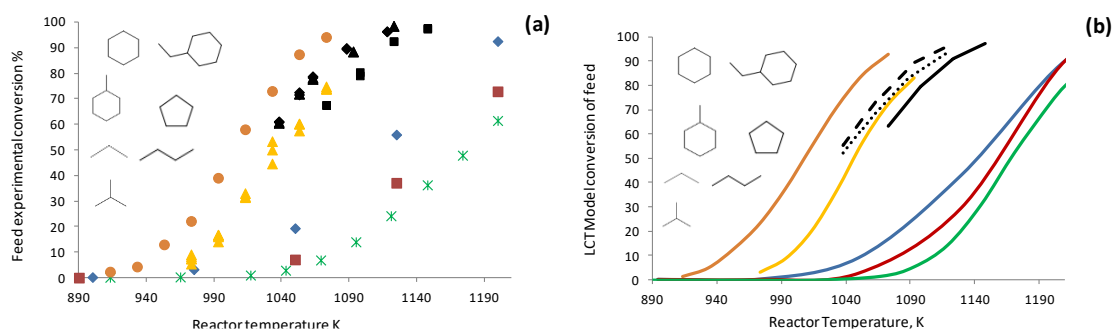
Figure 7.1: Conversion of feed molecule vs. reactor temperature for 8 different experiments: Experiment shown by dots (a), LCT model simulation shown by lines (b): ♦ ── **Hefei experiment on ethyl-cyclohexane pyrolysis at 1013 mbara,** ■ ── **Hefei experiment on methyl-cyclohexane pyrolysis at 1013 mbara,** ✳ ── **Hefei experiment on cyclohexane pyrolysis at 1013 mbara,** ● ── **LCT experiment on cyclohexane pyrolysis at 1700 mbara,** ▲ ── **LCT experiment on cyclopentane pyrolysis at 1700 mbara,** ■ ── **LCT experiment on propane pyrolysis at 1700 mbara,** ▲ ── ── **LCT experiment on n-butane pyrolysis at 1700 mbara,** ♦ ⋯⋯ **LCT experiment on iso-butane pyrolysis at 1700 mbara**

From Figure 7.1, it can be seen that as per experiment as well as model, propane, n-butane and iso-butane conversions are comparable to that of cyclopentane. Some product trends of pyrolysis of propane, n-butane and iso-butane are also comparable to those of cyclopentane - for the products propylene and 1,3-butadiene, as shown in Figure 7.2. Here, propylene yield is among the highest for a given feed conversion, and 1,3-butadiene is among the lowest for these molecules compared to other cycloalkanes.
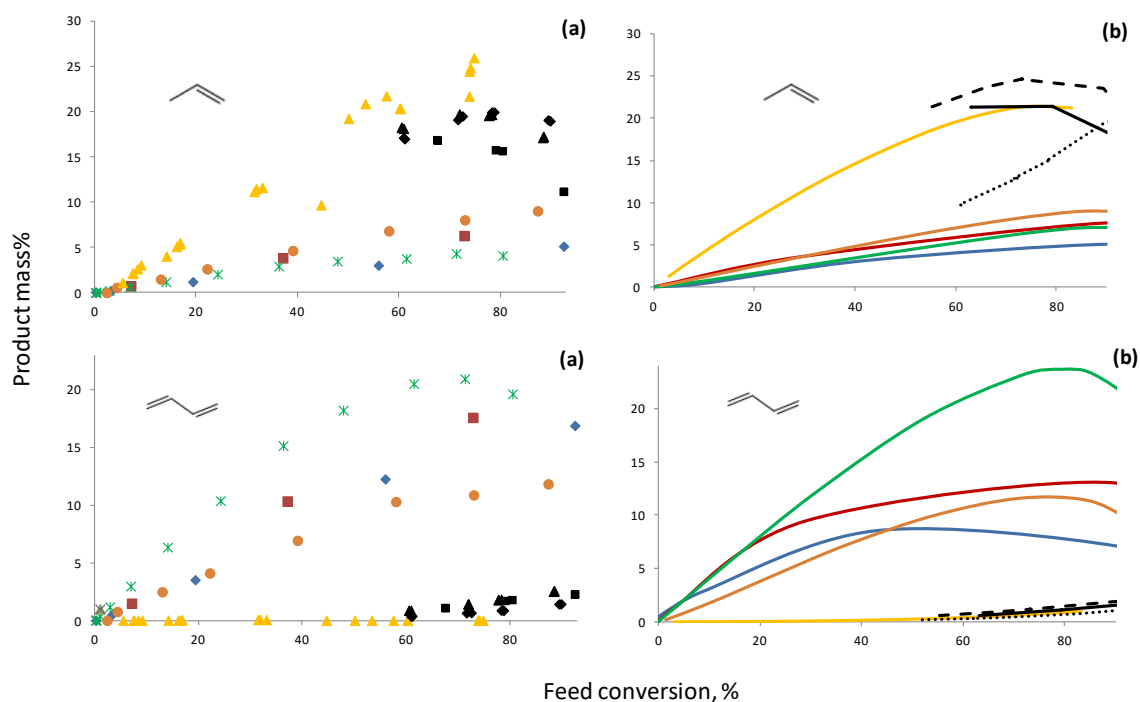
Figure 7.2: Mass% of propylene and 1,3-butadiene in pyrolysis product: Experiment shown by dots (a), LCT model simulation shown by lines (b): ◆ ── Hefei experiment on ethyl-cyclohexane pyrolysis at 1013 mbara, ■ ── Hefei experiment on methyl-cyclohexane pyrolysis at 1013 mbara, ✳ ── Hefei experiment on cyclohexane pyrolysis at 1013 mbara, ● ── LCT experiment on cyclohexane pyrolysis at 1700 mbara, ▲ ── LCT experiment on cyclopentane pyrolysis at 1700 mbara, ■ ── LCT experiment on propane pyrolysis at 1700 mbara, ▲ ─ ─ LCT experiment on n-butane pyrolysis at 1700 mbara, ◆ ⋯⋯ LCT experiment on iso-butane pyrolysis at 1700 mbara

Propane, n-butane and iso-butane are also unique for their methane and benzene trends. They produce the highest methane and lowest benzene in comparison to all the cycloalkanes, for the same feed conversion. This is shown in Figure 7.3
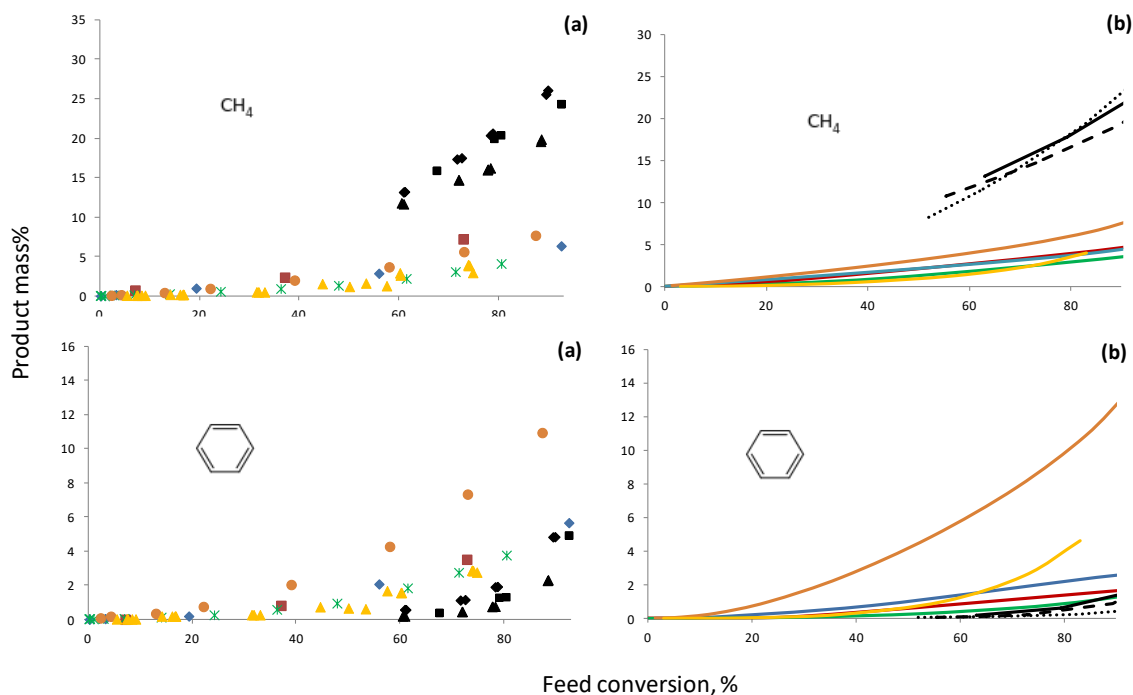
Figure 7.3: Mass% of methane and benzene in pyrolysis product: Experiment shown by dots (a), LCT model simulation shown by lines (b): ◆ ▬▬ **Hefei experiment on ethyl-cyclohexane pyrolysis at 1013 mbara,** ■ ▬▬ **Hefei experiment on methyl-cyclohexane pyrolysis at 1013 mbara,** ✳ ▬▬ **Hefei experiment on cyclohexane pyrolysis at 1013 mbara,** ● ▬▬ **LCT experiment on cyclohexane pyrolysis at 1700 mbara,** ▲ ▬▬ **LCT experiment on cyclopentane pyrolysis at 1700 mbara,** ■ ▬▬ **LCT experiment on propane pyrolysis at 1700 mbara,** ▲ ▬ ▬ **LCT experiment on n-butane pyrolysis at 1700 mbara,** ◆ ······ **LCT experiment on iso-butane pyrolysis at 1700 mbara**

The above figures show some similarities of trends between open chain alkanes and cycloalkanes. This information would be handy when formulating a surrogate of a petrochemical cut based on product spectrum. Moreover, the main objective of this thesis was the modeling of pyrolysis of important cycloalkanes, and that has been accomplished. However, there could be further interesting species to model, as discussed in the next section on path forward.

7.2. Path forward

Naphtha has the carbon number range of C_5-C_9. Among the naphthenic cut, the highest carbon number evaluated in this thesis was C_8 (ethyl-cyclohexane). The next logical step would be to try propyl-cyclohexane and butyl-cyclohexane. There is literature available on these[12-15]. Also interesting would be to model the pyrolysis of the three isomers of dimethyl-cyclohexane (C_8) on which ignition delay times have been tested[16]. Poly-ring naphthenics like decalin, 1,3-dimethyladmantane[17] and norbornane would also be interesting. These molecules are shown pictorially in Figure 7.4.

(propyl, butyl cyclohexane)

(dimethyl cycloohexanes)

(decalin, dimethyl-adamantane, norbornane)
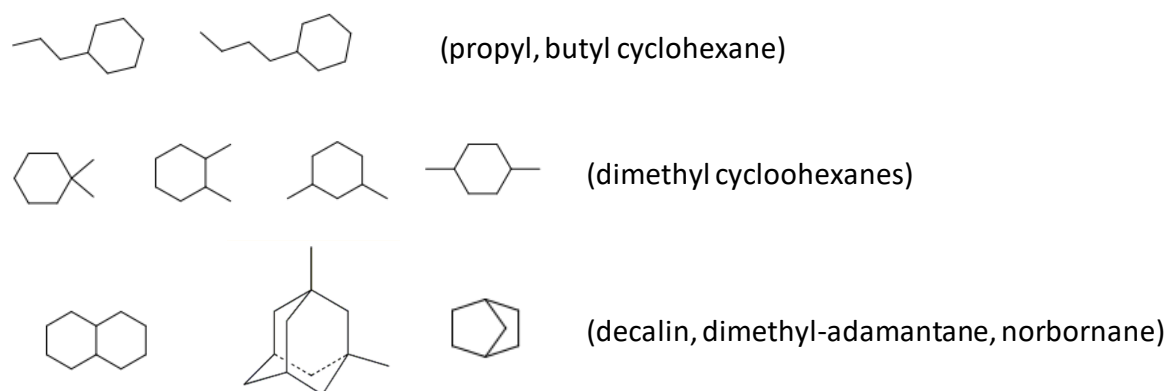
Figure 7.4: Path forward – molecules interesting for future studies

Study of the pyrolysis of these molecules would enhance our understanding of pyrolysis of biomass derived fuels. As a next step, surrogate formulations can be evaluated with the knowledge of the product spectra of the studied molecules. What would be interesting is to represent a petrochemical cut composed of hundreds of molecules by very few molecules and still match the pyrolysis product spectrum.

7.3. References

1.Van de Vijver, R.; Vandewiele, N. M.; Vandeputte, A. G.; Van Geem, K. M.; Reyniers, M. F.; Green, W. H.; Marin, G. B., Rule-based ab initio kinetic model for alkyl sulfide pyrolysis. *Chemical Engineering Journal* **2015,** 278, 385-393.

2.Vandewiele, N. M.; Van Geem, K. M.; Reyniers, M. F.; Marin, G. B., Genesys: Kinetic model construction using chemo-informatics. *Chemical Engineering Journal* **2012,** 207, 526-538.

3.Li, Y.; Zhou, C. W.; Somers, K. P.; Zhang, K. W.; Curran, H. J., The oxidation of 2-butene: A high pressure ignition delay, kinetic modeling study and reactivity comparison with isobutene and 1-butene. *Proceedings of the Combustion Institute* **2017,** 36, (1), 403-411.

4.Wang, K.; Villano, S. M.; Dean, A. M., Fundamentally-based kinetic model for propene pyrolysis. *Combustion and Flame* **2015,** 162, (12), 4456-4470.

5.Ranzi, E.; Frassoldati, A.; Grana, R.; Cuoci, A.; Faravelli, T.; Kelley, A. P.; Law, C. K., Hierarchical and comparative kinetic modeling of laminar flame speeds of hydrocarbon and oxygenated fuels. *Progress in Energy and Combustion Science* **2012,** 38, (4), 468-501.

6.Sirjean, B.; Buda, F.; Hakka, H.; Glaude, P. A.; Fournet, R.; Warth, V.; Battin-Leclerc, F.; Ruiz-Lopez, M., The autoignition of cyclopentane and cyclohexane in a shock tube. *Proceedings of the Combustion Institute* **2007,** 31, 277-284.

7.H. Wang, E. D., B. Sirjean, D. A. Sheen, R. Tango, A. Violi, J. Y. W. Lai, F. N. Egolfopoulos, D. F. Davidson, R. K. Hanson, C. T. Bowman, C. K. Law, W. Tsang, N. P. Cernansky, D. L. Miller, R. P. Lindstedt *JetSurF*, 2.0; http://web.stanford.edu/group/haiwanglab/JetSurF/JetSurF2.0/index.html, 2010.

8.Tian, Z. M.; Tang, C. L.; Zhang, Y. J.; Zhang, J. X.; Huang, Z. H., Shock Tube and Kinetic Modeling Study of Cyclopentane and Methylcyclopentane. *Energy & Fuels* **2015,** 29, (1), 428-441.

9.Wang, Z.; Cheng, Z.; Yuan, W.; Cai, J.; Zhang, L.; Zhang, F.; Qi, F.; Wang, J., An experimental and kinetic modeling study of cyclohexane pyrolysis at low pressure. *Combustion and Flame* **2012,** 159, (7), 2243-2253.

10.Wang, Z. D.; Ye, L. L.; Yuan, W. H.; Zhang, L. D.; Wang, Y. Z.; Cheng, Z. J.; Zhang, F.; Qi, F., Experimental and kinetic modeling study on methylcyclohexane pyrolysis and combustion. *Combustion and Flame* **2014,** 161, (1), 84-100.

11.Wang, Z. D.; Zhao, L.; Wang, Y.; Bian, H. T.; Zhang, L. D.; Zhang, F.; Li, Y. Y.; Sarathy, S. M.; Qi, F., Kinetics of ethylcyclohexane pyrolysis and oxidation: An experimental and detailed kinetic modeling study. *Combustion and Flame* **2015,** 162, (7), 2873-2892.

12.Dubois, T.; Chaumeix, N.; Paillard, C. E., Experimental and Modeling Study of n-Propylcyclohexane Oxidation under Engine-relevant Conditions. *Energy & Fuels* **2009,** 23, (5-6), 2453-2466.

13.Ristori, A.; Dagaut, P.; El Bakali, A.; Cathonnet, M., The oxidation of N-propylcyclohexane: Experimental results and kinetic modeling. *Combustion Science and Technology* **2001,** 165, 197-228.

14.Tian, Z. M.; Zhang, Y. J.; Yang, F. Y.; Pan, L.; Jiang, X.; Huang, Z. H., Comparative Study of Experimental and Modeling Autoignition of Cyclohexane, Ethylcyclohexane, and n-Propylcyclohexane. *Energy & Fuels* **2014,** 28, (11), 7159-7167.

15.Rakotoalimanana, D. A.; Bounaceur, R.; Behar, F.; Burkle-Vitzthum, V.; Marquaire, P. M., Thermal cracking of n-butylcyclohexane at high pressure (100 bar)-Part 2: Mechanistic modeling. *Journal of Analytical and Applied Pyrolysis* **2016,** 120, 174-185.

16.Eldeeb, M. A.; Jouzdani, S.; Wang, Z. D.; Sarathy, S. M.; Akih-Kumgeh, B., Experimental and Chemical Kinetic Modeling Study of Dimethylcyclohexane Oxidation and Pyrolysis. *Energy & Fuels* **2016,** 30, (10), 8648-8657.

17.Qin, X. M.; Yue, L.; Wu, J. Z.; Guo, Y. S.; Xu, L.; Fang, W. J., Thermal Stability and Decomposition Kinetics of 1,3-Dimethyladamantane. *Energy & Fuels* **2014,** 28, (10), 6210-6220.

Appendix A

Appendix A shows the experimental data for cyclopentane pyrolysis and the model trends for the full range of products, including minor products.

Table A1: Experimental data of Cyclopentane pyrolysis (averaged over multiple experiments)

Run nr.	973K	993K	1013K	1033K	1053K	1073K
Feed Cyclopentane [gh⁻¹]	240	240	240	240	240	240
N2 Dilution [gh⁻¹]	0	0	0	0	0	0
N2 Internal Standard [gh⁻¹]	20	20	20	70	70	70
T-profile reactor [K]						
Tsetting [K]	973	993	1013	1033	1053	1073
CIT	622.4	628.4	633	529.2	527.3	526.6
T at 190 mm	974.8	995	1015.9	1034.6	1054.3	1073
T at 380 mm	1003.3	1020.1	1034.3	1050.4	1074.6	1094.1
T at 480 mm	973.4	993.2	1012.7	1033.2	1052.5	1073
T at 670 mm	960.9	978.9	996.6	1017.8	1037.6	1058.3
T at 860 mm	973.4	993.2	1012.7	1033.4	1052.7	1073
T at 1050 mm	980.5	997.5	1015	1035	1056.7	1076.2
T at 1240 mm	975.2	994.8	1014.1	1034.6	1053.9	1074.1
T at 1430 mm	761.9	781.9	795.2	855.6	875.2	896.5
COT	721.9	721.9	721.7	720.8	721.7	722.6
P-profile reactor [MPa]						
CIP	0.17	0.17	0.17	0.17	0.17	0.17
COP	0.17	0.17	0.17	0.17	0.17	0.17
Molar Flows [mol h⁻¹]						
H	14.28	14.28	14.35	15.16	15.11	15.25
C	7.13	7.13	7.12	6.85	7.03	6.98
H/C ratio [mol mol⁻¹] (in)	2.00	2.00	2.00	2.00	2.00	2.00
H/C ratio [mol mol⁻¹] (out)	2.00	2.00	2.02	2.21	2.15	2.18
Yields [mass%]						
H2	0.126	0.219	0.438	2.063	1.191	1.515
C2H4	1.949	4.532	8.991	17.261	19.699	25.339
C2H6	0.079	0.218	0.538	1.466	2.038	2.442
C2H2	0.000	0.000	0.002	0.007	0.008	0.010
CH4	0.070	0.176	0.505	1.545	2.915	3.837
C3H8	0.036	0.089	0.176	0.355	0.390	0.420
C3H6	2.124	5.372	11.176	9.706	20.391	24.469
PD	0.001	0.007	0.016	0.000	0.000	0.000
i-C4H10	0.006	0.010	0.018	0.000	0.028	0.043
n-C4H10	0.001	0.002	0.003	0.003	0.009	0.008
t-2-C4H8	0.003	0.007	0.014	0.021	0.090	0.112
1-C4H8	0.005	0.016	0.041	0.035	0.187	0.291
i-C4H8	0.168	0.488	0.919	0.000	0.031	0.000
c-2-C4H8	0.002	0.005	0.011	0.012	0.063	0.039
MeAc	0.000	0.000	0.000	0.001	0.000	0.110
1,3-C4H6	0.010	0.030	0.082	0.007	0.006	0.009
C7H10	0.000	0.000	0.023	0.000	0.000	0.000
Toluene	0.000	0.000	0.128	0.204	0.444	0.773
Ethylbenzene	0.000	0.000	0.009	0.000	0.000	0.018
xylene (m, p)	0.000	0.000	0.009	0.000	0.000	0.020
Styrene	0.000	0.000	0.050	0.119	0.315	0.524
3-methyl-1H-Indene	0.000	0.000	0.042	0.000	0.000	0.000
Indene	0.000	0.000	0.066	0.183	0.477	0.761
1,2-dihydro-Naphthalene	0.000	0.000	0.015	0.000	0.000	0.000
Naphthalene	0.000	0.000	0.057	0.214	0.521	1.071
1,3-cyclopentadiene	1.056	2.304	4.828	7.507	7.681	7.706
2-methyl-1,3-butadiene	0.077	0.318	0.198	0.037	0.024	0.061
Cyclopentane	92.439	83.328	68.548	55.362	39.803	26.104
Benzene	0.021	0.183	0.270	0.733	1.569	2.865
Cyclopentene	1.665	2.437	2.652	2.979	2.000	1.351
cis-2-pentene	0.043	0.000	0.000	0.000	0.000	0.000
1,4-pentadiene	0.119	0.004	0.000	0.180	0.120	0.103
trans-2-pentene	0.000	0.255	0.159	0.000	0.000	0.000
C10H10 monoaromatic	0.000	0.000	0.016	0.000	0.000	0.000
Total 34 compounds detected						
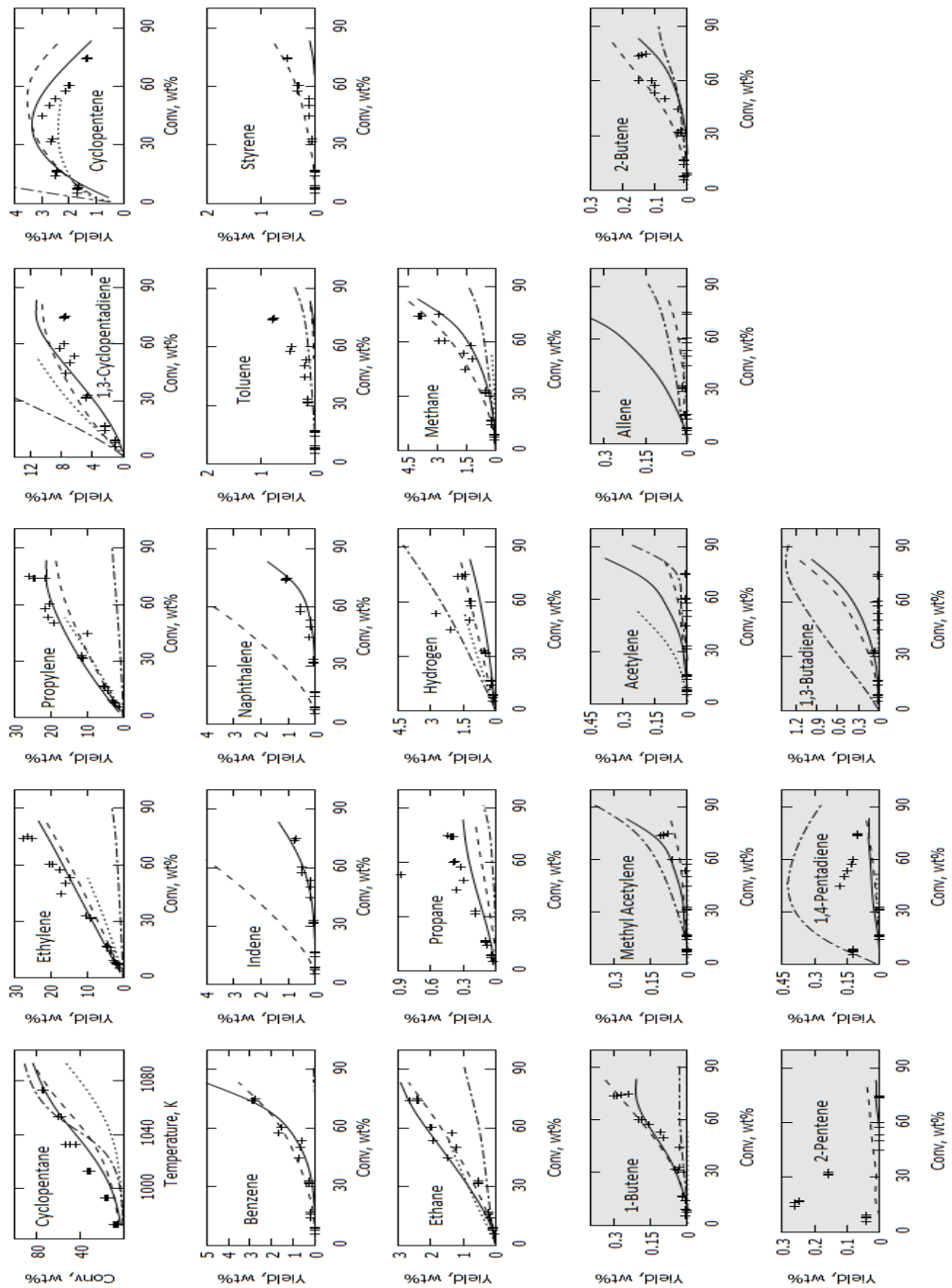
Figure A1: Experimental pyrolysis yields and model predictions for 22 products in continuous flow experiments at 0.5s residence time, 0.17MPa pressure, pure cyclopentane feed (✛ Experiment, —————— Genesys, — — — — Wang, ·········· Sirjean, — · — · — Tian)

Appendix B

Appendix B lists the LCT model valid for the 7 molecules in ChemKin format.

```
! Quick reference - Some important species nomenclature
!     H2          hydrogen
!     C2H4        ethylene
!     C2H6        ethane
!     CH4         methane
!     CCC         propane
!     C*CC        propylene
!     C6H12_R6    cyclohexane
!     CYC5H10         cyclopentane
!     BENZENE         benzene
!     CY13PD          1,3-cyclopentadiene
!     CYC5H8          cyclopentene
!     C*CC*C          1,3-butadiene
!     CC*CCC          2-pentene
!     C*CCC*C         1,4-pentadiene
!     toluene(3)  toluene
!     CYC6H5C*C   styrene
!     INDENE          indene
!     a2          naphthalene
!     CCCC        n-butane
!     C3C         i-butane
!     CH3cC6H11   methyl-cyclohexane
!     C2H5cC6H11  ethyl-cyclohexane


ELEMENTS
C   H   O   AR   N    HE
END
SPECIES
AR      !     InChI=1S/Ar
N2      !     InChI=1S/N2/c1-2
H2O     !     InChI=1S/H2O/h1H2
HE      !     InChI=1S/He
CC*CCC.     !      InChI=1S/C5H9/c1-3-5-4-2/h4-5H,1,3H2,2H3
C*CC*CC     !      InChI=1S/C5H8/c1-3-5-4-2/h3-5H,1H2,2H3
C*C.CC      !      InChI=1S/C4H7/c1-3-4-2/h1,4H2,2H3
CYPENE4.    !      InChI=1S/C5H7/c1-2-4-5-3-1/h1-2,5H,3-4H2
C*CC. !     InChI=1S/C3H5/c1-3-2/h3H,1-2H2
CYC6H10     !      InChI=1S/C6H10/c1-2-4-6-5-3-1/h1-2H,3-6H2
C2H3 !      InChI=1S/C2H3/c1-2/h1H,2H2
CH3  !      InChI=1S/CH3/h1H3
C*CCC.C     !      InChI=1S/C5H9/c1-3-5-4-2/h3-4H,1,5H2,2H3
C*CC.*C     !      InChI=1S/C4H5/c1-3-4-2/h3H,1-2H2
CYC6H9      !      InChI=1S/C6H9/c1-2-4-6-5-3-1/h1-2,5H,3-4,6H2
C*CC*C      !      InChI=1S/C4H6/c1-3-4-2/h3-4H,1-2H2
C#CCC !     InChI=1S/C4H6/c1-3-4-2/h1H,4H2,2H3
C6H11R_OLEF_42     !      InChI=1S/C6H11/c1-3-5-6-4-2/h5-6H,1,3-4H2,2H3
H2   !      InChI=1S/H2/h1H
C.*CC !     InChI=1S/C3H5/c1-3-2/h1,3H,2H3
MECY13PD    !      InChI=1S/C6H8/c1-6-4-2-3-5-6/h2-6H,1H3
C6H9R_OLEF_57      !      InChI=1S/C6H9/c1-4-5-6(2)3/h5-6H,1-2H2,3H3
CHD14 !     InChI=1S/C6H8/c1-2-4-6-5-3-1/h1-2,5-6H,3-4H2
C*CC.CC     !      InChI=1S/C5H9/c1-3-5-4-2/h3,5H,1,4H2,2H3
CC*CCCC     !      InChI=1S/C6H12/c1-3-5-6-4-2/h3,5H,4,6H2,1-2H3
MECYPE2.    !      InChI=1S/C6H11/c1-6-4-2-3-5-6/h4,6H,2-3,5H2,1H3
C2H4 !      InChI=1S/C2H4/c1-2/h1-2H2
CH4  !      InChI=1S/CH4/h1H4
C.*CCC      !      InChI=1S/C4H7/c1-3-4-2/h1,3H,4H2,2H3
ME4-CPENE3. !      InChI=1S/C6H9/c1-6-4-2-3-5-6/h2-4,6H,5H2,1H3
C*CCCC.C    !      InChI=1S/C6H11/c1-3-5-6-4-2/h3-4H,1,5-6H2,2H3


                    Page - 192
```

```
C6H7R_OLEF_85       !       InChI=1S/C6H7/c1-4-5-6(2)3/h2,5H,1H2,3H3
CC*CC !       InChI=1S/C4H8/c1-3-4-2/h3-4H,1-2H3
C6H7R_OLEF_2        !       InChI=1S/C6H7/c1-3-5-6-4-2/h5H,1-2,6H2
CC*CCC.C    !       InChI=1S/C6H11/c1-3-5-6-4-2/h3-5H,6H2,1-2H3
C*C*CC*C.C  !       InChI=1S/C6H7/c1-3-5-6-4-2/h5-6H,1H2,2H3
CYC5H9.     !       InChI=1S/C5H9/c1-2-4-5-3-1/h1H,2-5H2
C*CC*CCC.   !       InChI=1S/C6H9/c1-3-5-6-4-2/h3,5-6H,1-2,4H2
CC*CC.C     !       InChI=1S/C5H9/c1-3-5-4-2/h3-5H,1-2H3
CCC    !       InChI=1S/C3H8/c1-3-2/h3H2,1-2H3
CYC5H8      !       InChI=1S/C5H8/c1-2-4-5-3-1/h1-2H,3-5H2
C*CCC2.     !       InChI=1S/C5H9/c1-4-5(2)3/h4-5H,1-2H2,3H3
C2CCC.      !       InChI=1S/C5H11/c1-4-5(2)3/h5H,1,4H2,2-3H3
CY13PD      !       InChI=1S/C5H6/c1-2-4-5-3-1/h1-4H,5H2
CYC6H9A     !       InChI=1S/C6H9/c1-2-4-6-5-3-1/h1-3H,4-6H2
C#CC   !       InChI=1S/C3H4/c1-3-2/h1H,2H3
CCCC. !       InChI=1S/C4H9/c1-3-4-2/h1,3-4H2,2H3
H      !       InChI=1S/H
C*C*C !       InChI=1S/C3H4/c1-3-2/h1-2H2
C*CCCC       !       InChI=1S/C5H10/c1-3-5-4-2/h3H,1,4-5H2,2H3
C2H5  !       InChI=1S/C2H5/c1-2/h1H2,2H3
C5H5R_OLEF_7        !       InChI=1S/C5H5/c1-2-4-5-3-1/h1-2,5H,3H2
CCC. !       InChI=1S/C3H7/c1-3-2/h1,3H2,2H3
CYC6H7      !       InChI=1S/C6H7/c1-2-4-6-5-3-1/h1-5H,6H2
CC*CCCC.    !       InChI=1S/C6H11/c1-3-5-6-4-2/h4,6H,1,3,5H2,2H3
ME.CY3PE    !       InChI=1S/C6H9/c1-6-4-2-3-5-6/h2,4,6H,1,3,5H2
C5H7R_OLEF_4        !       InChI=1S/C5H7/c1-3-5-4-2/h5H,1-3H2
C*CCCC*C    !       InChI=1S/C6H10/c1-3-5-6-4-2/h3-4H,1-2,5-6H2
C6H7R_OLEF_91       !       InChI=1S/C6H7/c1-4-5-6(2)3/h5H,1-3H2
C*CCCC.     !       InChI=1S/C5H9/c1-3-5-4-2/h3H,1-2,4-5H2
C*CCC.C*C   !       InChI=1S/C6H9/c1-3-5-6-4-2/h3-5H,1-2,6H2
C*C.CCC     !       InChI=1S/C5H9/c1-3-5-4-2/h1,4-5H2,2H3
CC*C.CC     !       InChI=1S/C5H9/c1-3-5-4-2/h3H,4H2,1-2H3
CYPENE3.    !       InChI=1S/C5H7/c1-2-4-5-3-1/h1-3H,4-5H2
CCCC.C      !       InChI=1S/C5H11/c1-3-5-4-2/h3H,4-5H2,1-2H3
C*CCC !       InChI=1S/C4H8/c1-3-4-2/h3H,1,4H2,2H3
C6H9R_OLEF_56       !       InChI=1S/C6H9/c1-3-5-6-4-2/h4-5H,1,6H2,2H3
CC.C !       InChI=1S/C3H7/c1-3-2/h3H,1-2H3
C2H2 !       InChI=1S/C2H2/c1-2/h1-2H
C*C*CC*C.    !       InChI=1S/C5H5/c1-3-5-4-2/h1,3,5H,2H2
C*CC !       InChI=1S/C3H6/c1-3-2/h3H,1H2,2H3
CC*CC.       !       InChI=1S/C4H7/c1-3-4-2/h3-4H,1H2,2H3
C6H10_OLEF_17       !       InChI=1S/C6H10/c1-3-5-6-4-2/h3,5-6H,1,4H2,2H3
CY13PD5.    !       InChI=1S/C5H5/c1-2-4-5-3-1/h1-5H
C*CC.CCC    !       InChI=1S/C6H11/c1-3-5-6-4-2/h3,5H,1,4,6H2,2H3
C#CC. !       InChI=1S/C3H3/c1-3-2/h1H,2H2
C*C(C)CC.   !       InChI=1S/C5H9/c1-4-5(2)3/h1-2,4H2,3H3
CC.*CC      !       InChI=1S/C4H7/c1-3-4-2/h3H,1-2H3
C#CC*C      !       InChI=1S/C4H4/c1-3-4-2/h1,4H,2H2
C*C*CC      !       InChI=1S/C4H6/c1-3-4-2/h4H,1H2,2H3
C*C.C !       InChI=1S/C3H5/c1-3-2/h1H2,2H3
CC*CC.CC    !       InChI=1S/C6H11/c1-3-5-6-4-2/h3,5-6H,4H2,1-2H3
C2H6 !       InChI=1S/C2H6/c1-2/h1-2H3
C*CCC.      !       InChI=1S/C4H7/c1-3-4-2/h3H,1-2,4H2
C*CC.C*C    !       InChI=1S/C5H7/c1-3-5-4-2/h3-5H,1-2H2
C#CC.C      !       InChI=1S/C4H5/c1-3-4-2/h1,4H,2H3
CCC.C !       InChI=1S/C4H9/c1-3-4-2/h3H,4H2,1-2H3
BENZENE     !       InChI=1S/C6H6/c1-2-4-6-5-3-1/h1-6H
C2CC. !       InChI=1S/C4H9/c1-4(2)3/h4H,1H2,2-3H3
C3C. !       InChI=1S/C4H9/c1-4(2)3/h1-3H3
C2C*C !       InChI=1S/C4H8/c1-4(2)3/h1H2,2-3H3
C2C*C.       !       InChI=1S/C4H7/c1-4(2)3/h1H,2-3H3
```

```
C2.C*C        !       InChI=1S/C4H7/c1-4(2)3/h1-2H2,3H3
C6H13R_8      !       InChI=1S/C6H13/c1-4-5-6(2)3/h4-5H2,1-3H3
C2C.CC        !       InChI=1S/C5H11/c1-4-5(2)3/h4H2,1-3H3
C2C*CC        !       InChI=1S/C5H10/c1-4-5(2)3/h4H,1-3H3
C2CC.C2       !       InChI=1S/C6H13/c1-5(2)6(3)4/h5H,1-4H3
a2      !      InChI=1S/C10H8/c1-2-6-10-8-4-3-7-9(10)5-1/h1-8H
C*C(C)C.C     !       InChI=1S/C5H9/c1-4-5(2)3/h4H,2H2,1,3H3
C*C(C)CCC.    !       InChI=1S/C6H11/c1-4-5-6(2)3/h1-2,4-5H2,3H3
C*C(C.)CCC    !       InChI=1S/C6H11/c1-4-5-6(2)3/h2-5H2,1H3
C*C2CC*C      !       InChI=1S/C6H10/c1-4-5-6(2)3/h4H,1-2,5H2,3H3
C*CC(C)CC.    !       InChI=1S/C6H11/c1-4-6(3)5-2/h4,6H,1-2,5H2,3H3
C*CC*C.       !       InChI=1S/C4H5/c1-3-4-2/h1,3-4H,2H2
C*CC*CC.C     !       InChI=1S/C6H9/c1-3-5-6-4-2/h3-6H,1H2,2H3
C*CC.CCCC     !       InChI=1S/C7H13/c1-3-5-7-6-4-2/h3,5H,1,4,6-7H2,2H3
C*CC2C2C*C    !       InChI=1S/C8H14/c1-5-7(3)8(4)6-2/h5-8H,1-2H2,3-4H3
C*CC2CC       !       InChI=1S/C6H12/c1-4-6(3)5-2/h4,6H,1,5H2,2-3H3
C*CC2CC*CC    !       InChI=1S/C8H14/c1-4-6-7-8(3)5-2/h4-6,8H,2,7H2,1,3H3
C*CC2CC*CC.   !       InChI=1S/C8H13/c1-4-6-7-8(3)5-2/h4-6,8H,1-2,7H2,3H3
C*CCC*C       !       InChI=1S/C5H8/c1-3-5-4-2/h3-4H,1-2,5H2
C*CCC*CC      !       InChI=1S/C6H10/c1-3-5-6-4-2/h3-4,6H,1,5H2,2H3
C*CCC*CC.C    !       InChI=1S/C7H11/c1-3-5-7-6-4-2/h3-4,6-7H,1,5H2,2H3
C*CCC2        !       InChI=1S/C5H10/c1-4-5(2)3/h4-5H,1H2,2-3H3
C*CCC2C.C     !       InChI=1S/C7H13/c1-4-6-7(3)5-2/h4-5,7H,1,6H2,2-3H3
C*CCCC*CC     !       InChI=1S/C7H12/c1-3-5-7-6-4-2/h3-4,6H,1,5,7H2,2H3
C*CCCC*CC.    !       InChI=1S/C7H11/c1-3-5-7-6-4-2/h3-5H,1-2,6-7H2
C*CCCCC       !       InChI=1S/C6H12/c1-3-5-6-4-2/h3H,1,4-6H2,2H3
C*CCCCC.      !       InChI=1S/C6H11/c1-3-5-6-4-2/h3H,1-2,4-6H2
C.*CCCC       !       InChI=1S/C5H9/c1-3-5-4-2/h1,3H,4-5H2,2H3
C10H9 !      InChI=1S/C10H9/c1-2-6-10-8-4-3-7-9(10)5-1/h1-3,5-8H,4H2
C2.CCC*C      !       InChI=1S/C6H11/c1-4-5-6(2)3/h4,6H,1-2,5H2,3H3
C2C*CC.       !       InChI=1S/C5H9/c1-4-5(2)3/h4H,1H2,2-3H3
C2H3-ME2-CPANE3.  !      InChI=1S/C8H13/c1-3-8-6-4-5-7(8)2/h3,5,7-8H,1,4,6H2,2H3
C5H5-3-C5H4 !       InChI=1S/C10H9/c1-2-6-9(5-1)10-7-3-4-8-10/h1-7H,8H2
C5H5-3-C5H5 !       InChI=1S/C10H10/c1-2-6-9(5-1)10-7-3-4-8-10/h1-5,7H,6,8H2
C5H5C5H4      !       InChI=1S/C10H9/c1-2-6-9(5-1)10-7-3-4-8-10/h1-9H
C5H5C5H5      !       InChI=1S/C10H10/c1-2-6-9(5-1)10-7-3-4-8-10/h1-10H
C6H5C*CC*C    !       InChI=1S/C10H10/c1-2-3-7-10-8-5-4-6-9-10/h2-9H,1H2
C7H15-4       !       InChI=1S/C7H15/c1-3-5-7-6-4-2/h7H,3-6H2,1-2H3
CC*CC*CC.C    !       InChI=1S/C7H11/c1-3-5-7-6-4-2/h3-7H,1-2H3
CC*CCC        !       InChI=1S/C5H10/c1-3-5-4-2/h3,5H,4H2,1-2H3
CC*CCC*CC.    !       InChI=1S/C7H11/c1-3-5-7-6-4-2/h3-6H,1,7H2,2H3
CC*CCC*CC.C !       InChI=1S/C8H13/c1-3-5-7-8-6-4-2/h3-7H,8H2,1-2H3
CC*CCC2*CC.   !       InChI=1S/C8H13/c1-4-6-7-8(3)5-2/h4-6H,2,7H2,1,3H3
CC*CCC2C.C    !       InChI=1S/C8H15/c1-4-6-7-8(3)5-2/h4-6,8H,7H2,1-3H3
CC*CCCC*CC    !       InChI=1S/C8H14/c1-3-5-7-8-6-4-2/h3-6H,7-8H2,1-2H3
CC*CCCC*CC.   !       InChI=1S/C8H13/c1-3-5-7-8-6-4-2/h3-6H,1,7-8H2,2H3
CC*CCCC.C     !       InChI=1S/C7H13/c1-3-5-7-6-4-2/h3-5H,6-7H2,1-2H3
CCC(C.)*C     !       InChI=1S/C5H9/c1-4-5(2)3/h2-4H2,1H3
CH2*CPANE     !       InChI=1S/C6H10/c1-6-4-2-3-5-6/h1-5H2
CH2.CYC5      !       InChI=1S/C6H11/c1-6-4-2-3-5-6/h6H,1-5H2
CHD13 !      InChI=1S/C6H8/c1-2-4-6-5-3-1/h1-4H,5-6H2
CYC5H10       !       InChI=1S/C5H10/c1-2-4-5-3-1/h1-5H2
CYC5H4.CC     !       InChI=1S/C7H9/c1-2-7-5-3-4-6-7/h3-6H,2H2,1H3
CYC5H5CC      !       InChI=1S/C7H10/c1-2-7-5-3-4-6-7/h3-7H,2H2,1H3
CYC5H5CC.     !       InChI=1S/C7H9/c1-2-7-5-3-4-6-7/h3-7H,1-2H2
CYC6H11       !       InChI=1S/C6H11/c1-2-4-6-5-3-1/h1H,2-6H2
C6H12_R6      !       InChI=1S/C6H12/c1-2-4-6-5-3-1/h1-6H2
CYC6H5C*C     !       InChI=1S/C8H8/c1-2-8-6-4-3-5-7-8/h2-7H,1H2
Et4-CHEXE4.   !       InChI=1S/C8H13/c1-2-8-6-4-3-5-7-8/h2-4,8H,5-7H2,1H3
FULVENE       !       InChI=1S/C6H6/c1-6-4-2-3-5-6/h2-5H,1H2
INDENE        !       InChI=1S/C9H8/c1-2-5-9-7-3-6-8(9)4-1/h1-6H,7H2
```

```
INDENE.        !     InChI=1S/C9H7/c1-2-5-9-7-3-6-8(9)4-1/h1-7H
ME.CY13PD      !     InChI=1S/C6H7/c1-6-4-2-3-5-6/h2-4H,1,5H2
ME.CY14PD      !     InChI=1S/C6H7/c1-6-4-2-3-5-6/h2,4-5H,1,3H2
ME1-CPENE      !     InChI=1S/C6H10/c1-6-4-2-3-5-6/h4H,2-3,5H2,1H3
ME3-CHEXE5.    !     InChI=1S/C7H11/c1-7-5-3-2-4-6-7/h3-5,7H,2,6H2,1H3
ME3-CPENE      !     InChI=1S/C6H10/c1-6-4-2-3-5-6/h2,4,6H,3,5H2,1H3
ME3-CPENE3.    !     InChI=1S/C6H9/c1-6-4-2-3-5-6/h2,4H,3,5H2,1H3
ME3-CPENE4.    !     InChI=1S/C6H9/c1-6-4-2-3-5-6/h2,4-6H,3H2,1H3
ME4.-CHEXE     !     InChI=1S/C7H11/c1-7-5-3-2-4-6-7/h2-3,7H,1,4-6H2
ME45-CHEXE4.       !    InChI=1S/C8H13/c1-7-5-3-4-6-8(7)2/h3-4,7-8H,1,5-6H2,2H3
ME4-CPENE      !     InChI=1S/C6H10/c1-6-4-2-3-5-6/h2-3,6H,4-5H2,1H3
MECY24PD       !     InChI=1S/C6H8/c1-6-4-2-3-5-6/h2,4-5H,3H2,1H3
MECYPE1.       !     InChI=1S/C6H11/c1-6-4-2-3-5-6/h2-5H2,1H3
MECYPE4.       !     InChI=1S/C6H11/c1-6-4-2-3-5-6/h2,6H,3-5H2,1H3
toluene(3)     !     InChI=1S/C7H8/c1-7-5-3-2-4-6-7/h2-6H,1H3
C10H11(15)     !     InChI=1S/C10H11/c1-2-6-9(5-1)10-7-3-4-8-10/h1-7,9-10H,8H2
pdt15(16)      !     InChI=1S/C10H11/c1-2-6-9(5-1)10-7-3-4-8-10/h1-5,7,9H,6,8H2
pdt16(17)      !     InChI=1S/C10H11/c1-2-3-4-7-10-8-5-6-9-10/h2-8H,1,9H2
pdt20(18)      !     InChI=1S/C10H11/c1-2-3-4-7-10-8-5-6-9-10/h2-9H,1H3
pdt21(19)      !     InChI=1S/C10H11/c1-8-4-2-5-9-6-3-7-10(8)9/h2-8,10H,1H3
pdt27(20)      !     InChI=1S/C10H11/c1-8-4-2-5-9-6-3-7-10(8)9/h2-6,8H,7H2,1H3
pdt55(23)      !     InChI=1S/C10H11/c1-2-6-9(5-1)10-7-3-4-8-10/h1-6,10H,7-8H2
pdt58(24)      !     InChI=1S/C10H11/c1-2-3-4-7-10-8-5-6-9-10/h2-3,5-9H,1,4H2
C5H6a(28)      !     InChI=1S/C5H6/c1-3-5-4-2/h3,5H,1-2H2
pdt39(34)      !     InChI=1S/C10H11/c1-2-6-9(5-1)10-7-3-4-8-10/h1-3,5,7-9H,4,6H2
C10H10(43)     !     InChI=1S/C10H10/c1-2-6-9(5-1)10-7-3-4-8-10/h1-7,9H,8H2
C10H10(45)     !     InChI=1S/C10H10/c1-2-6-9(5-1)10-7-3-4-8-10/h1-3,5,7-8H,4,6H2
C10H10(46)     !     InChI=1S/C10H10/c1-2-6-9(5-1)10-7-3-4-8-10/h1-3,5-9H,4H2
C10H10(47)     !     InChI=1S/C10H10/c1-2-6-9(5-1)10-7-3-4-8-10/h1,3,5-8H,2,4H2
prod_9(66)     !     InChI=1S/C6H8/c1-6-4-2-3-5-6/h2-4H,5H2,1H3
addC(80)       !     InChI=1S/C7H9/c1-2-7-5-3-4-6-7/h2-5,7H,1,6H2
C7H9(83)       !     InChI=1S/C7H9/c1-3-5-7-6-4-2/h3-7H,1-2H2
C7H9(85)       !     InChI=1S/C7H9/c1-7-5-3-2-4-6-7/h2-5,7H,1,6H2
C7H9J(88)      !     InChI=1S/C7H9/c1-2-6-4-7(3-1)5-6/h1-3,6-7H,4-5H2
S(102)         !     InChI=1S/C10H10/c1-8-6-7-9-4-2-3-5-10(8)9/h2-8H,1H3
C7H8(105)      !     InChI=1S/C7H8/c1-2-6-4-7(3-1)5-6/h1-3,6H,4-5H2
C7H8(106)      !     InChI=1S/C7H8/c1-7-5-3-2-4-6-7/h2-5H,1,6H2
S(109)         !     InChI=1S/C10H10/c1-8-6-9-4-2-3-5-10(9)7-8/h2-8H,1H3
S(110)         !     InChI=1S/C10H10/c1-8-6-9-4-2-3-5-10(9)7-8/h2-6,8H,7H2,1H3
C10H9(112)     !     InChI=1S/C10H9/c1-2-6-9(5-1)10-7-3-4-8-10/h1-3,5-8H,4H2
prod1(114)     !     InChI=1S/C10H9/c1-2-7-10(6-1)8-4-3-5-9(8)10/h1-9H
C10H8(116)     !     InChI=1S/C10H8/c1-2-6-9(5-1)10-7-3-4-8-10/h1-8H
C5H7J(117)     !     InChI=1S/C5H7/c1-3-5-4-2/h1,3-5H,2H3
C6H7(121)      !     InChI=1S/C6H7/c1-6-4-2-3-5-6/h2-6H,1H2
C6H7(122)      !     InChI=1S/C6H7/c1-2-5-4-6(5)3-1/h1-3,5-6H,4H2
prod2(126)     !     InChI=1S/C10H9/c1-2-6-10(7-3-1)8-4-5-9-10/h1-9H
c10h9(128)     !     InChI=1S/C10H9/c1-2-6-10-8-4-3-7-9(10)5-1/h1-9H
C7H7(131)      !     InChI=1S/C7H7/c1-7-5-3-2-4-6-7/h2-6H,1H2
prod5(132)     !     InChI=1S/C10H9/c1-2-3-7-10-8-5-4-6-9-10/h1-9H
C7H10(145)     !     InChI=1S/C7H10/c1-2-7-5-3-4-6-7/h3-5H,2,6H2,1H3
C7H10(146)     !     InChI=1S/C7H10/c1-2-7-5-3-4-6-7/h3,5-6H,2,4H2,1H3
C8H9J(156)     !     InChI=1S/C8H9/c1-2-8-6-4-3-5-7-8/h2-8H,1H2
C10H9(173)     !     InChI=1S/C10H9/c1-8-6-7-9-4-2-3-5-10(8)9/h2-7H,1H3
C10H9(174)     !     InChI=1S/C10H9/c1-8-6-7-9-4-2-3-5-10(8)9/h2-8H,1H2
pdt17(209)     !     InChI=1S/C10H11/c1-2-6-10(7-3-1)8-4-5-9-10/h1-6,8H,7,9H2
pdt18(211)     !     InChI=1S/C10H11/c1-2-3-7-10-8-5-4-6-9-10/h2-8H,1,9H2
C10H9(263)     !     InChI=1S/C10H9/c1-8-4-2-5-9-6-3-7-10(8)9/h2-7H,1H3
S(270)         !     InChI=1S/C10H10/c1-8-4-2-5-9-6-3-7-10(8)9/h2-6,7H2,1H3
S(271)         !     InChI=1S/C10H10/c1-8-4-2-5-9-6-3-7-10(8)9/h2,4-7H,3H2,1H3
S(272)         !     InChI=1S/C10H10/c1-8-4-2-5-9-6-3-7-10(8)9/h2-5,7H,6H2,1H3
norbornene(340)  !    InChI=1S/C7H10/c1-2-7-4-3-6(1)5-7/h1-2,6-7H,3-5H2
```

```
C#CCCC.      !       InChI=1S/C5H7/c1-3-5-4-2/h1H,2,4-5H2
C2C*CC2      !       InChI=1S/C6H12/c1-5(2)6(3)4/h1-4H3
C2H    !     InChI=1S/C2H/c1-2/h1H
C3C    !     InChI=1S/C4H10/c1-4(2)3/h4H,1-3H3
C3H3R  !     InChI=1S/C3H3/c1-3-2/h1H3
C5H8   !     InChI=1S/C5H8/c1-3-5-4-2/h1H,4-5H2,2H3
C6H11R_OLEF_13     !       InChI=1S/C6H11/c1-4-6(3)5-2/h4-6H,1H2,2-3H3
C6H11R_OLEF_22     !       InChI=1S/C6H11/c1-4-5-6(2)3/h4-6H,2H2,1,3H3
C6H12_OLEF_13      !       InChI=1S/C6H12/c1-4-5-6(2)3/h5H,4H2,1-3H3
CCCC   !     InChI=1S/C4H10/c1-3-4-2/h3-4H2,1-2H3
C*CCC.CC     !       InChI=1S/C6H11/c1-3-5-6-4-2/h3,6H,1,4-5H2,2H3
C10H10(C6)   !       InChI=1S/C10H10/c1-2-6-10-8-4-3-7-9(10)5-1/h1-7,10H,8H2
C10H10(C6_2)       !       InChI=1S/C10H10/c1-2-6-10-8-4-3-7-9(10)5-1/h1-10H
C10H11(1)    !       InChI=1S/C10H11/c1-2-3-7-10-8-5-4-6-9-10/h2-6,8-9H,1,7H2
C10H11(12)   !       InChI=1S/C10H11/c1-2-6-10-8-4-3-7-9(10)5-1/h1-7,9-10H,8H2
C10H11(C6)   !       InChI=1S/C10H11/c1-2-6-10-8-4-3-7-9(10)5-1/h1-6,9H,7-8H2
C6H5   !       InChI=1S/C6H5/c1-2-4-6-5-3-1/h1-5H
A(1)   !     InChI=1S/C7H9/c1-7-5-3-2-4-6-7/h2-7H,1H3
C9H10(C5)    !       InChI=1S/C9H10/c1-2-5-9-7-3-6-8(9)4-1/h1-6,8-9H,7H2
C9H11(1)     !       InChI=1S/C9H11/c1-2-6-9-7-4-3-5-8-9/h2-5,7-9H,1,6H2
C9H11(C5)    !       InChI=1S/C9H11/c1-2-5-9-7-3-6-8(9)4-1/h1-5,8-9H,6-7H2
A(5)   !     InChI=1S/C7H9/c1-7-5-3-2-4-6-7/h2-5H,6H2,1H3
B(2)   !     InChI=1S/C7H10/c1-7-5-3-2-4-6-7/h2-3,6H,4-5H2,1H3
A(2)   !     InChI=1S/C7H9/c1-7-5-3-2-4-6-7/h2-3,5-6H,4H2,1H3
C(1)   !     InChI=1S/C7H11/c1-7-5-3-2-4-6-7/h2-3,6-7H,4-5H2,1H3
pdt12(7)     !       InChI=1S/C10H11/c1-2-3-7-10-8-5-4-6-9-10/h2-10H,1H2
A(4)   !     InChI=1S/C7H9/c1-7-5-3-2-4-6-7/h3-6H,2H2,1H3
B(1)   !     InChI=1S/C7H10/c1-7-5-3-2-4-6-7/h3-7H,2H2,1H3
B(3)   !     InChI=1S/C7H10/c1-7-5-3-2-4-6-7/h2-3,5H,4,6H2,1H3
B(4)   !     InChI=1S/C7H10/c1-7-5-3-2-4-6-7/h3,5-6H,2,4H2,1H3
B(5)   !     InChI=1S/C7H10/c1-7-5-3-2-4-6-7/h2-5,7H,6H2,1H3
C(2)   !     InChI=1S/C7H11/c1-7-5-3-2-4-6-7/h2-3,5,7H,4,6H2,1H3
C(3)   !     InChI=1S/C7H11/c1-7-5-3-2-4-6-7/h3,5-7H,2,4H2,1H3
CH3cC6H11    !InChI=1S/C7H14/c1-7-5-3-2-4-6-7/h7H,2-6H2,1H3
CH3S3XcC6H10       !InChI=1S/C7H13/c1-7-5-3-2-4-6-7/h3,7H,2,4-6H2,1H3
SXC7H13            !InChI=1S/C7H13/c1-3-5-7-6-4-2/h3-4H,1,5-7H2,2H3
SAXC7H13     !InChI=1S/C7H13/c1-3-5-7-6-4-2/h3,5H,1,4,6-7H2,2H3
CH3S2XcC6H10       !InChI=1S/C7H13/c1-7-5-3-2-4-6-7/h5,7H,2-4,6H2,1H3
PX7-2C7H13        !InChI=1S/C7H13/c1-3-5-7-6-4-2/h4,6H,1,3,5,7H2,2H3
C2H5cC6H11   !InChI=1S/C8H16/c1-2-8-6-4-3-5-7-8/h8H,2-7H2,1H3
PXCH2cC6H11  !InChI=1S/C7H13/c1-7-5-3-2-4-6-7/h7H,1-6H2
C2H5S3XcC6H10      !InChI=1S/C8H15/c1-2-8-6-4-3-5-7-8/h4,8H,2-3,5-7H2,1H3
S2XC8H15     !InChI=1S/C8H15/c1-3-5-7-8-6-4-2/h3,6H,1,4-5,7-8H2,2H3
SAXC8H15     !InChI=1S/C8H15/c1-3-5-7-8-6-4-2/h3,5H,1,4,6-8H2,2H3


END

THERMO ALL
298.00    600.00   1000.0

AR                       AR  1    0    0    0G   300.000  5000.000 1000.000      1
 2.50104422E+00 0.00000000E+00 0.00000000E+00 0.00000000E+00 0.00000000E+00      2
-7.45686320E+02 4.36103012E+00 2.50104422E+00 0.00000000E+00 0.00000000E+00      3
 0.00000000E+00 0.00000000E+00-7.45686320E+02 4.36103012E+00                     4
N2                       N   2              G   200.000  6000.000 1000.          1
 2.95257637E+00 1.39690040E-03-4.92631603E-07 7.86010195E-11-4.60755204E-15      2
-9.23948688E+02 5.87188762E+00 3.53100528E+00-1.23660988E-04-5.02999433E-07      3
 2.43530612E-09-1.40881235E-12-1.04697628E+03 2.96747038E+00                     4
H2O                      H   2O  1    0    0G   300.000  5000.000 1550.000        1
 2.12664307E+00 3.95064411E-03-1.34445915E-06 2.02233655E-10-1.12832177E-14      2
```

```
-2.96648416E+04 9.94130947E+00 3.99815645E+00-5.64426779E-04 2.69352862E-06    3
-1.38822387E-09 2.22299458E-13-3.02772009E+04-2.19584030E-02                   4
HE                      HE  1    0    0    0G    200.000  6000.000 1000.        1
 2.50000000E+00 0.00000000E+00 0.00000000E+00 0.00000000E+00 0.00000000E+00    2
-7.45375000E+02 9.28723974E-01 2.50000000E+00 0.00000000E+00 0.00000000E+00    3
 0.00000000E+00 0.00000000E+00-7.45375000E+02 9.28723974E-01 0.00000000E+00    4
CH3cC6H11  7/28/ 9 THERMC   7H  14    0    0G    300.000  5000.000 1381.000    11
 2.20212024E+01 3.32076617E-02-1.15857904E-05 1.82324838E-09-1.06797389E-13    2
-3.07694299E+04-1.03212094E+02-8.90848849E+00 9.69226774E-02-5.76085502E-05    3
 1.48743771E-08-1.11357718E-12-1.92643459E+04 6.57804644E+01                   4
CC*CCC.              C  5H  90   00    0G    300.000  5000.000 1383.000         1
 1.39508285E+01 2.01263468E-02-6.69959786E-06 1.02236764E-09-5.86783095E-14    2
 1.35507343E+04-4.64281309E+01 2.78566466E-01 4.91010353E-02-2.92269915E-05    3
 8.60443966E-09-9.79386462E-13 1.86103578E+04 2.80783499E+01                   4
C*CC*CC             C  5  H  8             G250.000   5000.000  995.00          1
 1.26201910E+01 1.92830754E-02-6.35331597E-06 9.66898096E-10-5.56038457E-14    2
 3.32989577E+03-4.18262714E+01 3.20951733E+00 2.07351136E-02 4.62969093E-05    3
-7.10496765E-08 2.72693854E-11 7.00362101E+03 1.25774857E+01                   4
C*C.CC              C  4H  70   00    0G    300.000  5000.000 1384.000          1
 1.09041248E+01 1.56004034E-02-5.15263323E-06 7.81966469E-10-4.47124131E-14    2
 2.31547473E+04-3.17582025E+01 9.73775192E-01 3.65439698E-02-2.13262937E-05    3
 6.17176578E-09-6.88972608E-13 2.68427248E+04 2.23976108E+01                   4
CYPENE4.            C  5  H  7             G250.000   5000.000  995.00          1
 1.16898525E+01 1.87381300E-02-6.28979168E-06 9.69111589E-10-5.61732599E-14    2
 2.18802402E+04-3.98762220E+01 3.31454796E+00 2.88454894E-03 9.22616705E-05    3
-1.15075535E-07 4.16659026E-11 2.59985943E+04 1.28072116E+01                   4
C*CC.               C  3H  50    0    G    300.000  1500.000                    1
-1.04119000e+00 3.69600000e-02-3.26500000e-05 1.59600000e-08-3.23100000e-12    2
 1.90400000e+04 2.72500000e+01-1.04119000e+00 3.69600000e-02-3.26500000e-05    3
 1.59600000e-08-3.23100000e-12 1.90400000e+04 2.72500000e+01                   4
CYC6H10             C  6H  10    0    0G    300.000  5000.000 1392.000          1
 1.60811950E+01 2.53669984E-02-8.74760281E-06 1.36572651E-09-7.95518468E-14    2
-9.52829324E+03-6.79771626E+01-6.42702467E+00 7.69721740E-02-5.37392770E-05    3
 1.91548574E-08-2.77729519E-12-1.62031190E+03 5.32418985E+01                   4
C2H3                C  2  H  3             G250.000   5000.000  995.00          1
 5.13696945E+00 6.11668772E-03-1.88246429E-06 2.70800443E-10-1.48859136E-14    2
 3.36214297E+04-3.85852804E+00 3.79141287E+00-1.86819380E-03 3.03455017E-05    3
-3.48492572E-08 1.22076455E-11 3.45522798E+04 5.95819910E+00                   4
CH3                 C  1  H  3             G250.000   5000.000  995.00          1
 3.38082042E+00 4.98551865E-03-1.50096686E-06 2.12965349E-10-1.16164943E-14    2
 1.64453942E+04 2.61296777E+00 3.93682449E+00 7.92915830E-04 7.77015640E-06    3
-7.97563501E-09 2.54245960E-12 1.64316520E+04 4.20283340E-01                   4
C*CCC.C             C  5H  90   00    0G    300.000  5000.000 1377.000          1
 1.25528869E+01 2.18617958E-02-7.31365206E-06 1.11700907E-09-6.40945021E-14    2
 1.41227434E+04-3.74830182E+01 1.29614698E+00 4.20858948E-02-1.85413979E-05    3
 2.45588348E-09 2.70172155E-13 1.86869030E+04 2.52072403E+01                   4
C*CC.*C             C  4  H  5             G250.000   5000.000  995.00          1
 9.77008116E+00 1.24918304E-02-4.09648338E-06 6.19085886E-10-3.53821382E-14    2
 3.40765245E+04-2.61745867E+01 3.44746329E+00 1.38807267E-02 3.00307035E-05    3
-4.65132913E-08 1.79035327E-11 3.65242766E+04 1.02740842E+01                   4
CYC6H9              C  6H  9    0    0G    300.000  5000.000 1396.000           1
 1.57757308E+01 2.29119263E-02-7.86274116E-06 1.22355692E-09-7.11069741E-14    2
 1.41828333E+04-6.30151719E+01-5.51570747E+00 7.45070998E-02-5.62467883E-05    3
 2.20897753E-08-3.54975415E-12 2.13847403E+04 5.06632363E+01                   4
C*CC*C              C  4  H  6             G250.000   5000.000  995.00          1
 1.19556464E+01 1.22672423E-02-3.93122853E-06 5.85090162E-10-3.30143922E-14    2
 7.85431705E+03-4.17640258E+01 3.25524335E+00 4.79625845E-03 7.13172330E-05    3
-9.27004253E-08 3.41754317E-11 1.16870812E+04 1.07260430E+01                   4
C#CCC               C  4H  60   00    0G    300.000  5000.000 1392.000          1
 1.01146465E+01 1.35087922E-02-4.33746662E-06 6.45591027E-10-3.64359064E-14    2
 1.54407941E+04-2.61830433E+01 1.00560156E+00 3.54102801E-02-2.47645499E-05    3
```

```
   9.43986710E-09-1.50590870E-12 1.85485930E+04 2.25288661E+01             4
C6H11R_OLEF_42          C  6H  110   00   0G   300.000  5000.000 1386.000   1
 1.73497230E+01 2.42992581E-02-8.06718654E-06 1.22899794E-09-7.04669444E-14   2
 9.45352856E+03-6.31618830E+01-9.62104286E-01 6.54822212E-02-4.30992333E-05   3
 1.46845265E-08-2.04781019E-12 1.59777149E+04 3.57601709E+01             4
H2                      H 2             G250.000  5000.000  995.00          1
 3.22770892E+00 3.61118604E-04 1.14741888E-07-4.42240471E-11 3.68714813E-15   2
-9.63053778E+02-2.76293460E+00 3.40382289E+00 5.74298087E-05-3.68915737E-08   3
 4.65683374E-10-2.27012042E-13-1.01811589E+03-3.71227566E+00             4
C.*CC                   C  3H  50   00   0G   300.000  5000.000 1386.000    1
 7.96851074E+00 1.09467224E-02-3.55913400E-06 5.34296872E-10-3.03288114E-14   2
 2.82342610E+04-1.78010231E+01 1.33016068E+00 2.53011885E-02-1.50891258E-05   3
 4.62012972E-09-5.68632486E-13 3.06616838E+04 1.82716598E+01             4
MECY13PD                C  6 H  8             G250.000  5000.000  995.00     1
 1.35155434E+01 2.23997349E-02-7.67892811E-06 1.20176098E-09-7.04912905E-14   2
 6.23974428E+03-5.16805660E+01 3.24645205E+00 1.46783079E-02 7.78307500E-05   3
-1.05580593E-07 3.91927085E-11 1.07092715E+04 1.00007098E+01             4
C6H9R_OLEF_57           C  6H  90   00   0G   300.000  5000.000 1395.000    1
 1.52476429E+01 2.21612950E-02-7.11466688E-06 1.05374080E-09-5.91955565E-14   2
 3.09748694E+04-5.17716276E+01 3.78631346E-03 6.11592505E-02-4.63186728E-05   3
 1.93159320E-08-3.34488058E-12 3.59521077E+04 2.89328843E+01             4
CHD14                   C  6H  8    0    0G   300.000  5000.000 1369.000    1
 1.76883674E+01 2.00067698E-02-7.14996880E-06 1.14314548E-09-6.76953796E-14   2
 3.45242039E+03-8.02538079E+01-5.49947822E+00 6.82134483E-02-4.29985903E-05   3
 1.21493314E-08-1.16666693E-12 1.20744433E+04 4.63551821E+01             4
C*CC.CC                 C  5 H  9             G250.000  5000.000  995.00     1
 1.21894316E+01 2.29650435E-02-7.89876632E-06 1.23905621E-09-7.28360235E-14   2
 8.26099895E+03-3.85268935E+01 3.35662800E+00 2.00665487E-02 5.43662269E-05   3
-7.92670868E-08 2.98996169E-11 1.19200974E+04 1.35962181E+01             4
CC*CCCC                 C  6H  120   00   0G   300.000  5000.000 1383.000    1
 1.77103841E+01 2.64778391E-02-8.83281481E-06 1.35000947E-09-7.75659391E-14   2
-1.56673384E+04-6.80934953E+01-7.08135086E-01 6.57429851E-02-3.96593132E-05   3
 1.18924713E-08-1.39267152E-12-8.87559453E+03 3.21934584E+01             4
MECYPE2.                C  6H  11   0    0G   300.000  5000.000 1402.000    1
 1.60098556E+01 2.69610909E-02-9.16669878E-06 1.41749807E-09-8.20133137E-14   2
 1.19077048E+03-6.57311602E+01-7.69861576E+00 8.47024459E-02-6.33907516E-05   3
 2.47256878E-08-3.93690066E-12 9.15435332E+03 6.07030856E+01             4
C2H4                    C 2 H 4             G250.000  5000.000  995.00       1
 4.45387927E+00 9.40070604E-03-3.08614191E-06 4.68494519E-10-2.68872449E-14   2
 4.06075369E+03-2.89394035E+00 3.87057114E+00-6.52547530E-03 4.84652385E-05   3
-5.25238499E-08 1.79235685E-11 5.08135398E+03 4.46240150E+00             4
CH4                     C 1 H 4             G250.000  5000.000  995.00       1
 1.79580743E+00 9.50671464E-03-3.27779914E-06 5.17040096E-10-3.05675769E-14   2
-9.89071825E+03 9.25644206E+00 4.14960776E+00-6.07725144E-03 2.94431435E-05   3
-2.75886052E-08 8.58430159E-12-1.00560789E+04-5.64708683E-01             4
C.*CCC                  C  4H  70   00   0G   300.000  5000.000 1390.000    1
 1.14109996E+01 1.50775193E-02-4.92003881E-06 7.40761798E-10-4.21419824E-14   2
 2.41294752E+04-3.47941547E+01 9.34428543E-02 4.16407289E-02-2.88401107E-05   3
 1.05944168E-08-1.60991194E-12 2.80439365E+04 2.59388668E+01             4
ME4-CPENE3.             C  6 H 9             G250.000  5000.000  995.00      1
 1.33394673E+01 2.53575239E-02-8.70126684E-06 1.36071605E-09-7.97126238E-14   2
 8.91606345E+03-5.07961938E+01 3.22857846E+00 1.76972614E-03 1.23685962E-04   3
-1.52211571E-07 5.48040398E-11 1.41080961E+04 1.39113592E+01             4
C*CCCC.C                C  6H  110   00   0G   300.000  5000.000 1378.000    1
 1.58134423E+01 2.62055525E-02-8.78833499E-06 1.34501291E-09-7.72927675E-14   2
 9.99107879E+03-5.36030593E+01 1.07866468E+00 5.42160884E-02-2.66383491E-05   3
 5.24474301E-09-1.25304103E-13 1.58027132E+04 2.78965254E+01             4
C6H7R_OLEF_85           C  6H  70   00   0G   300.000  5000.000 1401.000    1
 1.68732328E+01 1.52616566E-02-4.83046409E-06 7.11834226E-10-3.99156834E-14   2
 4.87028098E+04-6.24203505E+01 4.25133781E-01 6.18527691E-02-5.62012937E-05   3
 2.64794351E-08-4.93353042E-12 5.35746468E+04 2.29803386E+01             4
```

```
CC*CC                   C   4H   80   00   0G    300.000   5000.000 1377.000    1
 1.10278429E+01 1.79778091E-02-5.99064462E-06 9.14791566E-10-5.25221749E-14    2
-7.40468650E+03-3.58028425E+01 7.39903864E-01 3.73000350E-02-1.78363117E-05    3
 3.13265966E-09 4.51791572E-14-3.33756876E+03 2.11605814E+01                   4
C6H7R_OLEF_2            C   6H   70   00   0G    300.000   5000.000 1390.000    1
 1.55810239E+01 1.65720182E-02-5.49866038E-06 8.38169845E-10-4.80901574E-14    2
 5.13996188E+04-5.25699854E+01 1.09154560E+00 5.14482539E-02-3.79702572E-05    3
 1.47557167E-08-2.35915029E-12 5.63263633E+04 2.48801694E+01                   4
CC*CCC.C                C   6H  110   00   0G    300.000   5000.000 1375.000    1
 1.54112939E+01 2.65816951E-02-8.95846989E-06 1.37554437E-09-7.92131366E-14    2
 8.58631901E+03-5.18122700E+01 1.63774968E+00 5.05310519E-02-2.10853067E-05    3
 1.93241307E-09 5.70666671E-13 1.42572185E+04 2.51882346E+01                   4
C*C*CC*C.C              C   6H   70   00   0G    300.000   5000.000 1395.000    1
 1.59802721E+01 1.61182137E-02-5.22557035E-06 7.83481478E-10-4.44520339E-14    2
 4.78578188E+04-5.68376495E+01 1.13024359E+00 5.49769242E-02-4.50152744E-05    3
 1.95531582E-08-3.44565284E-12 5.25927413E+04 2.14295709E+01                   4
CYC5H9.                 C   5H   9    0   0G    300.000   5000.000 1378.000    1
 1.24946381E+01 2.23549938E-02-7.51362241E-06 1.15415415E-09-6.65065318E-14    2
 6.45390040E+03-4.65796398E+01-5.78089755E+00 5.92878731E-02-3.26281412E-05    3
 7.06409844E-09-1.75407888E-13 1.32581249E+04 5.34176945E+01                   4
C*CC*CCC.               C   6H   90   00   0G    300.000   5000.000 1398.000    1
 1.71103713E+01 1.95732877E-02-6.28292006E-06 9.35655448E-10-5.28543559E-14    2
 2.33520860E+04-6.24467584E+01-1.92535116E+00 7.00031213E-02-5.83565449E-05    3
 2.55977310E-08-4.52314896E-12 2.93338771E+04 3.76184250E+01                   4
CC*CC.C                 C   5H   90   00   0G    300.000   5000.000 1383.000    1
 1.39300622E+01 2.06694554E-02-6.92242374E-06 1.05912215E-09-6.08755907E-14    2
 5.58904734E+03-5.04428048E+01-8.01436277E-01 5.19717772E-02-3.12688918E-05    3
 9.21890340E-09-1.03864473E-12 1.10209142E+04 2.97874223E+01                   4
CCC                     C   3H   80   0    G    300.000   1500.000               1
 3.09800000e-01 3.19600000e-02-1.09800000e-05-2.20100000e-09 1.67200000e-12    2
-1.42100000e+04 2.18200000e+01 3.09800000e-01 3.19600000e-02-1.09800000e-05    3
-2.20100000e-09 1.67200000e-12-1.42100000e+04 2.18200000e+01                   4
CYC5H8                  C 5 H 8          G250.000   5000.000   995.00           1
 1.09471908E+01 2.20004767E-02-7.50750599E-06 1.17198302E-09-6.86090646E-14    2
-1.49895259E+03-3.76255775E+01 3.41284343E+00-2.95321012E-03 1.13384138E-04    3
-1.35616965E-07 4.83167358E-11 2.73519148E+03 1.24276946E+01                   4
C*CCC2.                 C   5H   90   00   0G    300.000   5000.000 1396.000    1
 1.27473248E+01 2.16806739E-02-6.90664871E-06 1.01692977E-09-5.68882738E-14    2
 1.46987538E+04-4.00461281E+01-8.00950619E-01 5.58578042E-02-4.07401424E-05    3
 1.65463991E-08-2.81532770E-12 1.91717327E+04 3.18544234E+01                   4
C2CCC.                  C   5H  110   00   0G    300.000   5000.000 1386.000    1
 1.53749278E+01 2.36488372E-02-7.80352198E-06 1.18247532E-09-6.75336739E-14    2
-2.09179419E+03-5.61974544E+01-7.33806094E-01 5.93339807E-02-3.75727296E-05    3
 1.23449569E-08-1.66217380E-12 3.71276545E+03 3.10340773E+01                   4
CY13PD                  C 5 H 6          G250.000   5000.000   995.00           1
 8.54224876E+00 2.14442757E-02-8.49864028E-06 1.54187677E-09-1.04980310E-13    2
 1.27177699E+04-2.43630856E+01 2.02640754E-01 2.16857125E-02 4.89543516E-05    3
-8.47163463E-08 3.67450866E-11 1.59781268E+04 2.38173249E+01 1.72796300E+04    4
CYC6H9A                 C   6H   9    0   0G    300.000   5000.000 1397.000    1
 1.58947534E+01 2.28094575E-02-7.82756299E-06 1.21812113E-09-7.07938932E-14    2
 6.91420824E+03-6.48620185E+01-6.19827413E+00 7.68379097E-02-5.89414439E-05    3
 2.34266254E-08-3.79372950E-12 1.43242497E+04 5.28987999E+01                   4
C#CC                    C   3H   40   0    G    300.000   1500.000               1
 4.44044000e-01 2.79100000e-02-2.29700000e-05 1.06500000e-08-2.08600000e-12    2
 2.14500000e+04 1.92800000e+01 4.44044000e-01 2.79100000e-02-2.29700000e-05    3
 1.06500000e-08-2.08600000e-12 2.14500000e+04 1.92800000e+01                   4
CCCC.                   C   4H   90   00   0G    300.000   5000.000 1383.000    1
 1.21292760E+01 1.92303581E-02-6.35210364E-06 9.63442844E-10-5.50587041E-14    2
 3.14649752E+03-3.87691952E+01 2.50236717E-01 4.39975071E-02-2.51204523E-05    3
 7.02130797E-09-7.38569852E-13 7.58942478E+03 2.61197949E+01                   4
H                       H 1             G250.000   5000.000   995.00           1
```

```
    2.50000000E+00-7.95201043E-16 3.26879084E-19-5.29212490E-23 3.32525944E-27    2
    2.54724189E+04-4.55747022E-01 2.50000000E+00-1.16585069E-14 2.88298298E-17    3
   -2.72743723E-20 8.88391551E-24 2.54724189E+04-4.55747022E-01                   4
C*C*C              C  3H   40   00    0G   300.000  5000.000 1398.000            1
    7.62282540E+00 9.02079046E-03-2.84486166E-06 4.18164325E-10-2.34048079E-14    2
    2.00277136E+04-1.78500629E+01 6.72827931E-01 2.67900841E-02-2.05084351E-05    3
    8.48363518E-09-1.43885647E-12 2.22765341E+04 1.89127736E+01                   4
C*CCCC             C  5H  100   00    0G   300.000  5000.000 1386.000            1
    1.48559323E+01 2.17591025E-02-7.19194271E-06 1.09245029E-09-6.25175564E-14    2
   -1.01357366E+04 5.37935447E+01-1.03155314E+00 5.71908168E-02-3.69342122E-05    3
    1.22979706E-08-1.66699878E-12-4.44795547E+03 3.21336978E+01                   4
C2H5               C  2 H  5            G250.000   5000.000  995.00              1
    4.74777319E+00 1.14086285E-02-3.81375099E-06 5.87463020E-10-3.41128644E-14    2
    1.22404195E+04-1.52590277E+00 3.87193994E+00-3.57531865E-04 3.69680741E-05    3
   -4.21755109E-08 1.45890315E-11 1.31715059E+04 6.49792536E+00                   4
C5H5R_OLEF_7       C  5H   50   00    0G   300.000  5000.000 1401.000            1
    1.01505802E+01 1.59876252E-02-5.18072650E-06 7.71253848E-10-4.35045929E-14    2
    3.54441480E+04-3.37682370E+01-6.74028831E+00 5.95481236E-02-4.84388138E-05    3
    2.03252598E-08-3.41829547E-12 4.08192259E+04 5.53570369E+01                   4
CCC.               C  3 H  7            G250.000   5000.000  995.00              1
    7.30431994E+00 1.64557482E-02-5.52962303E-06 8.54945669E-10-4.97776639E-14    2
    8.62895463E+03-1.30921375E+01 3.67314085E+00 8.10468193E-03 4.16530868E-05    3
   -5.39342658E-08 1.95389722E-11 1.04876498E+04 1.01167533E+01                   4
CYC6H7             C  6 H  7            G250.000   5000.000  995.00              1
    1.35382730E+01 1.96580119E-02-6.57919738E-06 1.01114272E-09-5.84824728E-14    2
    1.84873078E+04-5.00530569E+01 3.16325139E+00 4.96970340E-03 1.00577180E-04    3
   -1.27740795E-07 4.66004147E-11 2.33438960E+04 1.39777610E+01                   4
CC*CCCC.           C  6H  110   00    0G   300.000  5000.000 1383.000            1
    1.72344752E+01 2.44534656E-02-8.17417936E-06 1.25095526E-09-7.19334388E-14    2
    9.36514899E+03-6.26896173E+01 7.11982681E-02 6.11627994E-02-3.71777513E-05    3
    1.12841645E-08-1.34881341E-12 1.56848440E+04 3.07248261E+01                   4
ME.CY3PE           C  6H   9   0    0G   300.000  5000.000 1397.000             1
    1.55253807E+01 2.26952550E-02-7.78674225E-06 1.21154467E-09-7.04009230E-14    2
    1.66821247E+04-6.06580293E+01-5.56694215E+00 7.36839564E-02-5.53767882E-05    3
    2.15935138E-08-3.43929665E-12 2.38203827E+04 5.19864005E+01                   4
C5H7R_OLEF_4       C  5H   70   00    0G   300.000  5000.000 1394.000            1
    1.31582023E+01 1.59913089E-02-5.17224017E-06 7.74154500E-10-4.38730610E-14    2
    3.61613624E+04-4.05342701E+01-3.68500495E-01 4.99607908E-02-3.83484099E-05    3
    1.56931663E-08-2.63151754E-12 4.06089732E+04 3.12508702E+01                   4
C*CCCC*C           C  6H  100   00    0G   300.000  5000.000 1389.000            1
    1.71030051E+01 2.22520476E-02-7.36290668E-06 1.12019727E-09-6.41933515E-14    2
    1.61094466E+03-6.33817222E+01-1.58111740E+00 6.60376180E-02-4.66425841E-05    3
    1.72030216E-08-2.60295960E-12 8.07157628E+03 3.68924287E+01                   4
C6H7R_OLEF_91      C  6H   70   00    0G   300.000  5000.000 1404.000            1
    1.73860768E+01 1.52187181E-02-4.77907548E-06 6.98892931E-10-3.89733397E-14    2
    3.68648099E+04-6.72199557E+01-1.45979557E+00 7.00668544E-02-6.65076238E-05    3
    3.20906011E-08-6.05069158E-12 4.22768033E+04 3.00711258E+01                   4
C*CCCC.            C  5H   90   00    0G   300.000  5000.000 1386.000            1
    1.44005264E+01 1.97092525E-02-6.52672481E-06 9.92646930E-10-5.68527283E-14    2
    1.49179297E+04-4.85075997E+01-2.58380960E-01 5.26374151E-02-3.44775847E-05    3
    1.16929988E-08-1.62204571E-12 2.01435390E+04 3.06932604E+01                   4
C*CCC.C*C          C  6H   90   00    0G   300.000  5000.000 1394.000            1
    1.69217162E+01 2.02745051E-02-6.64939177E-06 1.00413073E-09-5.72454107E-14    2
    1.87471882E+04-6.27655758E+01-2.18694516E+00 6.81744607E-02-5.32242977E-05    3
    2.18126748E-08-3.63901712E-12 2.50260820E+04 3.86524442E+01                   4
C*C.CCC            C  5H   90   00    0G   300.000  5000.000 1393.000            1
    1.51281236E+01 1.94672484E-02-6.36000283E-06 9.56509512E-10-5.43548307E-14    2
    6.48551508E+03-5.60802180E+01-1.26889762E+00 6.00957525E-02-4.54439072E-05    3
    1.82672238E-08-3.01555274E-12 1.19341632E+04 3.11362643E+01                   4
CC*C.CC            C  5H   90   00    0G   300.000  5000.000 1380.000            1
    1.37353741E+01 2.03439296E-02-6.79753127E-06 1.03964039E-09-5.97474299E-14    2
```

```
     1.76402734E+04-4.59206529E+01 1.29040803E+00 4.51418975E-02-2.41474358E-05      3
     5.84115878E-09-4.33028114E-13 2.24208168E+04 2.24860310E+01                      4
CYPENE3.              C  5 H  7          G250.000   5000.000  995.00         1
     1.06474261E+01 2.02650090E-02-6.96375857E-06 1.08993650E-09-6.38709230E-14      2
     1.38512698E+04-3.66655051E+01 3.44073715E+00-6.76555946E-03 1.18203983E-04      3
    -1.39331253E-07 4.94268405E-11 1.80578173E+04 1.19976209E+01                      4
CCCC.C                C  5H  110   00   0G    300.000   5000.000 1374.000        1
     1.35801553E+01 2.57007789E-02-8.61531433E-06 1.31717179E-09-7.56204233E-14      2
    -1.81397687E+03-4.40993293E+01 1.61305710E+00 4.54134320E-02-1.69608936E-05      3
     3.43375656E-10 8.11921117E-13 3.23568098E+03 2.32124148E+01                      4
C*CCC                 C  4H  80    0    G    300.000   1500.000 1387.000        1
     1.26432000e+01-3.29800000e-02 1.04000000E-04-8.60400000E-08 2.30500000E-11      2
    -3.01500000e+03-2.90500000e+01 1.26432000e+01-3.29800000e-02 1.04000000E-04      3
    -8.60400000e-08 2.30500000e-11-3.01500000e+03-2.90500000e+01                      4
C6H9R_OLEF_56         C  6H  90    00   0G    300.000   5000.000 1379.000        1
     1.50776632E+01 2.23181031E-02-7.51903351E-06 1.15404708E-09-6.64397089E-14      2
     3.03850371E+04-4.93557387E+01 2.11290738E+00 4.73071139E-02-2.39636704E-05      3
     5.11078024E-09-2.32118509E-13 3.54660923E+04 2.22351298E+01                      4
CC.C                  C  3H  70    00   0G    300.000   5000.000 2005.000        1
     6.64310809E+00 1.76632020E-02-6.16182917E-06 9.72800565E-10-5.72132951E-14      2
     6.92489529E+03-1.01243352E+01 1.26930988E+00 2.59284993E-02-8.24926075E-06      3
    -6.26105316E-10 5.66591257E-13 9.11166358E+03 2.01341842E+01                      4
C2H2                  C  2 H  2          G250.000   5000.000  995.00         1
     5.55471770E+00 3.18957832E-03-7.24857154E-07 7.23331981E-11-2.51539262E-15      2
     2.54058225E+04-9.25224497E+00 3.16199256E+00 4.47311476E-03 9.90510161E-06      3
    -1.54679125E-08 6.01696129E-12 2.62946259E+04 4.35281165E+00                      4
C*C*CC*C.             C  5H  50    00   0G    300.000   5000.000 1405.000        1
     1.36558977E+01 1.08518034E-02-3.34807788E-06 4.84602881E-10-2.68465864E-14      2
     5.42966301E+04-4.56608695E+01-6.67215895E-02 5.14757556E-02-4.97079493E-05      3
     2.43064162E-08-4.62253667E-12 5.81655338E+04 2.49327338E+01                      4
C*CC                  C  3H  60    0    G    300.000   1500.000                 1
     6.52688000e-01 2.66300000e-02-1.05000000e-05-6.17800000e-10 1.05200000e-12      2
     1.04900000e+03 2.08000000e+01 6.52688000e-01 2.66300000e-02-1.05000000e-05      3
    -6.17800000e-10 1.05200000e-12 1.04900000e+03 2.08000000e+01                      4
CC*CC.                C  4 H  7          G250.000   5000.000  995.00         1
     9.00592483E+00 1.82962505E-02-6.29119816E-06 9.86908242E-10-5.80241836E-14      2
     1.21946209E+04-2.24194410E+01 3.59557341E+00 1.17960970E-02 4.60927734E-05      3
    -6.26412695E-08 2.30966904E-11 1.46698268E+04 1.06828242E+01                      4
C6H10_OLEF_17         C  6H  100   00   0G    300.000   5000.000 1397.000        1
     1.75702119E+01 2.16172947E-02-6.94584290E-06 1.03508221E-09-5.84967660E-14      2
    -1.72310860E+03-6.77572748E+01-2.70633902E+00 7.45959873E-02-6.08701035E-05      3
     2.62352998E-08-4.57474014E-12 4.72326967E+03 3.90938822E+01                      4
CY13PD5.              C  5 H  5          G250.000   5000.000  995.00         1
     9.56337366E+00 1.74277088E-02-6.86085196E-06 1.23916759E-09-8.41087417E-14      2
     2.81845298E+04-2.81373712E+01 5.16970848E-01 2.76670206E-02 2.33775674E-05      3
    -5.70072196E-08 2.66905847E-11 3.12367412E+04 2.17162771E+01 3.27225830E+04      4
C*CC.CCC              C  6H  110   00   0G    300.000   5000.000 1389.000        1
     1.80253708E+01 2.41255461E-02-7.99497365E-06 1.21508898E-09-6.95453883E-14      2
     2.59599220E+03-6.98935509E+01-1.67092996E+00 7.04546430E-02-4.98293638E-05      3
     1.85057353E-08-2.83100082E-12 9.39727137E+03 3.57648479E+01                      4
C#CC.                 C  3H  30    00   0G    300.000   5000.000 1408.000        1
     5.97267636E+00 8.72048085E-03-2.61041135E-06 3.63542319E-10-1.94760001E-14      2
     3.95927159E+04-5.80819449E+00 1.65624248E+00 2.23786482E-02-1.92521682E-05      3
     9.41110668E-09-1.84566147E-12 4.07474390E+04 1.61268904E+01                      4
C*C(C)CC.             C  5H  90    00   0G    300.000   5000.000 1386.000        1
     1.43384820E+01 1.97919496E-02-6.53760081E-06 9.92081589E-10-5.67242623E-14      2
     1.32346016E+04-4.89324582E+01 4.68545013E-01 5.08287869E-02-3.28321734E-05      3
     1.10701587E-08-1.53859015E-12 1.82022025E+04 2.60667610E+01                      4
CC.*CC                C  4H  70    00   0G    300.000   5000.000 1372.000        1
     1.03320448E+01 1.61768613E-02-5.43223765E-06 8.33386702E-10-4.79812129E-14      2
     2.17589915E+04-2.91623411E+01 2.53889446E+00 2.87212472E-02-1.02182629E-05      3
```

```
-2.71525032E-10 6.42033719E-13 2.50725726E+04 1.47691902E+01                      4
C#CC*C                    C  4  H  4          G250.000   5000.000   995.00         1
 9.04541763E+00 1.03871808E-02-3.32212637E-06 4.91824173E-10-2.76553801E-14       2
 3.08686673E+04-2.28856712E+01 3.47803575E+00 1.18315513E-02 2.60611301E-05       3
-4.03398290E-08 1.55437552E-11 3.30130762E+04 9.15414001E+00                      4
C*C*CC                    C  4H  6O  0    G   300.000  1500.000                    1
 1.05031000e+00 3.35100000e-02-1.93100000e-05 4.88500000e-09-2.60300000e-13       2
 1.77800000e+04 1.98900000e+01 1.05031000e+00 3.35100000e-02-1.93100000e-05       3
 4.88500000e-09-2.60300000e-13 1.77800000e+04 1.98900000e+01                      4
C*C.C                     C  3H  50  00   0G   300.000  5000.000 1374.000          1
 0.61101805E+01 0.14673395E-01-0.53676822E-05 0.86904932E-09-0.51932006E-13       2
 0.25532442E+05-0.83555712E+01 0.25544033E+01 0.10986798E-01 0.30174305E-04       3
-0.47253568E-07 0.19771073E-10 0.27150242E+05 0.13207592E+02 0.28582707E+05       4
CC*CC.CC                  C  6H  110  00  0G   300.000  5000.000 1386.000          1
 1.73411293E+01 2.48324385E-02-8.28915784E-06 1.26589723E-09-7.26833480E-14       2
 1.45484137E+03-6.72502063E+01-2.03939278E+00 6.83311874E-02-4.50879773E-05       3
 1.52566757E-08-2.09665621E-12 8.35784277E+03 3.74582617E+01                      4
C2H6                      C  2H  6O  0    G   300.000  1500.000 1385.000           1
 1.47024000e+00 1.57400000e-02 3.43900000e-06-9.10200000e-09 3.02700000e-12       2
-1.15400000e+04 1.43800000e+01 1.47024000e+00 1.57400000e-02 3.43900000e-06       3
-9.10200000e-09 3.02700000e-12-1.15400000e+04 1.43800000e+01                      4
C*CCC.                    C  4  H  7          G250.000   5000.000   995.00         1
 9.01129493E+00 1.78224718E-02-6.11882433E-06 9.61533885E-10-5.66587059E-14       2
 2.08621124E+04-2.02163898E+01 3.61805296E+00 1.70792436E-02 2.88046477E-05       3
-4.50844246E-08 1.72023007E-11 2.30455089E+04 1.13542111E+01                      4
C*CC.C*C                  C  5  H  7          G250.000   5000.000   995.00         1
 1.21100701E+01 1.81366348E-02-5.74950057E-06 8.40260753E-10-4.66828667E-14       2
 1.75046152E+04-3.91194455E+01 3.07025477E+00 1.52135202E-02 5.78441967E-05       3
-8.14214479E-08 3.05842632E-11 2.12473267E+04 1.42144852E+01                      4
C#CC.C                    C  4  H  5          G250.000   5000.000   995.00         1
 8.79521050E+00 1.31541041E-02-4.43334152E-06 6.85004021E-10-3.98388370E-14       2
 3.48300463E+04-1.91847953E+01 3.57930669E+00 1.61259055E-02 1.82148606E-05       3
-3.26645265E-08 1.29055942E-11 3.67589447E+04 1.04296413E+01                      4
CCC.C                     C  4H  90  00   0G   300.000  5000.000 1371.000          1
 1.03004042E+01 2.13639548E-02-7.13730002E-06 1.08806685E-09-6.23362617E-14       2
 2.32046100E+03-2.78575581E+01 1.81936554E+00 3.33607633E-02-9.03129347E-06       3
-2.32329667E-09 1.17866889E-12 6.11094177E+03 2.05700953E+01                      4
BENZENE                   C  6  H  6          G250.000   5000.000   995.00         1
 1.26767192E+01 1.77039663E-02-5.88135612E-06 8.98454171E-10-5.17051712E-14       2
 3.85789357E+03-4.91638510E+01 3.21118589E+00-1.47463528E-03 1.09301575E-04       3
-1.34073726E-07 4.83816863E-11 8.57478417E+03 1.06912516E+01                      4
C2CC.                     C  4H  9  0    0G   300.000  5000.000 1388.000           1
 1.21606184E+01 1.97410873E-02-6.79331097E-06 1.05883041E-09-6.15941215E-14       2
 1.89429181E+03-3.99434775E+01-2.41823941E-01 4.59113706E-02-2.75593803E-05       3
 8.50493368E-09-1.09259320E-12 6.56265361E+03 2.77944816E+01                      4
C3C.                      C  4H  9  0    0G   300.000  5000.000 1371.000           1
 1.06255654E+01 2.10520049E-02-7.24673634E-06 1.12970527E-09-6.57239734E-14       2
 8.99515063E+01-3.48930806E+01 3.00309826E+00 2.87551563E-02-2.88463154E-06       3
-5.91231913E-09 1.91820725E-12 3.85174260E+03 9.80237511E+00                      4
C2C*C                     C  4H  8  0    0G   300.000  5000.000 1388.000           1
 1.12258330E+01 1.81795798E-02-6.20348592E-06 9.61444458E-10-5.57088057E-14       2
-7.69983777E+03-3.73306704E+01 9.38433173E-01 3.90547287E-02-2.16437148E-05       3
 5.87267077E-09-6.14435479E-13-3.74817891E+03 1.91442985E+01                      4
C2C*C.                    C  4H  7  0    0G   300.000  5000.000 1389.000           1
 1.10957600E+01 1.57810049E-02-5.38419615E-06 8.34360121E-10-4.83401481E-14       2
 2.24175827E+04-3.40426822E+01 1.87632434E+00 3.54486107E-02-2.13104949E-05       3
 6.73400492E-09-9.03166339E-13 2.58712914E+04 1.62429161E+01                      4
C2.C*C                    C  4H  7  0    0G   300.000  5000.000 1386.000           1
 1.20751223E+01 1.53848479E-02-5.34522638E-06 8.38553838E-10-4.90033930E-14       2
 1.02792066E+04-4.16923478E+01 2.32429586E-01 4.23582063E-02-2.93986340E-05       3
 1.09304927E-08-1.73072388E-12 1.45426253E+04 2.22928497E+01                      4


                    Page-202
```

```
C6H13R_8                      C 6 H 13           G   3E+02    1E+03    6E+02         1
 2.03977783E+00 5.28033178E-02-9.42672497E-06-1.67159938E-08 8.49829047E-12         2
-8.97200085E+02 1.84780605E+01 2.03977783E+00 5.28033178E-02-9.42672497E-06         3
-1.67159938E-08 8.49829047E-12-8.97200085E+02 1.84780605E+01                        4
C2C.CC                        C   5H  11   0   0G   300.000  5000.000 1378.000       1
 1.39073137E+01 2.54249890E-02-8.74289372E-06 1.36202712E-09-7.92041157E-14         2
-4.05125857E+03-4.79619044E+01 2.42901065E+00 4.24407315E-02-1.30562253E-05         3
-1.97621133E-09 1.29529180E-12 1.01587957E+03 1.73279484E+01                        4
C2C*CC                        C   5H  10   0   0G   300.000  5000.000 1385.000       1
 1.39945443E+01 2.29446582E-02-7.82594153E-06 1.21260230E-09-7.02518457E-14         2
-1.31576943E+04-5.04083848E+01 1.20274147E+00 4.78872107E-02-2.48144766E-05         3
 5.73514355E-09-3.91266685E-13-8.15212335E+03 2.01592579E+01                        4
C2CC.C2                       C   6H  13   0   0G   300.000  5000.000 1382.000       1
 1.72636647E+01 2.98860721E-02-1.03029673E-05 1.60781818E-09-9.36098414E-14         2
-8.60075173E+03-6.54282999E+01 1.18032830E+00 5.89645469E-02-2.72495146E-05         3
 4.45927638E-09 1.08370225E-13-2.03623910E+03 2.41787594E+01                        4
a2                            C 10 H  8           G250.000   5000.000  995.00        1
 1.88932067E+01 2.93950430E-02-1.00738902E-05 1.57111221E-09-9.18229630E-14         2
 8.97132774E+03-8.17698032E+01 2.79311186E+00 2.01362562E-02 1.15406329E-04         3
-1.57218086E-07 5.85760475E-11 1.58378019E+04 1.42271544E+01                        4
C*C(C)C.C                     C   5H   9   0   0G   300.000  5000.000 1391.000       1
 1.44097619E+01 2.05368238E-02-7.01029136E-06 1.08682831E-09-6.29905018E-14         2
 5.08792724E+03-5.21221602E+01 1.98024477E-01 5.27870144E-02-3.52636898E-05         3
 1.25416751E-08-1.88227749E-12 1.01773154E+04 2.46388562E+01                        4
C*C(C)CCC.                    C   6H  11   0   0G   300.000  5000.000 1391.000       1
 1.73660563E+01 2.47543194E-02-8.45119156E-06 1.31035396E-09-7.59514758E-14         2
 9.16086456E+03-6.38235508E+01 2.49943006E-01 6.30361731E-02-4.11725030E-05         3
 1.41157447E-08-2.02238094E-12 1.53316983E+04 2.87984616E+01                        4
C*C(C.)CCC                    C   6H  11   0   0G   300.000  5000.000 1395.000       1
 1.82026718E+01 2.44812048E-02-8.35996384E-06 1.29643763E-09-7.51546950E-14         2
 2.33876532E+03-7.06546759E+01-1.47932805E+00 7.22802333E-02-5.37942381E-05         3
 2.13741487E-08-3.53072969E-12 9.04209177E+03 3.44874859E+01                        4
C*C2CC*C                      C   6H  10   0   0G   300.000  5000.000 1385.000       1
 1.74835555E+01 2.33022983E-02-8.12229539E-06 1.27703467E-09-7.47438738E-14         2
-4.27145620E+02-6.96127438E+01-1.17304406E+00 6.48535274E-02-4.38408615E-05         3
 1.55461220E-08-2.32628592E-12 6.36039564E+03 3.14833690E+01                        4
C*CC(C)CC.                    C   6H  11   0   0G   300.000  5000.000 1394.000       1
 1.73861820E+01 2.48639479E-02-8.51628366E-06 1.32329621E-09-7.68158066E-14         2
 9.82508224E+03-6.45964415E+01-1.18772130E+00 6.79720472E-02-4.72509497E-05         3
 1.74232687E-08-2.68819423E-12 1.63584394E+04 3.53476416E+01                        4
C*CC*C.                       C 4 H 5             G250.000   5000.000  995.00        1
 1.23776496E+01 9.05826570E-03-2.66197795E-06 3.66550547E-10-1.93463815E-14         2
 3.81463434E+04-4.16531920E+01 3.14692687E+00 1.03428831E-02 4.94025216E-05         3
-7.06960726E-08 2.69248870E-11 4.17567334E+04 1.17449969E+01                        4
C*CC*CC.C                     C   6H   90   0   G   300.000  5000.000  995.043       1
 1.36288339E+01 2.45055787E-02-8.07546311E-06 1.23042786E-09-7.08589527E-14         2
 1.27234636E+04-4.54653810E+01 2.56830777E+00 2.90638735E-02 4.52075606E-05         3
-7.47713655E-08 2.91501468E-11 1.69000816E+04 1.77668995E+01                        4
C*CC.CCCC                     C   7H  13   0   0G   300.000  5000.000 1392.000       1
 2.06977799E+01 2.93585249E-02-9.99754351E-06 1.54773305E-09-8.96230815E-14         2
-1.23454647E+03-8.35627043E+01-2.01707658E+00 8.08915559E-02-5.43383904E-05         3
 1.88066108E-08-2.66059253E-12 6.81102828E+03 3.89797235E+01                        4
C*CC2C2C*C                    C   8H  14O   0   G   300.000  5000.000 1397.000       1
 2.31216526E+01 3.22679047E-02-1.10624691E-05 1.72001335E-09-9.98889563E-14         2
-8.54417127E+03-9.64070233E+01-3.39329492E+00 9.64829297E-02-7.17993705E-05         3
 2.83771811E-08-4.65159749E-12 4.94547635E+02 4.52834596E+01                        4
C*CC2CC                       C   6H  12   0   0G   300.000  5000.000 1395.000       1
 1.77647790E+01 2.70640158E-02-9.26909165E-06 1.44014826E-09-8.35925744E-14         2
-1.52266214E+04-7.01703436E+01-1.94060316E+00 7.24156002E-02-4.95665820E-05         3
 1.79679943E-08-2.72638950E-12-8.25548278E+03 3.59999294E+01                        4
C*CC2CC*CC                    C   8H  14O   0   G   300.000  5000.000 1392.000       1
```

```
                                2.27569297E+01 3.20337404E-02-1.08965939E-05 1.76766038E-09-1.07658054E-13    2
                               -8.79858434E+03-9.24488993E+01-3.52871122E+00 9.64527709E-02-7.25420541E-05    3
                                2.91089521E-08-4.81755217E-12 6.33485942E+01 4.77114052E+01                   4
C*CC2CC*CC.              C   8H  13O   0         G   300.000  5000.000 1429.000              1
  2.06044827E+01 3.28438922E-02-1.02124819E-05 1.48173684E-09-8.18503766E-14                2
  1.11062105E+04-7.85311763E+01-5.41553369E+00 1.09294255E-01-9.59247533E-05                3
  4.44822053E-08-8.15825083E-12 1.84010148E+04 5.53569281E+01                                4
C*CCC*C                  C   5H   8   0   0G     300.000  5000.000 1384.000              1
  1.42768623E+01 1.88159014E-02-6.57659206E-06 1.03593904E-09-6.07122376E-14                2
  5.39346728E+03-5.30057983E+01-1.75387474E+00 5.48379612E-02-3.78390191E-05                3
  1.36354531E-08-2.06221527E-12 1.11819982E+04 3.37287469E+01                                4
C*CCC*CC                 C   6H  10   0   0G     300.000  5000.000 1384.000              1
  1.69466806E+01 2.37401746E-02-8.26935463E-06 1.29957655E-09-7.60397786E-14                2
 -2.44118906E+01-6.55228850E+01-1.39746950E+00 6.33921002E-02-4.07814788E-05                3
  1.34649374E-08-1.85010966E-12 6.76101988E+03 3.42921290E+01                                4
C*CCC*CC.C               C   7H  11O   0         G   300.000  5000.000 1388.000              1
  1.99615117E+01 2.67949058E-02-8.90403101E-06 1.35726309E-09-7.77930107E-14                2
  1.29586403E+04-8.09620265E+01-3.25044213E+00 7.74144755E-02-4.85168539E-05                3
  1.41791003E-08-1.42983928E-12 2.12209809E+04 4.47146303E+01                                4
C*CCC2                   C   5H  10   0   0G     300.000  5000.000 1393.000              1
  1.46491909E+01 2.25422061E-02-7.72053001E-06 1.19958604E-09-6.96317745E-14                2
 -1.11652332E+04-5.42252285E+01-1.83685605E+00 6.07709466E-02-4.21592576E-05                3
  1.56103972E-08-2.43142766E-12-5.34864282E+03 3.45203543E+01                                4
C*CCC2C.C                C   7H  13   0   0G     300.000  5000.000 1388.000              1
  2.03567043E+01 2.90995795E-02-9.88389595E-06 1.52769885E-09-8.83710401E-14                2
  4.24531228E+03-7.93620817E+01-9.80209200E-01 7.49851411E-02-4.61241216E-05                3
  1.39102988E-08-1.60937310E-12 1.20407233E+04 3.66178582E+01                                4
C*CCCC*CC                C   7H  120  00   0G    300.000  5000.000 1385.000              1
  1.99533937E+01 2.69862952E-02-9.01257795E-06 1.37944131E-09-7.93507506E-14                2
 -3.90664781E+03-7.76648901E+01-1.22112151E+00 7.44173491E-02-4.91015985E-05                3
  1.66357387E-08-2.29429269E-12 3.65374662E+03 3.67847305E+01                                4
C*CCCC*CC.               C   7H  110  00   0G    300.000  5000.000 1391.000              1
  2.02760587E+01 2.46190490E-02-8.16879873E-06 1.24354877E-09-7.12724561E-14                2
  1.44005635E+04-7.95044447E+01-2.19263086E+00 7.91838736E-02-5.93639137E-05                3
  2.33051148E-08-3.74441807E-12 2.19727763E+04 4.03930415E+01                                4
C*CCCCC                  C   6H  12   0   0G     300.000  5000.000 1392.000              1
  1.78337529E+01 2.67377658E-02-9.10036773E-06 1.40819768E-09-8.15124244E-14                2
 -1.42062860E+04-6.83818851E+01-1.35275205E+00 6.98655426E-02-4.59408022E-05                3
  1.56967343E-08-2.21296175E-12-7.34368617E+03 3.53120691E+01                                4
C*CCCCC.                 C   6H  11   0   0G     300.000  5000.000 1392.000              1
  1.74129892E+01 2.45984185E-02-8.37352752E-06 1.29588349E-09-7.50182758E-14                2
  1.08613574E+04-6.32669814E+01-6.17484828E-01 6.54674092E-02-4.36872486E-05                3
  1.51936842E-08-2.18414423E-12 1.72739396E+04 3.40544957E+01                                4
C.*CCCC                  C 5 H 9                 G100.000  5000.000  1017.13             1
  8.93810632E+00 2.86334301E-02-1.14841044E-05 2.10564723E-09-1.45909299E-13                2
  2.26286935E+04-1.82126913E+01 1.83489161E+00 3.94405565E-02-2.16372070E-06                3
 -2.05583532E-08 9.49371329E-12 2.49596263E+04 2.05320209E+01                                4
C10H9                    C 10 H 9                G250.000  5000.000  995.00              1
  2.18329544E+01 2.95028152E-02-1.03239940E-05 1.63876848E-09-9.71150469E-14                2
  2.23120698E+04 1.08056691E+02 2.74356801E+00 4.91149446E-02 4.62268820E-05                3
 -9.39460703E-08 3.84141117E-11 2.89390638E+04-1.84564254E+00                                4
C2.CCC*C                 C   6H  11   0   0G     300.000  5000.000 1393.000              1
  1.73789104E+01 2.49141494E-02-8.54341211E-06 1.32855830E-09-7.71639569E-14                2
  9.67894432E+03-6.52997897E+01-1.12223791E+00 6.74746771E-02-4.63673789E-05                3
  1.68609510E-08-2.56700270E-12 1.62284521E+04 3.43937767E+01                                4
C2C*CC. C*CC.C2          C   5H   9   0   0G     300.000  5000.000 1390.000              1
  1.37488172E+01 2.12968670E-02-7.31667112E-06 1.13927711E-09-6.62322897E-14                2
  4.95421087E+03-5.11769915E+01-1.34298397E+00 5.40081872E-02-3.39256108E-05                3
  1.08403561E-08-1.41074702E-12 1.04932841E+04 3.08504001E+01                                4
C2H3-ME2-CPANE3.         H  13C   8   0   0g     300.000  2500.0001000.000              1
  0.64209614E+01 0.62674135E-01-0.32978089E-04 0.85348679E-08-0.88029800E-12                2
```

```
   0.14806009E+05-0.84813452E+01-0.25783868E+01 0.86955927E-01-0.48542046E-04    3
   0.15747531E-08 0.63646944E-11 0.17143477E+05 0.37692928E+02                    4
C5H5-3-C5H4            C  10 H  9              G250.000   5000.000  995.00         1
 2.26968258E+01 2.71542781E-02-9.14685780E-06 1.41076502E-09-8.17776069E-14      2
 3.30647933E+04-9.83268437E+01 2.47191615E+00 2.64970206E-02 1.15396314E-04      3
-1.64810260E-07 6.24782531E-11 4.11471913E+04 1.95345553E+01                     4
C5H5-3-C5H5            C  10 H  10             G250.000   5000.000  995.00         1
 2.28382374E+01 2.96675462E-02-1.01750341E-05 1.59306174E-09-9.34310788E-14      2
 2.23811106E+04-1.00798999E+02 2.56184984E+00 3.09704893E-02 1.08770192E-04      3
-1.59106631E-07 6.06344902E-11 3.03869570E+04 1.68743521E+01                     4
C5H5C5H4              C  10 H  9              G250.000   5000.000  995.00          1
 2.33318140E+01 2.63110645E-02-8.74633325E-06 1.33534814E-09-7.68079442E-14      2
 4.06482672E+04-1.00860806E+02 2.37215788E+00 2.77874014E-02 1.13816680E-04      3
-1.64387219E-07 6.25660749E-11 4.89174821E+04 2.07456607E+01                     4
C5H5C5H5              C  10 H  10             G250.000   5000.000  995.00          1
 2.36143513E+01 2.83176791E-02-9.55593472E-06 1.47860709E-09-8.59351200E-14      2
 2.67651404E+04-1.03795209E+02 2.42639284E+00 2.20189617E-02 1.37831943E-04      3
-1.89655963E-07 7.11474441E-11 3.55101317E+04 2.10739803E+01                     4
C6H5C*CC*C            C  10 H  10             G250.000   5000.000  995.00          1
 2.09656519E+01 3.20402610E-02-1.11648705E-05 1.76527985E-09-1.04262730E-13      2
 1.50409847E+04-8.70169113E+01 2.75771317E+00 3.30845263E-02 9.60255958E-05      3
-1.42922057E-07 5.45562901E-11 2.22363590E+04 1.86835494E+01                     4
C7H15-4               C   7H  15  0   0G   300.000   5000.000 1382.000            1
 2.16368842E+01 3.23324804E-02-1.09273807E-05 1.68357060E-09-9.71774091E-14      2
-1.05873616E+04-8.59104470E+01-3.79155767E-02 7.56726570E-02-4.07473634E-05      3
 9.32678943E-09-4.92360745E-13-2.35605303E+03 3.30426690E+01                     4
CC*CC*CC.C            C   7H  11O   0   G   300.000   5000.000 1392.000           1
 1.97162810E+01 2.57349529E-02-8.88780777E-06 1.45433064E-09-8.89123490E-14      2
 9.87731302E+03-7.97127945E+01-2.67089394E+00 8.11237460E-02-6.23997773E-05      3
 2.53892000E-08-4.23959092E-12 1.73615979E+04 3.94563140E+01                     4
CC*CCC                C   5H  10  0   0G   300.000   5000.000 1389.000            1
 1.41109267E+01 2.28348272E-02-7.78626835E-06 1.20627491E-09-6.98795983E-14      2
-1.14336507E+04-5.01601163E+01-5.41560551E-01 5.39629918E-02-3.23508738E-05      3
 9.77416037E-09-1.18534668E-12-5.98606169E+03 2.97142748E+01                     4
CC*CCC*CC.            C   7H  11O   0   G   300.000   5000.000 1424.000           1
 1.73039532E+01 2.89396278E-02-9.06501195E-06 1.32279136E-09-7.33937275E-14      2
 1.46316916E+04-6.29046491E+01-4.14162478E+00 8.97320109E-02-7.52022020E-05      3
 3.37258610E-08-6.05041647E-12 2.08818595E+04 4.82595363E+01                     4
CC*CCC*CC.C           C   8H  13O   0   G   300.000   5000.000 1392.000           1
 2.17242946E+01 3.07097479E-02-1.03903693E-05 1.67181375E-09-1.01112352E-13      2
 8.09123335E+03-8.68721164E+01-3.36291274E+00 9.20779032E-02-6.89949267E-05      3
 2.76123631E-08-4.56210036E-12 1.65613429E+04 4.69397663E+01                     4
CC*CCC2*CC.           C   8H  13O   0   G   300.000   5000.000 1392.000           1
 2.22392089E+01 3.05909718E-02-1.04735321E-05 1.70020001E-09-1.03382803E-13      2
 8.33072706E+03-9.08987373E+01-3.86341905E+00 9.48950293E-02-7.23263678E-05      3
 2.92568932E-08-4.86707462E-12 1.70897912E+04 4.81546169E+01                     4
CC*CCC2C.C            C   8H  15  0   0G   300.000   5000.000 1386.000            1
 2.31436210E+01 3.38457042E-02-1.14994771E-05 1.77778175E-09-1.02852422E-13      2
-1.22216762E+03-9.25477704E+01-7.18688766E-01 8.38333604E-02-4.93137251E-05      3
 1.37850162E-08-1.38965026E-12 7.63705452E+03 3.76447456E+01                     4
CC*CCCC*CC            C   8H  14O   0   G   300.000   5000.000 1392.000           1
 2.22462799E+01 3.21365164E-02-1.08001256E-05 1.73598331E-09-1.05137477E-13      2
-9.03793646E+03-8.84412036E+01-3.03406314E+00 9.36687258E-02-6.92687099E-05      3
 2.75029068E-08-4.52098797E-12-4.64382209E+02 4.65223282E+01                     4
CC*CCCC*CC.           C   8H  13O   0   G   300.000   5000.000 1427.000           1
 1.99343416E+01 3.34077889E-02-1.04057937E-05 1.51178175E-09-8.35943785E-14      2
 1.08601969E+04-7.37865371E+01-4.29414667E+00 1.03330228E-01-8.76491482E-05      3
 3.98186002E-08-7.21505410E-12 1.77893045E+04 5.13484577E+01                     4
CC*CCCC.C             C   7H  13  0   0G   300.000   5000.000 1379.000            1
 2.00522952E+01 2.90375466E-02-9.79903704E-06 1.50841035E-09-8.70206514E-14      2
 4.01078575E+03-7.59217636E+01 1.92192199E-01 6.87557473E-02-3.70909926E-05      3
```

```
       8.46587268E-09-4.34596882E-13 1.15461566E+04 3.30601003E+01                 4
CCC(C.)*C               C  5 H  9             G100.000  5000.000  2064.69           1
-2.58061857E+01 7.14245046E-02-2.49290219E-05 1.98784004E-09-2.07416429E-14        2
 2.91693408E+04 1.85131760E+02 4.53308205E-01 5.16416677E-02-3.31441045E-05        3
 1.19335995E-08-2.10809336E-12 1.16988955E+04 2.33591140E+01                       4
CH2*CPANE               C  6H  10    0    0G   300.000  5000.000 1398.000           1
 1.51543120E+01 2.56820761E-02-8.75342789E-06 1.35604540E-09-7.85633700E-14        2
-7.04013929E+03-6.22980730E+01-7.96083119E+00 8.07721106E-02-5.90441962E-05        3
 2.22704598E-08-3.41797721E-12 8.37948711E+02 6.13896445E+01                       4
CH2.CYC5                C  6H  11    0    0G   300.000  5000.000 1396.000           1
 1.57570715E+01 2.74323411E-02-9.38652970E-06 1.45781968E-09-8.46055825E-14        2
 2.59239941E+03-6.38756773E+01-7.37988965E+00 8.04871317E-02-5.54172422E-05        3
 1.94406677E-08-2.75597440E-12 1.06959378E+04 6.06843985E+01                       4
CHD13                   C  6H   8    0    0G   300.000  5000.000 1396.000           1
 1.53625259E+01 2.08675112E-02-7.19203048E-06 1.12251633E-09-6.53733380E-14        2
 4.62118283E+03-6.26703913E+01-5.81337476E+00 7.22248431E-02-5.52161741E-05        3
 2.16975324E-08-3.46304555E-12 1.17578006E+04 5.03398935E+01                       4
CYC5H10                 C  5H  10    0    0G   300.000  5000.000 1395.000           1
 1.30254911E+01 2.48383373E-02-8.44096370E-06 1.30515909E-09-7.55185013E-14        2
-1.72098432E+04-5.43094696E+01-7.18452311E+00 6.97305020E-02-4.53463755E-05        3
 1.45624513E-08-1.81443636E-12-1.00158290E+04 5.49588019E+01                       4
CYC5H4.CC               C  7 H  9             G250.000  5000.000  995.00            1
 1.59948100E+01 2.55285077E-02-8.73641126E-06 1.36280123E-09-7.97104186E-14        2
 1.74434927E+04-5.97326824E+01 3.03045549E+00 2.17437418E-02 8.12375586E-05        3
-1.15377579E-07 4.34358269E-11 2.27908944E+04 1.66542626E+01                       4
CYC5H5CC                C  7 H  10            G250.000  5000.000  995.00            1
 1.58651439E+01 2.79394455E-02-9.69763447E-06 1.53225961E-09-9.05287344E-14        2
 2.61296666E+03-6.24069138E+01 3.13390645E+00 2.50074565E-02 7.62925862E-05        3
-1.10731287E-07 4.18460308E-11 7.82536663E+03 1.24112804E+01                       4
CYC5H5CC.               C  7 H  9             G250.000  5000.000  995.00            1
 1.67084092E+01 2.47016408E-02-8.36604630E-06 1.29470491E-09-7.52747971E-14        2
 2.88745726E+04-6.35019178E+01 2.93558407E+00 2.25473177E-02 8.15915039E-05        3
-1.17070402E-07 4.42594370E-11 3.44630435E+04 1.71842935E+01                       4
CYC6H11                 C  6H  11    0    0G   300.000  5000.000 1383.000           1
 1.86458108E+01 2.59191581E-02-8.98642697E-06 1.40867513E-09-8.23019080E-14        2
-2.20908469E+03-8.30368337E+01-7.55161902E+00 8.15848964E-02-5.10686816E-05        3
 1.43337921E-08-1.30910474E-12 7.31251697E+03 5.94079764E+01                       4
C6H12_R6                C  6H  12    0    0G   300.000  5000.000 1375.000           1
 1.88139366E+01 2.85260968E-02-9.93095425E-06 1.56087712E-09-9.13588355E-14        2
-2.58750745E+04-8.80894762E+01-8.02645333E+00 8.19981028E-02-4.56638045E-05        3
 9.73071753E-09-1.93332062E-13-1.57539369E+04 5.91311538E+01                       4
CYC6H5C*C               C  8 H  8             G250.000  5000.000  995.00            1
 1.68023303E+01 2.47000145E-02-8.50911919E-06 1.33693601E-09-7.86393619E-14        2
 9.71520030E+03-6.58692142E+01 3.03145259E+00 2.21443007E-02 8.26468008E-05        3
-1.18228557E-07 4.46575325E-11 1.53227672E+04 1.49055143E+01                       4
Et4-CHEXE4.             H  13C   8    0    0g   300.000  2500.0001000.000           1
 0.37956057E+01 0.66251226E-01-0.34927998E-04 0.90117558E-08-0.92288276E-12        2
 0.13822503E+05 0.60197468E+01-0.10048960E+01 0.61370064E-01 0.15959886E-04        3
-0.61096692E-07 0.27985142E-10 0.15846463E+05 0.34760132E+02                       4
FULVENE                 C  6 H  6             G250.000  5000.000  995.00            1
 1.36544324E+01 1.65769997E-02-5.38277527E-06 8.08106029E-10-4.59021786E-14        2
 2.01766700E+04-5.12787847E+01 3.09599618E+00 6.97346368E-03 8.75547699E-05        3
-1.14026501E-07 4.20131388E-11 2.48545362E+04 1.25545146E+01                       4
INDENE                  C  9 H  8             G250.000  5000.000  995.00            1
 1.88368714E+01 2.56716206E-02-8.74517201E-06 1.36156792E-09-7.94931211E-14        2
 1.06734623E+04-8.04100709E+01 2.81487568E+00 1.29770906E-02 1.26620351E-04        3
-1.67203638E-07 6.18367253E-11 1.76789399E+04 1.59870706E+01                       4
INDENE.                 C  9 H  7             G250.000  5000.000  995.00            1
 1.71417957E+01 2.66272358E-02-9.87449801E-06 1.62941249E-09-9.90710901E-14        2
 2.52156972E+04-7.00087679E+01 3.34187991E+00 1.04106192E-02 1.22644272E-04        3
-1.59563946E-07 5.85920585E-11 3.15111116E+04 1.43332422E+01                       4
```

```
ME.CY13PD              C 6  H 7              G250.000   5000.000  995.00        1
 1.45174085E+01 1.84377017E-02-6.02350335E-06 9.06757804E-10-5.16009479E-14    2
 2.33198428E+04-5.47655885E+01 3.01525223E+00 1.13553504E-02 8.50316862E-05    3
-1.13951906E-07 4.23363880E-11 2.82485133E+04 1.39324733E+01                   4
ME.CY14PD              C 6  H 7              G250.000   5000.000  995.00        1
 1.44565700E+01 1.84897187E-02-6.04762727E-06 9.11221083E-10-5.18880750E-14    2
 2.04403233E+04-5.45050926E+01 3.02160467E+00 1.00127837E-02 8.88049838E-05    3
-1.17627383E-07 4.35460118E-11 2.54112901E+04 1.41488722E+01                   4
ME1-CPENE             C   6H  10   0   0G   300.000   5000.000 1395.000        1
 1.59521101E+01 2.46510254E-02-8.41203526E-06 1.30412493E-09-7.55919007E-14    2
-8.91446649E+03-6.44144756E+01-4.91712820E+00 7.35579200E-02-5.22811143E-05    3
 1.92470571E-08-2.89983018E-12-1.69520424E+03 4.75896811E+01                   4
ME3-CHEXE5.           C   7H  11   0   0G   300.000   5000.000 1396.000        1
 1.90438569E+01 2.74218415E-02-9.43315378E-06 1.47022739E-09-8.55324241E-14    2
 9.01033463E+03-8.06211311E+01-6.43921773E+00 8.96313848E-02-6.84655980E-05    3
 2.73244623E-08-4.47113949E-12 1.76032633E+04 5.53064282E+01                   4
ME3-CPENE             C 6  H 10             G100.000   5000.000  864.69        1
 7.96492437E+00 3.69369293E-02-1.50483059E-05 2.88342544E-09-2.09138086E-13    2
-3.95631882E+03-1.91034934E+01 1.73949466E+00 1.48061094E-02 1.11690968E-04    3
-1.62946892E-07 6.74295777E-11-9.75745546E+02 2.10350264E+01                   4
ME3-CPENE3.           C 6  H 9              G100.000   5000.000  888.51        1
 7.59634476E+00 3.54550616E-02-1.47528214E-05 2.84367546E-09-2.06198850E-13    2
 1.06912144E+04-1.79373346E+01 1.79975165E+00 1.81093600E-02 8.78692292E-05    3
-1.29183099E-07 5.24252082E-11 1.34360270E+04 1.89922207E+01                   4
ME3-CPENE4.           C 6  H 9              G250.000   5000.000  995.00        1
 1.18737936E+01 2.66674566E-02-9.34959555E-06 1.48810084E-09-8.83633494E-14    2
 1.69755663E+04-3.79147012E+01 3.46196612E+00 5.64717432E-03 1.05000517E-04    3
-1.30508046E-07 4.69897879E-11 2.13642372E+04 1.62665481E+01                   4
ME4.-CHEXE            H  11C   7   0   0g   300.000   2500.0001000.000         1
 0.28502486E+01 0.58037020E-01-0.30927393E-04 0.80569906E-08-0.83240560E-12    2
 0.15883772E+05 0.93479624E+01-0.11838361E+01 0.52514601E-01 0.16400212E-04    3
-0.55834374E-07 0.25293012E-10 0.17650957E+05 0.33838818E+02                   4
ME45-CHEXE4.          H  13C   8   0   0g   300.000   2500.0001000.000         1
 0.52813272E+01 0.64073831E-01-0.33641900E-04 0.86630534E-08-0.88697870E-12    2
 0.14110026E+05-0.37532773E+01-0.26962185E+01 0.76894678E-01-0.18441484E-04    3
-0.30146531E-07 0.17883915E-10 0.16558562E+05 0.39176411E+02                   4
ME4-CPENE             C 6  H 10             G100.000   5000.000  874.36        1
 8.10981607E+00 3.66902777E-02-1.49131700E-05 2.85538064E-09-2.07047195E-13    2
-4.14700214E+03-1.99282474E+01 1.82875916E+00 1.49799009E-02 1.08871584E-04    3
-1.57508853E-07 6.45108493E-11-1.12034691E+03 2.05576590E+01                   4
MECY24PD              C 6  H 8              G250.000   5000.000  995.00        1
 1.40580165E+01 2.15354916E-02-7.24899040E-06 1.11901354E-09-6.49595978E-14    2
 5.40839282E+03-5.30684017E+01 3.13743005E+00 1.13148172E-02 8.97437994E-05    3
-1.18526221E-07 4.37287529E-11 1.02609528E+04 1.30259334E+01                   4
MECYPE1.              C   6H  11   0   0G   300.000   5000.000 1394.000        1
 1.54547638E+01 2.76827900E-02-9.47114624E-06 1.47081229E-09-8.53524134E-14    2
 3.28192530E+02-6.22074071E+01-6.12930089E+00 7.53466299E-02-4.86782800E-05    3
 1.57165645E-08-2.00805545E-12 8.08332011E+03 5.46625403E+01                   4
MECYPE4.              C   6H  11   0   0G   300.000   5000.000 1402.000        1
 1.60098556E+01 2.69610909E-02-9.16669878E-06 1.41749807E-09-8.20133137E-14    2
 1.19077048E+03-6.57311602E+01-7.69861576E+00 8.47024459E-02-6.33907516E-05    3
 2.47256878E-08-3.93690066E-12 9.15435332E+03 6.07030856E+01                   4
toluene(3)            C 7  H 8              G250.000   5000.000  995.00        1
 1.44137278E+01 2.45700700E-02-8.48963715E-06 1.33482944E-09-7.85248143E-14    2
-8.61705750E+02-5.29116093E+01 3.19482612E+00 1.18547044E-02 9.78322810E-05    3
-1.28291603E-07 4.71602635E-11 4.23308969E+03 1.55393380E+01                   4
C10H11(15)            C 10 H 11             G250.000   5000.000  995.00        1
 2.32414507E+01 3.18229957E-02-1.07493695E-05 1.66203512E-09-9.65438997E-14    2
 3.04381856E+04-1.00956740E+02 2.41914259E+00 2.50754487E-02 1.35775888E-04    3
-1.87863332E-07 7.04734316E-11 3.90598613E+04 2.18962152E+01                   4
pdt15(16)             C 10 H 11             G250.000   5000.000  995.00        1
```

```
    2.28623499E+01 3.24263112E-02-1.10580976E-05 1.72219186E-09-1.00589784E-13    2
    2.93880614E+04-9.81446763E+01 2.49999891E+00 2.70202867E-02 1.28635234E-04    3
   -1.80003482E-07 6.77001381E-11 3.77602535E+04 2.16978624E+01                   4
pdt16(17)               C  10  H  11           G250.000   5000.000  995.00        1
    2.26679790E+01 3.29075899E-02-1.13730929E-05 1.78806572E-09-1.05193265E-13    2
    2.72846985E+04-9.52558756E+01 2.59339668E+00 4.00478554E-02 8.87499962E-05    3
   -1.39586047E-07 5.40801563E-11 3.49212433E+04 1.97909829E+01                   4
pdt20(18)               C  10  H  11           G250.000   5000.000  995.00        1
    2.20283789E+01 3.37835595E-02-1.18059970E-05 1.86920531E-09-1.10510787E-13    2
    2.70026515E+04-9.09107997E+01 2.69143418E+00 4.18305108E-02 8.11134503E-05    3
   -1.30767943E-07 5.08971927E-11 3.43007179E+04 1.96178642E+01                   4
pdt21(19)               C  10  H  11           G250.000   5000.000  995.00        1
    2.22313916E+01 3.32116599E-02-1.14124899E-05 1.78753475E-09-1.04855926E-13    2
    2.07495480E+04-9.68454010E+01 2.58862201E+00 2.77023789E-02 1.24231541E-04    3
   -1.74407885E-07 6.55985941E-11 2.88404461E+04 1.88352544E+01                   4
pdt27(20)               C  10  H  11           G250.000   5000.000  995.00        1
    2.18608748E+01 3.37613286E-02-1.16814655E-05 1.83898203E-09-1.08284034E-13    2
    2.05784633E+04-9.40217113E+01 2.65750757E+00 2.94688358E-02 1.17631266E-04    3
   -1.67101592E-07 6.30154282E-11 2.84342341E+04 1.87991737E+01                   4
pdt55(23)               C  10  H  11           G250.000   5000.000  995.00        1
    2.27282403E+01 3.24846645E-02-1.10614637E-05 1.72103713E-09-1.00458454E-13    2
    2.80546589E+04-9.78578971E+01 2.50327337E+00 2.78088752E-02 1.25597710E-04    3
   -1.76676467E-07 6.65386388E-11 3.63360191E+04 2.10034876E+01                   4
pdt58(24)               C  10  H  11           G250.000   5000.000  995.00        1
    2.26489156E+01 3.27427271E-02-1.12644987E-05 1.76326243E-09-1.03381647E-13    2
    3.72866490E+04-9.23704581E+01 2.55307612E+00 4.04151766E-02 8.73829022E-05    3
   -1.38170963E-07 5.36068424E-11 4.49053085E+04 2.26677195E+01                   4
C5H6a(28)               C   5  H   6           G250.000   5000.000  995.00        1
    1.31147007E+01 1.39322313E-02-4.42099767E-06 6.52509437E-10-3.66224548E-14    2
    2.46532756E+04-4.42576772E+01 3.13492110E+00 2.14159978E-02 3.34926373E-05    3
   -5.77093666E-08 2.29076358E-11 2.82549109E+04 1.19575079E+01                   4
pdt39(34)               C  10  H  11           G250.000   5000.000  995.00        1
    2.29762788E+01 3.22393723E-02-1.09553909E-05 1.70164156E-09-9.91919809E-14    2
    2.91367198E+04-9.94336083E+01 2.47196254E+00 2.70717488E-02 1.28879475E-04    3
   -1.80454466E-07 6.78940005E-11 3.75536144E+04 2.11757855E+01                   4
C10H10(43)              C  10  H  10           G250.000   5000.000  995.00        1
    2.18289580E+01 3.05240529E-02-1.05022119E-05 1.64921350E-09-9.69733683E-14    2
    2.67373867E+04-9.25602465E+01 2.66010944E+00 3.32382438E-02 9.74765670E-05    3
   -1.45781049E-07 5.58091771E-11 3.42325491E+04 1.83167709E+01                   4
C10H10(45)              C  10  H  10           G250.000   5000.000  995.00        1
    2.29112524E+01 2.93719901E-02-9.99364058E-06 1.55576993E-09-9.08708192E-14    2
    2.28713436E+04-9.95475535E+01 2.51883029E+00 3.17586031E-02 1.06387541E-04    3
   -1.56802660E-07 5.98921962E-11 3.08697260E+04 1.85314808E+01                   4
C10H10(46)              C  10  H  10           G250.000   5000.000  995.00        1
    2.22445077E+01 2.99621002E-02-1.02194717E-05 1.59455053E-09-9.33209917E-14    2
    2.63272088E+04-9.50482493E+01 2.58522647E+00 3.44345225E-02 9.54303238E-05    3
   -1.44490724E-07 5.55290264E-11 3.39305296E+04 1.82454390E+01                   4
C10H10(47)              C  10  H  10           G250.000   5000.000  995.00        1
    2.30636331E+01 2.89472540E-02-9.72948479E-06 1.50095831E-09-8.70862497E-14    2
    2.32415544E+04-1.00931531E+02 2.44935488E+00 3.27572732E-02 1.03704637E-04    3
   -1.54346106E-07 5.91301253E-11 3.12577729E+04 1.80844971E+01                   4
prod_9(66)              C   6  H   8           G250.000   5000.000  995.00        1
    1.30985089E+01 2.29595971E-02-7.86981967E-06 1.23024801E-09-7.20783252E-14    2
    6.13658476E+03-4.73372436E+01 3.26076320E+00 1.03407600E-02 8.97913592E-05    3
   -1.16888495E-07 4.28420750E-11 1.06768778E+04 1.30521199E+01                   4
addC(80)                C   7  H   9           G250.000   5000.000  995.00        1
    1.63747914E+01 2.49722526E-02-8.44856631E-06 1.30822284E-09-7.61079381E-14    2
    2.25528662E+04-6.24029057E+01 2.96521213E+00 1.74786842E-02 9.54052739E-05    3
   -1.30285000E-07 4.85664302E-11 2.82610812E+04 1.74976079E+01                   4
C7H9(83)                C   7  H   9           G250.000   5000.000  995.00        1
    1.61374303E+01 2.55799018E-02-8.84529780E-06 1.38916842E-09-8.16635463E-14    2
```

```
    2.18995247E+04-6.00784271E+01 3.06360073E+00 3.08740144E-02 5.44197572E-05     3
   -8.87314738E-08 3.45536464E-11 2.68410449E+04 1.46871346E+01                    4
C7H9(85)                  C 7  H 9              G250.000    5000.000  995.00        1
 1.60802208E+01 2.54265187E-02-8.67523163E-06 1.35223116E-09-7.90767936E-14        2
 2.82040919E+04-6.10472000E+01 3.02810633E+00 2.20318327E-02 8.06544877E-05        3
-1.14918845E-07 4.33090872E-11 3.35671124E+04 1.57534232E+01                       4
C7H9J(88)                 C 7  H 9              G250.000    5000.000  995.00        1
 1.48278014E+01 2.84350489E-02-1.01210462E-05 1.62082077E-09-9.64763674E-14        2
 2.31175376E+04-6.34331859E+01 3.26010428E+00-9.13507099E-03 1.73250284E-04        3
-2.06146947E-07 7.34377877E-11 2.95816068E+04 1.32304458E+01                       4
S(102)                    C 10 H 10             G250.000    5000.000  995.00        1
 2.02202543E+01 3.31715410E-02-1.22705227E-05 2.02786416E-09-1.23543056E-13        2
 5.09455510E+03-8.32235830E+01 3.23408127E+00 2.16739721E-02 1.25329076E-04        3
-1.70739867E-07 6.35283408E-11 1.24245356E+04 1.84867853E+01                       4
C7H8(105)                 C 7  H 8              G250.000    5000.000  995.00        1
 1.31566478E+01 2.72147204E-02-9.84904601E-06 1.59954165E-09-9.62760754E-14        2
 1.43067034E+04-4.69929512E+01 3.51147531E+00 1.05012348E-02 9.89902952E-05        3
-1.27362121E-07 4.63847101E-11 1.89730566E+04 1.32943293E+01                       4
C7H8(106)                 C 7  H 8              G250.000    5000.000  995.00        1
 1.36578575E+01 2.81481092E-02-9.95129326E-06 1.57973466E-09-9.33936987E-14        2
 3.02605944E+04-5.38176572E+01 3.25944820E+00-2.70084202E-03 1.46070274E-04        3
-1.76328313E-07 6.30404564E-11 3.59265322E+04 1.43693971E+01                       4
S(109)                    C 10 H 10             G250.000    5000.000  995.00        1
 1.85644106E+01 3.64186700E-02-1.33604347E-05 2.18721901E-09-1.32325583E-13        2
 2.20995190E+04-7.72128924E+01 3.25956311E+00 2.25571843E-02 1.21177527E-04        3
-1.64090463E-07 6.07737370E-11 2.88773300E+04 1.53011318E+01                       4
S(110)                    C 10 H 10             G250.000    5000.000  995.00        1
 1.87077425E+01 3.58468242E-02-1.32972434E-05 2.19622930E-09-1.33703314E-13        2
 5.10979214E+03-7.84350670E+01 3.35063037E+00 2.21146339E-02 1.21167620E-04        3
-1.64114089E-07 6.08010637E-11 1.19020046E+04 1.43509452E+01                       4
C10H9(112)                C 10 H 9              G250.000    5000.000  995.00        1
 2.28306132E+01 2.70009817E-02-9.07601229E-06 1.39760684E-09-8.09195582E-14        2
 3.50999318E+04-9.88120164E+01 2.45415590E+00 2.75533755E-02 1.12738495E-04        3
-1.62388807E-07 6.17150611E-11 4.31827639E+04 1.96303931E+01                       4
prod1(114)                C 10 H 9              G250.000    5000.000  995.00        1
 2.38798560E+01 2.54195731E-02-8.27431022E-06 1.24409255E-09-7.07195881E-14        2
 4.42338683E+04-1.06521828E+02 2.26074882E+00 2.36503245E-02 1.28070196E-04        3
-1.79667338E-07 6.78845713E-11 5.29262305E+04 1.97296567E+01                       4
C10H8(116)                C 10 H 8              G250.000    5000.000  995.00        1
 2.21715504E+01 2.48738071E-02-8.31664351E-06 1.27753861E-09-7.38517298E-14        2
 3.53794187E+04-9.71735123E+01 2.51070252E+00 2.54744285E-02 1.09015916E-04        3
-1.56551883E-07 5.94832468E-11 4.31750385E+04 1.70924452E+01                       4
C5H7J(117)                C 5  H 7              G250.000    5000.000  995.00        1
 1.28268016E+01 1.64659544E-02-5.34930983E-06 8.05230619E-10-4.59247458E-14        2
 3.32517792E+04-4.12200800E+01 3.18490047E+00 2.39738693E-02 3.04439990E-05        3
-5.47398491E-08 2.18398363E-11 3.67177378E+04 1.30228306E+01                       4
C6H7(121)                 C 6  H 7              G250.000    5000.000  995.00        1
 1.46586547E+01 1.83540499E-02-6.03721626E-06 9.14415492E-10-5.23042381E-14        2
 3.26736008E+04-5.30950552E+01 3.03541070E+00 1.54469336E-02 7.31636493E-05        3
-1.02276680E-07 3.84682926E-11 3.74437691E+04 1.52690362E+01                       4
C6H7(122)                 C 6  H 7              G250.000    5000.000  995.00        1
 1.51800569E+01 1.73086061E-02-5.43127401E-06 7.91962369E-10-4.39096961E-14        2
 2.79285445E+04-6.02528765E+01 2.87077864E+00 2.42200781E-03 1.14044401E-04        3
-1.44267266E-07 5.27355286E-11 3.35648164E+04 1.50835830E+01                       4
prod2(126)                C 10 H 9              G250.000    5000.000  995.00        1
 2.29744371E+01 2.65954882E-02-8.82550310E-06 1.34764303E-09-7.75523274E-14        2
 3.72475564E+04-1.00568000E+02 2.40296945E+00 2.55174204E-02 1.19086507E-04        3
-1.68962530E-07 6.39701567E-11 4.54887228E+04 1.94148571E+01                       4
c10h9(128)                C 10 H 9              G250.000    5000.000  995.00        1
 2.19319136E+01 2.81169450E-02-9.55892299E-06 1.48613244E-09-8.66787876E-14        2
 3.01262119E+04-9.61204243E+01 2.57598851E+00 2.18032003E-02 1.26772264E-04        3
```

```
-1.74817560E-07 6.55555076E-11 3.81427665E+04 1.80910717E+01                    4
C7H7(131)               C 7  H 7           G250.000  5000.000  995.00           1
 1.58899925E+01 1.99843620E-02-6.61783367E-06 1.00700314E-09-5.77803520E-14    2
 1.82887283E+04-6.29636743E+01 2.94445654E+00 1.34803197E-02 9.14405682E-05    3
-1.23819882E-07 4.61602888E-11 2.37632590E+04 1.39902061E+01                    4
prod5(132)              C 10 H 9           G250.000  5000.000  995.00           1
 2.16068676E+01 2.86835306E-02-9.89522678E-06 1.55239427E-09-9.11540138E-14    2
 4.73123448E+04-8.95977315E+01 2.65758802E+00 3.52818666E-02 8.50424928E-05    3
-1.32326106E-07 5.12005785E-11 5.45278283E+04 1.90352924E+01                    4
C7H10(145)              C 7  H 10          G250.000  5000.000  995.00           1
 1.69415688E+01 2.63340854E-02-8.88368489E-06 1.37393685E-09-7.98823513E-14    2
 1.42662840E+03-6.65988674E+01 2.91484861E+00 1.91647428E-02 9.77324638E-05    3
-1.34248177E-07 5.01221538E-11 7.36442498E+03 1.68124136E+01                    4
C7H10(146)              C 7  H 10          G250.000  5000.000  995.00           1
 1.69415688E+01 2.63340854E-02-8.88368489E-06 1.37393685E-09-7.98823513E-14    2
 1.60275562E+03-6.67548658E+01 2.91484861E+00 1.91647428E-02 9.77324638E-05    3
-1.34248177E-07 5.01221538E-11 7.54055220E+03 1.66564153E+01                    4
C8H9J(156)              C 8  H 9           G250.000  5000.000  995.00           1
 1.58394770E+01 2.94693813E-02-1.00254050E-05 1.55272067E-09-9.02851690E-14    2
 2.70672310E+04-6.02992892E+01 2.95450226E+00 1.81238411E-02 1.02262853E-04    3
-1.37451971E-07 5.08566713E-11 3.27573382E+04 1.75065322E+01                    4
C10H9(173)              C 10 H 9           G250.000  5000.000  995.00           1
 1.94167497E+01 3.22928220E-02-1.19340963E-05 1.96607849E-09-1.19472737E-13    2
 1.99841153E+04-8.12231515E+01 3.23546970E+00 2.40334339E-02 1.11024967E-04    3
-1.54454213E-07 5.77824332E-11 2.68334268E+04 1.49976484E+01                    4
C10H9(174)              C 10 H 9           G250.000  5000.000  995.00           1
 1.92697967E+01 3.15349491E-02-1.13497720E-05 1.83822872E-09-1.10444580E-13    2
 3.03447592E+04-7.49253763E+01 3.08764071E+00 2.50948235E-02 1.06129621E-04    3
-1.49076872E-07 5.59475535E-11 3.71043559E+04 2.08479602E+01                    4
pdt17(209)              C 10 H 11          G250.000  5000.000  995.00           1
 2.27371323E+01 3.24117648E-02-1.09963145E-05 1.70823141E-09-9.96238565E-14    2
 2.89749778E+04-9.88853419E+01 2.49854596E+00 2.74004198E-02 1.26757074E-04    3
-1.77816587E-07 6.69217477E-11 3.72783706E+04 2.01387734E+01                    4
pdt18(211)              C 10 H 11          G250.000  5000.000  995.00           1
 2.19871226E+01 3.37225157E-02-1.17230671E-05 1.85064899E-09-1.09194611E-13    2
 2.54601037E+04-9.24265066E+01 2.67258076E+00 3.75422048E-02 9.38055865E-05    3
-1.43413045E-07 5.51207080E-11 3.29585262E+04 1.90233617E+01                    4
C10H9(263)              C 10 H 9           G250.000  5000.000  995.00           1
 1.82028943E+01 3.37857452E-02-1.27122663E-05 2.11966419E-09-1.29864853E-13    2
 2.05948485E+04-7.35185744E+01 3.46642607E+00 2.29269031E-02 1.09328548E-04    3
-1.50444777E-07 5.59890815E-11 2.69977874E+04 1.49408540E+01                    4
S(270)                  C 10 H 10          G250.000  5000.000  995.00           1
 1.90492915E+01 3.55759246E-02-1.34688752E-05 2.25646262E-09-1.38697722E-13    2
 5.58122806E+03-8.02804987E+01 3.49126249E+00 2.44938851E-02 1.14223469E-04    3
-1.57655466E-07 5.87209643E-11 1.23222118E+04 1.30154861E+01                    4
S(271)                  C 10 H 10          G250.000  5000.000  995.00           1
 1.86119063E+01 3.64393576E-02-1.33901024E-05 2.19455319E-09-1.32876199E-13    2
 2.00646020E+04-7.69105765E+01 3.26971302E+00 2.42354678E-02 1.16376610E-04    3
-1.59363923E-07 5.92049796E-11 2.67752172E+04 1.54084348E+01                    4
S(272)                  C 10 H 10          G250.000  5000.000  995.00           1
 1.74938871E+01 3.73397474E-02-1.40754134E-05 2.34981500E-09-1.44095429E-13    2
 5.77587956E+03-7.08864882E+01 3.58158675E+00 2.10081032E-02 1.19471201E-04    3
-1.60104653E-07 5.90077120E-11 1.21217195E+04 1.41381525E+01                    4
norbornene(340)         C 7  H 10          G100.000  5000.000  814.30           1
 7.64096378E+00 4.20189270E-02-1.76575349E-05 3.45463281E-09-2.54194573E-13    2
 3.63302243E+03-2.03966218E+01 9.80678914E-01 4.08987264E-03 1.82344474E-04    3
-2.66826902E-07 1.15434482E-10 7.05992873E+03 2.47489268E+01                    4
C#CCCC.                 C   5H  70   00   0G  300.000  5000.000 1396.000        1
 1.16127647E+01 1.81015783E-02-5.75303577E-06 8.42978543E-10-4.69514458E-14    2
 3.66457107E+04-3.23950513E+01 1.50966455E+00 4.43877634E-02-3.28637336E-05    3
 1.38516958E-08-2.45610725E-12 3.99246754E+04 2.09770450E+01                    4
```

```
C2C*CC2                 C 6  H 12          G    3E+02    1E+03   6E+02     1
 1.54690000E+00 4.52500000E-02 2.14800039E-07-1.92200000E-08 7.15000001E-12   2
-1.00000000E+04 2.14800000E+01 1.54690000E+00 4.52500000E-02 2.14800039E-07   3
-1.92200000E-08 7.15000001E-12-1.00000000E+04 2.14800000E+01                  4
C2H                     C 2  H 1           G    3E+02    1E+03   6E+02     1
 4.50092000E+00 3.01500000E-03-3.34999999E-06 2.88499999E-09-9.03599998E-13   2
 6.69300000E+04-4.99700000E-01 4.50092000E+00 3.01500000E-03-3.34999999E-06   3
 2.88499999E-09-9.03599998E-13 6.69300000E+04-4.99700000E-01                  4
C3C                     C 4  H 10          G    3E+02    1E+03   6E+02     1
-7.16852001E-01 4.96100000E-02-2.89700000E-05 7.66399998E-09-5.09299998E-13   2
-1.79800000E+04 2.61100000E+01-7.16852001E-01 4.96100000E-02-2.89700000E-05   3
 7.66399998E-09-5.09299998E-13-1.79800000E+04 2.61100000E+01                  4
C3H3R                   C 3  H 3           G    3E+02    1E+03   6E+02     1
 2.03607000E+00 2.53500000E-02-2.80300000E-05 1.70400000E-08-4.09600000E-12   2
 4.06900000E+04 1.25300000E+01 2.03607000E+00 2.53500000E-02-2.80300000E-05   3
 1.70400000E-08-4.09600000E-12 4.06900000E+04 1.25300000E+01                  4
C5H8                    C   5H   80   00  0G   300.000  5000.000 1396.000     1
 1.20470639E+01 2.01758339E-02-6.42365708E-06 9.43267454E-10-5.26303368E-14   2
 1.15717891E+04-3.76084567E+01 7.37254328E-01 4.89425421E-02-3.53414696E-05   3
 1.44826138E-08-2.50855593E-12 1.53028350E+04 2.23631271E+01                  4
C6H11R_OLEF_13          C   6H  110   00  0G   300.000  5000.000 1389.000     1
 1.76057566E+01 2.41340087E-02-7.95504037E-06 1.20548482E-09-6.88702584E-14   2
 9.82289696E+03-6.56606541E+01-1.36991628E+00 6.86962191E-02-4.81528942E-05   3
 1.78167298E-08-2.72371515E-12 1.63877815E+04 3.61662241E+01                  4
C6H11R_OLEF_22          C   6H  110   00  0G   300.000  5000.000 1391.000     1
 1.55985958E+01 2.64020351E-02-8.54820814E-06 1.27457136E-09-7.19404555E-14   2
 9.16861810E+03-5.43273482E+01-4.74402491E-01 6.43953863E-02-4.34481911E-05   3
 1.61328085E-08-2.53958715E-12 1.47436733E+04 3.19000097E+01                  4
C6H12_OLEF_13           C 6  H 12          G    3E+02    1E+03   6E+02     1
 3.40158759E+00 4.22351796E-02 1.17874770E-05-3.93739126E-08 1.74971840E-11   2
-1.07657707E+04 1.27025210E+01 3.40158759E+00 4.22351796E-02 1.17874770E-05   3
-3.93739126E-08 1.74971840E-11-1.07657707E+04 1.27025210E+01                  4
CCCC                    C   4H  100   0   G   300.000  1500.000 1385.000     1
 1.49392000E+00 3.79000000E-02-8.75400000E-06-6.93600000E-09 3.26100000E-12   2
-1.73000000E+04 1.80600000E+01 1.49392000E+00 3.79000000E-02-8.75400000E-06   3
-6.93600000E-09 3.26100000E-12-1.73000000E+04 1.80600000E+01                  4
pdt12(7)                C 10 H 11          G250.000   5000.000  995.00      1
 2.23135412E+01 3.32244979E-02-1.14746814E-05 1.80290528E-09-1.06012410E-13   2
 3.47295961E+04-9.26655150E+01 2.61054478E+00 3.74490816E-02 9.51872456E-05   3
-1.45388287E-07 5.59016749E-11 4.23625857E+04 2.09442246E+01                  4
C10H11(12)              C 10 H 11          G250.000   5000.000  995.00      1
 2.19654393E+01 3.34692525E-02-1.14931415E-05 1.80095188E-09-1.05692614E-13   2
 2.72566370E+04-9.62611538E+01 2.61460869E+00 2.38126074E-02 1.34885836E-04   3
-1.84590247E-07 6.89140153E-11 3.54366558E+04 1.87522776E+01                  4
C*CCC.CC                C   6H  11   0   0G   300.000  5000.000 1381.000     1
 1.73835224E+01 2.43481782E-02-8.32416451E-06 1.29233306E-09-7.49891815E-14   2
 9.36150243E+03-6.28631507E+01 4.71970553E-02 5.93593191E-02-3.31064149E-05   3
 8.18079613E-09-5.95483828E-13 1.59332092E+04 3.21954367E+01                  4
C10H10(6)               H 10 C 10          G100.000   5000.000  881.07      1
 1.32324398E+01 4.54041206E-02-1.89970723E-05 3.69160550E-09-2.69707809E-13   2
 2.45744489E+04-4.76895352E+01 1.07560153E-01 4.03915016E-02 9.95135936E-05   3
-1.69194060E-07 7.23972955E-11 2.93946057E+04 2.81976290E+01                  4
C10H10(6_2)             H 10 C 10          G100.000   5000.000  799.28      1
 1.41070824E+01 4.59429878E-02-1.98056781E-05 3.94073477E-09-2.93264469E-13   2
 1.13143241E+04-5.58008846E+01-1.78610506E+00 3.58313679E-02 1.67414750E-04   3
-2.92546932E-07 1.36335385E-10 1.67185480E+04 3.52274497E+01                  4
C10H11(1)               H 11 C 10          G100.000   5000.000  950.02      1
 1.48649228E+01 4.54752242E-02-1.91189222E-05 3.69239056E-09-2.67228900E-13   2
 2.27192810E+04-5.03986283E+01-1.27897357E-01 5.88361539E-02 3.83602416E-05   3
-9.17818882E-08 3.93669069E-11 2.78137460E+04 3.29839078E+01                  4
C10H11(6)               H 11 C 10          G100.000   5000.000  884.24      1
```

```
    1.36513234E+01 4.78058258E-02-1.99143976E-05 3.85972246E-09-2.81535454E-13    2
    2.51600532E+04-4.99615471E+01-2.59266714E-02 4.27731320E-02 1.02115939E-04    3
   -1.73710813E-07 7.41146865E-11 3.01944107E+04 2.91304462E+01                   4
C6H5                    C   6H   5          G   300.00   5000.00 1000.00           1
    .157758892E+02 .965110900E-02-.942941600E-06-.546911100E-09 .102652200E-12    2
    .330269797E+05-.617628096E+02 .114355700E+00 .362732400E-01 .115828600E-05    3
   -.219696400E-07 .846355600E-11 .383605400E+05 .238011700E+02                   4
A(1)                    C 7 H 9            G250.000   5000.000   995.00            1
    1.57622838E+01 2.56940088E-02-8.75964011E-06 1.36402965E-09-7.96845640E-14    2
    1.41291740E+04-6.13308821E+01 3.03738129E+00 1.54560552E-02 9.92192776E-05    3
   -1.32984900E-07 4.92531909E-11 1.97007380E+04 1.52678825E+01                   4
C9H10(C5)               H 10 C 9           G100.000   5000.000   812.46            1
    1.22813224E+01 4.50244400E-02-1.94253049E-05 3.85371681E-09-2.85728291E-13    2
    5.75604282E+03-4.56975455E+01-1.11478468E+00 3.20098431E-02 1.50397794E-04    3
   -2.55128426E-07 1.16217274E-10 1.05390886E+04 3.21882270E+01                   4
C9H11(1)                H 11 C 9           G100.000   5000.000  1049.23            1
    2.71677986E+01 1.37745440E-02 4.44171246E-06-2.74657194E-09 2.39589595E-13    2
    2.01893491E+04-1.17855765E+02 8.22498560E-01 5.03956191E-02 4.33200457E-05    3
   -8.54175752E-08 3.37497661E-11 2.92304658E+04 2.72504179E+01                   4
C9H11(C5)               H 11 C 9           G100.000   5000.000  1042.14            1
    9.06605587E+00 5.02163835E-02-2.12128046E-05 4.05610434E-09-2.89483080E-13    2
    3.10458926E+04-2.31848418E+01 1.51910338E+00 3.71598295E-02 5.80669607E-05    3
   -8.53540659E-08 3.04416302E-11 3.49008832E+04 2.44849717E+01                   4
A(5)                    C 7 H 9            G100.000   5000.000   906.07            1
    1.21244923E+01 3.12056192E-02-1.12460242E-05 2.08105379E-09-1.51382106E-13    2
    1.47477085E+04-4.03341918E+01 1.90836399E+00 1.90127348E-02 1.03790143E-04    3
   -1.52349995E-07 6.17151739E-11 1.89507896E+04 2.09229769E+01                   4
B(2)                    C 7 H 10           G100.000   5000.000   939.44            1
    1.06701257E+01 3.68938865E-02-1.47976637E-05 2.80448260E-09-2.01693527E-13    2
    3.09284728E+03-3.11317991E+01 1.52225816E+00 3.25636269E-02 6.12225257E-05    3
   -1.00183439E-07 4.02556027E-11 6.72147416E+03 2.25947531E+01                   4
A(2)                    H  9C   7          G   100.000  5000.000   906.07          1
    1.21246045E+01 3.12054222E-02-1.12459079E-05 2.08102584E-09-1.51379758E-13    2
    1.47476633E+04-4.03348194E+01 1.90832279E+00 1.90132518E-02 1.03788185E-04    3
   -1.52347227E-07 6.17138856E-11 1.89507914E+04 2.09231226E+01                   4
C(1)                    C   7H  11   0   0G   300.000  5000.000  1397.000          1
    1.89758894E+01 2.75593560E-02-9.49776643E-06 1.48206423E-09-8.62913212E-14    2
    8.88863535E+03-8.02843572E+01-6.21686008E+00 8.84427311E-02-6.65933964E-05    3
    2.61806776E-08-4.22694208E-12 1.74495858E+04 5.43203303E+01                   4
A(4)                    H  9C   7          G   100.000  5000.000   896.75          1
    9.64672726E+00 3.63727337E-02-1.50067101E-05 2.88186188E-09-2.08679572E-13    2
    1.99552524E+04-2.95912581E+01 1.40037447E+00 2.76905002E-02 7.55669230E-05    3
   -1.20991193E-07 5.00872796E-11 2.32623072E+04 1.94867352E+01                   4
B(1)                    H  10C   7         G   100.000  5000.000  1111.91          1
    1.76624358E+01 2.46148740E-02-8.36906416E-06 1.81214239E-09-1.48458943E-13    2
    1.10353453E+03-7.12461517E+01 1.41695699E+00 4.06805731E-02 2.71241990E-05    3
   -5.37436172E-08 2.00489455E-11 7.33580821E+03 2.06317904E+01                   4
B(3)                    H  10C   7         G   100.000  5000.000   908.96          1
    1.00919738E+01 3.79001261E-02-1.54510527E-05 2.94452018E-09-2.12079722E-13    2
    2.69639577E+03-3.05528196E+01 1.25777593E+00 3.30667946E-02 6.46558124E-05    3
   -1.08712324E-07 4.50484549E-11 6.10804016E+03 2.11563539E+01                   4
B(4)                    H  10C   7         G   100.000  5000.000   908.96          1
    1.00920516E+01 3.78999897E-02-1.54509723E-05 2.94450086E-09-2.12078099E-13    2
    2.87249104E+03-3.07092528E+01 1.25774752E+00 3.30671497E-02 6.46544713E-05    3
   -1.08710434E-07 4.50475781E-11 6.28416802E+03 2.10004567E+01                   4
B(5)                    H  10C   7         G   100.000  5000.000   873.43          1
    1.00254538E+01 3.78290191E-02-1.52857372E-05 2.91884106E-09-2.11472350E-13    2
    3.46890776E+03-3.06532300E+01 1.32604293E+00 2.45528236E-02 9.87351187E-05    3
   -1.53737083E-07 6.45570091E-11 7.01463737E+03 2.17374753E+01                   4
C(2)                    H  11C   7         G   100.000  5000.000   909.33          1
    1.02450380E+01 4.08821189E-02-1.64256101E-05 3.14034056E-09-2.28111327E-13    2
```

```
      6.33910643E+03-3.36182582E+01 1.67045358E+00 1.99179810E-02 1.14956725E-04     3
     -1.64149904E-07 6.52758485E-11 1.03246966E+04 2.02745706E+01                     4
C(3)                       H  11C   7          G   100.000  5000.000 1063.20          1
      1.76430650E+01 2.65399439E-02-8.65888177E-06 1.79185868E-09-1.45639251E-13     2
      1.04315841E+04-7.01653778E+01 1.86448398E+00 2.74738649E-02 7.24570020E-05     3
     -1.00759948E-07 3.61224745E-11 1.70891043E+04 2.24544387E+01                     4
CH3S3XcC6H10               C   7H  13          G   300.000  5000.000 1000.00          1
      1.03348618E+01 4.61843472E-02-1.85362834E-05 3.40560247E-09-2.35026588E-13     2
     -1.45879600E+03-3.28619133E+01 8.37449953E-01 4.11173018E-02 5.36493239E-05     3
     -8.77748284E-08 3.33242543E-11 2.59352100E+03 2.37217819E+01                     4
SXC7H13              THERMC   7H  13   0   0G   300.000  5000.000 1383.000           51
      2.05321062E+01 2.85988588E-02-9.64125534E-06 1.48314293E-09-8.55245930E-14     2
      5.35259833E+03-7.70635568E+01-3.37870970E-01 7.22549356E-02-4.22499105E-05     3
      1.14646497E-08-1.05306924E-12 1.30682289E+04 3.67608087E+01                     4

SAXC7H13             THERMC   7H  13   0   0G   300.000  5000.000 1389.000           51
      2.09278134E+01 2.92841022E-02-1.00899640E-05 1.57425554E-09-9.16505991E-14     2
     -1.41296217E+03-8.39475707E+01-1.66945935E+00 7.93202117E-02-5.20231516E-05     3
      1.74804211E-08-2.40912996E-12 6.75927466E+03 3.84730831E+01                     4
CH3S2XcC6H10               C   7H  13          G   300.000  5000.000 1000.00          1
      1.03158717E+01 4.61934335E-02-1.85375133E-05 3.40553426E-09-2.35007960E-13     2
     -1.32487102E+03-3.27296134E+01 7.45909772E-01 4.14463096E-02 5.31236301E-05     3
     -8.73955330E-08 3.32220018E-11 2.74046996E+03 2.41966640E+01                     4
PX7-2C7H13           THERGC   7H  13   0   0G   300.000  5000.000 1000.000           51
      0.19699223E+02 0.27305672E-01-0.77966097E-05 0.11003983E-08-0.62440192E-13     2
      0.65118008E+04-0.73263214E+02-0.65700984E+00 0.80941029E-01-0.64745480E-04     3
      0.32671579E-07-0.79607354E-11 0.12720174E+05 0.33642590E+02                     4
C2H5cC6H11           THERGC   8H  16   0   0G   300.000  5000.000 1391.000           71
      0.18926668E+02 0.46028376E-01-0.16598082E-04 0.27614144E-08-0.17525178E-12     2
     -0.30882613E+05-0.82036865E+02-0.73650422E+01 0.10403100E+00-0.55678032E-04     3
      0.82958991E-08 0.16235853E-11-0.22308957E+05 0.58822647E+02                     4
PXCH2cC6H11                C   7H  13          G   300.000  5000.000 1000.00          1
      1.06259372E+01 4.57870480E-02-1.83465982E-05 3.36704649E-09-2.32189546E-13     2
     -1.02890079E+02-3.41844211E+01 9.16358329E-02 4.61754024E-02 4.36941468E-05     3
     -7.97423013E-08 3.09823602E-11 4.09141275E+03 2.70747064E+01                     4
C2H5S3XcC6H10        THERMC   8H  15   0   0G   300.000  5000.000 1371.000           21
      2.45832536E+01 3.52272488E-02-1.21864870E-05 1.90774123E-09-1.11364343E-13     2
     -1.15433828E+04-1.11494199E+02-7.88540984E+00 9.92968351E-02-5.39691868E-05     3
      1.06980695E-08 3.38821695E-14 7.43536102E+02 6.67862450E+01                     4
S2XC8H15             THERMC   8H  15   0   0G   300.000  5000.000 1384.000           61
      2.38137997E+01 3.29111978E-02-1.11043362E-05 1.70913415E-09-9.85919191E-14     2
      1.21766863E+03-9.32787751E+01-6.59887138E-01 8.48568447E-02-5.09516976E-05     3
      1.45505436E-08-1.49835714E-12 1.01939871E+04 3.99394662E+01                     4
SAXC8H15             THERMC   8H  15   0   0G   300.000  5000.000 1390.000           61
      2.41485380E+01 3.36466429E-02-1.15692934E-05 1.80261649E-09-1.04847473E-13     2
     -5.51631150E+03-9.97977435E+01-1.90098561E+00 9.15067740E-02-6.01588113E-05     3
      2.02337556E-08-2.78235289E-12 3.87213558E+03 4.12376344E+01                     4
END


REACTIONS KCAL/MOLE MOLES
C*CC+C2H3=C*CCC2. 6.75E+11    0      8.1579
CC*CC+C2H3=C6H11R_OLEF_13     1.33E+12    0      7.823
C2H4+C2H5=CCCC.  7.76E+11    0      9.8086
C*CC+C2H5=CCCC.C  1.91E+11    0      9.4737
C2H2+C2H5=C.*CCC  1.98E+12    0      10.5263
C*CC+C.*CC=C6H11R_OLEF_22     6.75E+11    0      8.1579
C*CC+C.*CC=CC*CCC.C    1.37E+12    0      6.3158
C2H2+C.*CC=C5H7J(117)  1.42E+13    0      7.3684
C2H4+C.*CC=CC*CCC.     5.56E+12    0      6.6507
C2H4+C*C.C=C*C(C)CC.    3.06E+12    0      6.5072
C2H4+CC.C=C2CCC.  6.52E+11    0      8.6842
```

```
C*CC*CC+CH3=C6H11R_OLEF_22    1.20E+12    0      11.7943
C2H2+CH3=C.*CC    1.89E+13    0      11.0287
C#CC+CH3=CC.*CC  3.07E+13    0      11.8421
C*C*CC+CH3=CC*C.CC      1.86E+12    0      10.311
C*CC*CC+CH3=C6H11R_OLEF_13    1.18E+12    0      11.4593
C*C*C+CH3=C*C.CC  7.43E+12    0      10.311
C#CCC+CH3=CC*C.CC 3.07E+13    0      11.8421
C#CC.+C#CC.=BENZENE  3.160E+55  -12.550  22.264
C*CC+CH3=CCC.C    1.83E+12    0      9.9761
C*CC*C+CH3=C*CCC2.      2.40E+12    0      11.7943
C*C*C+H=C*CC.      2.20E+13    0      6.4833
C#CCC+H=C*C.CC    1.05E+14    0      5.5024
C*CCCC+H=CCCC.C  5.56E+13    0      3.8517
C*CCC+H=CCCC.      6.46E+13    0      5.3828
C*C*CC+H=CC.*CC    4.76E+13    0      4.5694
C2H2+H=C2H3 4.19E+14    0      5.311
C2H4+H=C2H5 2.13E+14    0      4.4258
C*CC+H=CC.C 5.56E+13    0      3.8517
C#CC+H=C*C.C      1.05E+14    0      5.5024
C5H8+H=C*C.CCC    1.05E+14    0      5.5024
C*C*CC+H=CC*CC.    5.50E+13    0      6.4833
C*CCC+H=CCC.C    5.56E+13    0      3.8517
C*C*CC+H=C*C.CC    5.78E+13    0      5.5263
C#CCC+H=C.*CCC    5.51E+13    0      6.9378
CC*CC+H=CCC.C    1.35E+14    0      4.8086
C*CC+H=CCC. 6.46E+13    0      5.3828
C*C*C+H=C*C.C    1.91E+14    0      4.5694
C#CC+H=C.*CC    5.51E+13    0      6.9378
CCC+CH3=CC.C+CH4  2.08E+13    0.00E+00    1.54E+01
CCC+CH3=CCC.+CH4  5.99E+13    0.00E+00    1.77E+01
CCC+H=CC.C+H2    2.65E+14    0.00E+00    1.02E+01
CCC+H=CCC.+H2    7.51E+14    0.00E+00    1.28E+01
C*C.C+C2H4=C*CC+C2H3    2.52E+13    0      16.3876
C.*CC+C2H4=C*CC+C2H3    3.40E+13    0      15.3828
CCC.+C2H4=CCC+C2H3      5.68E+12    0      21.4833
C*CC.+C2H4=C*CC+C2H3    7.56E+13    0      32.4641
CC.C+C2H4=CCC+C2H3      7.28E+12    0      22.1053
C2H5+C2H4=C2H6+C2H3      5.68E+12    0      21.4833
C.*CC+C2H6=C*CC+C2H5    4.43E+13    0      12.8947
C*CC.+C2H6=C*CC+C2H5    9.85E+13    0      29.9761
CCC.+C2H6=CCC+C2H5      7.40E+12    0      18.9952
CH3+C2H6=CH4+C2H5 4.56E+13    0      17.7033
CC.C+C2H6=CCC+C2H5      9.49E+12    0      19.6172
C*C.C+C2H6=C*CC+C2H5    3.28E+13    0      13.8995
H+C2H6=H2+C2H5    7.03E+14    0      12.799
CH3+C*CC=CH4+C*CC.      5.65E+12    0      13.8517
CC.+C*CC=CCC+C*CC.      1.18E+12    0      15.7656
H+C*CC=H2+C*CC.    7.28E+13    0      9.1866
C*C.C+C*CC=C*CC+C*CC.    4.07E+12    0      10.0478
CCC.+C*CC=CCC+C*CC.      9.17E+11    0      15.1435
CH3+C*CC=CH4+C.*CC      8.75E+12    0      20.1914
H+C*CC=H2+C.*CC    1.81E+14    0      17.2488
CC.C+C*CC=CCC+C.*CC      1.82E+12    0      22.1053
C*CC.+C*CC=C*CC+C.*CC    1.89E+13    0      32.4641
CCC.+C*CC=CCC+C.*CC      1.42E+12    0      21.4833
C*C.C+C*CC=C*CC+C.*CC    6.30E+12    0      16.3876
H+C*CC=H2+C*C.C    1.79E+14    0      14.3541
CH3+C*CC=CH4+C*C.C      9.69E+12    0      17.9904
CCC.+C*CC=CCC+C*C.C      1.57E+12    0      19.2823
CC.C+C*CC=CCC+C*C.C      2.01E+12    0      19.9043
CC.C+CCC=CCC+CCC. 9.49E+12    0      19.6172
```

```
C2H5+C*CC*C=C2H6+C*CC.*C        3.22E+12    0      19.2344
CC.C+C*CC*C=CCC+C*CC.*C 4.12E+12    0      19.8565
C*CC.+C*CC*C=C*CC+C*CC.*C        4.28E+13    0      30.2153
CCC.+C*CC*C=CCC+C*CC.*C 3.22E+12    0      19.2344
C.*CC+C*CC*C=C*CC+C*CC.*C        1.92E+13    0      13.134
C*C.C+C*CC*C=C*CC+C*CC.*C        1.43E+13    0      14.1388
CCC.+C*C*CC=CCC+C*CC.*C 9.17E+11    0      15.1435
CH3+C*C*CC=CH4+C*CC.*C   5.65E+12    0      13.8517
C*C.C+C*C*CC=C*CC+C*CC.*C        4.07E+12    0      10.0478
C2H5+C*C*CC=C2H6+C*CC.*C 9.17E+11    0      15.1435
CC.C+C*C*CC=CCC+C*CC.*C 1.18E+12    0      15.7656
C2H3+C*C*CC=C2H4+C*CC.*C        5.49E+12    0      9.0431
H+C*C*CC=H2+C*CC.*C     7.28E+13    0      9.1866
C*CC.+C*C*CC=C*CC+C*CC.*C        1.22E+13    0      26.1244
C.*CC+C*C*CC=C*CC+C*CC.*C        5.49E+12    0      9.0431
C2H5+C#CCC=C2H6+C#CC.C 2.33E+12    0      14.0431
C2H3+C#CCC=C2H4+C#CC.C 1.39E+13    0      7.9426
C*CC.+C#CCC=C*CC+C#CC.C 3.10E+13    0      25.0239
H+C#CCC=H2+C#CC.C 1.89E+14    0      8.6124
C*C.C+C#CCC=C*CC+C#CC.C 1.03E+13    0      8.9474
CC.C+C#CCC=CCC+C#CC.C   2.99E+12    0      14.6651
CCC.+C#CCC=CCC+C#CC.C   2.33E+12    0      14.0431
C.*CC+C#CCC=C*CC+C#CC.C 1.39E+13    0      7.9426
CH3+C#CCC=CH4+C#CC.C    1.44E+13    0      12.7512
C2H3+C*C*CC=C2H4+C#CC.C 8.50E+12    0      15.3828
CCC.+C*C*CC=CCC+C#CC.C 1.42E+12    0      21.4833
C*CC.+C*C*CC=C*CC+C#CC.C        1.89E+13    0      32.4641
C.*CC+C*C*CC=C*CC+C#CC.C        8.50E+12    0      15.3828
CH3+C*C*CC=CH4+C#CC.C   8.75E+12    0      20.1914
H+C*C*CC=H2+C#CC.C      1.81E+14    0      17.2488
CC.C+C*C*CC=CCC+C#CC.C 1.82E+12    0      22.1053
C*C.C+C*C*CC=C*CC+C#CC.C        6.30E+12    0      16.3876
C2H5+C*C*CC=C2H6+C#CC.C 1.42E+12    0      21.4833
C*CC.+C*CCC=C*CC+C.*CCC 1.89E+13    0      32.4641
C2H3+C*CCC=C2H4+C.*CCC  8.50E+12    0      15.3828
CCC.+C*CCC=CCC+C.*CCC   1.42E+12    0      21.4833
H+C*CCC=H2+C.*CCC 1.81E+14    0      17.2488
C*C.C+C*CCC=C*CC+C.*CCC 6.30E+12    0      16.3876
C2H5+C*CCC=C2H6+C.*CCC  1.42E+12    0      21.4833
C.*CC+C*CCC=C*CC+C.*CCC 8.50E+12    0      15.3828
CC.C+C*CCC=CCC+C.*CCC   1.82E+12    0      22.1053
CH3+C*CCC=CH4+C.*CCC    8.75E+12    0      20.1914
C*C.C+C*CCC=C*CC+C*CCC. 1.64E+13    0      13.8995
H+C*CCC=H2+C*CCC. 3.52E+14    0      12.799
CCC.+C*CCC=CCC+C*CCC.    3.70E+12    0      18.9952
C*CC.+C*CCC=C*CC+C*CCC. 4.92E+13    0      29.9761
C2H3+C*CCC=C2H4+C*CCC.  2.21E+13    0      12.8947
C2H5+C*CCC=C2H6+C*CCC.  3.70E+12    0      18.9952
CH3+C*CCC=CH4+C*CCC.     2.28E+13    0      17.7033
CC.C+C*CCC=CCC+C*CCC.    4.75E+12    0      19.6172
C.*CC+C*CCC=C*CC+C*CCC. 2.21E+13    0      12.8947
C.*CC+C*CCC=C*CC+C*C.CC 9.40E+12    0      13.1818
H+C*CCC=H2+C*C.CC 1.79E+14    0      14.3541
CCC.+C*CCC=CCC+C*C.CC   1.57E+12    0      19.2823
CH3+C*CCC=CH4+C*C.CC    9.69E+12    0      17.9904
C*CC.+C*CCC=C*CC+C*C.CC 2.09E+13    0      30.2632
CC.C+C*CCC=CCC+C*C.CC   2.01E+12    0      19.9043
C2H5+C*CCC=C2H6+C*C.CC 1.57E+12    0      19.2823
C2H3+C*CCC=C2H4+C*C.CC 9.40E+12    0      13.1818
C*C.C+C*CCC=C*CC+C*C.CC 6.97E+12    0      14.1866
CC.C+C*CCC=CCC+CC*CC.    2.54E+12    0      14.0909
```

```
H+C*CCC=H2+CC*CC. 1.59E+14      0      7.3684
C*C.C+C*CCC=C*CC+CC*CC. 8.77E+12      0      8.3732
C.*CC+C*CCC=C*CC+CC*CC. 1.18E+13      0      7.3684
C2H5+C*CCC=C2H6+CC*CC. 1.98E+12      0      13.4689
C*CC.+C*CCC=C*CC+CC*CC. 2.63E+13      0      24.4498
CCC.+C*CCC=CCC+CC*CC.  1.98E+12      0      13.4689
C2H3+C*CCC=C2H4+CC*CC. 1.18E+13      0      7.3684
CH3+C*CCC=CH4+CC*CC.   1.22E+13      0      12.177
C.*CC+CC*CC=C*CC+CC*CC. 1.10E+13      0      9.0431
C2H3+CC*CC=C2H4+CC*CC. 1.10E+13      0      9.0431
CCC.+CC*CC=CCC+CC*CC.  1.83E+12      0      15.1435
CH3+CC*CC=CH4+CC*CC.   1.13E+13      0      13.8517
C2H5+CC*CC=C2H6+CC*CC. 1.83E+12      0      15.1435
H+CC*CC=H2+CC*CC. 1.46E+14      0      9.1866
CC.C+CC*CC=CCC+CC*CC.  2.35E+12      0      15.7656
C*CC.+CC*CC=C*CC+CC*CC. 2.44E+13      0      26.1244
C*C.C+CC*CC=C*CC+CC*CC. 8.13E+12      0      10.0478
CH3+CC*CC=CH4+CC.*CC   1.94E+13      0      17.9904
C*CC.+CC*CC=C*CC+CC.*CC 4.18E+13      0      30.2632
C2H5+CC*CC=C2H6+CC.*CC 3.14E+12      0      19.2823
CCC.+CC*CC=CCC+CC.*CC  3.14E+12      0      19.2823
CC.C+CC*CC=CCC+CC.*CC  4.03E+12      0      19.9043
H+CC*CC=H2+CC.*CC 3.59E+14      0      14.3541
C*C.C+CC*CC=C*CC+CC.*CC 1.39E+13      0      14.1866
C2H3+CC*CC=C2H4+CC.*CC  1.88E+13      0      13.1818
C.*CC+CC*CC=C*CC+CC.*CC 1.88E+13      0      13.1818
H+CCCC=H2+CCCC.   7.03E+14      0      12.799
CCC.+CCCC=CCC+CCCC.    7.40E+12      0      18.9952
C2H5+CCCC=C2H6+CCCC.   7.40E+12      0      18.9952
CH3+CCCC=CH4+CCCC.     4.56E+13      0      17.7033
C*CC.+CCCC=C*CC+CCCC.  9.85E+13      0      29.9761
C2H3+CCCC=C2H4+CCCC.   4.43E+13      0      12.8947
CC.C+CCCC=CCC+CCCC.    9.49E+12      0      19.6172
C.*CC+CCCC=C*CC+CCCC.  4.43E+13      0      12.8947
C*C.C+CCCC=C*CC+CCCC.  3.28E+13      0      13.8995
H+CCCC=H2+CCC.C   4.88E+14      0      10.1435
C*C.C+CCCC=C*CC+CCC.C  2.35E+13      0      11.6029
CCC.+CCCC=CCC+CCC.C    5.29E+12      0      16.6986
C2H3+CCCC=C2H4+CCC.C   3.16E+13      0      10.5981
C.*CC+CCCC=C*CC+CCC.C  3.16E+13      0      10.5981
C2H5+CCCC=C2H6+CCC.C   5.29E+12      0      16.6986
C*CC.+CCCC=C*CC+CCC.C  7.04E+13      0      27.6794
CC.C+CCCC=CCC+CCC.C    6.78E+12      0      17.3206
CH3+CCCC=CH4+CCC.C     3.26E+13      0      15.4067
CC.C+CY13PD=CCC+C5H5R_OLEF_7 2.69E+12      0      22.1053
C*CC.+CY13PD=C*CC+C5H5R_OLEF_7      2.79E+13      0      32.4641
C.*CC+CY13PD=C*CC+C5H5R_OLEF_7      1.25E+13      0      15.3828
C2H3+CY13PD=C2H4+C5H5R_OLEF_7 1.25E+13      0      15.3828
CH3+CY13PD=CH4+C5H5R_OLEF_7  1.29E+13      0      20.1914
H+CY13PD=H2+C5H5R_OLEF_7      4.73E+14      0      15.0957
CCC.+CY13PD=CCC+C5H5R_OLEF_7 2.10E+12      0      21.4833
C2H5+CY13PD=C2H6+C5H5R_OLEF_7 2.10E+12      0      21.4833
C*C.C+CY13PD=C*CC+C5H5R_OLEF_7      9.29E+12      0      16.3876
C*C.C+CY13PD=C*CC+CY13PD5.    9.29E+12      0      16.3876
C*CC.+CY13PD=C*CC+CY13PD5.    2.79E+13      0      32.4641
CC.C+CY13PD=CCC+CY13PD5.      2.69E+12      0      22.1053
C2H5+CY13PD=C2H6+CY13PD5.     2.10E+12      0      21.4833
CCC.+CY13PD=CCC+CY13PD5.      2.10E+12      0      21.4833
C.*CC+CY13PD=C*CC+CY13PD5.    1.25E+13      0      15.3828
CCC.+C5H8=CCC+C#CCCC.  3.70E+12      0      18.9952
C2H3+C5H8=C2H4+C#CCCC. 2.21E+13      0      12.8947
```

```
C.*CC+C5H8=C*CC+C#CCCC. 2.21E+13      0      12.8947
CH3+C5H8=CH4+C#CCCC.     2.28E+13      0      17.7033
CC.C+C5H8=CCC+C#CCCC.    4.75E+12      0      19.6172
H+C5H8=H2+C#CCCC. 3.52E+14      0      12.799
C2H5+C5H8=C2H6+C#CCCC. 3.70E+12      0      18.9952
C*CC.+C5H8=C*CC+C#CCCC. 4.92E+13      0      29.9761
C*C.C+C5H8=C*CC+C#CCCC. 1.64E+13      0      13.8995
C.*CC+C*CC*CC=C*CC+C5H7J(117) 8.50E+12      0      15.3828
H+C*CC*CC=H2+C5H7J(117) 1.81E+14      0      17.2488
CCC.+C*CC*CC=CCC+C5H7J(117)   1.42E+12      0      21.4833
C2H3+C*CC*CC=C2H4+C5H7J(117) 8.50E+12      0      15.3828
CC.C+C*CC*CC=CCC+C5H7J(117)   1.82E+12      0      22.1053
CH3+C*CC*CC=CH4+C5H7J(117)    8.75E+12      0      20.1914
C*C.C+C*CC*CC=C*CC+C5H7J(117) 6.30E+12      0      16.3876
C*CC.+C*CC*CC=C*CC+C5H7J(117) 1.89E+13      0      32.4641
C2H5+C*CC*CC=C2H6+C5H7J(117)  1.42E+12      0      21.4833
C2H3+C*CC*CC=C2H4+C*CC.C*C    5.49E+12      0      9.0431
C2H5+C*CC*CC=C2H6+C*CC.C*C    9.17E+11      0      15.1435
CC.C+C*CC*CC=CCC+C*CC.C*C     1.18E+12      0      15.7656
C*CC.+C*CC*CC=C*CC+C*CC.C*C   1.22E+13      0      26.1244
C.*CC+C*CC*CC=C*CC+C*CC.C*C   5.49E+12      0      9.0431
CCC.+C*CC*CC=CCC+C*CC.C*C     9.17E+11      0      15.1435
C*C.C+C*CC*CC=C*CC+C*CC.C*C   4.07E+12      0      10.0478
CCC.+CYC5H8=CCC+CYPENE3.      4.19E+12      0      21.4833
C.*CC+CYC5H8=C*CC+CYPENE3.    2.51E+13      0      15.3828
CC.C+CYC5H8=CCC+CYPENE3.      5.37E+12      0      22.1053
C*CC.+CYC5H8=C*CC+CYPENE3.    5.58E+13      0      32.4641
C2H3+CYC5H8=C2H4+CYPENE3.     2.51E+13      0      15.3828
C*C.C+CYC5H8=C*CC+CYPENE3.    1.86E+13      0      16.3876
C2H5+CYC5H8=C2H6+CYPENE3.     4.19E+12      0      21.4833
C2H3+CYC5H8=C2H4+CYPENE4.     1.25E+13      0      15.3828
CC.C+CYC5H8=CCC+CYPENE4.      2.69E+12      0      22.1053
C*CC.+CYC5H8=C*CC+CYPENE4.    2.79E+13      0      32.4641
C*C.C+CYC5H8=C*CC+CYPENE4.    9.29E+12      0      16.3876
C2H5+CYC5H8=C2H6+CYPENE4.     2.10E+12      0      21.4833
C.*CC+CYC5H8=C*CC+CYPENE4.    1.25E+13      0      15.3828
CCC.+CYC5H8=CCC+CYPENE4.      2.10E+12      0      21.4833
C*CC.+C*CCCC=C*CC+C*CC.CC     2.63E+13      0      24.4498
CC.C+C*CCCC=CCC+C*CC.CC 2.54E+12      0      14.0909
C2H3+C*CCCC=C2H4+C*CC.CC      1.18E+13      0      7.3684
CCC.+C*CCCC=CCC+C*CC.CC 1.98E+12      0      13.4689
H+C*CCCC=H2+C*CC.CC      1.59E+14      0      7.3684
C.*CC+C*CCCC=C*CC+C*CC.CC     1.18E+13      0      7.3684
CH3+C*CCCC=CH4+C*CC.CC 1.22E+13      0      12.177
C*C.C+C*CCCC=C*CC+C*CC.CC     8.77E+12      0      8.3732
C2H5+C*CCCC=C2H6+C*CC.CC      1.98E+12      0      13.4689
C*C.C+C*CCCC=C*CC+C*C.CCC     6.97E+12      0      14.1866
C.*CC+C*CCCC=C*CC+C*C.CCC     9.40E+12      0      13.1818
H+C*CCCC=H2+C*C.CCC      1.79E+14      0      14.3541
CC.C+C*CCCC=CCC+C*C.CCC 2.01E+12      0      19.9043
CCC.+C*CCCC=CCC+C*C.CCC 1.57E+12      0      19.2823
C2H5+C*CCCC=C2H6+C*C.CCC      1.57E+12      0      19.2823
C*CC.+C*CCCC=C*CC+C*C.CCC     2.09E+13      0      30.2632
C2H3+C*CCCC=C2H4+C*C.CCC      9.40E+12      0      13.1818
CH3+C*CCCC=CH4+C*C.CCC 9.69E+12      0      17.9904
C2H5+C*CCCC=C2H6+C*CCC.C      2.64E+12      0      16.6986
CH3+C*CCCC=CH4+C*CCC.C 1.63E+13      0      15.4067
C2H3+C*CCCC=C2H4+C*CCC.C      1.58E+13      0      10.5981
C*C.C+C*CCCC=C*CC+C*CCC.C     1.17E+13      0      11.6029
CCC.+C*CCCC=CCC+C*CCC.C 2.64E+12      0      16.6986
H+C*CCCC=H2+C*CCC.C      2.44E+14      0      10.1435
```

```
CC.C+C*CCCC=CCC+C*CCC.C 3.39E+12     0      17.3206
C*CC.+C*CCCC=C*CC+C*CCC.C      3.52E+13    0      27.6794
C.*CC+C*CCCC=C*CC+C*CCC.C      1.58E+13    0      10.5981
C2H3+CC*CCCC=C2H4+CC*CCC.C     1.58E+13    0      10.5981
CH3+CC*CCCC=CH4+CC*CCC.C       1.63E+13    0      15.4067
CCC.+CC*CCCC=CCC+CC*CCC.C      2.64E+12    0      16.6986
C2H5+CC*CCCC=C2H6+CC*CCC.C     2.64E+12    0      16.6986
H+CC*CCCC=H2+CC*CCC.C   2.44E+14    0      10.1435
C*C.C+CC*CCCC=C*CC+CC*CCC.C    1.17E+13    0      11.6029
CC.C+CC*CCCC=CCC+CC*CCC.C      3.39E+12    0      17.3206
C.*CC+CC*CCCC=C*CC+CC*CCC.C    1.58E+13    0      10.5981
C*CC.+CC*CCCC=C*CC+CC*CCC.C    3.52E+13    0      27.6794
C2H3+CC*CCCC=C2H4+CC*CCCC.     2.21E+13    0      12.8947
C2H5+CC*CCCC=C2H6+CC*CCCC.     3.70E+12    0      18.9952
C*CC.+CC*CCCC=C*CC+CC*CCCC.    4.92E+13    0      29.9761
CCC.+CC*CCCC=CCC+CC*CCCC.      3.70E+12    0      18.9952
C*C.C+CC*CCCC=C*CC+CC*CCCC.    1.64E+13    0      13.8995
CC.C+CC*CCCC=CCC+CC*CCCC.      4.75E+12    0      19.6172
C.*CC+CC*CCCC=C*CC+CC*CCCC.    2.21E+13    0      12.8947
CH3+CC*CCCC=CH4+CC*CCCC.       2.28E+13    0      17.7033
H+CC*CCCC=H2+CC*CCCC.   3.52E+14    0      12.799
C2H3+CC*CCCC=C2H4+CC*CC.CC     1.18E+13    0      7.3684
H+CC*CCCC=H2+CC*CC.CC   1.59E+14    0      7.3684
CH3+CC*CCCC=CH4+CC*CC.CC       1.22E+13    0      12.177
C2H5+CC*CCCC=C2H6+CC*CC.CC     1.98E+12    0      13.4689
C*C.C+CC*CCCC=C*CC+CC*CC.CC    8.77E+12    0      8.3732
CCC.+CC*CCCC=CCC+CC*CC.CC      1.98E+12    0      13.4689
C.*CC+CC*CCCC=C*CC+CC*CC.CC    1.18E+13    0      7.3684
C*CC.+CC*CCCC=C*CC+CC*CC.CC    2.63E+13    0      24.4498
CC.C+CC*CCCC=CCC+CC*CC.CC      2.54E+12    0      14.0909
C2H3+CC*CCCC=C2H4+C*CC.CCC     5.49E+12    0      9.0431
H+CC*CCCC=H2+C*CC.CCC   7.28E+13    0      9.1866
C*CC.+CC*CCCC=C*CC+C*CC.CCC    1.22E+13    0      26.1244
C2H5+CC*CCCC=C2H6+C*CC.CCC     9.17E+11    0      15.1435
C*C.C+CC*CCCC=C*CC+C*CC.CCC    4.07E+12    0      10.0478
CC.C+CC*CCCC=CCC+C*CC.CCC      1.18E+12    0      15.7656
C.*CC+CC*CCCC=C*CC+C*CC.CCC    5.49E+12    0      9.0431
CCC.+CC*CCCC=CCC+C*CC.CCC      9.17E+11    0      15.1435
CH3+CC*CCCC=CH4+C*CC.CCC       5.65E+12    0      13.8517
H+CHD14=H2+CYC6H7 4.03E+14    0      6.1962
C2H5+CHD14=C2H6+CYC6H7 4.19E+12    0      21.4833
CH3+CHD14=CH4+CYC6H7    2.58E+13    0      20.1914
CC.C+C*CCCC*C=CCC+C*CCC.C*C    5.07E+12    0      14.0909
CCC.+C*CCCC*C=CCC+C*CCC.C*C    3.96E+12    0      13.4689
C.*CC+C*CCCC*C=C*CC+C*CCC.C*C  2.37E+13    0      7.3684
C2H5+C*CCCC*C=C2H6+C*CCC.C*C   3.96E+12    0      13.4689
C*CC.+C*CCCC*C=C*CC+C*CCC.C*C  5.26E+13    0      24.4498
H+C*CCCC*C=H2+C*CCC.C*C 3.18E+14    0      7.3684
C2H3+C*CCCC*C=C2H4+C*CCC.C*C   2.37E+13    0      7.3684
C*C.C+C*CCCC*C=C*CC+C*CCC.C*C  1.75E+13    0      8.3732
CH3+C*CCCC*C=CH4+C*CCC.C*C     2.44E+13    0      12.177
H+C*CCCC=H2+C*CCCC.     3.52E+14    0      12.799
C*CC.+C*CCCC=C*CC+C*CCCC.      4.92E+13    0      29.9761
CC.C+C*CCCC=CCC+C*CCCC. 4.75E+12    0      19.6172
C.*CC+C*CCCC=C*CC+C*CCCC.      2.21E+13    0      12.8947
CCC.+C*CCCC=CCC+C*CCCC. 3.70E+12    0      18.9952
C*C.C+C*CCCC=C*CC+C*CCCC.      1.64E+13    0      13.8995
CH3+C*CCCC=CH4+C*CCCC. 2.28E+13    0      17.7033
C2H3+C*CCCC=C2H4+C*CCCC.       2.21E+13    0      12.8947
C2H5+C*CCCC=C2H6+C*CCCC.       3.70E+12    0      18.9952
H+H=H2          6.40E+17     -1       0
```

```
C2H3+C2H3=C*CC*C  9.34E+12    0      0
CH3+C2H3=C*CC      2.83E+13    0      0
CH3+C2H5=CCC       1.23E+15   -5.62E-01  2.04E-02
C2H5+C2H5=CCCC     8.73E+14   -0.699     -0.0032
C2H3+C2H5=C*CCC    1.62E+13    0      0
C*CC.+C2H5=C*CCCC 1.52E+13    0      0
C*CC.+C*CC.=C*CCCC*C   1.91E+13   -0.166      -0.62
CH3+C*CC.=C*CCC    2.67E+13    0      0
C2H3+C.*CC=C*CC*CC     9.34E+12    0      0
CH3+C.*CC=CC*CC    2.83E+13    0      0
C2H3+CCC.=C*CCCC   1.62E+13    0      0
C.*CC+CCC.=CC*CCCC     1.62E+13    0      0
CH3+CCC.=CCCC      1.41E+13    0      -1.1244
CYC6H10=C2H4+C*CC*C    3.34E+09    2      66.63
CH3+CH3=C2H6       1.32E+13    0      -0.9569
C.*CC+H=C*CC       1.91E+14    0      0.4067
CC*CCCC.+H=CC*CCCC     1.94E+14    0      0.3349
CC.*CC+H=CC*CC     2.36E+14    0      0.4785
CC*CC.+H=C*CCC     5.83E+13   0.176  0.125
C2H5+H=C2H6 1.94E+14    0      0.3349
CC.C+H=CCC  9.55E+13    0      0.4545
C*CC.*C+H=C*C*CC   5.83E+13   0.176  0.125
CCC.+H=CCC  1.94E+14    0      0.3349
C*C.CC+H=C*CCC     2.36E+14    0      0.4785
CH3+H=CH4   1.94E+14    0      0.3349
C#CC.C+H=C*C*CC    1.91E+14    0      0.4067
C*CCC.C+H=C*CCCC   9.55E+13    0      0.4545
CCCC.+H=CCCC       1.94E+14    0      0.3349
C*CCCC.+H=C*CCCC   1.94E+14    0      0.3349
C*CCC.+H=C*CCC     1.94E+14    0      0.3349
CCC.C+H=CCCC       9.55E+13    0      0.4545
C*CC.CC+H=C*CCCC   5.83E+13   0.176  -0.125
C*CC.+H=C*CC       1.91E+14    0      0.4067
C5H5R_OLEF_7+H=CY13PD  3.19E+12   0.359  -0.205
CC*CCC.C+H=CC*CCCC     9.55E+13    0      0.4545
C.*CCC+H=C*CCC     3.88E+13   0.32   0
C5H7J(117)+H=C*CC*CC   1.91E+14    0      0.4067
CYC6H7+H=CHD14     5.83E+13   0.176  0.125
C#CCCC.+H=C5H8     1.94E+14    0      0.3349
CYPENE4.+H=CYC5H8 9.55E+13    0      0.4545
C2H3+H=C2H4 1.91E+14    0      0.4067
C*C.C+H=C*CC       2.36E+14    0      0.4785
C*C.CCC+H=C*CCCC   2.36E+14    0      0.4785
C*CC*CCC.=ME.CY3PE     2.52E+10    0      6.8421
C2H3+C*C*C=C2H4+C#CC.  2.30E+12    0      15.2
C2H5+C*C*C=C2H6+C#CC.  3.14E+13    0      14.4
C*C*C+C*CC.*C=C#CC.+C*CC*C  1.30E+13    0      20.2
C*C*C+C*CC.*C=C#CC.+C*C*CC  5.20E+13    0      20.6
C*C*C+C#CC.C=C#CC.+C#CCC    1.52E+13    0      14.3
C#CC.+C*C*CC=C*C*C+C#CC.C   2.94E+13    0      27.1
C*C*C+C.*CCC=C#CC.+C*CCC    3.60E+12    0      20.5
C*C*C+C*CCC.=C#CC.+C*CCC    2.88E+12    0      15.1
C*C*C+C*C.CC=C#CC.+C*CCC    1.79E+13    0      33.2
C#CC.+C*CCC=C*C*C+CC*CC.    8.78E+12    0      27.2
C*C*C+CC*CC.=C#CC.+CC*CC    3.13E+13    0      19.7
C*C*C+CC.*CC=C#CC.+CC*CC    1.60E+13    0      15.5
C2H4+C#CC.=C5H7R_OLEF_4 1.14E+12   0.214 3.25
CH3+C#CC.=C*C*CC   2.08E+13    0      0
C*C*C+C#CC.=C6H7R_OLEF_91   1.14E+12   0.214 3.25
C#CC+C#CC.=C6H7R_OLEF_85    1.02E+14    0      26.8
C*C*C+C#CC.=C6H7R_OLEF_2    1.14E+12   0.214 3.25
```

Page-219

```
C*CC+C#CC.=C6H9R_OLEF_56      5.69E+11    0.214 3.25
C#CC+C#CC.=C*C*CC*C.C   5.69E+11    0.214 3.25
C*CC+C#CC.=C6H9R_OLEF_57      5.69E+11    0.214 3.25
C2H2+C#CC.=C*C*CC*C.    1.14E+12    0.214 3.25
C#CC.+H=C*C*C    3.88E+13    0.2    0
C*C.C+C*C*C=C*CC+C#CC.  1.88E+13    0    15.1
C.*CC+C*C*C=C*CC+C#CC.  1.60E+13    0    15.5
H+C*C*C=H2+C#CC.  3.13E+13    0    8.4
C*CCC*C+H=C*CC.C*C+H2  7.14E+13    0    9.418049438
C*CCC*C+CH3=C*CC.C*C+CH4  7.73E+13 0    26.04974545
C*CC.+C*C*C=C*CC+C#CC.  3.13E+13    0    19.7
C3C=CC.C+CH3      1.10E+26    -2.61 90.4306
H+C3C=H2+C2CC.    1.05E+15    0    12.799
CH3+C3C=CH4+C2CC. 6.85E+13    0    17.7033
C2H5+C3C=C2H6+C2CC.    1.11E+13    0    18.9952
CC.C+C3C=CCC+C2CC.     1.42E+13    0    19.6172
C*CC.+C3C=C*CC+C2CC.   1.48E+14    0    29.9761
C.*CC+C3C=C*CC+C2CC.   6.64E+13    0    12.8947
C*C.C+C3C=C*CC+C2CC.   4.93E+13    0    13.8995
CCC.+C3C=CCC+C2CC.     1.11E+13    0    18.9952
C2H3+C3C=C2H4+C2CC.    6.64E+13    0    12.8947
C.*CC+C3C=C*CC+C3C.    9.64E+12    0    8.4211
CH3+C3C=CH4+C3C.  9.94E+12    0    13.2297
C2H3+C3C=C2H4+C3C.     9.64E+12    0    8.4211
C*CC.+C3C=C*CC+C3C.    2.14E+13    0    25.5024
C2H5+C3C=C2H6+C3C.     1.61E+12    0    14.5215
H+C3C=H2+C3C.    1.36E+14    0    7.8708
C*C.C+C3C=C*CC+C3C.    7.15E+12    0    9.4258
CC.C+C3C=CCC+C3C. 2.07E+12    0    15.1435
CCC.+C3C=CCC+C3C. 1.61E+12    0    14.5215
C2C*C+H=C3C.     1.26E+13    0    13.2536
C2C*C+H=C2CC.    3.42E+13    0    6.1962
C*CC+CH3=C2CC.    1.80E+14    0    31.8182
CCC.+C2C*C=CCC+C2.C*C   1.83E+12    0    15.1435
H+C2C*C=H2+C2.C*C 1.46E+14    0    9.1866
CH3+C*C.C=C2C*C  2.67E+13    0    0
C.*CC+C2C*C=C*CC+C2.C*C 1.10E+13    0    9.0431
C2H5+C2C*C=C2H6+C2.C*C 1.83E+12    0    15.1435
C*C.C+C2C*C=C*CC+C2.C*C 8.13E+12    0    10.0478
CC.C+C2C*C=CCC+C2.C*C   2.35E+12    0    15.7656
C*CC.+C2C*C=C*CC+C2.C*C 2.44E+13    0    26.1244
CH3+C2C*C=CH4+C2.C*C    4.13E+13    0    13.8517
C2H3+C2C*C=C2H4+C2.C*C 1.10E+13    0    9.0431
C2.C*C+H=C2C*C   1.91E+14    0    0.4067
C*C*C+CH3=C2.C*C 1.44E+16    0    12.9665
CC.C+C2C*C=CCC+C2C*C.   3.64E+12    0    22.1053
C*C.C+C2C*C=C*CC+C2C*C. 1.26E+13    0    16.3876
CH3+C2C*C=CH4+C2C*C.    1.75E+13    0    20.1914
H+C2C*C=H2+C2C*C. 3.61E+14    0    17.2488
C*CC.+C2C*C=C*CC+C2C*C. 3.78E+13    0    32.4641
C2H3+C2C*C=C2H4+C2C*C. 1.70E+13    0    15.3828
C2C*C.+H=C2C*C   1.91E+14    0    0.4067
C.*CC+C2C*C=C*CC+C2C*C. 1.70E+13    0    15.3828
C2H5+C2C*C=C2H6+C2C*C. 2.84E+12    0    21.4833
CCC.+C2C*C=CCC+C2C*C.   2.84E+12    0    21.4833
C#CC+CH3=C2C*C.  1.20E+16    0    13.445
C3H3R+C2C*C=C#CC+C2.C*C 5.65E+12    0    13.8517
C#CC.+C2C*C=C*C*C+C2.C*C      3.29E+13    0    9.0431
C2H+C2C*C=C2H2+C2.C*C 5.65E+12    0    13.8517
C2C*C+CH3=C2C.CC 4.58E+15    0    9.5694
C2C*CC+H=C2C.CC 7.62E+13    0    4.2105
```

```
C2C*CC+CH3=C2CC.C2      2.22E+15    0      11.0766
C2C*CC2+H=C2CC.C2 8.07E+13    0      5.0239
C2C*C+C2H5=C6H13R_8     4.79E+14    0      9.067
C6H12_OLEF_13+H=C6H13R_8       7.62E+13    0       4.2105
C*CC+CYC6H11=C*CC.+C6H12_R6    2.09E+12    0      13.72008761
C*CCCCC=C*CC.+CCC.      7.94E+15    0      70.74
C*CCCC.=C*CC.+C2H4      1.48E+13    0      20.681
C*CCC.C=C2H3+C*CC 1.65E+14    0      36.971
C.*CCCC=CCC.+C2H2 1.27E+15    0      33.219
C*C.CCC=C2H5+C*C*C      1.84E+14    0      31.703
C*CCC.C*C=C2H3+C*CC*C   1.71E+15    0      45.099
C*CCCCC.=C*CCC.+C2H4    7.05E+13    0      30.74162679
C*CC.CCC=C*CC*C+C2H5    3.88E+14    0      37.006
CC*CC.CC=C*CC*CC+CH3    1.41E+14    0      38.65
MECYPE2.=CYC5H8+CH3     1.69E+14    0      31.104
C*CC(C)CC.=C2H4+CC*CC.  1.82E+13    0      0
C2.CCC*C=CH3+C*CCC*C    9.88E+13    0      30.963
C2.CCC*C=C*CC+C*CC.     1.81E+13    0      19.717
C*CCCC.C=C*CC+C*CC.     6.41E+12    0      21.063
C*C(C)CCC.=C2H4+C2.C*C  2.88E+13    0      21.127
C*C(C.)CCC=CCC.+C*C*C   2.82E+15    0      55.625
C7H15-4=C2H5+C*CCCC     5385299619  0      3.361448034
CC*CCCC.=C2H4+CC*CC.    23501860694 0      13.12012145
C*CCCC*CC.=C*CC.+C*CC*C 6.09E+03    0      -1.818664648
C*CCC2C.C=C*CC.+CC*CC   1.43E-02    0      0.886413987
C*CCC*CC.C=C2H3+C*CC*CC 2.01E+12    0      30.31362957
C*CC2CC*CC.=CC*CC.+C*CC*C      1.28E+11    0      20.07984948
CC*CCCC*CC.=CC*CC.+C*CC*C      1.00E+11    0      22.30848653
CC*CCCC.C=CC*CC.+C*CC   3.92E+02    0      -1.246506605
CC*CCC2C.C=CC*CC.+CC*CC 8.30E+11    0      13.80567213
CYC5H9.=CYC5H8+H  1.85E+14    0      36.83533593
C*CC.CC=C*CC*CC+H 1.62E+14    0      46.637
CC*CCC.=C*CC*CC+H 2.34E+13    0      33.222
C*CCCC.=C*CCC*C+H 1.44E+13    0      36.916
C*CCC.C=H+C*CC*CC 1.45E+13    0      33.857
C*CCC.C=H+C*CCC*C 2.62E+14    0      38.596
CC*CC.C=H+C*CC*CC 2.85E+14    0      48.52
CYC6H9=CHD14+H    2.01E+14    0      35.027
CYC6H9=CHD13+H    8.94E+13    0      34.592
CYC6H11=CYC6H10+H 2.06E+14    0      36.802
C*CCCCC.=H+C*CCCC*C     1.19E+14    0      36.919
MECYPE4.=H+ME3-CPENE    2.05E+14    0      0
MECYPE4.=H+ME4-CPENE    2.76E+14    0      36.642
C2.CCC*C=H+C*C2CC*C     1.05E+13    0      34.983
C*CCCC.C=H+C*CCC*CC     5.40E+13    0      36.771
C*CCCC.C=H+C*CCCC*C     3.20E+14    0      38.41
CH2.CYC5=H+CH2*CPANE    1.35E+13    0      35.395
MECYPE1.=H+CH2*CPANE    3.12E+14    0      41.485
MECYPE1.=H+ME1-CPENE    5.77E+14    0      36.873
C*C(C)CCC.=H+C*C2CC*C   9.76E+13    0      36.934
CYC6H9A=CHD13+H   4.22E+12    0      42.52513658
C6H12_R6+CH3=CYC6H11+CH4       4.90E+13    0      14.21626921
C*CC.+CYC5H10=C*CC+CYC5H9.     5.27E+13    0      23.52969861
CYC5H10+C2H5=CYC5H9.+C2H6      1.61E+13    0      13.55748391
CYC5H10+CC.C=CYC5H9.+CCC       7.66E+12    0      15.79781577
CYC5H10+CCC.=CYC5H9.+CCC       5.89E+12    0      14.78642058
CYC5H10+CH3=CYC5H9.+CH4 1.61E+13    0      13.55748391
CYC5H10+C2H3=CYC5H9.+C2H4      1.56E+13    0      9.09461564
C6H12_R6+C2H5=CYC6H11+C2H6     2.55E+13    0      15.98179214
CC*CC.+C*CC*C=CC*CC+C*CC.*C    9.00E+12    0      16.73154863
CHD13+C2H5=CYC6H7+C2H6 1.29E+13    0      8.726792137
```

```
CHD13+CH3=CYC6H7+CH4      1.76E+13    0      10.01406162
CC*CC.+C6H12_R6=CC*CC+CYC6H11 1.74E+13   0      23.39456106
C6H12_R6+H=CYC6H11+H2     1.14E+15    0      9.418049438
CYC5H10+H=CYC5H9.+H2      2.57E+14    0      8.518049438
CHD13+H=CYC6H7+H2 3.14E+14   0      4.969139573
C*CCCC*CC+H=CC*CCC*CC.+H2    1.52E+15    0      7.153357094
C*CCCC*CC+H=C*CCC*CC.C+H2    1.52E+15    0      7.153357094
ME3-CPENE+H=ME3-CPENE3.+H2   3.04E+15    0      6.153357094
ME3-CPENE+H=ME3-CPENE4.+H2   3.04E+15    0      6.153357094
CC*CCCC*CC+H=CC*CCC*CC.C+H2   3.04E+15    0      7.153357094
ME3-CPENE+H=ME4-CPENE3.+H2   3.04E+15    0      7.153357094
C*CC.CC=CC*CCC.    1.79E+12    0      31.408
C*CCCCC.=C*CCC.CC 1.77E+12    0      16.813
C*CCC.CC=CH3+C*CCC*C    9.41E+14    0      38.65
C*CCC.CC=C*CCC+C2H3    5.87E+15    0      46.75604821
C*CC.CC=C*CCCC.    1.27E+13    0      49.564
C*CC.CC=C*CCC.C    1.56E+13    0      45.93
C*CCCC.=C*CCC.C    9.01E+12    0      38.073
C*CC.CC=CC*CC.C    5.54E+12    0      36.188
CC*CCC.=CC*CC.C    4.85E+12    0      30.559
C*CCCC.=C.*CCCC    9.36E+10    0      19.551
C*CCC.C=C.*CCCC    4.14E+11    0      28.104
C*CCCC.=C*C.CCC    2.81E+11    0      25.796
C*CCC.C*C=C*CC*CC.C    1.84E+12    0      31.266
C*CCCCC.=C*CC.CCC 2.19E+17    0      45.35503639
C*CC.CCC=CC*CC.CC 8.97E+12    0      36.951
C*CC.CCC=CC*CCC.C 6.83E+11    0      28.84
MECYPE4.=MECYPE2. 4.24E+13    0      43.309
CH2.CYC5=MECYPE2. 9.04E+12    0      37.972
CH2.CYC5=MECYPE1. 6.39E+12    0      36.535
C*C(C)CCC.=C*C(C.)CCC    4.06E+10    0      13.447
C*CC.CCC=CC*CCCC. 4.27E+12    0      32.21660989
CC*CC.CC=CC*CCC.C 6.11E+13    0      48.99360989
C*C(C)C.C=C2C*CC. 5.84E+13    0      7.842435043
C*C(C)CC.=CCC(C.)*C    16107696030 0      18.0125106
C*CCCCC.=C*CCCC.C 1946369589  0      12.95765171
C*CCC.=C.*CCC     217960214   0      15.79478342
CC*CCC.C=CC*CCCC. 284200848.5 0      14.23227222
CC*CCCC*CC.=CC*CCC*CC.C 39909845686 0      21.67112991
C*CCCC*CC.=CC*CCC*CC.    22755709550 0      19.18079034
C*CC2CC*CC.=CC*CCC2*CC.   20487623026 0      18.82026436
CC*CCCC.C=C*CC.CCCC    4427620458  0      8.032329316
CC*CCC*CC.=CC*CC*CC.C    3.66E+11    0      28.6340559
C6H12_R6=C*CCCCC  2.455E+20   -0.97 92.86
CYC5H10=C*CCCC    1.25E+16    0      85.106
C*CC.+CC*CC.=C*CCCC*CC 1.02E+13    0      -0.666958291
CC*CC.+CC*CC.=CC*CCCC*CC    8.04E+12    0      -1.127097863
CC*CC.+CC*CC.=C*CC2C2C*C    1.89E+12    0      -3.73099906
CC*CC.+CC*CC.=C*CC2CC*CC    3.01E+12    0      -2.00388094
CC*CC.+C2H5=C*CC2CC    1.09E+13    0      -0.683730513
CYPENE3.+CH3=ME3-CPENE 1.00E+14    0      0
CC*CC.+CH3=CC*CCC 1.94E+13    0      -0.683730513
CC*CC.+CH3=C*CCC2 1.94E+13    0      -0.683730513
CC*CC.+C2H5=CC*CCCC    3.65E+12    0      -0.683730513
C6H7(121)=C6H7(122)    1.22E+12    0      4.743135857
CYC6H7=C6H7(122) 1.03E+13    0      37.7745913
prod2(126)=prod1(114)    1.03E+13    0      37.7745913
C5H5C5H4=prod1(114)    2.30E+12    0      9.842213546
C*CCCC.=CYC5H9.    3.09E+10    0      16.62869137
C*C(C)CCC.=MECYPE1.    3.09E+10    0      16.62869137
C*CC(C)CC.=MECYPE2.    3.09E+10    0      16.62869137
```

```
C2.CCC*C=MECYPE4. 3.09E+10    0    16.62869137
C*CC*CC.C=ME4-CPENE3.  3.09E+10   0    16.62869137
C*CC.C*C=CYPENE3. 3.09E+10   0    16.62869137
C*CCCC.C=MECYPE4. 5.55E+10   0    14.185
CC*CCCC.=MECYPE2. 5.55E+10   0    14.185
CC*CCCC*CC.=C2H3-ME2-CPANE3. 5.55E+10   0    14.185
C7H9(83)=addC(80) 9.96E+12   0    38.29192988
pdt16(17)=pdt15(16)   9.96E+12   0    38.29192988
C7H9(85)=C7H9J(88)    4.89E+11   0    14.22387371
C*CCCCC.=CYC6H11 5.85E+09   0    8.368
C*CCC.C*C=CYC6H9 5.85E+09   0    8.368
C*CCC*CC.C=ME3-CHEXE5. 5.85E+09   0    8.368
pdt20(18)=pdt21(19)   7.88E+11   0    21.6853494
C*CCCCC.=CH2.CYC5 2.06E+10   0    6.268
prod5(132)=prod2(126) 2.05E+12   0    7.797282793
C*CC2CC*CC.=ME45-CHEXE4.   5.55E+10   0    14.185
C*CCCC*CC.=ME4.-CHEXE   5.55E+10   0    14.185
C7H9(83)=C7H9(85) 5.55E+10   0    14.185
CC*CCCC*CC.=Et4-CHEXE4. 5.55E+10   0    14.185
prod5(132)=c10h9(128)  1.96E+12   0    5.244058168
pdt16(17)=pdt17(209)   1.43E+12   0    33.08811634
C7H8(106)=C7H8(105)    2.77E+11   0    1.354281672
CYC5H5CC.=CY13PD5.+C2H4 4.11E+13   0    15.27254343
addC(80)=CY13PD+C2H3   1.87E+15   0    46.75604821
CYC5H4.CC=FULVENE+CH3 9.68E+14   0    42.02121315
pdt27(20)=INDENE+CH3   1.57E+14   0    24.43586375
ME4-CPENE3.=CY13PD+CH3 5.73E+15   0    44.20285903
ME3-CPENE4.=CY13PD+CH3 1.56E+14   0    32.91709669
C10H11(15)=CY13PD5.+CY13PD    2.08E+14   0    21.71402312
C8H9J(156)=BENZENE+C2H3 4.15E+14   0    22.63007662
CCC.=C2H4+CH3    8.46E+13   0    31.37006558
C*CCC.=C2H4+C2H3 1.47E+14   0    37.46296913
C*CC.CC=C*CC*C+CH3    4.36E+14   0    38.71526437
CYPENE4.=CY13PD+H 2.19E+14   0    34.66527132
CYC6H7=BENZENE+H  5.52E+13   0    30.02398009
c10h9(128)=a2+H   2.92E+13   0    18.42859164
ME4-CPENE3.=prod_9(66)+H    1.67E+15   0    49.70624198
CYPENE3.=CY13PD+H 1.47E+15   0    50.75977728
C5H5-3-C5H4=C10H8(116)+H    2.43E+15   0    58.37500293
C10H9(112)=C10H8(116)+H 1.81E+15   0    54.1941383
C5H5C5H4=C10H8(116)+H   1.59E+14   0    42.6873123
ME.CY13PD=FULVENE+H    7.75E+14   0    47.80869396
C6H7(121)=FULVENE+H    1.57E+13   0    30.67299137
ME.CY14PD=FULVENE+H    1.31E+15   0    53.040535
ME4-CPENE3.=MECY13PD+H 8.56E+14   0    49.40845758
ME3-CPENE4.=MECY24PD+H 4.41E+13   0    36.46702369
C8H9J(156)=CYC6H5C*C+H 1.58E+14   0    21.94957517
pdt18(211)=C6H5C*CC*C+H 1.92E+14   0    34.03177417
pdt27(20)=S(270)+H    3.32E+13   0    23.23949082
C10H9=a2+H  1.13E+19   0    25.65901882
C7H8(106)=C7H7(131)+H  1.55E+15   0    35.27229881
C7H9J(88)=C7H8(105)+H  8.90E+16   0    35.6857438
CC*CC.=C*CC*C+H   2.52E+14   0    48.44312763
C*CCC.=C*CC*C+H   3.03E+13   0    34.56058239
C*CC.*C=C#CC*C+H  5.71E+14   0    48.75738016
C#CC.C=C#CC*C+H   1.06E+14   0    46.92281647
ME.CY13PD+CY13PD=prod_9(66)+CY13PD5.    3.41E+12   0    15.4600566
prod_9(66)+CH3=ME.CY13PD+CH4 5.47E+12   0    13.4600566
CY13PD+CH3=CY13PD5.+CH4 3.00E+11   0    5
CY13PD+CYPENE3.=CY13PD5.+CYC5H8    1.74E+12   0    15.0600566
C2H3+CY13PD=C2H4+CY13PD5.    2.02E+13   0    5.960056596
```

```
CY13PD+CYPENE4.=CY13PD5.+CYC5H8      2.05E+12    0      8.360056596
C10H10(46)+CY13PD5.=C10H9(112)+CY13PD    7.80E+11    0     14.05497891
C10H10(43)+CY13PD5.=C5H5-3-C5H4+CY13PD   7.80E+11    0     14.05497891
C10H10(45)+CY13PD5.=C5H5-3-C5H4+CY13PD   4.97E+12    0     23.91333787
C10H10(45)+CY13PD5.=C10H9(112)+CY13PD    4.97E+12    0     23.91333787
C7H7(131)+CY13PD=toluene(3)+CY13PD5.     3.41E+12    0     15.4600566
CH3+C7H10(146)=CH4+CYC5H4.CC 1.88E+13    0     10.4600566
C10H10(45)+CH3=C5H5-3-C5H4+CH4      1.88E+13    0     10.4600566
C10H10(45)+CH3=C10H9(112)+CH4 1.88E+13    0     10.4600566
C10H10(45)+C*CC.C*C=C10H9(112)+C*CC*CC    3.41E+12    0     15.4600566
C10H10(45)+C*CC.C*C=C5H5-3-C5H4+C*CC*CC   3.41E+12    0     15.4600566
CH3+C7H10(145)=CH4+CYC5H4.CC 1.88E+13    0     10.4600566
C5H5-3-C5H5+CH3=C5H5-3-C5H4+CH4      3.75E+13    0     10.4600566
C10H10(47)+CH3=C10H9(112)+CH4 3.75E+13    0     10.4600566
C10H10(47)+C*CC.C*C=C10H9(112)+C*CC*CC    6.83E+12    0     15.4600566
INDENE+CH3=INDENE.+CH4 1.88E+13    0     10.4600566
INDENE+C*CC.C*C=INDENE.+C*CC*CC      3.41E+12    0     15.4600566
ME.CY14PD+INDENE=MECY24PD+INDENE.      1.71E+12    0     15.4600566
MECY24PD+CH3=ME.CY14PD+CH4      5.47E+12    0     13.4600566
CH3+S(272)=CH4+C10H9(263)      9.38E+12    0     10.4600566
S(102)+CH3=C10H9(173)+CH4      4.63E+12    0     9.460056596
toluene(3)+C2H3=C7H7(131)+C2H4      5.89E+12    0     8.860056596
toluene(3)+CH3=C7H7(131)+CH4 5.47E+12    0     13.4600566
CH3+CYC5H8=CH4+CYPENE4. 1.42E+13    0     14.7600566
CH3+CYC5H8=CH4+CYPENE3. 2.25E+13    0     14.32360042
CH3+C*CC*CC=CH4+C*CC.C*C      5.47E+12    0     13.4600566
C2H4+CH3=C2H3+CH4 1.42E+13    0     19.7787761
C*CC*C+CH3=C*CC.*C+CH4 1.53E+13    0     16.9600566
CY13PD+C2H4=norbornene(340)   20000000000 0     24.7
CYC5H8=CY13PD+H2  2.24E+13    0     60
prod_9(66)+H=ME.CY13PD+H2      2.31E+14    0     11.3600566
CY13PD+H=CY13PD5.+H2   8.54E+14    0     7.660766147
C10H10(45)+H=C5H5-3-C5H4+H2    1.71E+14    0     7.660766147
C10H10(45)+H=C10H9(112)+H2    1.71E+14    0     7.660766147
C5H5-3-C5H5+H=C5H5-3-C5H4+H2 3.41E+14    0     7.660766147
C10H10(47)+H=C10H9(112)+H2    3.41E+14    0     7.660766147
INDENE+H=INDENE.+H2    1.71E+14    0     7.660766147
MECY24PD+H=ME.CY14PD+H2 2.31E+14    0     11.3600566
toluene(3)+H=C7H7(131)+H2      2.31E+14    0     11.3600566
H+CYC5H8=H2+CYPENE4.   6.00E+14    0     12.5600566
H+CYC5H8=H2+CYPENE3.   1.41E+14    0     8.869251408
CH4+H=CH3+H2      2.03E+14    0     14.63411555
C2H4+H=C2H3+H2   6.28E+14    0     18.57677532
prod_9(66)=MECY24PD    2.82E+14    0     29.33873706
MECY13PD=prod_9(66)    4.98E+13    0     26.0102518
CYC5H5CC=norbornene(340)      60000000000 0     5
CYC5H5CC=C7H10(145)    4.98E+13    0     26.0102518
C7H10(146)=C7H10(145)    9.95E+13    0     27.81209642
C10H10(43)=C5H5-3-C5H5    2.64E+13    0     22.32859164
C10H10(43)=C10H10(46)    2.82E+14    0     29.33873706
C5H5C5H5=C10H10(43)    4.98E+13    0     26.0102518
C10H10(45)=C10H10(47)    3.71E+13    0     28.55246535
C5H5-3-C5H5=C10H10(45)    1.05E+14    0     28.75338766
C10H10(46)=C10H10(45)    2.79E+13    0     23.22859164
pdt15(16)=pdt39(34)    2.82E+14    0     29.33873706
C10H11(15)=pdt15(16)    4.98E+13    0     26.0102518
C5H5-3-C5H4=C10H9(112)    4.57E+13    0     31.5570769
C5H5C5H4=C5H5-3-C5H4    2.62E+13    0     19.64693148
C6H7(121)=ME.CY13PD    4.49E+12    0     16.50840718
S(109)=S(110)    9.95E+13    0     27.81209642
S(271)=S(272)    9.95E+13    0     27.81209642
```

```
S(271)=S(270)        9.95E+13    0      27.81209642
ME.CY13PD=ME.CY14PD     4.39E+13    0      35.87183388
CYC5H5CC.=CYC5H4.CC     3.03E+12    0      28.32951395
pdt39(34)=pdt55(23)     9.13E+13    0      31.5570769
pdt21(19)=pdt27(20)     4.69E+13    0      30.13689244
pdt58(24)=pdt20(18)     3.65E+12    0      30.34969841
C10H9(174)=C10H9(173)   3.01E+12    0      23.1404753
pdt16(17)=pdt20(18)     7.79E+11    0      28.43863068
CYPENE4.=CYPENE3. 4.71E+13    0      47.7717275
C*CCC.=CC*CC.        7.22E+12    0      30.48361116
C*CC.*C=C#CC.C     1.17E+12    0      32.91869841
CY13PD5.+H=CY13PD 2.60E+14    0      0
CY13PD=C5H6a(28)  1.35E+15    0      80.45
CY13PD5.+C2H5=CYC5H5CC 3.24E+13    0      -1.912912354
ME.CY14PD+CH3=C7H10(146)    8.06E+12    0      -0.77590279
ME.CY13PD+CH3=C7H10(145)    8.06E+12    0      -0.77590279
INDENE.+CH3=S(102)     3.09E+12    0      -1.37254343
INDENE.+CH3=S(109)     3.09E+12    0      -1.37254343
CY13PD5.+CY13PD5.=C5H5C5H5    5.00E+13    0      0
CY13PD5.+CH3=MECY13PD   3.24E+13    0      -1.912912354
CYPENE3.+H=CYC5H8 1.22E+14    0      0.48732032
C7H9(85)=A(5)     17.19E6 1.81 23.3
C7H9(85)=A(1)     1.09E6 1.92 24.6
A(5)=A(1)     4.34E4 2.63 42.5
H+toluene(3)=A(1)     5.69E+13 0      5.19
H+toluene(3)=A(2)     5.69E+13 0      5.19
H+toluene(3)=A(4)     5.69E+13 0      5.19
H+toluene(3)=A(5)     5.69E+13 0      5.19
END
REACTIONS
CH3cC6H11=CYC6H11+CH3                5.93E+64    -14.15      108486
CH3cC6H11+H=CH3S3XcC6H10+H2          2.07E+07    2.12       6441.2
CH3cC6H11+CH3=CH3S3XcC6H10+CH4       7.18E+01    3.26       11303.0
CH3S3XcC6H10=SXC7H13                3.29E+28    -5.27       28275
SXC7H13=C*CCC.+C*CC     5.50E+11    0.55       28084.3
SXC7H13=SAXC7H13     1.55E+02    2.83       15566.2
SAXC7H13=C*CC*C+CCC.     3.39E+11    0.66       32262.9
CH3cC6H11+H=CH3S2XcC6H10+H2          2.08E+07    2.10       6474.4
CH3cC6H11+CH3=CH3S2XcC6H10+CH4       6.68E+01    3.21       11418.0
CH3S2XcC6H10=PX7-2C7H13             1.44E+28    -5.21       27888
PX7-2C7H13=CC*CCC.+C2H4     9.12E+11    0.31       27237.8
C2H5cC6H11=CYC6H11+C2H5              5.93E+64    -14.15      108486
C2H5cC6H11+H=C2H5S3XcC6H10+H2        2.07E+07    2.12       6441.2
C2H5cC6H11+CH3=C2H5S3XcC6H10+CH4     7.18E+01    3.26       11303.0
C2H5S3XcC6H10=S2XC8H15              3.29E+28    -5.27       28275
S2XC8H15=C*CCC.+C*CCC     5.50E+11    0.55       28084.3
S2XC8H15=SAXC8H15     1.55E+02    2.83       15566.2
SAXC8H15=C*CC*C+CCCC.     3.39E+11    0.66       32262.9
BENZENE+CH3=A(1) 7.40E+13    0      9976.076555
CH3+CHD14=C(1)        7.40E+13    0      9976.076555
CH3+CHD13=C(2)        7.40E+13    0      9976.076555
CH3+CHD13=C(3)        7.40E+13    0      9976.076555
H+B(2)=C(1)        6.28E+13        0    3253.588517
H+B(5)=C(1)        6.28E+13        0    3253.588517
H+B(5)=C(2)        6.28E+13        0    3253.588517
H+B(3)=C(2)        6.28E+13        0    3253.588517
H+B(4)=C(3)        6.28E+13        0    3253.588517
H+B(1)=C(3)        6.28E+13        0    3253.588517
B(2)+H=A(5)+H2                3.19E+08    1.700    2480.0
B(2)+CH3=A(5)+CH4            2690    2.897    3446
B(2)+C2H5=A(5)+C2H6          2690    2.897    3446
```

```
B(2)+C*CC.=A(5)+C*CC          389.2   3.12     9480
B(2)+CC*CC.=A(5)+CC*CC         389.2   3.12     9480
C*CC*C+C6H5=C10H11(1)          1.5E12 0 0
C10H11(1)=C10H11(C6)           4.6E10 0 24500
C10H11(C6)=C10H10(C6)+H        5E13 0 0
C10H10(C6)=a2+H2               5E13 0 0
C*CC*C.+BENZENE=pdt12(7)       1.5E12 0 0
pdt12(7)=C10H11(12)            4.6E10 0 24500
C10H11(12)=C10H10(C6_2)+H      5E13 0 0
C10H10(C6_2)=a2+H2             5E13 0 0
BENZENE+C*CC.=C9H11(1)  5E13 0 0
C9H11(1)=C9H11(C5)      5E13 0 0
C9H11(C5)=C9H10(C5)+H   5E13 0 0
C9H10(C5)=INDENE+H2     5E13 0 0
B(2)+CC*CC.=A(5)+C*CCC         389.2   3.12     9480
B(2)+CY13PD5.=A(5)+CY13PD      389.2   3.12     9480
B(2)+C*CC.=A(2)+C*CC          389.2   3.12     9480
B(2)+CC*CC.=A(2)+CC*CC         389.2   3.12     9480
B(2)+CC*CC.=A(2)+C*CCC         389.2   3.12     9480
B(2)+CY13PD5.=A(2)+CY13PD      389.2   3.12     9480
B(2)+H=A(2)+H2                 3.19E+08   1.700   2480
B(2)+CH3=A(2)+CH4             2690    2.897    3446
B(2)+C2H5=A(2)+C2H6           2690    2.897    3446
CH3+C*CC*C=CH4+C*CC*C.  .9367E+06 2.0  11360.34
H+C*CC*C=H2+C*CC*C.  .5776E+08 2.0  10398.54
CH3+BENZENE=CH4+C6H5  .6245E+06 2.0  10654.35
H+BENZENE=H2+C6H5                         .1500E+15   .000  10000
B(1)+H=A(1)+H2                 3.19E+08   1.700   2480.0
B(1)+CH3=A(1)+CH4            2690    2.897    3446
B(1)+C2H5=A(1)+C2H6            2690    2.897    3446
B(1)+C*CC.=A(1)+C*CC          389.2   3.12     9480
B(1)+CC*CC.=A(1)+CC*CC         389.2   3.12     9480
B(1)+CC*CC.=A(1)+C*CCC         389.2   3.12     9480
B(1)+CY13PD5.=A(1)+CY13PD      389.2   3.12     9480
B(1)+H=A(4)+H2                 3.19E+08   1.700   2480.0
B(1)+CH3=A(4)+CH4             2690    2.897    3446
B(1)+C2H5=A(4)+C2H6           2690    2.897    3446
B(1)+C*CC.=A(4)+C*CC          389.2   3.12     9480
B(1)+CC*CC.=A(4)+CC*CC         389.2   3.12     9480
B(1)+CC*CC.=A(4)+C*CCC         389.2   3.12     9480
B(1)+CY13PD5.=A(4)+CY13PD      389.2   3.12     9480
B(3)+H=A(2)+H2                 3.19E+08   1.700   2480.0
B(3)+CH3=A(2)+CH4            2690    2.897    3446
B(3)+C2H5=A(2)+C2H6           2690    2.897    3446
B(3)+C*CC.=A(2)+C*CC          389.2   3.12     9480
B(3)+CC*CC.=A(2)+CC*CC         389.2   3.12     9480
B(3)+CC*CC.=A(2)+C*CCC         389.2   3.12     9480
B(3)+CY13PD5.=A(2)+CY13PD      389.2   3.12     9480
B(3)+H=A(5)+H2                 3.19E+08   1.700   2480.0
B(3)+CH3=A(5)+CH4            2690    2.897    3446
B(3)+C2H5=A(5)+C2H6           2690    2.897    3446
B(3)+C*CC.=A(5)+C*CC          389.2   3.12     9480
B(3)+CC*CC.=A(5)+CC*CC         389.2   3.12     9480
B(3)+CC*CC.=A(5)+C*CCC         389.2   3.12     9480
B(3)+CY13PD5.=A(5)+CY13PD      389.2   3.12     9480
B(4)+H=A(2)+H2                 3.19E+08   1.700   2480.0
B(4)+CH3=A(2)+CH4            2690    2.897    3446
B(4)+C2H5=A(2)+C2H6           2690    2.897    3446
B(4)+C*CC.=A(2)+C*CC          389.2   3.12     9480
B(4)+CC*CC.=A(2)+CC*CC         389.2   3.12     9480
B(4)+CC*CC.=A(2)+C*CCC         389.2   3.12     9480
```

```
B(4)+CY13PD5.=A(2)+CY13PD      389.2   3.12    9480
B(4)+H=A(4)+H2                 3.19E+08   1.700   2480.0
B(4)+CH3=A(4)+CH4             2690    2.897   3446
B(4)+C2H5=A(4)+C2H6           2690    2.897   3446
B(4)+C*CC.=A(4)+C*CC         389.2   3.12    9480
B(4)+CC*CC.=A(4)+CC*CC        389.2   3.12    9480
B(4)+CC*CC.=A(4)+C*CCC        389.2   3.12    9480
B(4)+CY13PD5.=A(4)+CY13PD      389.2   3.12    9480
B(5)+H=A(5)+H2                3.19E+08   1.700   2480.0
B(5)+CH3=A(5)+CH4            2690    2.897   3446
B(5)+C2H5=A(5)+C2H6          2690    2.897   3446
B(5)+C*CC.=A(5)+C*CC        389.2   3.12    9480
B(5)+CC*CC.=A(5)+CC*CC       389.2   3.12    9480
B(5)+CC*CC.=A(5)+C*CCC       389.2   3.12    9480
B(5)+CY13PD5.=A(5)+CY13PD     389.2   3.12    9480
B(5)+H=A(1)+H2               3.19E+08   1.700   2480.0
B(5)+CH3=A(1)+CH4           2690    2.897   3446
B(5)+C2H5=A(1)+C2H6         2690    2.897   3446
B(5)+C*CC.=A(1)+C*CC        389.2   3.12    9480
B(5)+CC*CC.=A(1)+CC*CC       389.2   3.12    9480
B(5)+CC*CC.=A(1)+C*CCC       389.2   3.12    9480
B(5)+CY13PD5.=A(1)+CY13PD     389.2   3.12    9480
END
```